UAB
Universitat Autònoma de Barcelona

UAB

Universitat Autònoma de Barcelona

Genetics and Microbiology Department

Faculty of Biosciences

Mycobacteria factors responsible for modifying the antitumour activity in bladder cancer

SANDRA GUALLAR GARRIDO

Bellaterra, 2021

DOCTORAL THESIS

Programa de Doctorat en Microbiologia
Menció Doctor Internacional – International Doctoral Research Component
Departament de Genètica i Microbiologia
Universitat Autònoma de Barcelona
2021

Mycobacteria factors responsible for modifying the antitumour activity in bladder cancer

Sandra Guallar Garrido

Doctoral thesis to obtain the PhD in Microbiology by the Department of Genetics and Microbiology from Universitat Autònoma de Barcelona

Thesis director and Tutor   Doctorand

Dr Esther Julián Gómez   Sandra Guallar Garrido

Bellaterra, 2021

Als meus pares

ACKNOWLEDGEMENTS | AGRAÏMENTS

Desprès de tants anys són moltes les persones que d'una manera o una altra m'han ajudat en aquest procés tant dintre com fora del laboratori.

Primer de tot, m'agradaria agrair a la Dra Esther Julián l'increïble oportunitat que m'ha brindat per arribar fins aquí avui. Agrair des del primer moment en que va decidir agafar dos estudiants de grau enlloc d'un, que va confiar en mi per continuar durant el màster i finalment, acollir-me per fer el doctorat. Ella no només ha estat la meva directora i tutora de tesi, sinó que també ha sigut el meu recolzament incondicional durant tots aquests anys, i no només en ciència! Moltes gràcies Esther per haver confiat en mi, per ajudar-me a créixer en tots els aspectes de la meva vida, per compartir el teu temps i coneixement, la paciència i sobretot, la dedicació incansable en aquesta tesi. T'estaré sempre increïblement agraïda.

També donar les gràcies a la Dra Marina Luquin per la seva aportació en aquesta tesi, sense ella no hagués sigut la mateixa. Gràcies per compartir amb mi la teva experiència, per ensenyar-me a treballar amb lípids, pel teu esperit crític i, sobretot, per la teva pau i tranquil·litat que desprens dins i fora del laboratori.

Vull agrair a tot el laboratori, és una llista llarga, però absolutament tothom ha sigut imprescindible per fer aquesta feina. Des de la Dra Estela Noguera que em va acollir amb els braços ben oberts des del primer dia, tot i estar en ple caos de la tesi, i que només ara he pogut entendre. També per totes les hores que hem passat al laboratori, a l'estabulari i fora. Gràcies per totes les teves converses, i en definitiva, per la teva ajuda fins l'últim moment. Gràcies a la Dra Marta Llorens, mai oblidaré que tu em vas ensenyar a fer la meva primera cromato. També agrair a tots els d'estudiants que han estat al laboratori al llarg d'aquests anys: a la Mercè, l'Alba, la Júlia, la Marina, l'Elisenda i l'Anna, sempre us recordaré per la vostra ajuda i implicació. Natali, muchas gracias por ser tan cercana y por traernos un poquito de Equador aquí. Farny, tu has sigut LA estudiant de màster, la teva diversió, bogeries i riures al laboratori sense poder parar no els oblidaré mai, gràcies per tant. Gràcies per la vostra ajuda Irati i l'Arnau, sense dubte heu viscut els més estressants! I, sobretot, gràcies als compis de tesi, Marc, Víctor i Paula, han sigut molt moments al vostre costat, amb estrès i amb molta feina però també moltes tardes de desconnexió i diversió. Marc, vam començar a la vegada i cada cop queda menys, moltes gràcies per les hores de poyata i estabu. Víctor, muchas gracias por todos los consejos, por tu dedicación y perfeccionismo, por pasarte horas y horas mirando biofilms en microscopia y, sobretodo, por estar siempre ahí. Paula, ¿y tu? No tengo palabras para agradecerte todo lo que has hecho en estos años. Gracias por cosas tan tontas como obligarme a ir al SAF o sembrarme unos inóculos, como

ACKNOWLEDGEMENTS | AGRAÏMENTS

absolutamente todo, gracias por entenderme, apoyarme, estar ahí siempre, y por dejarlo todo por poder brindar por nosotras. Muchas, muchas gracias!

Moltes gràcies a les nenes de la uni Laies, Nuria i Martes, em sento molt privilegiada de seguir contant amb vosaltres. Podem dir que el grau de Micro ens ha dona coses molt macro! Núria gràcies pels teu positivisme i filosofia de vida; Marta gràcies per totes les tardes i nits de birres, jocs i riures. I a tu Marta, gràcies, gràcies i gràcies. Gràcies per ajudar-me a relativitzar les coses, per encabir les nostres quedades per fer-me desconnectar i per estar sempre al meu costat, ets molt gran! I a tu Iris, gràcies per aquestes tardes de desconnexió i estar sempre aquí, gràcies!

Com no podia ser diferent, moltes gràcies a la meva família per entendre que em perdés dinars, sopars i mil quedades familiars per estar fora, haver de pesar animals o haver d'escriure la ditxosa tesi. Gràcies al Padrí, Tati, Edu, Iñaki i Aleix per fer que cada visita a Botarell es convertís en una festa, i gràcies a la Meri per aquell viatge a Granada tant especial! Gracias yaya por estar ahí, por tu apoyo y por recordarme que puedo con todo y que todo se acaba. També moltes gràcies a la família política per fer-me sentir tant valorada i tractar-me sempre amb tant de carinyo.

Gràcies Tete, Míriam per estar al meu costat i ajudar-me quan ho necessito. I sobretot als nens, que sense saber-ho, et recarreguen d'energia amb un sol somriure.

Joel, i tu? Moltes gràcies pel teu amor i recolzament en aquesta carrera, per haver suportat preocupacions i plors quan un experiment no sortia o per celebrar la publicació d'un article. Gràcies per la teva ajuda alhora de fer un dibuix, un esquema o un text. Et prometo que aquesta és l'única tesi que faré a la meva vida!

I no podia acabar de cap altra manera que agraint als meus pares haver arribat fins aquí. Gràcies papa, mama per entendre que la nena volia ser científica i permetrem el luxe de marxar a Barcelona, per haver-me recolzat en cada decisió que he pres, per estar al meu costat cada dia durant aquest llarg camí, per entendre el meu estrès i fatiga, per anar allà on fes falta i sobretot, per deixar-me volar i ser la persona que soc ara. Perquè aquesta tesi em direu que l'he treballada jo, però és gràcies a vosaltres.

INDEX

Index of tables

Index of figures

ABSTRACT

The current treatment for non-muscle-invasive BC (NMIBC) patients consists of a tumour resection followed by intravesical instillation of the live form of *Mycobacterium bovis* BCG. Since 1990, *M. bovis* BCG is the preferred and most efficacious treatment regarding avoiding BC recurrence and progression that lead to an improvement of the survival rate of BC patients. Nonetheless, *M. bovis* BCG treatment has some limitations. Around 30 % of patients do not respond to *M. bovis* BG therapy, and about 70 % suffer side effects. Besides, 8 % of BC patients need to stop the treatment due to the severe impacts. Otherwise, different *M. bovis* BCG substrains, which vary in their lipidic content, are used indistinctively worldwide.

Looking for an efficacious and safe alternative, the antitumoral effect of the *Mycolicibacterium brumae* has been described. *M. brumae* is an environmental, non-pathogenic and fast-growing mycobacterium that showed similar antitumour activity than *M. bovis* BCG *in vitro* and *in vivo*. *M. brumae* inhibit tumour proliferation *in vitro* and induce a local immune response into the bladder and systemic immune response, favourable for tumour elimination *in vivo*.

One crucial issue is the culture media used for mycobacteria growth. Contrary to most research laboratories that use Middlebrook media to grow *M. bovis* BCG, *M. bovis* BCG is massively produced using Sauton medium due to not containing animal-derived components. Nowadays, the mechanism of action of *M. bovis* BCG and the antigens involved in its antitumoral effect are still unknown. Therefore, the culture media composition used to grow mycobacteria can modify its antigenic profile and, in turn, its antitumour effect, as shown when *M. bovis* BCG is used as a vaccine against tuberculosis. Thus, this thesis aims to evaluate the influence of culture media compositions and the antitumoral response triggered by *M. bovis* BCG or *M. brumae*. Initially, culture media composition was optimised for *M. brumae* growth using different culture media that differ on the amino acid source and glycerol concentrations. Then, the antigenic profile of *M. bovis* BCG and *M. brumae* grown in different culture media and their antitumoral effect *in vitro* and *in vivo* were analysed. Otherwise, a systemic immune response triggered by subcutaneous vaccination with *M. bovis* BCG or *M. brumae* before intravesical treatments was also evaluated in tumour-bearing mice.

M. bovis BCG and *M. brumae* require a specific composition to maximise their biomass production, although those compositions did not imply an increased antitumoral response *in vitro* and *in vivo*. Both mycobacteria species showed a different lipidic pattern depending on the culture media used for their growth, being the lipidic profile of *M. bovis* BCG corroborated in five *M. bovis* BCG substrains. *M. brumae* grown in Sauton A60 and *M. bovis* BCG grown in Sauton G15 triggered a better antitumoral response than the rest of the conditions. Finally, subcutaneous vaccination followed by intravesical treatment triggered a

more robust systemic immune response than the immune response triggered by the intravesical treatments alone.

In conclusion, culture medium composition impacts the antitumoral effect of *M. bovis* BCG and *M. brumae*. Moreover, vaccination with *M. brumae* or *M. bovis* BCG followed by intravesical treatment can be considered a boosting strategy to improve the outcomes of the intravesical treatment.

RESUMEN

El tratamiento actual para el cáncer de vejiga (CV) no músculo invasivo consiste en la resección del tumor seguida de instilaciones intravesicales de la forma viva de *Mycobacterium bovis* Calmette-Guérin (BCG). Des de 1990, *M. bovis* BCG es el tratamiento de elección y el más eficaz para evitar la recurrencia y progresión de la enfermedad, que conlleva a una mejora en la tasa de supervivencia de los pacientes con CV. No obstante, este tratamiento tiene algunas limitaciones. El 30 % de los pacientes no responden a la terapia con *M. bovis* BCG, y alrededor del 70 % de los enfermos sufren efectos adversos, haciendo que el 8 % de ellos se vean obligados a interrumpir el tratamiento. Además, distintas cepas de *M. bovis* BCG que difieren en el contenido lipídico son usadas indistintamente en el mundo.

En la búsqueda de una alternativa eficaz y segura, se ha descrito el efecto antitumoral de *Mycolicibacterium brumae*. *M. brumae* es una micobacteria ambiental, no patógena y de crecimiento rápido que mostró una actividad antitumoral *in vitro* e *in vivo* similar a *M. bovis* BCG. *M. brumae* es capaz de parar la proliferación tumoral *in* vitro, y además, induce una respuesta inmunitaria tanto local, en la vejiga, como sistémica, favorable para la eliminación del tumor *in vivo*.

Un tema crucial son los medios de cultivo utilizados para el crecimiento de las micobacterias. A diferencia de la mayoría de los laboratorios de investigación donde *M. bovis* BCG se cultiva en medios Middlebrook, para la producción a escala industrial se utiliza el medio Sauton ya que no contiene productos de origen animal. Actualmente, se desconoce el mecanismo de acción de *M. bovis* BCG y que antígenos están implicados en su actividad antitumoral. Motivo por el cual, la modificación del medio de cultivo utilizado para el crecimiento de las micobacterias podrá alterar su perfil antigénica y, en consecuencia, su efecto antitumoral, como ya se ha visto con *M. bovis* BCG cuando se usa como vacuna contra la tuberculosis. Por lo tanto, el objetivo de esta tesis consistió en evaluar la influencia de los medios de cultivo en la actividad antitumoral de *M. bovis* BCG o *M. brumae* crecidos en distintas formulaciones del medio Sauton en las que variaba la fuente de aminoácidos y la concentración de glicerol. Después se analizó el perfil antigénico de *M. bovis* BCG y de *M. brumae* crecidos en los diferentes medios de cultivo, y finalmente, se evaluó su actividad antitumoral *in vitro* e *in vivo*. Por otro lado, se analizó la respuesta inmunitaria sistémica desencadenada por una vacunación subcutánea con *M. bovis* BCG o *M. brumae* previa al tratamiento intravesical en ratones con tumor.

Se observó que *M. bovis* BCG y *M. brumae* requieren una composición específica de medio de cultivo para maximizar la biomasa obtenida, a pesar de que esta condición no siempre implicó una mejor actividad antitumoral *in vitro* e *in vivo*. Por otro lado, ambas micobacterias mostraron un perfil antigénico diferente en función del medio de cultivo usado para su crecimiento, siendo estas modificaciones en el perfil antigénico de *M. bovis* BCG corroboradas en cinco subcepas más. *M. brumae* crecido en Sauton A60 y *M. bovis* BCG crecido en Sauton G15 desencadenaron una respuesta antitumoral más eficiente.

Finalmente, la vacunación subcutánea previa al tratamiento intravesical desencadenó una respuesta sistémica más robusta que la producida por el tratamiento intravesical únicamente.

En conclusión, los medios de cultivo utilizados para el crecimiento de micobacterias muestran un impacto sobre la actividad antitumoral de *M. bovis* BCG y *M. brumae*. Además, la vacunación con *M. brumae* o *M. bovis* BCG, previa al tratamiento intravesical, puede ser considerada una estrategia de refuerzo para mejorar los resultados del tratamiento intravesical.

RESUM

El tractament actual pel càncer de bufeta (CB) no múscul invasiu consisteix en la resecció del tumor seguida d'instil·lacions intravesicals de la forma viva del *Mycobacterium bovis* Calmette-Guérin (BCG). Des del 1990, el *M. bovis* BCG és el tractament d'elecció i el més eficaç per evitar la recurrència i progressió de la malaltia, conduint a una millora de la taxa de supervivència dels pacients amb CB. No obstant, aquest tractament té algunes limitacions. El 30 % dels pacients no responen a la teràpia amb *M. bovis* BCG i al voltant del 70 % dels malalts pateixen efectes secundaris, fent que el 8 % d'ells hagin d'interrompre la teràpia. D'altra banda, diferents subsoques de *M. bovis* BCG que varien en el seu contingut lipídic, s'utilitzen sense distinció arreu del món.

En la recerca d'una alternativa eficaç i segura, s'ha descrit l'efecte antitumoral de *Mycolicibacterium brumae*. El *M. brumae* és un micobacteri ambiental, no patògen i de creixement ràpid amb una activitat antitumoral *in vitro* i *in vivo* semblant a la del *M. bovis* BCG. El *M. brumae* es capaç d'aturar la proliferació tumoral *in vitro*, i a més, indueix una resposta immune tant local, a la bufeta, com sistèmica, favorable per l'eliminació del tumor *in vivo*.

Un tema crític són els medis de cultiu utilitzats per al creixement dels micobacteris. A diferència de la majoria de laboratoris de recerca on el *M. bovis* BCG és crescut en medis Middlebrook, per la producció a escala industrial s'utilitza medi Sauton ja que no conté components d'origen animal. Actualment, es desconeix el mecanisme d'acció del *M. bovis* BCG i quin són els antígens implicats en l'efecte antitumoral. Per tant, la modificació del medi de cultiu utilitzat pel creixement dels micobacteris podria alterar el seu perfil antigènic i, en conseqüència, la seva resposta antitumoral, com ja s'ha vist amb *M. bovis* BCG quan s'utilitza com a vacuna contra la tuberculosi. Per tant, l'objectiu d'aquesta tesi va ser avaluar la influència dels medis de cultiu en l'activitat antitumoral del *M. bovis* BCG o del *M. brumae*. Primerament, es va optimitzar el creixement del *M. brumae* crescut en diferents formulacions del medi Sauton que variaven en la font d'aminoàcids i el contingut de glicerol. Després, es va analitzar el perfil antigènic del *M. bovis* BCG i del *M. brumae* crescuts en diferents medis de cultiu, i finalment, es va avaluar la seva activitat antitumoral *in vitro* i *in vivo*. D'altra banda, es va analitzar la resposta immunitaria sistèmica desencadenada per una vacunació subcutània amb el *M. bovis* BCG o el *M. brumae* prèvia al tractament intravesical en ratolins amb tumor.

Es va observar que el *M. bovis* BCG i el *M. brumae* requereixen una composició específica de medi de cultiu per maximitzar la biomassa obtinguda, tot i que aquesta condició no sempre va implicar una millor activitat antitumoral *in vitro* i *in vivo*. D'altra banda, ambdós micobacteris van mostrar un perfil lipídic diferent en funció del medi de cultiu utilitzat pel seu creixement, sent aquestes modificacions en el perfil lipídic de *M. bovis* BCG corroborades en cinc subsoques més. El *M. brumae* crescut en el Sauton A60 i el *M. bovis* BCG crescut en el medi Sauton G15 van desencadenar una resposta antitumoral més

eficient. Finalment, la vacunació subcutània prèvia al tractament intravesical va desencadenar una resposta sistèmica més robusta que la produïda pel tractament intravesical únicament.

En conclusió, els medis de cultiu utilitzats pel creixement de micobacteris mostren un impacte sobre l'activitat antitumoral de *M. bovis* BCG i *M. brumae*. A més, la vacunació amb el *M. brumae* o amb el *M. bovis* BCG, prèvia al tractament intravesical pot ser considerada una estratègia de reforç per millorar els resultats del tractament intravesical

.

ABBREVIATIONS

ATCC	American Type Culture Collection
A60	Sauton medium containing L-asparagine and 60 mL/L of glycerol
BC	Bladder Cancer
M. bovis BCG	*Mycobacterium bovis* bacillus Calmette-Guérin
BD	Becton & Dickinson
BSA	Bovine Serum Albumin
BSL	Biosafety Level
$CDCl_3$	Deuterate chloroform
CEEA	Comité de Ética de Experimentación Animal
CO_2	Carbon dioxide
ConA	Concanavaline A
CW	Cell Wall
CWE	Cell Wall Extract
CWS	Cell Wall Skeleton
DAT	Diacyl trehalose
DC	Dendritic Cell
DMEM	Dubelco's Modified Eagle's Medium
DMSO	Dimethyl Sulfoxide
DNA	Deoxyribonucleic acid
EAU	European Association of Urology
ELISA	Enzime-Linked Immunosorbent Assay
FBS	Fetal Bovine Serum
GAG	Glycosaminoglycans
GlcMM	Glucose Monomycolate
GPL	Glycopeptido lipid
GroMM	Glycerol Monomycolate
G15	Sauton medium containing 4 g/L of L-glutamate plus 15 mL/L of glycerol
G60	Sauton medium containing 4 g/L of L-glutamate plus 60 mL/L of glycerol
H	Healthy
^{1}H NMR	Proton Nuclear Magnetic Resonance
HK	Heat-killed
hpi	Hours post-infection
H&E	Hematoxylin and Eosin
Ig	Immunoglobuline
IL	Interleukin
ILC	Innate Lymphocyte Cells
IFN-γ	Interferon-γ
iv	Intravesical
LM	Lipomannan
LAM	Lipoarabinomannan
LB	Luria Bertoni
M. brumae	*Mycolicibacterium brumae*

MHC	Major Histocompatibility Complex
MK	Menakinone
MOI	Multiplicity of Infection
MTT	Thiazolyl blue tetrazolium bromide
NF-κβ	Nuclear Factor – κβ
NK	Natural Killer
NMIBC	Non-Muscle Invasive Bladder Cancer
NO	Nitric Oxide
NTM	Nontuberculous mycobacterial pathogens
OADC	Oleic-Albumine-Dextrose-Catalase
PB	Pentobarbital Buffer
PBS	Phosphate Buffered Saline
PDIM	Phtiocerol dimycocerosates
PE	Petroleum ether
PEC	Peritoneal Exudate Cells
PGL	Phenolic Glycolipid
PIM	Phosphatidylinositol mannosides
PLL	Poly-L-lisine
PMA	Phorbol 12-myristate 13-acetate
PTFE	Polytetrafluoroethylene
PUM	Phosphate Urea Magnesium sulphate buffer
OD	Optical Density
RPMI 1640	Roswell Park Memorial Institute 1640
RT	Room Temperature
sc	Subcutaneous
SD	Standard Deviation
SEM	Scanning Electron microscopy
SL	Sulfolipid
T^a	Temperature
TAT	Triacyl trehalose
TAMs	Tumour-associated macrophages
T_{EM}	Effector Memory CD4$^+$ T cells
TB	Tuberculosis
TBS	Tris-Buffered Saline
TDM	Trehalose dimycolate
TLC	Thin-layer chromatography
TLR	Toll-Like Receptor
TMM	Trehalose monomycoalte
TNF-α	Tumour Necrosis Factor-α
Treg	Regulatory T cells
TSA	Tryptic Soy Agar
vs	*versus*
WE	Wax Ester
WHO	World Health Organization

1 - INTRODUCTION

1.1 Mycobacteria

1.1.1.   Classification and diversity

Actinomycetales is an order formed by the families Mycobacteriaceae, Actinomycetaceae, Actinoplanaceae, Desmatophilaceae, Micromonosporaceae, Nocardiaceae, and Streptomycetaceae. Until 2018, the family Mycobacteriaceae only contained the genus *Mycobacterium*. Yet, an exhaustive study based on genetic and molecular characteristics developed in 2018 strongly suggests dividing the genus *Mycobacterium* into new five genera: *Mycobacterium, Mycolicibacterium, Mycolicibacter, Mycolicibacillus,* and *Mycobacteroides*[1].

Mycobacteria species are nonmotile, aerobic or microaerophilic rods from 1 to 10 μm of length [2]. They form rough or smooth colonies, and even some species can possess both morphologies when are grown on solid media at their optimal temperature of culture (from 25°C to 40°C) [3]. Besides, mycobacteria species have around 60-70% of guanine-cytosine in their desoxyribonucleic acid (DNA) [4].

They adopt a fuchsia colouration after performing a Zhiel-Nielsen stain, which permits differentiate mycobacterial species from the rest of the microorganisms. The primary dye, carbol-fuchsin, is retained into the cell wall of mycobacteria species after a destaining with acid alcohol. Consequently, mycobacteria species are also known as "acid-alcohol resistants" [5].

Until 2021, a total of 193 mycobacterial species have been described and validated (https://www.bacterio.net/genus/mycobacterium). Mycobacteria can be divided depending on their clinical relevance into 1) strict pathogens such as *Mycobacterium tuberculosis* complex or *Mycobacterium leprae* complex; 2) opportunistic and nontuberculous mycobacterial pathogens (NTM) such as *M. marinum*, which mainly infect immunosuppressed individuals; or 3) environmental mycobacteria that rarely or never cause disease, for instance, *Mycolicibacterium brumae* [6–8].

Environmental mycobacterial species account for up to 75% of the total described species. Because of the high versatility among species, Ernest Runyon proposed the first classification based on the growth rate and colony colouration in 1959 [9]. Accordingly, mycobacteria were divided into fast or slow-growing mycobacteria, whether they need one week or more to grow on solid and synthetic media; and into 1) photochromogens, whether they synthesise pigments when grown in the absence of light; 2) scotochromogens when species only synthesise pigments in the presence of light, or 3) nonphotochromogen when no pigmentation was observed, independently of growing in the presence of light or not.

Introduction

The classical classification of mycobacterial species based on the rate of growth, the presence/absence of pigmentation, the optimal temperature, biochemical tests, and other parameters are still required for describing a new species. Nowadays, this information needs to be supplemented with genome sequencing, assembly and mapping, [10].

1.1.2. Mycobacteria cell wall organisation

Mycobacteria are mainly characterised by their complex, highly hydrophobic and unique cell wall. Actually, mycobacterial cell envelopes are formed by up to 40% of lipids from their total cell dry mass compared to the 20% recorded in Gram-negative bacteria [11]. Several models have been suggested to unravel the structure of the mycobacterial cell envelope. However, the most recent model divides the envelope into four different layers [12]:

1) The conventional plasma membrane.
2) The periplasm.
3) The cell wall skeleton. It is formed by peptidoglycan covalently linked to arabinogalactan esterified by mycolic acids and a mycomembrane. Mycomembrane, also known as the outer membrane, is divided into the inner and the outer leaflet. While mycolic acids are contained in the inner leaflet, the outer leaflet possesses a wide range of lipids unbound or bound to lower layers.
4) The outermost layer. It is formed by a matrix of glucan that contains proteins, polysaccharides, and few lipids. It is also called a capsule-like structure in pathogenic species.
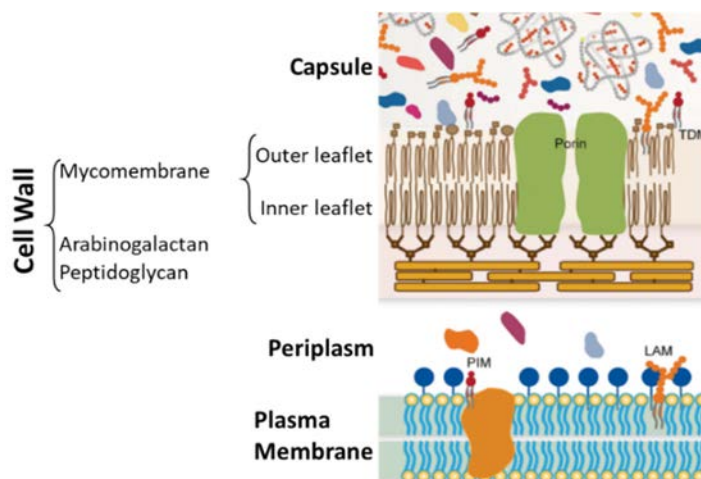
Figure 1. **Proposed model of the mycobacterial cell envelope.** The cell envelope possesses four different layers (plasma membrane, periplasm, cell wall and the capsule). Each layer is composed of several lipids. The plasma membrane contains phospholipids such as phosphatidylinositol mannosides (PIM) or lipoarabinomannan (LAM). The periplasm is mainly formed of proteins. The cell wall skeleton is made of peptidoglycan, arabinogalactan and mycolic acids, which are part of the inner leaflet of the mycomembrane. In the outer leaflet of the mycomembrane, there are several lipids, such as trehalose dimycolate (TDM). The capsule layer is a matrix of small lipids and proteins. Adapted from Daffé, 2019 [13].

1.1.3. Relevant mycobacterial cell wall components

As above mentioned, mycobacteria species are characterised by their complex cell wall formed by several lipids, which can differ among species and substrains. The most common lipids and their characteristics are assessed in this section and illustrated in Figure 2.

1.1.3.1 Mycolic acids

Mycolic acids have been found in several bacteria species, although their length differs among genera. For instance, mycolic acids from C*orynebacterium* are formed by 22-38 carbon atoms, mycolic acids from *Nocardia* contain 46-60 carbon atoms, and mycolic acids from *Mycobacterium* are the longest, having 60-90 carbon atoms [14].

Mycolic acids are the main characteristic of the mycobacterial cell envelope and are present in the inner leaflet of the mycomembrane. They are mostly found esterifying the pentaarbinofuranosyl units of arabinogalactan. Yet, they can also be found unbound as an ester of trehalose mono- and di-mycolates (TMM, TDM), glycerol monomycolate (GroMM) or glucose monomycolate (GlcMM) [15].

Mycolic acids structure corresponds to 3-hydroxy 2-alkyl-branched long-chains fatty acids [R_1-CH(OH)-CH(R_2)-COOH]. R_1 is a long aliphatic chain formed by 50-56 carbon atoms that contain different functional groups. Depending on the functional groups present on R_1, also called meromycolic chain, seven types of mycolic acids have been described (I-VII): α-, α'-, methoxy-, κ-, epoxy-, carboxy- and ω-1-methoxy- mycolate, respectively. Functional groups also seem to influence mycolic acid folding. For instance, α-mycolate from *M. tuberculosis* would be fully extended, methoxy-mycolate would be folded, and κ-mycolate would be fully folded. Moreover, double bonds or cyclopropane rings forming part of the mycolic acids can possess *cis*- and/or *trans* configuration [16]. R_2 is a short aliphatic chain formed by 22-26 carbon atoms [17].

Mycolic acid I has been described in all mycobacteria species, while the presence and combination of the other mycolic acids have been considered species-specific. Identifying the mycolic acid pattern by thin-layer chromatography, gas chromatography, mass spectrometry, nuclear magnetic resonance spectroscopy, or other techniques has been helpful to classify mycobacterial species. Nowadays, considering that several mycobacteria species can share the same mycolic acid pattern, other methods such as DNA sequencing are required to identify mycobacterial species [10].

Introduction

The mycolic acid pattern of some mycobacteria species is summarised in Table 1 [18].

Table 1.   The mycolic acid pattern of mycobacteria

Mycobacteria	Mycolic Acid Pattern						
	I	II	III	IV	V	VI	VII
Mycolicibacterium brumae	X	-	-	-	-	-	-
Mycolicibacterium fallax	X	-	-	-	-	-	-
Mycobacteroides chelonae	X	X	-	-	-	-	-
Mycobacteroides abscessus	X	X	-	-	-	-	-
Mycobacterium bovis BCG (Early Strains)	X	-	X	X	-	-	-
Mycobacterium gordonae	X	-	X	X	-	-	-
Mycobacterium tuberculosis	X	-	X	X	-	-	-
Mycobacterium marinum	X	-	X	X	-	-	-
Mycobacterium bovis BCG (Late strains)	X	-	-	X	-	-	-
Mycobacterium leprae	X	-	-	X	-	-	-
Mycolicibacterium phlei	X	-	-	X	X	-	-
Mycobacterium avium	X	-	-	X	-	X	-
Mycobacterium lepraemurum	X	-	-	X	-	X	-
Mycolicibacterium chubuense	X	X	-	X	-	X	-
Mycolicibacterium gilvum	X	X	-	X	-	X	-
Mycolicibacterium vaccae	X	X	-	X	-	X	-
Mycolicibacterium obuense	X	X	-	X	-	X	-
Mycolicibacterium alvei	X	-	-	-	-	-	X

1.1.3.2 Phthiocerol dimycocerates (PDIM)

PDIMs are formed by phthiocerol fatty acid plus two units of mycocerosic acid. They are one of the most abundant non-covalently bound lipids found in the outer leaflet of the mycomembrane. Their presence is restricted to slow-growing mycobacteria such as *M. tuberculosis, M. bovis, M. africanum, M. leprae* or *M. marinum* [19].

Several roles have been associated with PDIM. Firstly, PDIMs are crucial for giving structural support to the cell envelope of mycobacteria [20], which is highly related to their role as cell wall permeability barrier [21]. PDIM also favours macrophages invasion, modulates the host immune response during infection, and triggers phagosomal rupture and host cell apoptosis [22–24].

Moreover, PDIM might also be hiding several pathogen-associated molecular patterns (PAMPs) present in the mycobacterial cell wall, which would inhibit Toll-like receptor (TLR)/Myd88 signalling [24]. Besides, the spreading of PDIM into host epithelial membranes has been associated with increased infectivity and evasion of the immune system via Myd88

[25]. Finally, the presence of PDIMs has also been related to protection against reactive nitrogen intermediates produced by macrophages [26] and reduced macrophage recruitment to the site of *M. tuberculosis* infection [27].

1.1.3.3 Phenol glycolipids (PGLs)

PGLs are formed by a lipidic core composed of a phtiocerol and phenolphtiocerol esterified by polymethyl-branched fatty acids. PGLs have a molecule precursor in common with PDIMs. PGL from different mycobacterial species can present specific structures, and their accumulation in the outer leaflet of the mycomembrane can also differ [28].

The presence of PGLs is mainly restricted to opportunistic and pathogenic mycobacteria species such as *M. leprae, M. marinum, M. bovis* or *M. tuberculosis.* However, not all strains from the *M. tuberculosis* complex possess PGL, and the opportunistic *Mycobacterium gastri* does. Besides, some *Mycobacterium bovis* Calmette-Guérin (*M. bovis* BCG) substrains lost the ability to synthesise PDIM and/or PGL. For instance, *M. bovis* BCG-Moreau or -Glaxo synthesise neither PDIM nor PGL, and *M. bovis* BCG-Tice can produce PDIM but not PGL (see Figure 10).

PGL play a critical role in mycobacterial virulence. For instance, the presence of PGL-1 on *M. leprae* induces the secretion of nitric oxide (NO) that triggers nerve damage [29], and the presence of PGL in the *M. marinum* cell wall was related to an increased bacterial virulence [30]. Besides, high amounts of PGL and triacylglycerols (TAGs) expressed in *M. tuberculosis* were associated with a hypervirulent strain, as shown in the W-Beijing linage [19].

Some studies relate the great content of PGL in some *M. tuberculosis* clinical isolates with reduced phagocytosis by macrophages [31]. PGL can also inhibit TLR-2 to inhibit the release of proinflammatory cytokines[32], or the absence of PGL has also been related to a decreased Th17 response [33].

Contradictory results are also found regarding the triggered immunogenicity by *M. bovis* BCG as a vaccine against TB. Despite *M. bovis* BCG-Pasteur lacking PDIM and PGL seemed to trigger similar immunogenicity [34], other studies highlighted a reduced efficacy of *M. bovis* BCG mutant lacking PDIM and PGL [19].

Introduction

1.1.3.4 Trehalose-6,6-monomycolate (TMM)

Trehalose-6,6-monomycolate (TMM) is formed by trehalose esterified by one mycolic acid orientated to the cell plasma membrane [28]. TMM can be found linked to the mycolyl arabinogalactan peptidoglycan or used as a precursor to form trehalose dimycolates (TDM) [35]. Although the primary function of TMM seems to be giving structural support to the cell wall membrane[36], it can also induce the release of inflammatory cytokines such as TNF-α [37].

1.1.3.5 Trehalose-6,6-dimycolate (TDM)

Trehalose-6,6-dimycolate (TDM), previously known as *cord factor*, is formed by one trehalose esterified with two mycolic acids. This molecule triggers the production of proinflammatory cytokines such as TNF-α, IL-1β or IL-6 [38]. However, proinflammatory cytokines triggered by TDM can vary among species due to differences in the TDM composition, the presence of methoxy and k- groups of the meromycolic chain [14,39], or depending on cyclopropane rings [40].

1.1.3.6 Glycerol monomycolate (GroMM)

GroMM is a molecule found in the outer leaflet of the mycomembrane, and it is formed by one molecule of glycerol esterified by a mycolic acid, independently of the functional group. It was initially described in *M. tuberculosis* or *M. bovis* BCG, but it is present in most of the mycobacterial species [41].

GroMM is considered a stimulatory molecule able to trigger an increased infiltration of polymorphonuclear cells, robust T cell response and proinflammatory cytokines [42,43]. However, a Th2 response has also been described for GroMM in guinea pigs [44]. In fact, the immunostimulatory effect of GroMM could be modified by several factors such as the mycolic acid forming part of the molecule, mycolic acid folding, mycolic acid length, or mycolic acid conformation (*cis-* or *trans-* conformation). For instance, GroMM formed by α-mycolate (α-GroMM) seemed to facilitate the interaction with dendritic cells receptors triggering a faster immune response than GroMM containing κ-mycolate (κ -GroMM) [45]. However, liposomes containing κ-mycolic acids delayed tumour growth more efficiently than liposomes with α- or methoxy- mycolic acid.

When the length of mycolic acids of GroMM was analysed, it seems to modify the glycerol position required for the interaction with the receptor present on T-cells, crucial for its immunogenicity [41]. Otherwise, *cis-* conformation was associated with an inflammatory response, contrary to the *trans-* conformation that triggered an anti-inflammatory response [46].

After blocking GroMM-specific T cells from peripheral blood of latently TB infected or PPD+ patients with anti-Cd1a or -Cd1b, the immune response was abolished. Therefore, GroMM is presented to T cells through Cd1 molecules [41,43].

In general, few studies analyse the GroMM-triggered response, and further research is required to decipher the molecule modifications that alter its immunogenicity.

1.1.3.7 Sulfolipids (SLs)

SLs are sulphated acyl trehaloses described in *M. tuberculosis* and considered important virulence factors. SL-1 is the principal SL that inhibits mitochondrial oxidative phosphorylation, prevents the fusion of phagosome-lysosome, perpetuating the mycobacteria survival inside macrophages, and modulates the cytokine release of neutrophils and human monocytes [47]. SLs can act as TLR2 antagonists inhibiting the formation of TLR2/TLR1 and TLR2/TLR6 heterodimers that suppress the macrophage activation and, therefore, inhibit the immune response [48].

1.1.3.8 Diacyltrehalose (DAT) and Triacyltrehalose (TAT)

Diacyltrehalose (DAT), triacyltrehalose (TAT) and pentaacyl-trehalose (PAT) consist of trehalose esterified with two, three or five fatty acids, respectively. Acyltrehaloses are located on the outer layer of the cell envelope, noncovalently linked to peptidoglycan. They have been described in mycobacteria species such as *M. tuberculosis* or *M. fortuitum.* Although their function is still unclear, DATs and PATs seem to have a clear impact on the composition of the *M. tuberculosis* envelope. Besides, they can interfere in the mycobacteria uptake inhibiting mycobacteria recognition by phagocytic host cells [49]. Other studies suggest that DAT could also inhibit the release of proinflammatory cytokines and inhibit the proliferation of T cells by the release of IL-10 in a murine model [50].

1.1.3.9 Lipooligosaccharides (LOS)

LOSs is a glycolipid formed by a poly-O-acylated trehalose core, glycosylated by one or more oligosaccharide units. LOSs are surface-exposed glycolipids that were initially found in *M. kansasii* and *M. smegmatis.* Then, they have been identified in other mycobacteria species. Remarkably, not all *M. tuberculosis* complex strains contain LOSs [51]. LOSs are considered highly antigenic molecules. For instance, the absence of LOSs in *M. marinum* has been associated with a deficiency in entering macrophages, sliding motility and biofilm formation motility [51,52]. Additionally, the presence of LOS favoured the accumulation of proteins in the mycobacterial cell envelope of *M. marinum* [53].

1.1.3.10 Glycopeptidolipids (GPL)

GPL are present in the outer leaflet of non-tuberculous mycobacteria. In some species such as *M.* smegmatis, *M. avium* or *M. abscessus,* GPL structure consists of a lipopeptide core (D-Phe-D-allo-Thr-D-Ala-L-alaninol) esterified by a fatty acyl chain, formed by 28 carbons bound to the alaniol. However, the GPL structure of *Mycobacterium xenopi* contains a tetrapeptide core with two serines (L-Ser-L-Ser-L-Phe-D-allo-Thr), esterified by a fatty acyl chain formed by 12 carbons [54].

GPL function has been related to colony morphology, motility, biofilm formation, among others. For instance, *M. smegmatis* without or low GPL content showed a rough morphotype, increased cell hydrophobicity and cell aggregation [55]. While *M. smegmatis* containing GPL shows smooth morphotype with short cells that did not survive as long as *M. smegmatis* rough morphotype in J774 macrophages [56]. Similarly, *M. abscessus* smooth morphotype possess GPL. However, sequential passages of the smooth morphotype lead to rough colonies characterised by a decreased amount of GPL. Then, *M. abscessus* rough morphotype can form cords and has increased virulence [57,58].

Finally, differences in the terminal sugar in the oligosaccharide moiety enable the identification among *M. avium* serovars [59].

1.1.3.11 Lipomannan (LM) and Lipoarabinomannan (LAM)

LM are lipoglycans of high molecular weight structurally similar to PIM, yet formed by a phosphatidylinositol with 21 to 34 mannose residues. LM activates Myd88 via TLR2 in macrophages, which trigger a strong secretion of proinflammatory cytokines such as TNF-α or IL-12. However, Quesniaux *et al.* described that LM from *M. bovis* BCG could also trigger an anti-inflammatory effect. It was hypothesised that other receptors might recognise different structural motifs of LM [60].

LAM is formed by a mannan core branched with a polymer that contains arabinan chains [61]. Additionally, some mycobacteria species contain capping motifs at the end of the arabinan chains, which classify LAM into three groups: 1) LAM containing mannosyl caps (ManLAM), present in pathogenic species such as *M. tuberculosis* or *M. kansasii* [62], 2) LAM with phosphor-myo-inositol caps (PILAM) found, for instance, in *M. smegmatis* and 3) non-caped LAM, called araLAM present in *M. chelonae*, for instance [63].

It is well known that LAM can activate the innate immune response inducing cytokine production by macrophages and dendritic cells (DC). Several receptors such as TLRs or C-type lectins could be involved in activating those innate immune cells. Specifically, in the case of ManLAM, it can activate macrophages and DC through the interaction with a C-type lectin called Dectin-2, present on the surface of both immune cells, but not through TLR2 or TLR4 [54].

Moreover, LAM can activate CD1-restricted T cells through the interaction with CD1-b expressed in antigen-presenting cells such as DCs. This interaction triggers CD1-restricted T cell activation, proliferation and secretion of proinflammatory cytokines [54]. LAM also modulates the immune response through B cells by producing specific antibodies against LAM, synthesised after *M. bovis* BCG vaccination or *M. tuberculosis* infection [64].
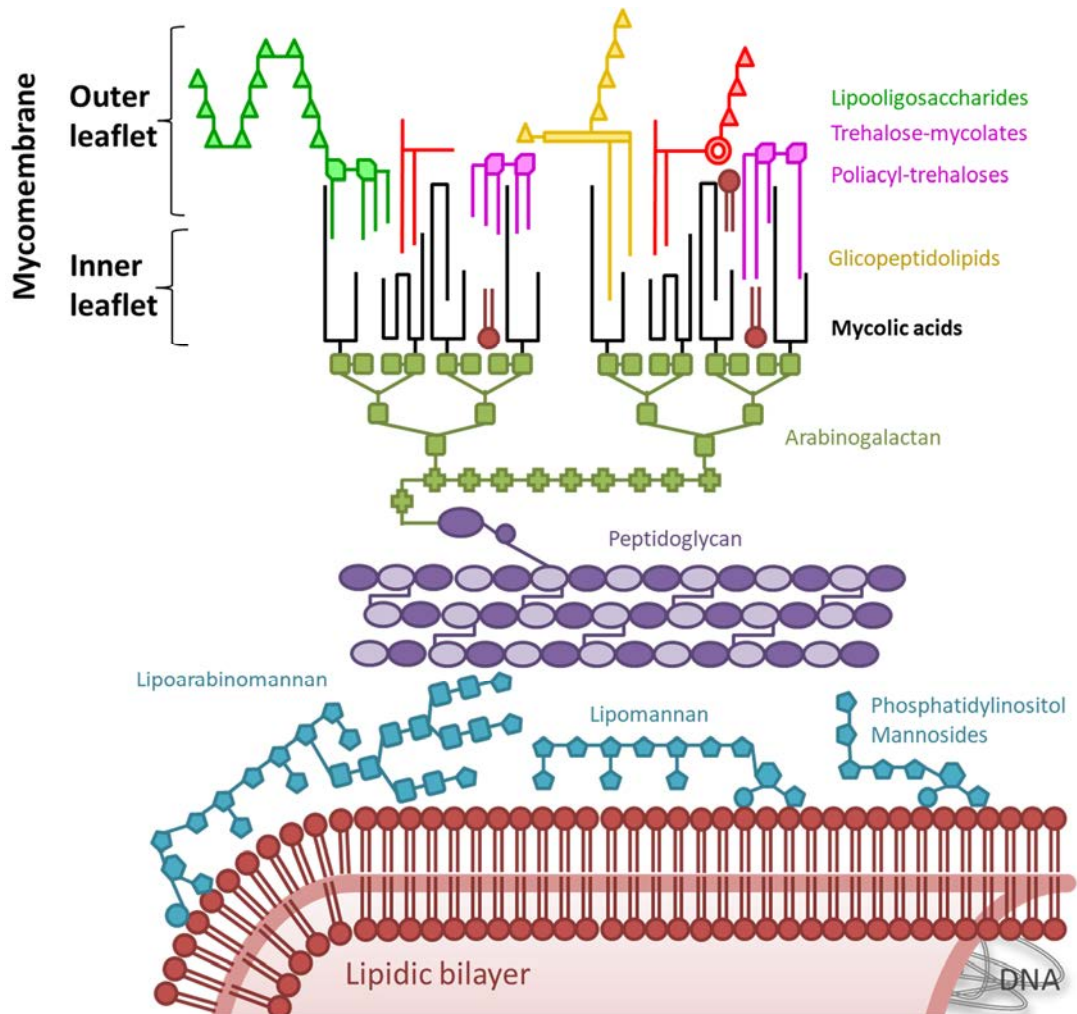
Figure 2. **Schematic representation of mycobacteria cell wall components.** Modified from Noguera-Ortega et al. [65]

1.1.3.12 Menaquinones (MK)

Menaquinones are the most common isoprenoid lipoquinones among mycobacterial species, being crucial in respiratory processes. The predominant structure of menaquinone in mycobacteria species contain nine isoprene units, identified as MK-9 [51]. However, other quinones have been described, such as sulfomenaquinone in *M. tuberculosis* or non-isoprenoid quinone in *M. avium* [16,66,67].

1.1.3.13 Phosphatidylinositol (PI) and Phosphatidylinositol mannosides (PIMs)

PI consists of diacylglycerol and a phosphodiester linked to an inositol ring formed by a 6 carbon polycyclic alcohol [61], which is covalently attached to the plasma membrane. PI reduction compromised *M. tuberculosis* viability, while its presence in the *M. tuberculosis* cell wall triggered high binding to macrophages [68].

Moreover, PI can be covalently attached to mannose residues (1-6), generating PIMs (PIM$_1$-PIM$_6$). PIMs are a family of glycolipids that can be found either in the inner leaflet covalently bound to the plasma membrane, or unbound forming part of the outer leaflet of the mycomembrane [61]. According to several studies, when *M. tuberculosis* or *M. smegmatis* infect macrophages, PIMs can intercalate into membrane phagosome, difficulting its maturation and, therefore, perpetuating mycobacteria survival [69]. Otherwise, PIMs can also inhibit host inflammatory responses via TLR-4 [70].

1.1.4. Mycobacteria metabolism

The slow growth of mycobacteria species has limited understanding the mycobacterial metabolism. However, advances in mycobacteria manipulation, genomics and bioinformatics triggered an increasing knowledge of enzymes implicated in the biosynthesis of the primary cell components. Moreover, most of the studies are focused on *M. tuberculosis* and its carbon metabolism processes [71–75]. Nowadays, the importance of both carbohydrates and fatty acids in the survival of other mycobacteria species has also been assessed.

1.1.4.1 Carbohydrate metabolism

Although several carbon sources such as glucose, mannose, fructose or galactose can be exploited by mycobacterial species [74,76–78], glycerol is the prefered carbon source used to grow mycobacterial species *in vitro* because it leads to maximal growth rates and yields [74,79]. Glycerol can be fastly assimilated, probably due to a presumed glyceroporin

described in some mycobacteria species such as *M. smegmatis,* facilitating glycerol diffusion through the mycobacterial cell wall [80].
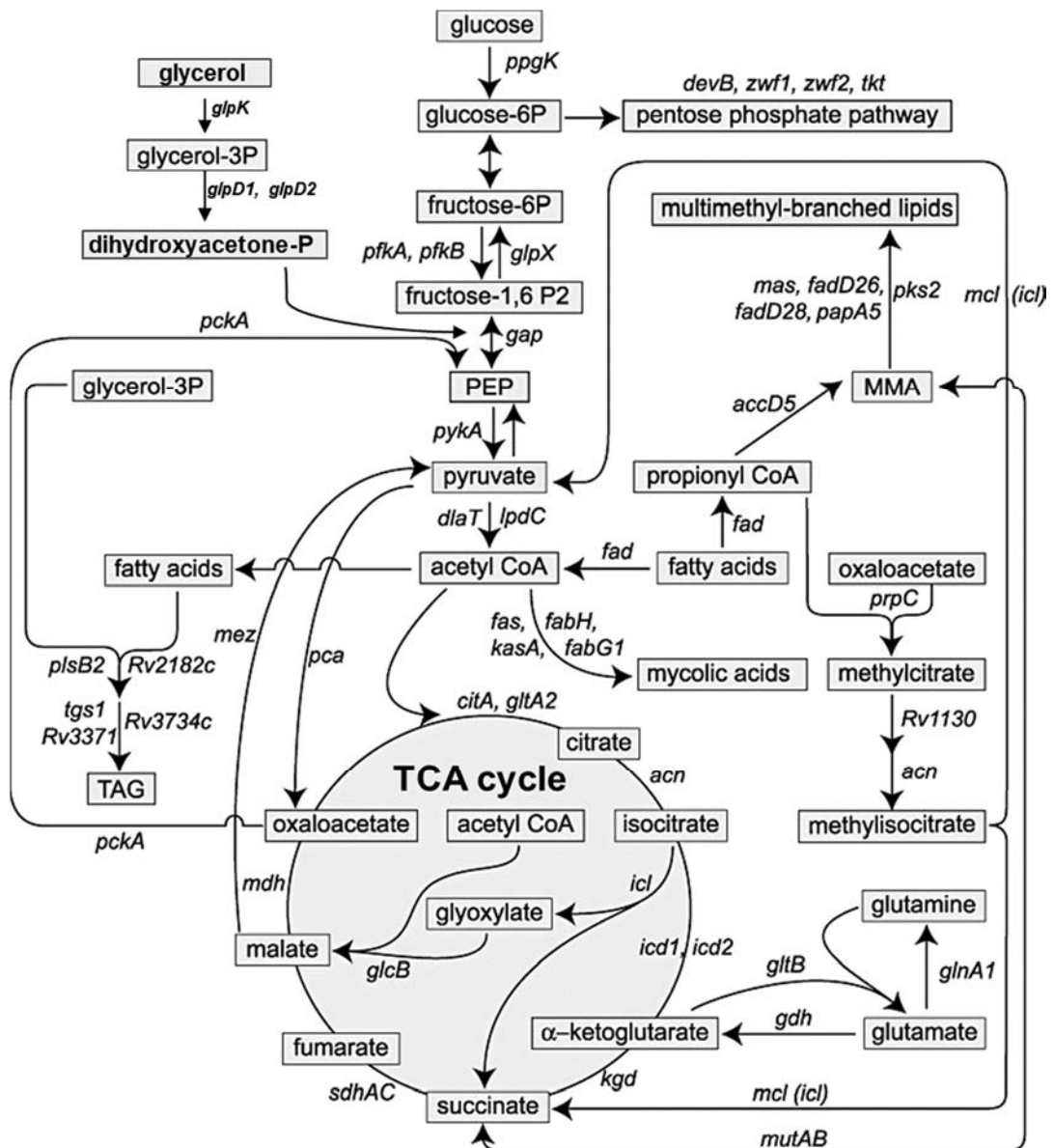
Figure 3. **Schematic representation of the pathways involved in central and lipid metabolism of *M. tuberculosis.*** PEP, phosphoenolpyruvate; MMA, methylmalonyl-CoA; TAG, triacylglycerol; TCA, tricarboxylic acid cycle. Lines may represent one or multiple reactions in a pathway. Gene symbols are shown next to the reactions. Modified from Shi *et al.* (2010) [78] and supplemented with Baughn *et al.* (2013) [74].

41

Introduction

According to glycerol metabolism studied in *M. tuberculosis* (Figure 3), when glycerol is incorporated into mycobacterial cells, it is converted to glyceraldehyde-3-phosphate (G3P).

Then, G3P is converted to dihydroxy-acetone phosphate (DHAP), and DHAP to phosphoenolpyruvate (PEP). PEP triggers the formation of pyruvate. Interestingly, some species such as *M. bovis*, *M. microti* or *M. africanum* require the addition of pyruvate into the medium due to a single nucleotide polymorphism in the gene encoding pyruvate kinase (*pykA*), which synthesises pyruvate from G3P. However, the mutation was reverted during *M. bovis* passages to obtain *M. bovis* bacillus Calmette-Guérin (BCG) [81].

Then, pyruvate evokes in Acetyl-Coa that enters into the tricarboxylic acid (TCA) cycle to catalyse ATP [74,78]. In the case of *M. bovis* BCG growing in a culture medium containing glycerol, a similar process has also been described [12].

Glycerol metabolism also implies the synthesis of lipids for mycobacterial cells. Once glycerol is converted to G3P, G3P can be acylated to form phosphatidic acid (PA). PA generates diphosphate-diacylglycerol (CDP-DAG), which is a precursor for the biosynthesis of phospholipids (PLs) [82]. For instance, CDP-DAG serves as a precursor of PI, PIMs, LM and LAM [83].

The product of glycerol glycolysis, Acetyl-CoA, can be carboxylated to obtain malonyl-CoA. Later, malonyl-CoA is condensed with an acyl-CoA to form β-ketoacyl-ACP. β-ketoacyl-ACP is elongated through two fatty acid synthases (FAS-I and FAS-II). Specifically, FAS-I generates fatty acids of 16-18 carbons and 24-26 carbons. Therefore, FAS-I will synthesise the α-branch of mycolic acids.

FAS-II elongates fatty acids formed by 12-16 carbons, synthesising the long meromycolic chains of mycolic acids [14]. Additionally, fatty acids of 16-20 carbons can be either extended to create phthiocerol or extended and methylated to synthesise mycocerosic acids. The esterification of both molecules synthesises PDIM. Otherwise, the esterification of one phenolphthiocerol and one mycocerosic acid trigger PGL production [30,84].

Besides, catabolism also involves the formation of triacylglycerol (TAGs). TAGs are formed after the addition of a fatty acyl-CoA to a diacylglycerol (DAGs). However, DAGs can be synthesised *de novo* or obtained after the dephosphorylation of PA. Remarkably, TAGs synthesis implies the downregulation TCA cycle, rerouting FASI products, and the DAG consumption [85]. Once synthesised, TAGs are found in lipid droplets present in the cytoplasm or/and accumulated in the cell wall of the mycobacteria [86,87]. Finally, the catabolism of glycerol has also been intimately related to the synthesis of other non-conventional lipids such as GroMM [44].

As above mentioned, other carbon sources can also be metabolised similarly to glycerol. For instance, glucose can be converted to fructose-6-phosphate, which is introduced to the

glycolysis pathway generating acetyl-CoA. Then, acetyl-CoA can be used to obtain energy or to create new molecules.

1.1.4.2 Nitrogen metabolism of mycobacteria

Contrary to carbohydrate metabolism, few studies have been performed to analyse the nitrogen metabolism of mycobacteria. In any case, the majority of studies are done on *M. tuberculosis.*

Amino acids are the preferred nitrogen source for mycobacteria species, yet they can also use inorganic sources such as ammonium [76]. Although *M. tuberculosis* can use all 20 amino acids, *M. tuberculosis* grown on L-glutamate or L-asparagine produces more biomass than grown on glutamine or asparagine [88]. Remarkably, an excess of amino acids triggers their accumulation into *M. tuberculosis* cytoplasm, leading to an increased cell size which may reflect the medium composition [88].

Nevertheless, not all mycobacteria species behave equally. For instance, when Agapova *et al*. compared the growth of *M. tuberculosis* and *M. smegmatis* growing in culture media containing several sources of amino acids, different amounts of biomass were achieved at the end of the experiment by both mycobacterial species. This result could indicate changes in nitrogen metabolism assimilation among them [88]. Besides, differences were also found in gene expression when *M. smegmatis* grew in different nitrogen compounds and concentrations In fact, transcriptional factors that regulate ammonia and nitrate uptake in other bacterial species have not been detected in *M. tuberculosis* [89].

One of the most studied proteins involved in nitrogen metabolism is the protein kinase G (PknG), which have a similar function in *M. tuberculosis, M. bovis* BCG and *M. smegmatis.* PknG is responsible for glutamine/L-glutamate homeostasis through the phosphorylation of glycogen accumulation regulator A (GarA). It is highly activated by an external supply of, mainly, L-glutamate and aspartate, but also by L-asparagine and glutamine or other stimuli. Moreover, carbon sources like glycerol can also trigger PknG activation. When PknG activity is low, unphosphorylated GarA activates the glutamate catabolising enzyme (GOGAT) to synthesise L-glutamate. Otherwise, when external stimuli stimulate PknG activity, GarA is phosphorylated and activates the glutamate dehydrogenase (GDH) to trigger glutamate catabolism. Therefore, GDH is essential to use L-glutamate as the only amino acid source (Figure 4) [12,90–92].
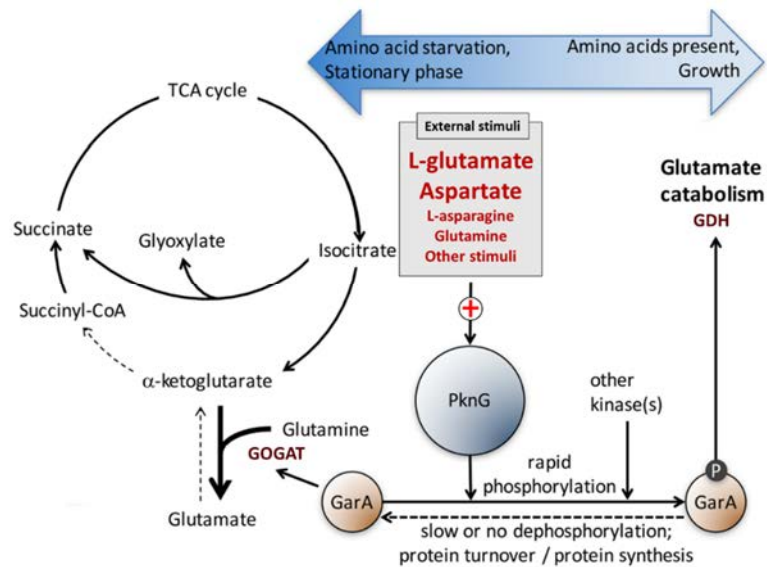
Figure 4. **A proposed model linking the Tricarboxylic Acid Cycle (TCA) with amino acid metabolism.** GOGAT: glutamate catabolising enzyme, GDH: glutamate dehydrogenase, GarA: glycogen accumulation regulator A, P: phosphorylation, PknG: protein kinase G. Modified from Rieck *et al.* (2017) [90].

Although the primary function of L-glutamate is as a nitrogen donor, other critical tasks have been described in the lifestyle and pathogenesis of *M. tuberculosis.* For instance, L-glutamate can serve as a carbon source when converted to α-ketoglutarate and be incorporated into the TCA cycle [92].

Otherwise, L-asparagine or aspartate can also be uptaken through a membrane transporter. The conversion of L-asparagine to aspartate generates ammonia, which is considered a virulence factor. Ammonia can alkalise the phagosome and, therefore, inhibits the phagolysosome fusion and maturation [92]. Otherwise, L-asparagine can also be quickly converted to L-glutamate.

Finally, *M. bovis* BCG GDH-deficient diminished its growth when cultured in high levels of asparagine or aspartate. It suggests that GDH is also necessary for asparagine metabolism [91,92].

1.1.4.3 Lipid metabolism of mycobacteria

It is further known the ability of mycobacterial species to accumulate neutral lipids in the form of lipid bodies in their cytoplasm. Lipid bodies are mainly formed by either TAGs and/or wax esters (WE). Besides, mycobacteria can also accumulate substantial amounts of DAGs and TAGs in the outer mycomembrane [85].

The exact causes that induce the formation of lipid bodies are still undeciphered. However, TAGs formation seems to be triggered in stress conditions [93]. Some stress conditions could be an elevated ratio of carbon:nitrogen in the culture media, the change of bacteria into a non-replicative state or starvation conditions, low nutrient availability, acidic pH in the culture medium, or low oxygen or high CO_2 concentration in the environment [78,85,94,95].

Remarkably, culture medium composition has a clear impact on TAGs formation and characteristics. For instance, *M. smegmatis* grown on different culture media produce TAGs formed by different fatty acids [96].

The primary function of TAGs is carbon and energy storage. However, TAGs accumulation have further implications. Mycobacteria can reduce their growth which can lead to antibiotic resistance [85]. Accordingly, *M. smegmatis, M. marinum, M. fortuitum* or *M. bovis* BCG containing lipid droplets showed increased resistance to antibiotics [97]. Besides, TAGs enable mycobacteria to persist during dormancy and also exit from the nonreplicating state [98].

Not only the factors triggering lipid bodies formation are unknown, but also their formation. One of the most plausible hypothesis consists of the aggregation of tiny lipid droplets present on the membrane to form small aggregates. When lipid aggregates are released to the cytoplasm, lipid-prebodies are produced. Finally, the following binding of small lipid bodies to lipid-prebodies generate mature lipid bodies (Figure 5) [85,99].

Otherwise, lipid bodies can also be degraded whenever are required by the microorganism. The energy produced from the oxidation of TAGs is twice the identical weight of protein or carbohydrates[85]. TAGs are hydrolysed to make available fatty acids that will be assimilated by β-oxidation, which provides acetyl CoA and energy for the glyoxylate pathway [78]. Therefore, TAGs can serve as a source of carbon and/or for being incorporated into newly synthesised lipids [87].

Lipid metabolism also differs among mycobacteria species. For instance, tuberculous mycobacteria can metabolise cholesterol, but few NTM can use it [100]. *M. tuberculosis* can exploit host-derived fatty acids to grow, being cholesterol the most common lipid. Then, cholesterol is degraded to propionyl-CoA, which synthesise cell wall lipids such as PDIM, SL-1, PAT or LOS [25,28]. Moreover, an excess of propionyl-CoA inside mycobacteria can induce the formation of new TAGs again [104,105].

45
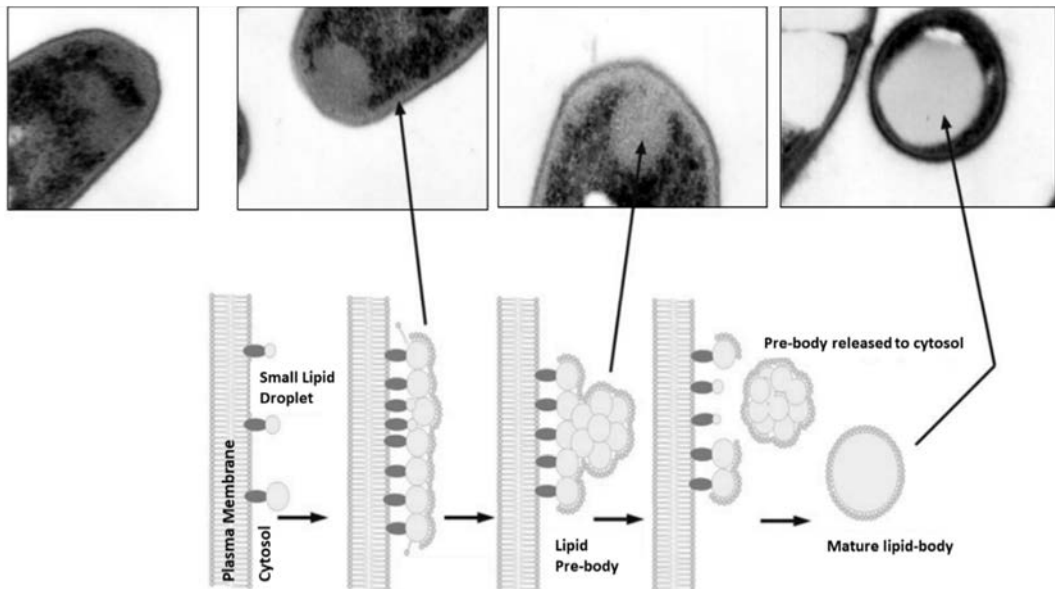
Figure 5. **Hypothetical stages for the formation of neutral lipid bodies in bacteria.** Modified from Wälterman et al. (2005) [101].

1.1.5. Cell wall remodelling depending on the mycobacteria stage

Mycobacteria cell wall is dynamic and heterogeneous, yet its components depend on the species, the environmental signals and lifetime. Nowadays, we have just started to understand how mycobacteria can remodel their cell envelope according to environmental conditions, which modify their interaction with the immune system. In this context, most articles are based on the study of *M. tuberculosis.*

Several approaches are used to study *M. tuberculosis* changes between active and latent disease. Accordingly, *in vitro* models have been developed to simulate the low nutrient and oxygen availability found in granulomas of latent tuberculosis (TB). One technique consists of culturing *M. tuberculosis* with gradual nutrient starvation to switch bacteria metabolism from a replicating to a nonreplicating persistent (NRP) state [102]. Otherwise, other authors culture mycobacteria as pellicles in which nutrients are gradually depleted [75,87,103].

M. tuberculosis in a replicating state converts acetyl-CoA to produce mycolic acids or peptidoglycan [87]. Similarly, virulence factors such as DATs, TATs, PATs, PDIMs, PGL, SL, TDM or TMM are further synthesised to confer infectivity to mycobacterial cells [87,104]. However, during NRP state, synthesis of mycolic acid, peptidoglycan, TMM, TDM, or PDIM decrease [105,106]. Moreover, trehalose from existing TMM and TDM is redistributed into the cytoplasm. Therefore, trehalose redistribution further reduces TDM and TMM levels,

and consequently, increases free mycolic acids present on the cell wall envelope [102]. The diminished TDM and TMM concentrations in *M. tuberculosis* have been related to a reduced pro-inflammatory response triggered in mouse macrophages [107].

Other lipids of the mycobacteria cell wall are increased in a nonreplicating stage such as LM and, especially, LAM. Considering that LAM inhibits phagosome maturation and LM triggers strong proinflammatory effects, LAM/LM ratio might be crucial in determining the virulence of *M. tuberculosis* [102,108]. Similarly, TAGs and wax esters (WE) are highly produced and accumulated on the cell envelope (Figure 6) [87].
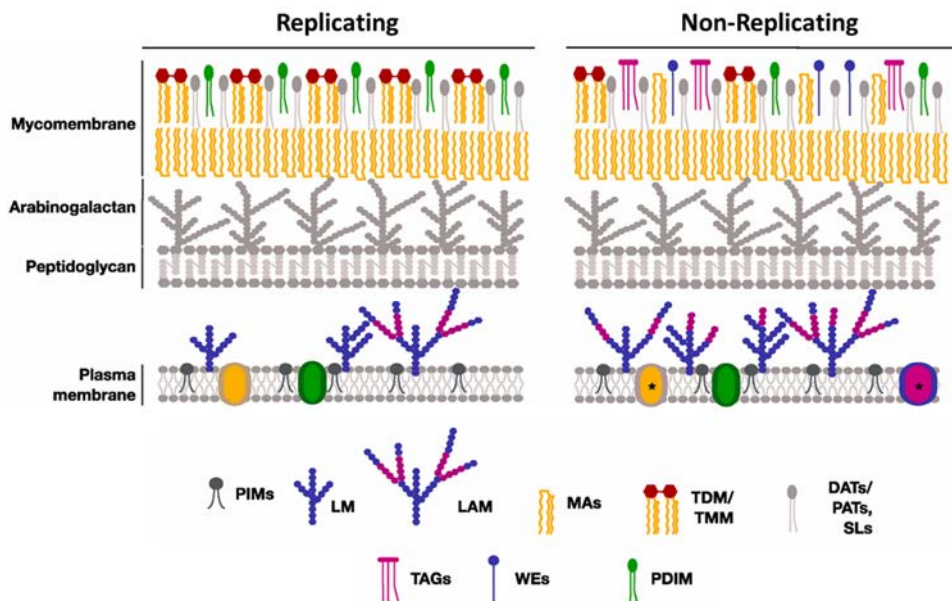
Figure 6. **Schematic model of *M. tuberculosis* cell envelope in a replicating or nonreplicating state.** PIMs: phosphatidylinositol mannosides; LM: lipomannan; LAM: Lipoarabinomannan, MAs: mycolic acids; TDM/TMM: trehalose dimycolate/trehalose monomycolate; DATs/PATs: diacyl trehalose, pentaacyl trehalose; SLs: Sulfolipids; TAGs: triacylglycerol; WEs: wax esters, PDIM: phthiocerol dimycocerosates; (PDIM). Modified from Stokas *et al.* (2020) [87].

Remarkably, *M. tuberculosis* characteristics observed in *in vitro* models can highly differ from its characteristics inside of the host. For instance, it has been proposed that *M. tuberculosis*, transmitted through the air, posses a highly hydrophobic cell envelope formed by a wide range of lipids and glycolipids. But when the mycobacterium enters into the alveolar space, several glycolipids and lipoglycans are degraded by hydrolases. Then, *M. tuberculosis* is phagocytised by alveolar macrophages and uses their own or host captured fatty acids to produce mycolic acids and survive during the latency stage. Finally, *M. tuberculosis* synthesises glycolipids to recover the highly hydrophobic envelope, escape from host cells and enable again its transmission [28,109,110].

Other mycobacteria species have also been studied when grown as pellicles *in vitro*, such as *M. smegmatis* or *M. bovis* BCG.

M. smegmatis enhances the glycolytic route during the first phases of the pellicle formation [12]. Besides, granuloma-like structures were observed when *M. smegmatis* grew in the presence of glycerol or cholesterol, in which cells contained high levels of LM and LAM. Otherwise, *M. smegmatis* cultured in minimal medium triggered a few granuloma-like structures and *M. smegmatis* cells produced PIMs and mycolic acid. The high hydrophobicity of cell surface found in the presence of glycerol or cholesterol supplementation also agreed with the described presence of those cell wall components [111].

When *M. bovis* BCG was cultured as a pellicle *in vitro*, the quantity of free mycolic acids was highly increased in the cell wall during pellicle maturation. In contrast, levels of mycolic acids decreased over time, similarly to *M. tuberculosis* [75,112].

1.1.6. Culture of mycobacteria

Culture media for growing mycobacteria was initially developed to detect *M. tuberculosis* in clinical specimens such as sputum, body fluids or tissues. Those samples are typically contaminated with microbiota, and the exposition to acids or alkali is required to recover mycobacteria [113]. The first isolation of *M. tuberculosis* was reached by Robert Koch in 1882 using a coagulated bovine serum [114]. However, mycobacteria colonies were very tiny in that medium [115]. Since that moment, several culture media were developed either in solid (egg- or agar-based) or in liquid form.

1.1.6.1 Egg-based culture media

The most frequent media used for the isolation of mycobacteria species from clinical samples are egg-based media such as Lowenstein-Jensen, American Trudeau Society (ATS) or Ogawa. They are composed of whole eggs, inorganic and organic salts, asparagine and glycerol. Additionally, malachite green is added to differentiate *M. tuberculosis* colonies from the medium colour and inhibit other microorganisms [113].

1.1.6.2 Agar-based culture media

Agar is added to culture media to obtain a solid medium. However, agar introduced in the culture composition can inhibit some mycobacterial species. Therefore, most agar-based media include ingredients to reduce its toxicity, such as bovine albumin or blood [113]. Middlebrook *et al.* established the most common used agar-based culture media [116,117]. Culture media were called "7H" media due to sequential changes in their formulations. Nowadays, 7H10 and 7H11 are the most widely used Middlebrook media in research laboratories. The main difference between 7H10 and 7H11 Middlebrook media remains on

the addition of casein hydrolysate into the 7H11 composition to enable the growth of fastidious *M. tuberculosis* strains.

Middlebrook media are distributed in dehydrated form, whose preparation and storage are critical as it is influenced negatively by daylight exposition and high temperature. Moreover, they must be supplemented with oleic acid, albumin, dextrose and catalase (OADC).

Remarkably, desiccation is the main limitation of solid media because mycobacteria require long periods of incubation.

1.1.6.3 Liquid culture media

The main components of mycobacteria liquid culture media compositions come from those proposed by Proskauer and Beck in 1894. However, other liquid media such as Kirchner, Sauton, Dubos or Middlebrook are also helpful [113].

Proskauer and Beck, and Sauton media are the only liquid media that do not contain animal products, and both have been classically prepared in-house. Therefore, variations from batch-to-batch can sporadically occur. Sauton media is used to produce *M. bovis* BCG massively. Then, mycobacteria are inoculated onto the medium surface and grown as pellicles [118].

Since Sauton media has been prepared in each laboratory, several compositions can be found in the literature. The main discrepancies are found in the amino acid source, being L-glutamate and L-asparagine, the most frequently used, and the carbon source. Glycerol and glucose are the most typically found in the compositions, yet their concentration also differs among formulas. Likewise, other inorganic compounds such as zinc sulphate are included by some authors as required for some mycobacteria enzymes, being another source of variability among the different laboratories. Some differences found in Sauton composition through the literature are shown in Table 2.

Kirchner's medium is a widely used medium to isolate *M. tuberculosis* from tissue or liquid body fluids that usually contain few amounts of cells.

The Dubos-liquid medium allows dispersed mycobacteria growth due to the presence of Tween-80.

Table 2. Compositions of Sauton medium. Extracted from Guallar-Garrido *et al.* (2020) [119]

	Sauton (1912)	Boyden *et al.* (1954)	Kusunose *et al.* (1976)	Chadwick *et al.* (1982)	Harth *et al.* (1997)	Petricevich *et al.* (2001)	Petricevich *et al.* (2001)	Batista *et al.* (2004)	Larsen et al. (2007)	Mehra et al. (2014)	Li *et al.* (2014)	Teknova
L-asparagine (g/L)	4	6	4	4,54		4	-		4	4	1	4
Sodium glutamate (g/L)							4					
L-glutamate (g/L)					2						2 to 8	
Soluble starch (g/L)								1				
Bacto-peptone (g/L)	-	-	-	-	-	-	-	16.6				-
Glycerol (mL/L)	60	30	53.3	60	60	60	30	60	60	60	2	17.8
Zinc sulphate (mg/L)	-	-	-	-	-	-	-	-	1	1		-
Sodium-potassium phosphate (g/L)						0.5		0.5				
Citric acid (g/L)	2	2	2	2	2	2.41	2	2.41	2	2	2	2
Potassium phosphate (g/L)	0.5	1.5	0.5	0.5	0.5		0.5		0.5	0.5	0.5	0.5
Ferric ammonium citrate (g/L)	0.05	0.05	0.05	0.05	0.05	0.495	0.05	0.495	0.05	0.05	0.05	0.05
Magnesium sulphate (g/L)	0.5	0.25	0.5	1	0.5	0.5	0.5	0.5	0.5	0.5	0.5	0.5
Tween 80 (mL/L)		-	-	-		-	-		0.5	0.5	0.5	0.15
Glucose (g/L)	-	10	-	-	-	-	-					2
pH	7.4	6.2	7.1	7.2	7.4	7.2-7.25	7	7.2-7.25	7	7		7

However, the most used culture media in research laboratories is Middlebrook 7H9. Similarly to 7H10 and 7H11, it is available commercially in a dehydrated form that is easily solubilised and sterilised. Then, it must be supplemented with albumin-dextrose-catalase (ADC). Contrary to 7H10 or 7H11 media, oleic acid is not incorporated in its composition because of the cleavage of Tween-80 releases enough oleate. Tween-80 is usually added to liquid 7H9 to avoid mycobacteria clumps. However, it has been described that its presence modifies superficial mycobacteria lipids [120]. Therefore, it should be avoided in studies related to host-pathogen interactions [121].

Independently of used the liquid media, it is essential to incubate mycobacteria in dark conditions. Additionally, mycobacteria cultures need to be controlled to avoid contamination [118].

Finally, mycobacteria growth is also influenced by the incubation characteristics. For instance, incubation temperature is a crucial factor to grow mycobacteria successfully. The vast majority of mycobacteria species grow at 37°C. However, the optimum temperature of some species can vary. For instance, the optimal temperature for *Mycobacterium ulcerans* growth is 30°C, while some fast-growing species such as *M. phlei* can indeed grow at 52°C [113].

1.1.7. Impact of culture media in mycobacteria characteristics

In 1987, Aboud-Zeid *et al.* suggested ensuring the constancy of *M. bovis* BCG strains during the manufacturing process to ensure its protective immunity considering that the antigens responsible for its activity were unknown[122]. Nowadays, some authors demonstrated the impact of culture media composition on the characteristics of mycobacteria [120,123–127], which might be critical in mycobacteria-host interactions [128].

Macroscopically, a liquid culture medium can modify the pellicle thickness, and a solid culture medium can alter the colony morphotype [129]. Besides, those changes can also imply different protein or lipid expression. For instance, the production of Adenosine 30,50-cyclic monophosphate (cAMP) in infected macrophages by *M. bovis* BCG grown in Sauton medium was increased compared to *M. bovis* BCG grown in Middlebrook 7H9. cAMP is responsible for inhibiting the union of lysosome and phagosome. Moreover, its massive secretion also triggered changes on the mycobacterial surface that caused cell aggregation [130]. Similarly, *M. bovis* BCG cells grown in modified Sauton were more resistant to reactive nitrogen intermediates than mycobacteria cells grown in Middlebrook 7H9 [124].

The immune response triggered by *M. bovis* BCG is also modified depending on the culture medium in which mycobacteria are grown. For instance, detergent in the culture medium

caused the capsule release of *M. bovis* BCG [131]. Later, the presence or absence of the capsule has been related to different protective efficacy of *M. bovis* BCG vaccination against *M. tuberculosis.* Especially, mice vaccination with encapsulated *M. bovis* BCG triggered higher antibody titers against a specific polysaccharide of the capsule, higher IFN-ɣ and IL-17 cytokine release by splenocytes, and more multifunctional CD4$^+$ T cells, compared to unencapsulated *M. bovis* BCG [120].

Another study reported that *M. bovis* BCG grown in Sauton medium persisted more inside macrophages, induced higher inflammatory reaction and was less effective against *M. tuberculosis* aerosol challenge than *M. bovis* BCG grown in Middlebrook 7H9[132]. Similarly, *M. bovis* BCG grown in Sauton medium containing glycerol triggered a more robust humoral immune response after intradermal vaccination than *M. bovis* BCG grown in Sauton enriched with bacto-peptone [127].

But this phenomena not only occurs in *M. bovis* BCG. *M. phlei* showed a high content of lipids and polysaccharides when growing in Sauton culture medium with 3% (w/v) of glycerol instead of 6% (w/v) of glucose [133]. *M. avium* subsp. hominissuis formed a thick pellicle growing in 7H9 Middlebrook medium supplemented with 0.2% glycerol, compared to grown on poor nutrient media. Besides, the addition of GPL in the culture media compositions triggered mycobacterial cells with high content of GPL [134]. *M. tuberculosis, M. marinum* and *M. smegmatis* also lost their capsule grown in detergent-containing media [131]. Finally, *M. tuberculosis* grown on glycerol showed an increased sensitivity to antibiotics *in vitro* [135].

1.1.7.1 Influence of inorganic compounds in mycobacteria metabolism

Mycobacteria growth can also be influenced by inorganic compounds which are extracellularly present. However, not all mycobacteria species behave equally.

For instance, Mg^{2+} is required by *M. tuberculosis, M. kansasii* and *M. smegmatis* grown in acidic media. However, other mycobacteria species such as *M. fortuitum*, *M. marinum*, *M. scrofulaceum, M. avium* or *M. chelone* can adequately grow in acidic conditions with limiting Mg^{2+} [136]. Besides, the presence of some inorganic compound can trigger a negative effect. For instance, the absence of inorganic phosphate triggered an up-regulation of α-glucans in the capsule of *M. tuberculosis, M. marinum* and *M. smegmatis* [137]. Other compounds are associated with improved mycobacteria growth. For instance, ferric ammonium citrate to grow *Mycobacterium haemophilum* [138] or Fe^{3+} to enable biofilm formation by *M. smegmatis* [2]. Similarly, zinc sulphate improved both *M. tuberculosis* or *M. bovis* BCG growth because the enzyme aspartate transaminase requires zinc to converts the aspartate to L-glutamate [75].

1.1.8. The downside of mycobacteria: Diseases triggered by mycobacteria

Only a minority of mycobacteria species are pathogenic or opportunistic pathogens, but due to the high incidence in some countries and the severity of their infections, their importance is undeniable.

M. tuberculosis Complex defines a group of pathogens capable of producing TB disease in humans and animals. The group is formed by species such as *M. tuberculosis*, *M. bovis*, *M. canetti, M. africanum*, *M. microti*, *M. caprae* [139]. TB affects to new 10 million people each year and is one of the ten causes of death worldwide. The disease affects both sexes, but the highest incidence is mainly found in adult men from South-East Asia, Africa, and the Western Pacific. Contrary, Eastern Mediterranean, the Americas, and Europe contained the lowest TB incidence according to the World Health Organization (WHO) in 2020. TB incidence is decreasing over the years, but improvements in a fast diagnosis and new treatments to face TB and drug-resistant TB are needed to reduce its incidence [140].

NTM includes environmental and atypical mycobacteria, and the number of described species is constantly increasing due to a wide variety of new methodologies that permit identify new isolates. NTM can form a biofilm-like structure and are mainly found in soil, dust, and natural and running water[2]. NTM can metabolise several environmental substances, such as aromatic hydrocarbons [2]. Although most NTM are non-pathogenic, some of them are opportunistic pathogens in immunocompromised patients. Some good examples are the case of *M. abscessus* present on cystic fibrosis patients [141] or the fish pathogen *M. marinum* that can cause zoonotic infections in humans [24]. Infections triggered by NTM include multiple diseases, from pulmonary infection to skin, device-associated infections, and blood infection. Symptoms vary depending on the infection site and the severity, from fever to death [142].

Another significant infection caused by a mycobacterium species is leprosy, specifically *M. leprae.* It is a neurological and dermatological disease caused by the infection of Schwann cells of the peripheral nervous system. Leprosy is curable, and early detection and appropriate and complete treatment are considered key factors to reduce its transmission and disease severity. *M. leprae* is likely transmitted by tiny droplets and close contact with untreated cases. Leprosy was eliminated as a public health problem globally in 2000, described as less than 1 case per 10000 population [143].

1.1.9.   The bright side of mycobacteria

As previously mentioned, most mycobacteria species are non-pathogenic, and they offer a wide range of advantages. The most valuable application of mycobacteria remains in using *M. bovis* BCG, the only commercially available vaccine, to prevent humans from TB. Parallelly, it is also the most successful discovery in the use of mycobacteria as antitumour treatment, specifically in non-muscle-invasive BC (NMIBC). The confluence of several coincidences triggered those discoveries (Figure 7).

In 1893, Dr Coley, the father of immunotherapy, reported that microorganisms have therapeutic benefit for patients. Specifically, he noted the efficacy of an inactivated product from *Streptococcus pyogenes* and *Serratia marcenses*, also called Coley's toxin, to treat patients affected by several types of cancer [144].

A few years later, *M. bovis* was isolated from mastitis of a tuberculous bovine by Nocard in 1904. Then, after 230 recultures, Drs Albert Calmette and Camille Guérin obtained an attenuated strain of *M. bovis* in 1921. The new strain called *M. bovis* Bacillus Calmette-Guérin (BCG), protected from TB in vaccinated animals, the reason why it was massively produced, distributed, and administrated around the world. Remarkably, it is still the only option for TB vaccine[145].

Then in 1928, Dr Pearl observed an inverse relationship between malignancies and tuberculous lesions after analysing over 1600 cadavers. Therefore, he suggested using *M. bovis* BCG as an antitumour treatment because its safety had been tested. Since 1930, several preclinical and clinical assays were performed using *M. bovis* BCG in different cancers. In 1976, Dr Morales conducted a successful trial in which 7 over 10 patients with NMIBC that had been treated with intravesical instillations of *M. bovis* BCG were tumour-free at the end of the study. This evidence was confirmed by a randomised trial in 1980. Finally, *M. bovis* BCG was accepted to treat NMIBC patients by the Food and Drug Administration (FDA) in 1990 [144]. Currently, *M. bovis* BCG is still the preferred and most efficacious treatment for NMIBC, even superior to chemotherapeutic drugs.
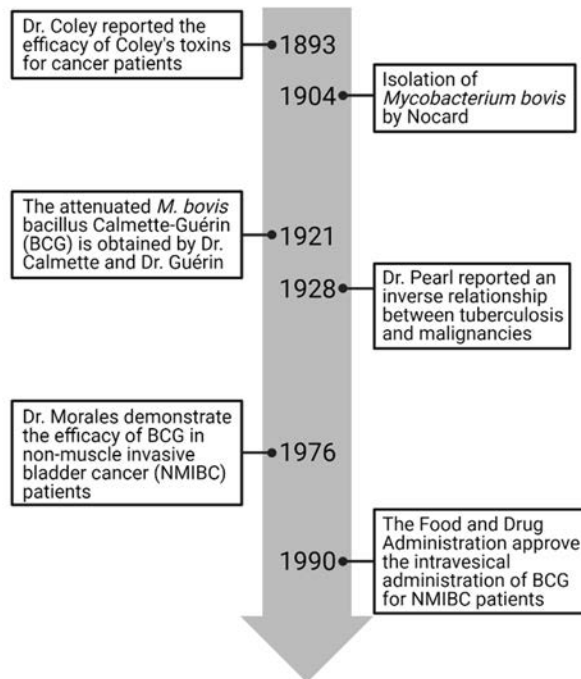
Figure 7. Historical summary of *M. bovis* BCG use as a treatment for non-muscle invasive bladder cancer patients

Due to the success of *M. bovis* BCG to treat BC tumours, *M. bovis* BCG alone or in combination with other elements such as chemotherapy has also been proposed to treat different types of cancers (Figure 8).

One of the most successful results was achieved in breast cancer patients that received *M. bovis* BCG plus allogeneic tumour cells in 1995 [146]. Accordingly, *M. bovis* BCG plus tumour cells and formalin increased patients' survival in 2015 [147]. Moreover, since 2003 other techniques such as obtaining a recombinant *M. bovis* BCG expressing MUC1 plus IL-2, GM-CSF, or CD80 seem to result in a breast cancer tumour growth inhibition [148–150].

Moreover, the whole live bacterium combined with 5-Fluorouracil, doxorubicin, and mitomycin seemed to improve the survival of gastric cancer patients in 2004 [151]. In the context of lung cancer, the combination of *M. bovis* BCG and maltose-binding protein from *Escherichia coli* triggered a Th1 response *in vivo* in 2011 [152]. Furthermore, the safety of *M. bovis* BCG with proton-beam radiotherapy was proved in hepatoma cancer patients in 2013 [153].

Introduction

M. bovis BCG components have also been of high interest. Heat Shock Protein 65 (HSP65) is the most analysed, which is the analogue of HSP70 of *M. tuberculosis*. For instance, HSP65 in breast cancer was able to induce immunogenicity in combination with repeat beta-hCG C-terminal peptide in 2006 [154]. Moreover, HSP65 in combination with PSA protected fibrosarcoma tumours expressing PSA in 2004 [155]. Then in 2006, HSP65 plus MUC1 demonstrated an antitumour lymphoma response through CTL activation [156], and the combination of HSP65 with CpG oligodeoxynucleotide and MUC1 induced a Th1 response that resulted in an inhibition of melanoma tumours in 2012 [157]. Interestingly, cervical cancer regression was addressed in *in vivo* models in 2005 and clinical trials in 2007 when treated with the combination of HSP65 plus E7 [158,159].

Other highly studied components of *M. bovis* BCG are molecules forming part of its cell wall. For instance, cell wall skeleton (CWS) of *M. bovis* BCG tested in lung cancer and melanoma reduced metastasis in mice [160]. Later in 2008, CWS efficiently eliminated metastases and the primary hepatoma tumour in guinea pigs [161]. Similarly, in 2009, CWS was intracutaneously administered to ovarian cancer patients, which triggered an improvement in survival and quality of life.

Moreover, CWS combined with the peptide WT1 rejected lung or leukaemia tumour cells expressing WT1 [162]. CWS with mitomycin C suppressed lung tumour growth [163]. Additionally, an increased antitumour effect was reached when CWS were administered in nanoparticles in the murine lymphoma model [164].

L-MTP-PE, muramyl tripeptide-phosphatidyl ethanolamine encapsulated in liposomes, prolonged the survival of dogs with oral melanoma [165]. Moreover, L-MTP-PE decreased the risk of recurrences and death in patients with osteosarcoma in 2014 [166] and was able to inhibit the primary tumour progression in combination with zoledronic acid in 2016 [167].

Other glycans, such as a complex polysaccharide in gelation microparticles called PS1, showed cytotoxicity in the murine sarcoma model [168]. Otherwise, LM from *M. bovis* BCG also demonstrated an antitumour effect in 2017, inhibiting lymphoma tumour growth [169].

Finally, back in 1990, the combination of deoxyribonucleic acid from *M. bovis* BCG, poly-L-lysine and carboxymethylcellulose was tested in the hepatoma guinea-pig model. It completely delayed the tumour growth of animals [171].
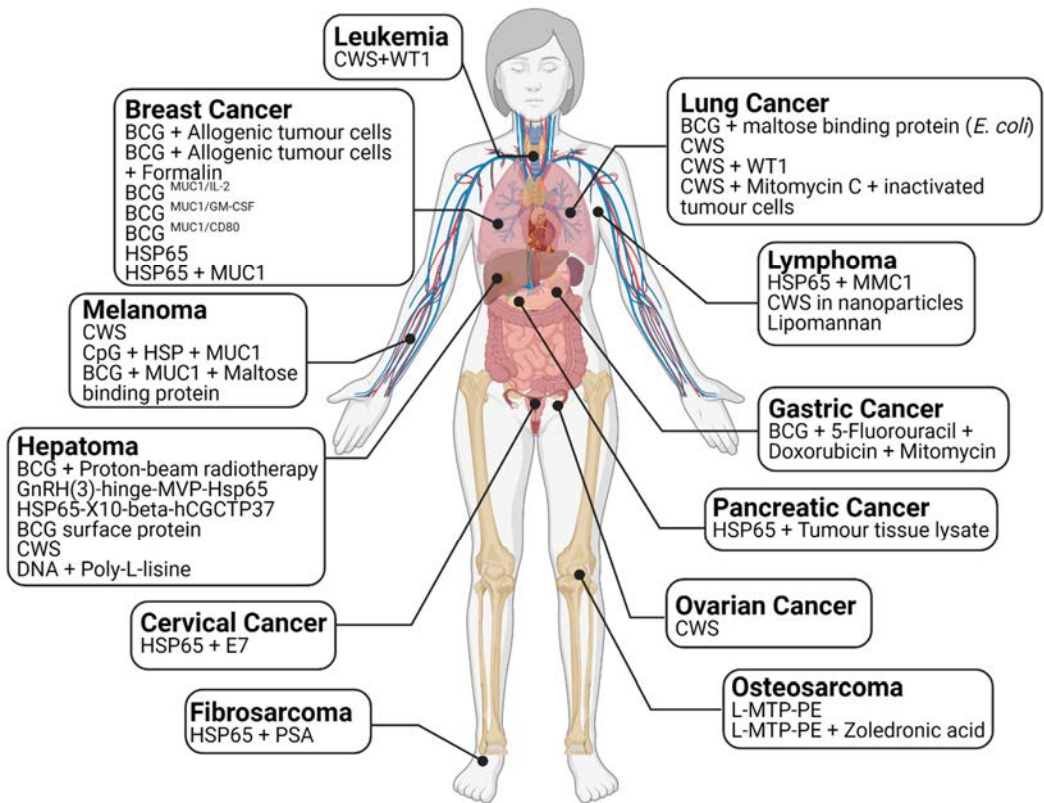
Figure 8. *M. bovis* BCG and *M. bovis* BCG compounds studied to treat several types of cancers. Data obtained from Noguera-Ortega *et al.* (2020) [65]

Additionally to *M. bovis* BCG, other mycobacteria and mycobacteria components have been assessed. Table 3 make a brief mention to the most successful results when using other mycobacteria to treat different kinds of cancer (extensively explained in Noguera-Ortega *et al.* (2020)) [65].

Table 3. Mycobacteria tested to treat different kinds of cancers

Mycobacterium	Form	Outcome	Cancer	Reference
Mycobacterium paragordonae	Heat-killed bacterium + cisplatin	Antitumour immune response	Colorectal cancer	[170]
Mycobacterium smegmatis	Recombinant *M. smegmatis* expressing MAGEA3 and SSX2	Reduction of tumour	Oesophagal cancer	[171]
	M. smegmatis with monosodium urate crystals	Delay melanoma formation	Melanoma	[172]
Mycobacterium obuense (IMM-101)	Heat-killed bacterium	Reduce metastatic burden, safe and tolerable Modulation immune system	Melanoma Pancreatic Cancer	[173,174] [175]
	Heat-killed plus Gemcitabine	Improve overall survival	Pancreatic Cancer	[176]
Mycobacterium phlei	Cell wall with *Salmonella Minnesota* (DETOX) plus subcutaneous IL-1 and allogenic colon tumour cell lines	Safe and effective	Colorectal cancer	[177]
	Cell wall plus photodynamic therapy	Increase antitumour effect	Breast cancer	[178]
Mycobacterium indicus pranii (MIP)	Whole live bacterium	Immune system activation and tumour suppression Immunotherapeutic effect	Melanoma Myeloma, Thymoma	[179–181] [182]
	MIP plus cisplatin and radiotherapy	Tolerability, improved quality of life, tumour size regression	Lung cancer	[183]
	MIP plus cisplatin and paclitaxel	Improved overall survival and progression-free survival	Lung Cancer	[184]
	MIP plus survivin and alum	Immunogenic and inhibit tumour growth	Breast Cancer	[185]
	MIP + 1'-S-1'-acetoxychavicol acetate and cisplatin	Control cancer progression	Breast Cancer	[186]
	MIP + Glycyrrhizin acid	Restrict solid tumour growth	Melanoma	[187]
	Heat-killed bacterium	Cytotoxic effect	Cervical, Lung, Cervical, Prostate, Liver, Bladder, Oral Cancer	[188]
	Heat-killed bacterium plus HPV16T epitope of the Human Papilloma Virus	Antigen-specific therapeutic effect	Cervical cancer	[189]
	Cell wall	Immunostimulatory effect	Melanoma	[190]
	Whole bacterium	Improve the quality of life, survival	Lung Cancer	[191–193]

Mycobacterium vaccae (IMM-201 or SRL172)		Increased patients' survival	Melanoma	[194]
	M. vaccae plus chemotherapy	Safe, tolerable, improve the response rate	Lung Cancer	[195]
		Safe, immune response	Mesothelioma	[196]
	M. vaccae plus IL-12	Prolong patients' survival	Melanoma	[197,198]
	M. vaccae with IL-12 and anti-her2 antibody	Increased immune response	Breast cancer	[199]
	PS4A proteoglycan	Immunostimulatory effect	Sarcoma	[200]
Mycobacterium bovis	CpG oligodeoxynucleotides of *M. bovis* inside liposomes	Increased antitumour activity	Melanoma	[201]
M. tuberculosis	Arabinomannan extract (Z-100) plus radiation	Tumour growth inhibition	Fibrosarcoma, Lung	[202]
	Z-100 plus *Corynebacterium parvum*	Prolongation antitumour effect	Sarcoma	[203]
	B16F10/ESAT-6-glycosylphosphatidylinositol-IL-21	Prolong survival, inhibit tumour growth	Melanoma	[204]
	B16F10-ESAT-6-gpi/IL-21	Inhibit tumour growth	Melanoma	[205]
	ESAT-2 plus IL-2	Regression tumour	Melanoma	[206]
	Tumour antigen-loaded-dendritic cells plus Rv2299c	Inhibit tumour growth	Colorectal cancer	[207]
	RelE	Inhibit tumour growth	Lung cancer	[208]
	HSP70	Inhibit tumour growth, size, increase survival	Leukaemia	[209]
		Prolong survival	Melanoma	[210]
	HSP70 plus human umbilical vein endothelial cell	Prolong survival, inhibit tumour growth	Hepatoma	[211]
	HSP70 plus thymidine kinase genes (HSV) and attenuated *S. typhimurium*	Suppress tumour growth	Melanoma	[212]
	HSP70 and Idiotype	Prolong survival	Lymphoma	[213]
	HSP70 and A20 tumour cells	Long tumour protection	Lymphoma	[214]
	HSP70 and CLIC1	Immunogenicity	Ovarian Cancer	[215]
	HSP70 and SigmE7	Cell immune response, antitumour effect	Cervical Cancer	[216]

1.2 Bladder Cancer: disease and treatment

The bladder is an organ of the urinary tract placed on the pelvic floor. It is a hollow formed by distensible muscular layers (inner epithelium, *lamina propria*, submucosa and muscle), which allow the storage and release of urine. The urine is produced after the blood filtration into the kidneys and arrives at the bladder through the ureters. Finally, muscular layers of the bladder are contracted to enable urination and, therefore, discharge the urine from the body.

The bladder can suffer common disorders such as urinary tract infections that can lead to bladder inflammation (cystitis), blood presence (haematuria) or difficulty and/or pain during urination (dysuria). Those symptoms can be easily confused with BC.

BC was the seventh most frequently diagnosed cancer in the male population around the world, according to the latest European Association of Urology report published in 2019. It decreased to the eleventh when women were included in the statistics. Therefore, the incidence rate per 100 000 person-year highly differs among genders, 9.0 for men and 2.2 for women [37]. There are several risk factors associated with BC development. However, tobacco is associated with 50% of the cases. Moreover, the exposure to aromatic amines, polycyclic aromatic and chlorinated hydrocarbons, mainly present in industrial plants account for 10% of cases. Finally, genetic predisposition, chlorination of drinking water or ionising radiation also seem to induce an increased risk to suffer BC.

There are three types of BC depending on the cellular tissue affected by the tumour:

- Transitional carcinoma: it counts for up to 90% of the diagnosed tumours. It is originated in the transitional epithelium of the bladder. While around 70% of the cases correspond to the tumour limited to bladder layers , the NMIBC, the other 30 % are called muscle-invasive BC (MIBC) because tumours can invade the muscle and closer organs such as the prostate, uterus, vagina, or abdomen
- Squamous cell carcinoma: it represents around 6 to 8% of the diagnosed cases, which originates in bladder cells after a prolonged inflammation.
- Adenocarcinoma: tumour cells from other organs such as lungs, pancreas, stomach, liver, or colon affect the bladder. It only represents 1 to 2 % of BC cases.

Following the American Joint Committee on Cancer and the International Union for Cancer Control, bladder tumours are classified depending on primary tumour invasion and lymph node and distant metastasis.

Therefore, primary tumours occurred into the bladder are divided into (Figure 9):

- T0: there is no proof of bladder tumours.
- Ta: non-invasive papillary carcinoma, which is characterised by a mushroom-shaped tumour and good prognosis.
- CIS: carcinoma *in situ*. It is a superficial and flat tumour that does not invade the *lamina propria*.
- T1: bladder tumour invades the subepithelial layer and the *lamina propria*.
- T2: bladder tumour invades the vesical muscular layer, superficially (T2a) or the deeply (T2b)
- T3: bladder tumour invades the perivesical fat layer, which can be observed microscopically (T3a) or macroscopically (T3b)
- T4: bladder tumour invades proximal organs such as prostatic stroma, uterus or vagina (T4a), or distant organs such as the pelvic wall or the abdominal wall (T4b)
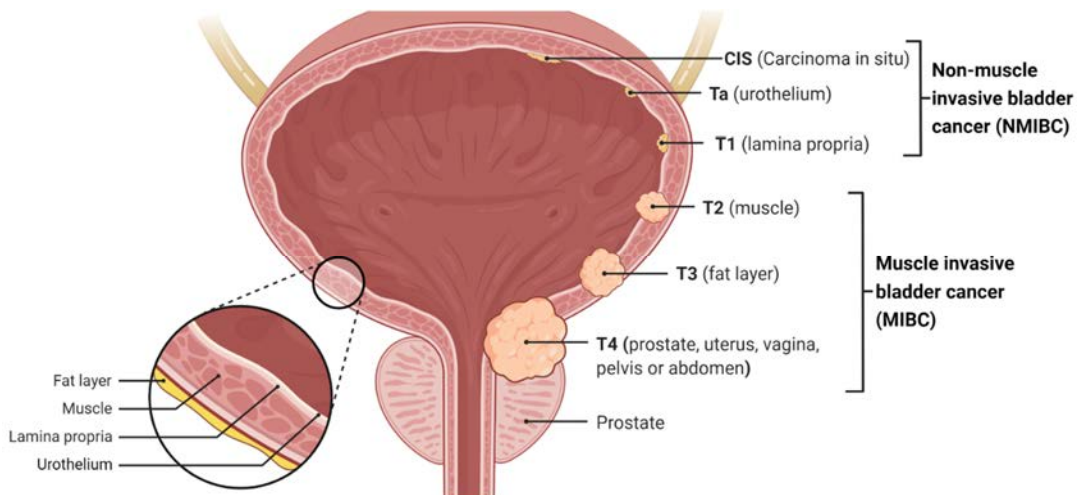
Figure 9.   **Bladder cancer staging.** Modified from Biorender.

Patients with BC are typically quickly diagnosed due to the presence of haematuria in the urine. Later, confirmation of BC diagnoses is based on a cystoscopic examination plus histologic evaluations of several bladder biopsies. Treatment starts once patients are diagnosed. Current treatment of NMIBC patients consists of transurethral resection to remove visible tumours present on the bladder surface. Then, patients follow a procedure based on the intravesical administration of millions of live *M. bovis* BCG once a week for six weeks, called the induction period. Whether the patient does not present adverse events can start the maintenance phase that differs between countries. Typically, patients receive intravesical instillations for six weeks every three months, for a total period of one to three years.

1.2.1   The history behind the use of M. bovis BCG strains as BC treatment

As previously mentioned in section 1.1.9, after shreds of scientific evidence provided by Dr Morales in the 70s, *M. bovis* BCG was established as the preferred and most successful treatment in terms of disease progression and free recurrence in NMIBC patients.

M. bovis BCG was distributed from Pasteur Institute worldwide to use and maintain this mycobacterium worldwide. However, different laboratories had used different protocols to grow the bacilli for more than four decades resulting in several *M. bovis* BCG substrains. Original mycobacteria suffered genetic modification such as deletions, duplications and insertions of sequences in its DNA[217].

After the natural depletion of the Region of Differentiation (RD) 1 plus several point mutations in the original *M. bovis,* the early substrains of *M. bovis* BCG (Birkhaug, Japan, Moreau, Russia and Sweden) were created. Then, the additional elimination of the RD2 generated the late group of *M. bovis* BCG substrains formed by *M. bovis* BCG Tice, Connaught, Frappier, Pasteur, Phipps, Prague, Danish and Glaxo[218].

Genetic modifications also involved modifications on the presence or absence of some lipids, such as PDIM or PGL, and proteins in the complex mycobacterial cell wall. Figure 10 shows the evolution of *M. bovis* BCG and the presence of PDIM and PGL in each substrain. Whether these modifications influence the immunogenicity and safety of *M. bovis* BCG substrains to vaccinate against TB or treat NMIBC patients is still unclear and under research due to inconclusive results [219].

In BC, Nowak *et al.* revised retrospectively 590 patients with T1HG NMIBC that were treated with *M. bovis* BCG-Moreau, -Tice or -RIVM substrains. The 5-year recurrence-free survival was superior in patients treated with either *M. bovis* BCG-Moreau (70.5%) or -Tice (66.7%) to the- RIVM (55.2%) substrain. Another recent study published by Del Giudice *et al.* compared the efficacy of *M. bovis* BCG Connaught, -Tice and -RIVM with secondary resection or not for high-risk NMIBC. Secondary resection, *M. bovis* BCG-Tice and *M. bovis* BCG-RIVM were associated with an improvement of recurrence-free survival compared to *M. bovis* BCG Connaught, being *M. bovis* BCG-Tice superior to the other *M. bovis* BCG substrains[220]. Contrary, another recent article reported that the recurrence-free survival was superior of *M. bovis* BCG Connaught compared to *M. bovis* BCG Tice [221].

However, a meta-analysis comparing ten different *M. bovis* BCG substrains was unsuccessful in finding differences in efficacy among *M. bovis* BCG strains, similarly to a wide range of studies [219,222–224].
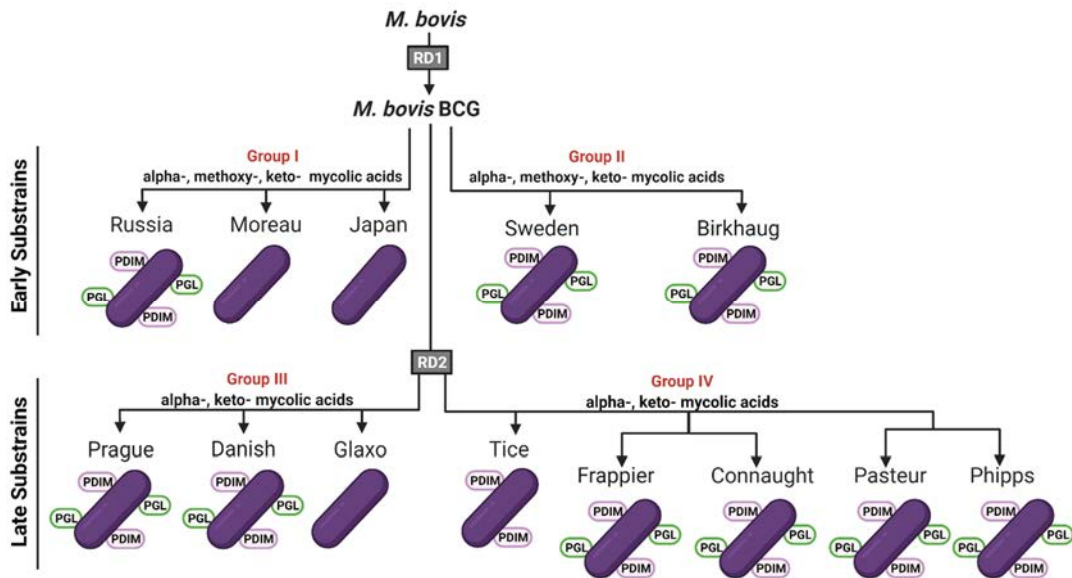
Figure 10. Evolution of *M. bovis* BCG and the presence of PDIM and PGL in each substrain. Information extracted from Secanella-Fandos *et al.* (2013) and Miyazaki *et al.* (2018) [225,226]

Safety could also be modified depending on the *M. bovis* BCG substrain. For instance, when *M. bovis* BCG OncoTice from Merck had to be substituted by SII Onco *M. bovis* BCG from the Serum Institute of India in New Zealand, some patients receiving SII Onco *M. bovis* BCG suffered higher discontinuation rates and severe complications than those previously reported with *M. bovis* BCG OntoTice[227]. In another study comparing *M. bovis* BCG-Tice, -Moreau and -RIVM, *M. bovis* BCG-Tice produced more local and mild events, while *M. bovis* BCG-RIVM produced more severe complications [223].

Further research is required to decipher whether there are differences among *M. bovis* BCG substrains regarding efficacy and safety and determine the critical characteristics of each *M. bovis* BCG strain responsible for different responses.

1.2.2 Mechanisms of action of *M. bovis* BCG

Although *M. bovis* BCG has been used for more than four decades to treat NMIBC patients, its exact mechanism of action is still undeciphered. It is known that *M. bovis* BCG exerts a direct antitumour effect that inhibits tumour cells proliferation. Additionally, it also induces the activation of the immune system to trigger an indirect immunotherapeutic response.

1.2.2.1 Direct antitumour effect of *M. bovis* BCG

Bladder cells are covered by a mucus layer formed by proteoglycans and glycosaminoglycans, called the GAG layer. It serves as a physical barrier that protects cells from infections and toxic substances [228] and also confers a high negative charge on the surface of bladder cells. However, the GAG expression is diminished in tumour bladder cells, triggering a decreased negative charge of the bladder cells' surface that favours mycobacteria adhesion, which also contains a negatively charged cell wall [229].

Finally, the presence of the fibronectin attachment protein (FAP) on the mycobacterial cell wall surface enables their union with the fibronectin present on the bladder cells' surface [230]. Then, *M. bovis* BCG is phagocytized, most likely by high-grade BC cells than low or non-malignant urothelial cells [231]. Its internalisation induces the release of NO, responsible for DNA and proteins damage and even cell apoptosis [230].

1.2.2.2 Indirect antitumour effect of *M. bovis* BCG

M. bovis BCG instillations also induce a local and systemic immune response. Specifically, *M. bovis* BCG serves as a source of PAMPs that are recognised by pattern recognition receptor (PRR) present on the surface of antigen-presenting cells (APCs) such as macrophages or DC.

The most studied PRRs are TLRs, which can activate the MyD88 signalling pathway. MyD88 triggers the activation of nuclear factor kappa-B (NK-κB) that enters into the nucleus and promote the expression of several cytokines and chemokines. The cytokine and chemokine release induce the infiltration of several immune cell populations such as granulocytes, macrophages, CD8+ cytotoxic T-cells (CTLs), NK neutrophils, and lymphocytes, among others into the bladder. Those cells, in turn, will continue releasing further cytokines into the bladder microenvironment to kill the tumour [230].

Paralellaly, *M. bovis* BCG antigens are also processed and presented on the surface of APCs and urothelial cells with major histocompatibility complex class II (MHC-II). MHC-II is recognised by CD4+ T cells that leads to their activation and differentiation [144]. Once CD4+ T cells are activated, CD4+ T cells release several cytokines such as IL-1, IL-2, IL-6, IL-8, IL-10, IL-17, IFN-ɣ that induce a proinflammatory immune response [144], that evokes in a tumour clearance [232]. Accordingly, the presence of CD4+ T cells and the substantial release of IFN-

γ have been associated with an improved response to *M. bovis* BCG in patients [233]. Besides, most cells express MHC-I molecules, recognised by CD8^{+} T cells. Therefore, the increased expression of MHC-I and MHC-II triggered after *M. bovis* BCG instillations have been associated with the treatment's positive outcomes (Figure 11) [234].

Figure 11. **Mechanism of action of *M. bovis* BCG in bladder cancer.** APC: antigen-presenting cells. Data
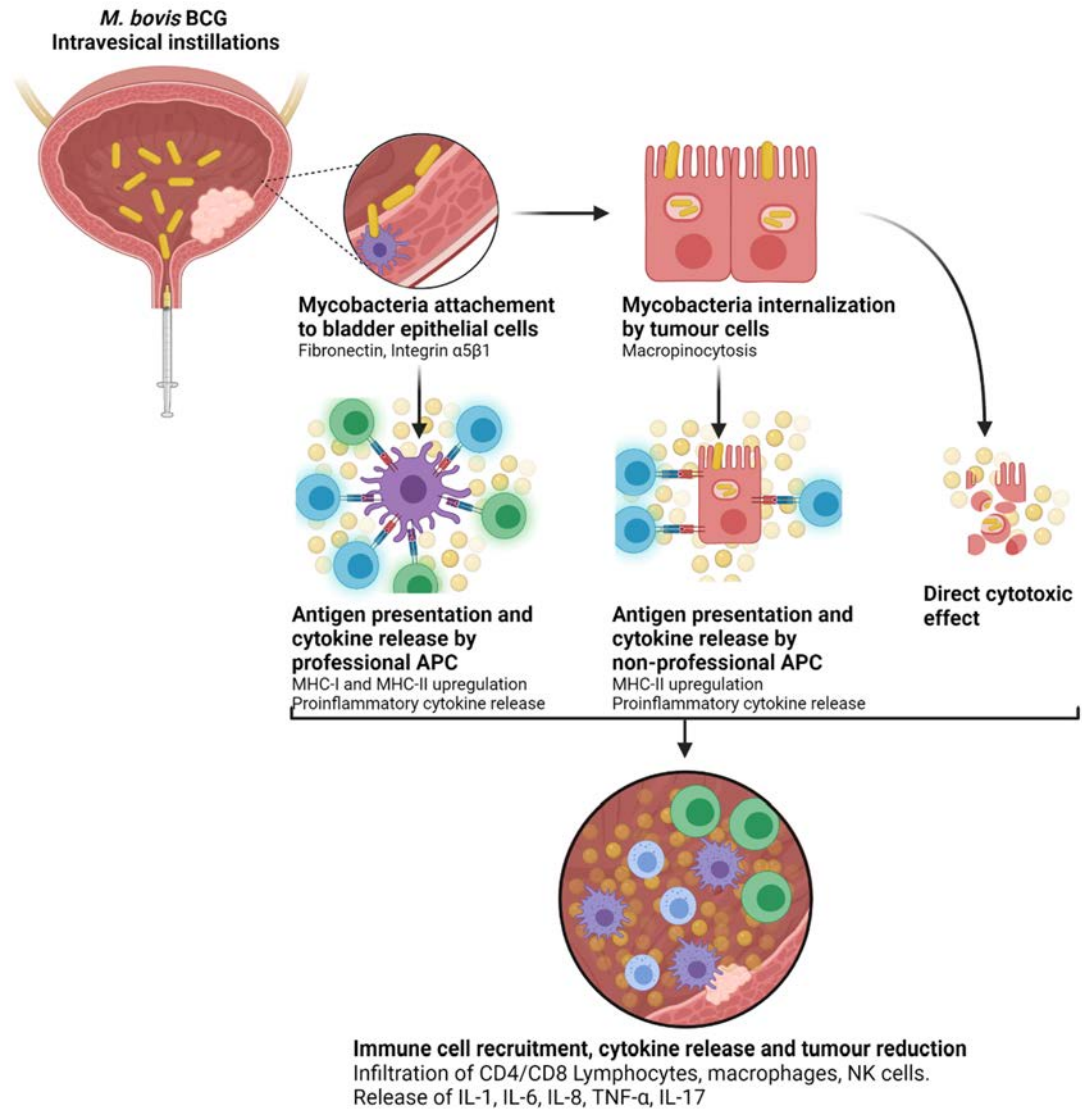
obtained from Redelman-Sidi, G (2014) [229]

Therefore, *M. bovis* BCG intravesical therapy induces the release of several cytokines, most of them part of a Th1 or Th17 response, leading to the success of the treatment. Otherwise, the release of IL-4 or IL-10 cytokines, or the infiltration of immune cells such as Tregs or tumour-associated macrophages (TAMs) typical from an anti-inflammatory or Th2 response, has been related to *M. bovis* BCG failure [233,235]. In fact, a high systemic immune-inflammation index, understood as a high ratio of neutrophils and platelet cells over lymphocytes, together with a tumour size above 3 cm, has been recently proposed as a low-cost predictor for *M. bovis* BCG failure and risk of BC progression in humans [236].

Finally, a systemic immune response is observed after *M. bovis* BCG therapy. Around 40 % of patients treated with *M. bovis* BCG experience a conversion to a positive tuberculin skin test. Besides, patients increase the number of lymphocytes, the mycobacteria-specific humoral response and the levels of cytokines and chemokines in sera. Unfortunately, moderate to severe systemic adverse effects may be produced at that moment[144].

1.2.2.3 Immune cells related with NMIBC and intravesical administration of *M. bovis* BCG

The following exposed immune cells have been related to a favourable or unfavourable outcome in BC patients.

<u>Neutrophils:</u> The presence of neutrophils in the bladder of BC patients seems to occur within 4-6 h after receiving *M. bovis* BCG instillations due to the cytokines, mainly IL-8, produced by BC cells [228]. Then, neutrophils release cytokines such as IL-1, IL-8, IL-12 and TNF-α that trigger CD4$^+$ T cell infiltration [237]. Moreover, they could act as antitumour cells due to producing reactive oxygen intermediates and the release of lytic enzymes and proapoptotic factors such as factor-related apoptosis-induced ligand (TRAIL) [144,233]. Moreover, *M. bovis* BCG-activated neutrophils can release neutrophils extracellular traps (NETs), a substance formed by DNA, elastin and histones. The formation of NETs has been related to preventing the release of *M. bovis* BCG out of the bladder, enhancing an increased immune response releasing cytokines, inducing immune cells infiltration such as T cells or macrophages [230], and inhibiting BC cells migration [238]. However, elevated neutrophil to lymphocyte ratio seems to be a predictor of poor prognosis of overall survival [239] and risk of recurrence [240] in NMIBC patients.

<u>Macrophages</u>: Macrophages can be found in a healthy human bladder, yet they are also recruited to the tumour after the instillation of *M. bovis* BCG. Two populations of macrophages have been described with very different functions. Macrophages in the presence of IFN-γ are polarised to M1, which release proinflammatory cytokines such as IL-6, IL-12 and TNF-α, and induce T cells infiltration into the bladder. Otherwise, macrophages can also be polarised to M2 in the presence of TGF-β or IL-10. M2 phenotype triggers an

immunosuppressive response and has been proposed as a predictor of *M. bovis* BCG treatment failure [229].

Dendritic cells (DCs): Despite a notable percentage of the total immune cells infiltrated into the tumour are DCs, most of them appeared to be phenotypically immature (low expression of CD80 and CD86), which difficult its beneficial effect. However, *M. bovis* BCG treatment induces DCs maturation that triggers the activation of other immune cells such as T cells, NKT cells or ɣδ T cells to eliminate BC cells [241].

Natural killer (NK): NK are cells from the innate immune system infiltrated into the bladder after *M. bovis* BCG treatments due to the presence of IFN-ɣ and IL-12 [229]. Nowadays, its role is still inconclusive. On the one hand, a baseline NK infiltration was associated with increased tumour size and high recurrence [242]. On the other hand, NK depletion abolished *M. bovis* BCG therapy benefits [243]. Similarly, NK presence was liked with improved survival of BC patients [244]. These contradictory shreds of evidence may be explained due to two NK cell populations with very different behaviour [228]. Further research is required to decipher the NK role in a BC context.

Innate lymphoid cells (ILC): ILC cells are formed by three subgroups: ILC1, ILC2 and ILC17, that correlate with Th1, Th2 and Th17 immune responses [245]. In 2017, Chevalier *et al.* published the only available paper regarding ILC and BC. Especifically, the production of IL-13 by ILC2 cells was associated with immunosuppression due to the recruitment of Myeloid-Derived Suppressor Cells (MDSC) [246].

MDSC: MDSC can be derived from monocytes, macrophages or dendritic cell progenitor (M-MDSC); or from neutrophil, eosinophil, basophil or mast cell progenitor (G-MDSC). M-MDSC can be differentiated to produce TAMs. Overall, MDSC inhibits T and NK cell functions and introduces Tregs' expansion through the release of NO, arginase-1 or inhibitory cytokines such as IL-10 or TGF-β [247]. Reduced survival has been reported in BC patients with high levels of MDSC into the bladder after *M. bovis* BCG administration[248].

Regulatory T cells (Tregs): Tregs is a population related to poor response and drastically diminished recurrence-free survival and progression-free survival in humans. Tregs are highly infiltrated among non-responders patients and are typically found in the stroma around the tumour, inhibiting the Th1 response induced by *M. bovis* BCG treatment [249].

T Lymphocytes: CD4$^+$ T cells and CD8$^+$ cytotoxic T cells are critical cells for the *M. bovis* BCG-mediated antitumour activity. CD4$^+$ T cells can develop different phenotypes: Th1, Th2 or Th17 phenotypes. Th1 phenotype is characterised by the release of proinflammatory cytokines such as IFN-ɣ, IL-2 and IL-12. Once in the tumour, CD4$^+$ T cells stimulate macrophages, and CD8$^+$ T cells triggered cytotoxicity [250]. Otherwise, CD4$^+$ T cells can be polarised to a Th2 phenotype, characterised by the release of mainly IL-4 or IL-10 that

promotes a humoral response. Although *M. bovis* BCG therapy can trigger a Th2 response, a massive influx to Th1 response producing proinflammatory cytokines is crucial for achieving an effective *M. bovis* BCG treatment [251]. Finally, CD4^{+} T cells can trigger a Th17 phenotype. Th17 cells are a novel subset of CD4^{+} T cells, which might play an essential role in tumour immunology. However, its function is poorly studied in BC. IL-1β, IL-6 or TGF-β trigger the differentiation of naïve CD4^{+} T cells to Th17 cells, characterised by releasing proinflammatory cytokines such as IL-17, IL-21 or IL-22. Higher levels of IL-17 has been found in BC patients compared to control groups [252].

γδ T cells: A resident population in mouse bladder, and probably in the healthy human bladder, γδ T cells are considered a subset of cells bridging innate and adaptative immunity [241], which are highly infiltrated into the bladder after intravesical instillations with *M. bovis* BCG [253]. Besides, vaccination with *M. bovis* BCG in NMIBC patients previous to receive the intravesical treatment resulted in enhanced cytotoxicity by γδ t cells [254] through the release of granulysin and perforin. [255]. γδ T cells can be activated by phosphoantigens and release proinflammatory cytokines.

1.2.2.4 Cytokines related with NMIBC and intravesical administration of *M. bovis* BCG

M. bovis BCG therapy is characterised by producing a cytokine and chemokine cascade due to the induced infiltration of several immune cells. The presence of IL-2, IL-12, IFN-γ and, more recently described, IL-17, together with the absence of IL-4 or IL-10, has been related to a beneficial response to *M. bovis* BCG therapy. In fact, the presence of some cytokines in the urine of patients has been proposed as a predictor for the outcome of *M. bovis* BCG treatment [229]. The role of the following molecules has been related to *M. bovis* BCG treatment.

- **IL-1β** is a proinflammatory cytokine produced by cells from the innate immune system, such as macrophages. Its expression after *M. bovis* BCG intravesical treatment has been related to the induction of the immune system [256].
- **IL-6** cytokine can be produced by monocytes, macrophages, lymphocytes, fibroblast or endothelial cells. It is a pleiotropic cytokine that, combined with other proinflammatory cytokines such as IFN-γ or IL-1, induce T cell or NK activation. However, its role in BC is controversial. *M. bovis* BCG treatment induces a high release of IL-6 that can enhance Th2 response, yet the absence of IL-4 and the high amount of IFN-γ may contradict its effect [257].
- **IL-8**, or adequately called CXCL-8, is a chemokine with controversial activity. CXCL-8 belong to a superfamily involved in tumour progression and angiogenesis. However, it also recruits immune cells such as macrophages or neutrophils to the bladder triggering a pro-inflammatory environment [258].

- **IL-10** is a controversial cytokine. While some authors relate a high intratumoral accumulation of IL-10 with CD8+ T cell proliferation, IL-10 in sera could be associated with poor prognostic of *M. bovis* BCG treatment [233].
- **IL-17** is a cytokine responsible for inducing a Th17 response. It can be produced by Th17 cells, γδ T cells, type 3 ILC or mast cells [245,259,260]. Its production by mast cells has been associated with positive outcomes from *M. bovis* BCG-treated patients [260].
- **IL-18** is a cytokine expressed by macrophages, DC or non-haematopoietic cells such as intestinal epithelial cells. The biological function of IL-18 is to prevent cell death. Accordingly, when IL-18 is added to the environment, immune effector cells such as T cells are increased, improving the efficacy of the immunotherapy [255].
- **IL-21** is a cytokine produced by circulating and infiltrating T cells able to activate antitumoral activity and induce the expansion of CD8+ T cells, NK and Th cells. Besides, it is related to the differentiation of B cells into plasmablasts. Overall, it is related to positive prognostic in NMIBC patients [232,233]
- **IFN-γ** is a cytokine produced by circulating and infiltrating T cells with antitumour activity. It is associated with BC favourable prognosis [233].
- **TNF-α** is a cytokine produced by monocytes and macrophages, T cells, B cells, NK cells and some tumour cells. It is responsible for the regulation of cell proliferation. Moreover, TNF-α has a potent antitumour activity and induce apoptosis in tumour cells [261]
- **NO** is a molecule released that can induce damage to DNA, proteins and even cell apoptosis and autophagy [230]. However, other authors manifest that iNOS can inactivate arginine related to an effective immune response, suppress T cells expansion and recruit MDSC, which would be detrimental for NMIBC patients [262].

1.2.3   Drawbacks of the use of *M. bovis* BCG for NMIBC patients

Around 70% of *M. bovis* BCG-treated NMIBC patients suffer common side effects such as flu-like symptoms and/or zone-focused irritation after receiving the treatment. According to the trial conducted by the European Organization for Research and Treatment of Cancer (EORTC), 8% of patients had to suspend the therapy due to toxicity [263]. Moreover, less than 1% of the patients suffer a disseminated infection and require antituberculosis treatment consisting of four antibiotics per day for four months, followed by two antimicrobials for two more months. Remarkably, when any severe side effect is reported in NMIBC patients, *M. bovis* BCG installations are immediately stopped, devoiding patients from the most efficacious treatment against NMIBC. Moreover, immune-deficient patients can not be treated with *M. bovis* BCG due to using a live bacterium.

Introduction

Apart from mycobacteria-associated limitations, there is an increasing problem related to the *M. bovis* BCG availability during the last decade after the closure of the Sanofi company, which distributed around the two continents with the highest incidence of NMIBC, Europe and North America. However, nowadays, Merck is trying to get over *M. bovis* BCG scarcity.

Several alternatives are studied to face *M. bovis* BCG limitations and adverse events. They are based on 1) modifying the current schedule of *M. bovis* BCG instillations, 2) improvement of *M. bovis* BCG itself, or 3) the total replacement of *M. bovis* BCG by other microorganisms (bacteria and mycobacteria) or compounds.

1.2.4   *M. bovis* BCG – based alternatives

As it has been mentioned, *M. bovis* BCG is the preferred treatment for NMIBC patients nowadays. However, its side effects lead to the development of other alternatives.

New research includes modifications in the way of delivering therapies to maximise the desired effect in NMIBC patients. For instance, hyperthermia [264], electromotive drug administration (EMDA) to improve drug penetration into biological membranes [265–267] or osmotic pump-like device able to deliver the drug slowly and prolongated in time [268]. Besides, these new delivery mechanisms are highly precious as they could also be applied to other alternatives. Some of the most studied alternatives using *M. bovis* BCG are explained below.

1.2.4.1   Modification of *M. bovis* BCG schedule

In 1976, when Dr Morales proposed using *M. bovis* BCG to treat NMIBC patients, he also considered the option of vaccination together with intravesical instillations of *M. bovis* BCG. However, the procedure was abandoned because patients vaccinated and intravesically treated simultaneously did not improve the therapy compared to only intravesical-treated patients [269]. Then, similar outcomes were achieved by other studies [270–272]. However, new research opens the possibility of a vaccination's beneficial effect.

On the one hand, a study published by Biot *et al.* in 2012 demonstrated an improvement of the triggered immune response of intravesical-treated mice that were previously vaccinated with *M. bovis* BCG. Specifically, they observed that subcutaneous immunization 21 days before intravesical administration generated a more robust infiltration of CD4+ and CD8+ T cells into the bladder. Besides, experimental data was supplemented with a retrospective study in which patients vaccinated with *M. bovis* BCG responded better to intravesical instillations than non-vaccinated patients [273]. Similarly, the high presence of IFN-ɣ and IL-21 before *M. bovis* BCG instillations in NMIBC patients have been related to favourable outcomes of the therapy, reinforcing that a prior vaccination could be favourable [233].

On the other hand, Rousseau *et al*. found that vaccination previous to *M. bovis* BCG instillations did not improve the total infiltration of CD4$^+$ and CD8$^+$ T cells into the bladder of tumour-bearing mice that were treated with at least three intravesical instillations. Therefore, suggesting that three or more intravesical instillations may overcome the beneficial effect triggered by a subcutaneous vaccination with *M. bovis* BCG [274].

Nowadays, there are two clinical trials in progress where NMIBC patients are previously vaccinated with *M. bovis* BCG Tokyo or RUTI (a proposed vaccine for TB) [275–277]. Additionally, another article published in 2019 manifests the safety of vaccinating NMIBC patients with *M. bovis* BCG and the ability to enhance the cytotoxicity of γδ T cells and NK against some tumour cells K562 or RT4, but not T24 [254].

Considering that patients who do not respond to *M. bovis* BCG therapy are among the main concerns among physicians, a boosting strategy could improve their response to the treatment. Therefore, further research is needed because the possible benefits of a mycobacterial vaccination are still unresolved.

Finally, achieve the most optimal schedule would able to reach improved outcomes, reduce side-effects, and diminish the requirement of *M. bovis* BCG. Accordingly, the Bladder Cancer Advocacy Network (BCAN) proposed that patients with intermediate-risk NMIBC can receive a weekly instillation of chemotherapy (mitomycin, gemcitabine or epirubicin) for six to eight weeks and follow a maintenance phase for one year; be treated with one-third of the current dose of *M. bovis* BCG, or avoid maintenance period with *M. bovis* BCG. Similarly, high-risk NMIBC patients can receive one-third of *M. bovis* BCG dose in both induction and maintenance phases or be treated with chemotherapy (mitomycin C, gemcitabine, epirubicin or a combination of gemcitabine/docetaxel) for a year. Especifically, the maintenance phase can be reduced from 3 to 1 year in the case of low-risk tumours, and cystectomy must be considered in high-risk tumours [276].

Remarkably, finding the proper maintenance schedule seems to be challenging due to many factors that could modify the outcome, such as the tumour stage of the patients, *M. bovis* BCG substrain used or the received dose [278].

1.2.4.2   Recombinant *M. bovis* BCG

Because of the necessity to improve BC treatment to reduce its pathogenicity and improve its antitumour effects, *M. bovis* BCG has been genetically modified.

M. bovis BCG Moreau was modified to express the S1 subunit of the pertussis toxin, which induced a Th1 immune response and immunogenicity in a murine BC model [279,280]. Similarly, a recombinant *M. bovis* BCG modified to release high levels of the STING agonist, c-di-AMP, increased the production of pro-inflammatory cytokines and increased the

antitumour effect [281]. Another approximation proposed by Nieuwenhuizen *et al.* consists of replacing the urease C from *M. bovis* BCG with a lysin of *Listeria monocytogenes.* Urease C is responsible for the neutralization of the phagosome; thus, its deletion leads to phagosome maturation. At the same time, listeriolysin alters the phagosome membranes, and mycobacterial antigens are released into the cytosol. The modified *M. bovis* BCG in Phase I clinical trials showed reduced pathogenicity and enhanced T cell responses. It is currently tested in Phase II [282].

The release of antimicrobial peptides by mammalian cells to face pathogens in the urinary tract reduce *M. bovis* BCG effectiveness. Consequently, the modification of *M. bovis* BCG to express proteins that inhibit those antimicrobial peptides enhanced an increased *M. bovis* BCG internalization, cytokine release and BC cells death [283].

Another plausible alternative to improve the current therapy is based on the encapsulation of *M. bovis* BCG cell wall skeleton, which seems to inhibit bladder tumour cells *in vitro* and *in vivo* [284]

1.2.4.3   Other *M. bovis* BCG alternatives

Several procedures have been proposed to diminish infections due to the live form of *M. bovis* BCG instillations. The most used method to kill mycobacteria is autoclaving. However, mycobacterial components can be altered, damaged, and even destroyed when exposed to high temperatures and pressure. Accordingly, most of the published studies testing the antitumour and immunostimulatory effect of HK-*M. bovis* BCG suggests a diminished antitumour and immunostimulatory impact [285].

Another method to inactivate mycobacteria is ɣ-irradiation, which maintain metabolically active mycobacterial cells, although they are not viable. Accordingly, ɣ-irradiated *M. bovis* BCG prolonged survival of BC tumour-bearing mice, yet less efficiently than its life form [286].

Otherwise, components such as CpG of *M. bovis* BCG, which TLR-9 recognises, showed an antitumour and immunostimulatory effect murine BC model [287]; or CW of *M. bovis* BCG stabilized using octa-arginine liposomes inhibited BC cell growth *in vitro* [288] and in the BC rat model [289].

1.2.5 Alternatives to *M. bovis* BCG

As previously mentioned, some alternatives for NMIBC patients are based on the complete replacement of *M. bovis* BCG. Some approaches are described below:

1.2.5.1 Chemotherapy

Mitomycin C, epirubicin, gemcitabine or pirarubicin are some of the most studied chemotherapeutic agents in a BC context. It has been shown that gemcitabine intravesically administered in BC patients was more efficient in reducing tumour growth than epirubicin or pirarubicin. [290]. Besides, combinations of chemotherapeutic agents or with *M. bovis* BCG have also been addressed. For instance, gemcitabine and docetaxel were well-tolerated and effective in patients unable to receive *M. bovis* BCG [291,292]. Similarly, *M. bovis* BCG with chemotherapeutic agents has been extensively reviewed and can reduce adverse effects and be valuable for patients with intermediate and high-risk NMIBC [293].

1.2.5.2 Checkpoint inhibitors

T cells can differentiate between healthy and tumour cells in a healthy immune system. Accordingly, T cells recognise proteins on the surface of healthy cells, called immune checkpoints. However, some tumour cells can express immune checkpoint molecules to survive and perpetuate the tumour inside the body. Scientists have developed molecules to block specifically checkpoints, called checkpoint inhibitors, and activate the antitumoral immune response with application in several kinds of cancer.

Regarding NMIBC, pembrolizumab, an anti-programmed receptor 1 (PD-1), granted accelerated approval by the FDA for treating high-risk *M. bovis* BCG-unresponsive patients unsuitable for cystectomy [294]. Besides, the combination of checkpoints with other therapies is also being tested. For instance, the POTOMAC study compares the effect of *M. bovis* BCG alone or in combination with durvalumab (an anti-PD-L1) in high-risk NMIBC patients[275].

1.2.5.3 Virus-Based Treatments

Viruses are an incredible tool to introduce genetic material into a specific and modify its behaviour. In phase I clinical trial, the Coxsackievirus A21 enterovirus induced BC cell lysis [295] and fowlpox virus encoding GM-CSF triggered local and systemic immune response [296]. Similarly, a recombinant adenovirus with a polyamide surfactant to facilitate the adherence to tumour cells showed improved recurrence-free survival in a phase II trial and is currently tested in phase III clinical trial [297].

1.2.5.4 Bacteria-Based Treatments

The use of other bacteria or bacteria-derived components has also been studied as substitutes for *M. bovis* BCG to avoid the undesirable effects triggered by the current treatment [298].

Accordingly, *Salmonella choleraesuis* improved BC tumour-bearing mice survival rates and triggered immune system response [299]. *Salmonella enterica* Ty21a also triggered an immune response, and it is in phase I clinical trial [300]. In the case of genera *Lactobacillus, Lactobacillus casei* showed an antitumour effect in a BC mouse model *in vivo* due to NK activation [301], or *Lactobacillus rhamnosus* triggered an improvement of mice survival rates after the infiltration of NK cells into the bladder [302].

Bacteria-derived components have also been postulated as promising alternatives. For instance, neutrophil-activating protein from *Helicobacter pylori,* recognised by TLR-2, reduced tumour growth and triggered a Th1 response in a BC mice model [303]; oncolytic virus expressing the enterotoxin A from *Staphylococcus aureus* showed antitumour activity in a subcutaneous murine model of BC [304], or simultaneous administration of enterotoxins A and B into the bladder also triggered an anti-angiogenic effect [305]. Besides, *Streptococcus*-derived immunomodulator OK-432 demonstrates cytotoxic activity in BC tumour cells *in vitro* [306] and reduced tumour size and metastasis when administered in the BC rat model [307].

Outstandingly, intravesical administration of exotoxin A fused to the humanized antibody against the epithelial cell adhesion molecules (EpCAM) from *Pseudomonas* showed a complete response in 44% of high-grade NMIBC patients who failed *M. bovis* BCG treatment when tested in a Phase II trial. Currently, it is being studied in a phase III trial [308].

1.2.5.5 Mycobacteria-based treatments

Mycobacteria species are characterised by their complex cell wall. Because some lipids and glycolipids are shared among mycobacterial species, the antitumour activity triggered by other mycobacterial species has also been assessed:

- *M. tuberculosis*: the transport phosphate protein PstS1 activated the immune system and prolonged survival rates in the BC mice model [309].
- *M. bovis*: the antigenic protein MPT-64 prolonged tumour-bearing mice survival while inducing IFN-ɣ production systemically [310].
- *M. phlei*: the complex formed by the cell wall and the nucleic acid, called MCNA, was a safe and effective alternative as a treatment for *M. bovis* BCG non-responders patients in a Phase III study [311,312]. However, CW of *M. phlei* (MCWE) formulated in mineral oil in water emulsion was tested in high-risk NMIBC patients, who had to stop the treatment due to side effects or treatment failure [313]. Otherwise, the

antitumour activity of the HK-*M. phlei* has been addressed with similar outcomes that the life form *in vitro* [286,314].

- *M. vaccae*: Few studies are available assessing the use of *M. vaccae* for BC treatment, with worse antitumour effect than *M. bovis* BCG [315]. *M. vaccae* has two morphotypes, the smooth and the rough morphotype, that diverge in the existence of polyester on the surface of the smooth morphotype. Later, the smooth morphotype was more efficient in inhibiting tumour cells than the rough morphotype *in vitro* [314].

- *M. smegmatis*: Although it is considered a nonpathogenic mycobacterium, several notifications of infection had restricted the use of its live form. However, *M. smegmatis* CW extracts, or *M. smegmatis* modified to express human TNF-α showed an antitumour and immunostimulatory effect either *in vitro* or *in vivo* [316].

- *M. kansasii*: The antigen 85 (Ag85) complex is a mycolyl transferase complex formed by three antigenic proteins (A, B and C), which is present in all mycobacterial species. Ag85 can be found either in the cytosol and the CW, and it is responsible for transporting TMM and TDM to the mycobacterial surface. Besides, it is also a fibronectin-binding protein that induces a Th1 response. Ag85 cDNA from *M. kansasii* or engineered DC expressing Ag85 inhibit tumour growth while activating the immune system in a mouse bladder tumour model [317,318].

- *Mycobacterium indicus* pranii (MIP) was previously known as *Mycobacterium w*. HK-MIP, combined with radiation, triggered 100% survival rates in a small clinical trial formed in five BC patients [310]. It has been recently demonstrated that MIP can induce tumour regression via Myd88/TLR2 [180].

1.2.5.6   *M. brumae*

As previously shown, an attractive approach to replace *M. bovis* BCG is to consider the use of non-pathogenic mycobacteria species. Accordingly, promising results have been obtained when *M. brumae* has been used *in vitro* and *in vivo*.

M. brumae is an environmental mycobacterium isolated from soil and water samples, firstly described in 1993 [319]. Its antitumour effect was discovered after comparing the inhibition triggered in seven different bladder tumour cell lines of a wide range of mycobacteria species. *M. brumae* was the only mycobacterium able to inhibit high-grade tumour cell growth, similarly to *M. bovis* BCG, and even superior in low-grade tumour cell lines. Additionally, it triggered an immune response based on proinflammatory cytokines and chemokines such as IL-6 or CXCL-8 in PBMCs [314].

Besides, HK-*M. brumae* triggered a similar inhibition of tumour cells growth than the live form *in vitro*, yet inducing less cytokine production [286].

Introduction

When *M. brumae* was tested in an orthotopic BC mice model, *M. brumae*-treated tumour-bearing mice survived longer than untreated or *M. bovis* BCG-treated tumour-bearing mice [314,320]. Moreover, it induced both local and systemic immune response. After *M. brumae* intravesical treatments, immune cells such as T, NK and NKT cells were infiltrated into the bladder and cytokines released in the urine. IgG antibody production or splenocytes proliferation demonstrated the systemic immune response also triggered after the therapy [321]

The safety of *M. brumae* has been extensively proved. None case of infection has been described along through the literature. *M. brumae* is also unable to persist inside human or mouse macrophages or tumour cells [314], and its safety has recently been demonstrated by intravenous administration of the live form in two animal models, *Galleria melonella* and mice [322].

Therefore, *M. brumae* is potentially interesting as an alternative to the current treatment of NMIBC patients due to several reasons. Firstly, the immunotherapeutic effect of *M. brumae* in different tumour cells. Second, *M. brumae* is a fast-growing mycobacterium, simplifying the manufacturing process compared with *M. bovis* BCG. Finally, the extensively studied safety of *M. brumae* would avoid several adverse effects found during *M. bovis* BCG instillations.
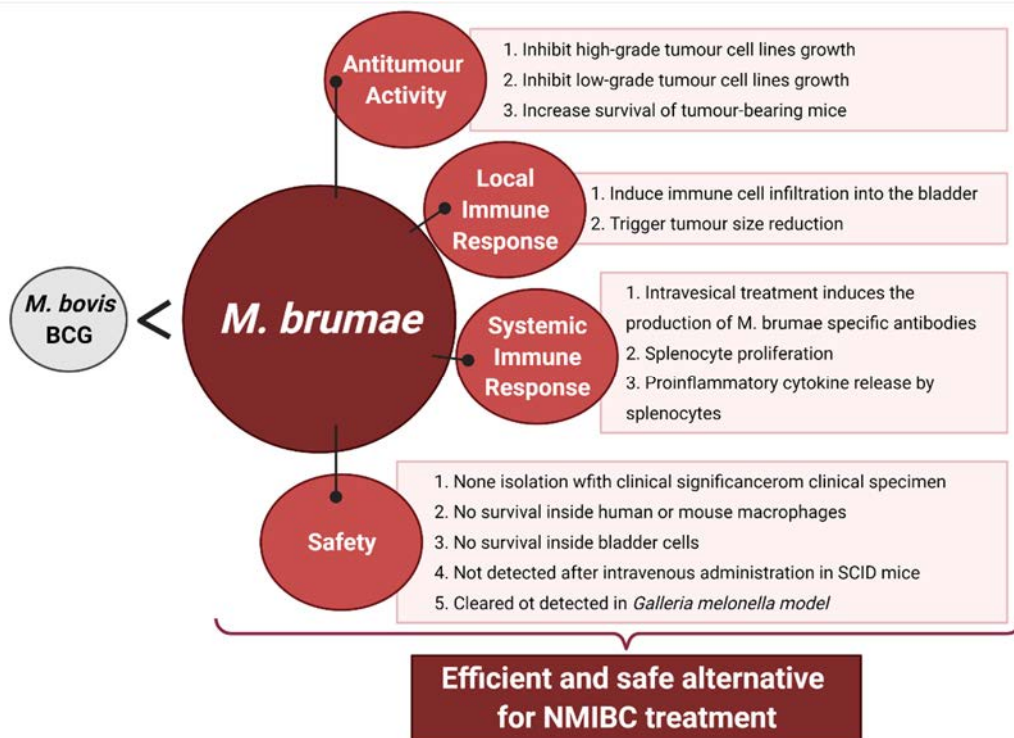
Figure 12. **Beneficial effect of *M. brumae*.** Information obtained from Noguera-Ortega (2015), Noguera-Ortega (2016), Noguera-Ortega (2018), Bach-Griera (2020) [314,320,322,323]

2 - RESEARCH GAP AND OBJECTIVES

M. bovis BCG is the preferred treatment for NMIBC patients. However, the side effects observed in 70 % of patients, together with the fact that 30 % of patients do not respond to *M. bovis* BCG treatment, lead to exploring further alternatives, such as using the nonpathogenic *M. brumae*. The exact mechanism of action of *M. bovis* BCG and, specifically, the antigens implicated in its antitumour response are still to be deciphered. Therefore, culture medium composition could modify mycobacteria characteristics, and consequently, their antitumour and immunostimulatory effect. Few studies report the impact of culture composition, and when these do exist, outcomes are limited to using *M. bovis* BCG as the vaccine for TB, but not for BC treatment [66]. Therefore, more work needs to be done when mycobacteria are produced for anticancer purposes to understand the mycobacteria mechanism of action and improve the treatment outcome.

Additionally, recent literature supports that subcutaneous vaccination with *M. bovis* BCG improves the immune response induced by intravesical instillations of *M. bovis* BCG for cancer treatment [170]. However, further information is required to decipher whether prior vaccination with either another mycobacterium such as *M. brumae* could be helpful for the treatment of BC.

Objectives

The first hypothesis was that mycobacteria's immunomodulatory and antitumour effect depends on the culture media used for their growth. The second hypothesis was that subcutaneous vaccination with *M. brumae* or *M. bovis* BCG boosts the immune response triggered by later intravesical instillations in tumour-bearing mice.

- ❖ Objective 1: To evaluate the impact of culture media composition in mycobacteria growth, physiological and physicochemical characteristics.
    - ◆ To optimize the growth of *M. brumae* in the different Sauton compositions.
    - ◆ To elucidate the lipidic profile and the microscopic appearance of *M. brumae* and *M. bovis* BCG grown on different culture media.
    - ◆ To determine the physicochemical characters of *M. brumae* and different *M. bovis* BCG sub-strains grown on different culture media.

- ❖ Objective 2: To study the antiproliferative and immunomodulatory effect of *M. brumae* and *M. bovis* BCG grown on different culture media.

- ❖ Objective 3: To analyse the antitumour effect of *M. brumae* and *M. bovis* BCG grown on different culture media in an orthotopic BC mouse model.

♦ To analyse tumour-bearing mice survival after intravesical treatment with *M. brumae* or *M. bovis* BCG grown on different culture media.

♦ To evaluate the local and systemic immune response triggered by mycobacteria intravesical treatments.

❖ Objective 4: To study the systemic immune response triggered by subcutaneous vaccination with *M. brumae* or *M. bovis* BCG previous to intravesical instillations in tumour-bearing mice.

3 - MATERIAL AND METHODS
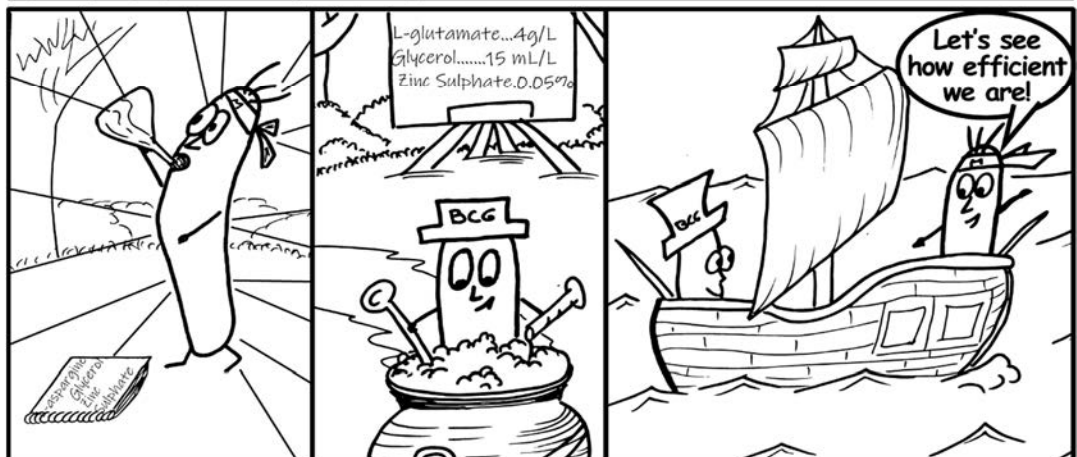
3.1   Growth of Bacteria Strains

M. brumae and *M. bovis* BCG Connaught were used to evaluate the impact of culture media composition. Besides, *M. bovis* BCG substrains were used to analyse the response to neutral red staining and analyse the lipid surface grown on different culture media. *Escherichia coli,* chosen as a negative control, was cultured in Luria Bertani (LB) solid medium.

Bacteria used are summarized in Table 4.

Table 4.   Characteristics of bacteria used in experiments

Bacteria	ATCC	Biosafety Level	Incubation Time (days)
M. brumae	51384	1	7
M. bovis BCG Connaught	35745	2	21-28
M. bovis BCG Glaxo	35741	2	21-28
M. bovis BCG Moreau	35736	2	21-28
M. bovis BCG Phipps	35734	2	21-28
M. bovis BCG Tice	27289	2	21-28
Escherichia coli	10536	1	1

ATCC: American Type Culture Collection

3.2   Culture media

The following culture media were used along through the experiments

3.2.1   Middlebrook 7H10

It is composed of agar Middlebrook 7H10 supplemented with 10% of Oleic-Albumin-Dextrose-Catalase (OADC). Firstly, OADC was prepared (Table 5):

Table 5.   OADC preparation

Component	Company	Volume
BSA (Bovine Serum Albumin)	Roche	5 g
Glucose	Panreac	2 g
NaCl	Panreac	0.85 g
Catalase	Sigma	4 mg
Oleic Acid	Sigma	0.05 g

Components were mixed one after the other (sequentially) in 100 mL of dH_2O and filtered into a sterile bottle using a 0.22 μm filter. After incubation at 37 °C for 24 hours, agar Middlebrook 7H10 medium was prepared (Table 6).

Material and Methods

Table 6.   Middlebrook 7H10 preparation

Component	Company	Volume
Middlebrook 7H10 medium	Difco	19 g
Glycerol	Panreac	5 mL

Components were mixed in 900 mL of dH$_2$O. The mixture was autoclaved at 121 °C for 10 min. After cooling the medium below 60 °C, OADC was carefully added under sterile conditions. Finally, the supplemented culture medium was mixed and plated in Petri dishes.

3.2.2   Middlebrook 7H9

It is composed of agar Middlebrook 7H9 supplemented with 10% of Albumin-Dextrose-Catalase (ADC). Firstly, ADC was prepared. Components were mixed in 100 mL of dH$_2$O and filtered using a 0.22 filter (Table 7). After incubation at 37 °C for 24 hours, ADC was used to complement Middlebrook 7H9 medium.

Table 7.   ADC preparation

Component	Company	Volume
BSA (Bovine Serum Albumin)	Roche	5 g
Glucose	Panreac	2 g
NaCl	Panreac	0.85 g
Catalase	Sigma	4 mg

Components were mixed in 900 mL of dH$_2$O (Table 8). The mixture was autoclaved at 121 °C for 10 min. After cooling the medium above 60 °C, ADC was carefully added under sterile conditions.

Table 8.   7H10 medium preparation

Component	Company	Volume
Middlebrook 7H9 medium	Difco	19 g
Glycerol	Panreac	5 mL

3.2.3   Sauton media

Different culture media compositions were used along through the experiment to evaluate the impact of the Sauton formula on mycobacteria growth. In all the cases, components were mixed in 800 mL of dH$_2$O and pH was adjusted to 7.2–7.3. Then, volume was adjusted to 1 L, and 50 mL were distributed in 100 mL glass bottles. All media were sterilized by autoclaving for 15 min at 121 °C.

The first set of experiments were performed to evaluate the influence of the zinc sulphate on *M. brumae* growth. Two different concentrations of glycerol (30 o 60 mL/L), L-asparagine (4 g/L) or L-glutamate (4 g/L) in the presence/absence of zinc sulphate were used (Table 9). When preparing 1L of culture media, 14 mg/L of zinc sulphate were dissolved into 10 mL of dH$_2$O. Then, 1 mL of the suspension was added to culture media.

Table 9.   Sauton composition to evaluate the zinc sulphate influence

Component	Company	Volume
L-glutamate or L-asparagine	Panreac	4 g
Citric Acid	Fluka	2 g
Potassium Dihydrogen Phosphate	Panreac	0.5 g
Ferric Ammonium Citrate	Sigma-Aldrich	0.05 g
Magnesium Sulphate Heptahydrate	Fluka	1 g
Zinc sulphate	Panreac	1.4 mg or ∅
Glycerol	Panreac	30 mL or 60mL

∅: no addition of zinc sulphate

Later, the influence of glycerol concentration together with the amino acid source was analyzed. Two concentrations of L-glutamate (2 or 4 g/L) or L-asparagine (4 g/L) were used in combination with three glycerol concentrations (15, 30 or 60 mL/L) (Table 10).

Table 10.   Sauton composition to evaluate the influence of glycerol

Component	Company	Volume
L-glutamate or L-asparagine	Panreac	2 g or 4 g
Citric Acid	Fluka	2 g
Potassium Dihydrogen Phosphate	Panreac	0.5 g
Ferric Ammonium Citrate	Sigma-Aldrich	0.05 g
Magnesium Sulphate Heptahydrate	Fluka	1 g
Zinc sulphate	Panreac	1.4 mg
Glycerol	Panreac	15 mL. 30 mL or 60mL

Finally, the following culture media (A60, G15 and G60) were the optimized compositions used to evaluate the antitumour and immunostimulatory effect of *M. brumae* and *M. bovis* BCG (Table 11).

Table 11.   Composition of the Optimized Sauton media: A60, G15 and G60

Component	Company	Sauton A60 Volume	Sauton G15 Volume	Sauton G60 Volume
L-asparagine	Scharlau	4 g	∅	∅
L-glutamate	Panreac	∅	4 g	4 g
Citric Acid	Fluka	2 g	2 g	2 g
Potassium Dihydrogen Phosphate	Panreac	0.5 g	0.5 g	0.5 g
Ferric Ammonium Citrate	Sigma-Aldrich	0.05 g	0.05 g	0.05 g
Magnesium Sulphate Heptahydrate	Fluka	1 g	1 g	1 g
Zinc sulphate	Panreac	1.4 mg	1.4 mg	1.4 mg
Glycerol	Panreac	60 mL	15 mL	60 mL

∅: no addition of the component

3.2.4   LB agar media

Components were mixed in 1 L of dH$_2$O and pH adjusted to ph=7. Then, 15 g of Bacteriological Agar (Schalau) was added and mixed. Finally, the mixture was autoclaved at 121 °C for 15 min. After cooling the medium below 60 °C, the culture medium was plated in Petri dishes (Table 12).

Table 12.   LB composition

Component	Company	Volume
Triptone	Scharlau	10 g
Yeast extract	Panreac	5 g
Sodium Chloride	Panreac	10 g

3.3   Bacteria storage and bacteria growth in liquid culture

Bacteria stock was conserved at -40°C in 20% skimmed milk for extended storage. Skimmed milk powder was solved in distilled water (20%, p/v) and autoclaved for 15 min at 115 °C. When milk suspension achieved room temperature, bacteria from solid media was scratched and added to Eppendorfs containing 1 mL of 20% skimmed milk.

To unfroze bacteria, 0.1 mL of bacteria suspension in 20% skimmed milk was extended on the surface of the appropriate culture medium contained in a Petri dish, according to bacteria requirements. Then, sequential passages in solid media were periodically performed to perform the experiments with fresh bacteria. Before incubating *M. brumae* or *M. bovis* BCG, Petri dishes were wrapped twice or three times with Parafilm®, respectively, to avoid culture medium desiccation. Bacteria were incubated at 37 °C for the required time. Once bacteria were properly grown, Petri dishes were maintained at room temperature for experiments or passages.

M. bovis BCG substrains and *M. brumae* colonies were scraped from Middlebrook 7H10 medium with a Kölle handle. Bacteria were transferred to a sterile glass tube containing glass beads and vortexed to disaggregate the clumps. Then, 3 mL of phosphate-buffered saline (PBS) were added to the tube and vortexed. Big clumps were allowed to settle for 20-30 min. After precipitation, the supernatant was transferred to a new glass tube where the turbidity was adjusted to McFarland 1. Then, 0.3 mL of a suspension containing 1.5 x 10^6 CFU was carefully added to the surface of each bottle containing 50 mL of liquid medium. Liquid cultures were incubated in static conditions for 11 or 28 days for M. brumae or *M. bovis* BCG, respectively.

Inoculums were corroborated by platting the solution in 7H10 Middlebrook plates. CFU/mL were obtained after incubating *M. bovis* BCG plates at 37 °C for three weeks and *M. brumae* plates for one week.

3.4   Biomass production in liquid media

Pellicles from mycobacteria grown on liquid media under static conditions were collected on day 11 for *M. brumae* and day 28 for *M. bovis* BCG. At that time point, mycobacteria were recovered from glass bottles by disrupting the pellicle with a sharply hit and throwing the mixture on a funnel covered with a filter. When the total of mycobacteria was recovered, mycobacteria extract was dried entirely under the hood.

3.5   Cell culture conditions

Several BC cell lines were chosen to evaluate the effect of *M. brumae* and *M. bovis* BCG grown on different culture media. BC cell lines have different origins, such as mice or human carcinomas, and in turn, can possess different grades of differentiation depending on the BC cell stage and origin. Additionally, the J774 mouse macrophages and the THP-1 human macrophages were also used in experiments.

Eukaryotic cells were conserved at -80ºC in cryovials containing 1 mL of 20% dimethyl sulfoxide (DMSO, Merck) in FBS at a concentration of 1 to $3 \cdot 10^6$ cells/mL. To unfroze eukaryotic cells, cell suspension stored in a cryovial was melted in a warm bath. Then, the suspension was transferred to a Falcon containing 5mL of complete culture media and centrifuged for 10 min at 300 *g*. Supernatant was discarded by decantation to eliminate DMSO from the medium. Pellet was resuspended in 5 mL of the required media. Periodical passages of eucaryotic cells were performed when cell confluency reached around 80% of the flask.

Origin, grade of differentiation and culture conditions are summarized in Table 13.

Table 13.   Differences among BC cell lines

BC cell line	Origin	Grade	Culture media
SW780	Human	BC Grade 1	DMEM/Ham's F12 nutrient mixture (Gibco)
5637	Human	BC Grade 2	DMEM-F12
T24	Human	BC Grade 3	DMEM-F12
MB49	Mice	BC Grade 3	Dulbecco's modified Eagle's medium (DMEM) with L-glutamine (Gibco)
J777	Mice	Macrophage	DMEM
THP-1	Human	Macrophage	Roswell Park Memorial Institute medium (RPMI) (Lonza)

Material and Methods

All culture media were supplemented with 10% Fetal Bovine Serum (FBS) (Lonza), complete media, and antibiotics when required. Cells were maintained in complete media with antibiotics (100 U/mL penicillin G (Laboratorios ERN) and 100 g/mL streptomycin (Laboratorio Reig Jofré) at 37°C in a humidified atmosphere with 5% CO_2.

3.6   Tumour growth inhibition experiments

BC cells attached to the bottom of the flask were resuspended using tripsine, which enable the breakage of peptide unions between protein cells and the plastic surface. Then, cells were resuspended in culture media without antibiotic and counted using a Neubauer Chamber. The concentration of BC cells was adjusted at 3×10^5 cells/mL, and 100 µL were added to each well of a 96 well-plate. Cells were incubated for 3 h at 37°C in a humidified atmosphere with CO_2.

Then, mycobacteria inoculum was prepared to infect BC cells. Mycobacteria from pellicles were recovered using a sterile Kölle handle and deposited on sterile paper to dry the cells under the hood. *M. brumae* and *M. bovis* BCG suspensions were prepared according to McF 1 turbidity, as previously explained in 4.3. The suspension was centrifuged at 1640 *g* for 10 min, and the supernatant was discarded. Pelleted bacteria were resuspended with the appropriate culture medium without antibiotic to achieve a final concentration of 3×10^6 bacteria/mL. The final suspension was sonicated three times for 30 sec, and 100 µL were used to infect each well. Infected BC cells were incubated at 37°C in a humidified atmosphere with CO_2 for three hours. Then, extracellular mycobacteria were removed by three washes per well with 200 µL of tempered PBS. Each well was refilled with 200 µL of the appropriate complete media, and the 96 well-plate was incubated at 37°C in a humidified atmosphere with CO_2 for 72 h.

After the incubation, the supernatant was recovered, centrifuged at 1000 *g* for 10 min, transferred to a new tube, and stored at -80°C for further cytokine analysis. Moreover, 3-(4,5-dimethylthiazol-2-yl)-2,5-diphenyltetrazolium bromide (MTT) colourimetric assay was performed to analyze the antitumour effect triggered by each mycobacterium. MTT is cleaved by active mitochondrial dehydrogenases, which in turn produce formazan crystals. Accordingly, culture media with 10 % MTT was distributed to each well (100 µL/well). The plate was incubated for 3 h at 37°C in a humidified atmosphere with 5% CO_2 to let the formation of formazan crystals. Then, 100 µL of acidic isopropanol were added to each well to solve the crystals, and the absorbance was measured at 550 nm with a reference wavelength of 630 nm (Infinite 100 PRO, Tecan, Switzerland).

Tumour growth inhibition was calculated at the absorbance value of infected cells divided by the absorbance value from non-infected cells (considered 100% of viability). Recorded data were multiplied by 100 to express the antiproliferative activity in a percentage.

3.7   Mycobacteria survival inside macrophages

J774 and THP-1 cell lines were used to analyze the mycobacterial burden inside macrophages.

THP-1 cells require to be differentiated to be attached to the bottom of the plates. Firstly, THP-1 cells were centrifuged at 300 g for 10 min and resuspended in culture media without antibiotic. After counting THP-1 cells through a Neubauer chamber, 8.5 x10^4 cells/well in 300 µL were seeded into a 48-well cell culture plate. Then, phorbol 12-myristate 13-acetate (PMA, Abcam) was added to each well at 100 nM in culture media for 48 h. Later, PMA was removed and replaced by complete media without antibiotic for 24 h. Finally, *M. brumae* and *M. bovis* BCG suspensions were prepared as previously explained in 4.3, and macrophages were infected at MOI 10 and 1, respectively.

J774 cells were detached from the culture flask following the same methodology as previously explained for BC cells in 4.6. Then, macrophages were counted and seeded into a 48-well cell culture plate at 6 x10^4 cells/well in 300 µL. After letting their adherence for 3 h at 37°C in a humidified atmosphere with 5% CO_2, they were infected with *M. bovis* BCG or *M. brumae* at MOI 1 and 10, respectively.

THP-1 and J774 infected macrophages were incubated for 3 h at 37°C in a humidified atmosphere with 5% CO_2. Three consecutive washes with tempered PBS were used to remove extracellular mycobacteria, and complete media with antibiotics was finally added to each well.

Plates were incubated at 37°C in a humidified atmosphere with 5% CO_2. At each time-point (3, 24, 48, 72, 96 and 120 hours), the supernatant was recovered, centrifuged at 1000 g for 10 min and transferred to a new tube. Then, it was stored at -80°C for further cytokine analysis. Macrophages attached to the bottom of the well were exposed to 0.1 % Triton X-100 (Sigma-Aldrich) for 15 min at 37 °C to lysate the cells and release the intracellular mycobacteria. Viable mycobacteria were counted through plating serial dilution on Middlebrook 7H10 plates.

3.8 Cytokine, Chemokine and Nitric Oxide (NO) Analysis

Commercially available enzyme immunoassays were used and followed according to the manufacturer's instructions to determine cytokines and chemokines in culture supernatants. Table 14 describes all cytokine or chemokine analyzed in experiments, the origin of the supernatant, and the commercial manufacturer of each cytokine.

Table 14.   Summary of cytokines analysed

Cytokine/Chemokine	Culture Supernatant	Company
IL-1β	Macrophages	Mabtech (Sweden)
IL-2	Splenocytes	Mabtech
IL-4	Splenocytes	Mabtech
IL-6	BC cells, macrophages, Peritoneal Exudate Cells (PECs)	Becton & Dickinson (BD, USA)
IL-8	BC cells	BD
IL-12 (p40)	Macrophages, PECs	Mabtech
IL-17	Splenocytes	Mabtech
CXCL-1 / KC	BC cells	R&D Systems (USA)
IFN-γ	Splenocytes/PECs	Mabtech
TNF-α	Macrophages, PECs	Mabtech

NO was also measured in J774 macrophages. The curve pattern consists of serial dilutions of 200 µM sodium nitrate (Panreac) in PBS and, 50 µL were added to 96-half well plates (Corning). Blank consisted of PBS without sodium nitrate. To analyse the NO concentration in the samples, 50 µL of culture supernatants were added to each well. Later, 100 µL of Griess Reagent (Sigma) was added to all wells, and the 96-well plate was incubated for 10 to 15 min at room temperature in the dark. Finally, absorbance was measured at 550 nm (Infinite 100 PRO, Tecan, Switzerland).

3.9 Extraction and analysis of mycobacterial lipids

Two different protocols were used to analyze the mycobacterial lipid content. One protocol was used to analyse the total lipid content of mycobacterial cells. In contrast, the other protocol was used to decipher the most superficial exposed lipids in the mycobacterial cell wall. Once lipid extraction was performed, lipid composition was analyzed by thin-layer chromatography (TLC).

3.9.1 Extraction of total non-covalent-linked lipids
Mycobacteria pellicles grown on the surface of the liquid media were recovered from inside the bottle with a sterile Kölle handle and dried under the hood to avoid the presence of culture media in the sample. To achieve the complete dryness, mycobacteria recovered with a Kölle handle was placed over a sterile filter paper, settling on a sterile Petri dish. Later, 0.2

g of dried mycobacteria was transferred to a glass bottle with a politetrafluoretile (PTFE) liner screw cap. Similarly, 0.2 g of mycobacteria grown on solid media, such as Middlebrook 7H10, were scratched and transferred to a glass bottle. A solution consisting of 5 mL of chloroform and 10 mL of methanol (chloroform:methanol, 1:2) was added to the bottles. Perfectly closed bottles were maintained in constant stirring overnight.

The day after, organic solvents were recovered in a new glass tube using a glass funnel covered with one filter paper. Collected organic solvents were evaporated inside a dry block heater at 37°C under a nitrogen stream, closed in a nitrogen atmosphere, and stored at 4°C. Otherwise, cellular debris was dried under the hood, collected from the filter paper, and mixed with 10 mL of chloroform and 5 mL of methanol (chloroform:methanol, 2:1) inside a glass bottle with a PTFE cap. Closed bottles were maintained in constant stirring overnight.

The following day, organic solvents were recovered in the same glass tube in which the previous organic phase was collected, as described above. Then, the tube containing the liquid phase was evaporated under a nitrogen stream. A mixture of 8 mL of chloroform, 4 mL of methanol, and 2 mL of 0.04% of $CaCl_2$ in dH2O was used to resuspend the lipidic extract. The mixture containing the lipids was transferred to a cone separatory funnel, mixed gently and let to settle until observing two transparent and differentiated phases. Then, the bottom phase corresponding to the lipidic extract was recovered in a new glass tube. Similarly, the upper phase corresponding to the most polar lipids were recovered into another tube. Both tubes were evaporated, closed, and saved at 4°C for TLC analysis.

3.9.2   Extraction of superficial non-covalent-linked lipids

Superficial lipid extraction was only performed after a proper growth of the pellicle, which means that the mycobacteria pellicle covered the whole surface of the liquid medium and reached a considerable thickness at day 11 for *M. brumae* and day 28 for *M. bovis* BCG.

Twenty mL of petroleum ether (40-60º) were added very softly on the top of the mycobacteria pellicle without touching the pellicle. The solvent was in contact with the pellicle for 5 min with the glass bottle hermetically closed. After the incubation, petroleum ether (40-60°C) was recovered with a glass Pasteur pipette and transferred to a glass tube. Finally, the liquid content of the glass tube was evaporated under nitrogen stream, closed and saved at 4°C for TLC analysis. Figure 14 shows the main steps to decipher the total lipidic content of mycobacteria cells.

Material and Methods

3.9.3 Analysis by TLC

Lipidic extracts obtained through total or superficial extraction were analyzed by one-dimensional (1D) -TLC in 20 cm x 20 cm silica gel plates (Merck). The lipidic extract was resuspended in 0.2 to 1 mL of chloroform, and 10 µL were deposited directly on a TLC plate using a capillary glass tube (Blaubrand ®). Samples were let to dry for 5 minutes at room temperature. TLC chamber was saturated for at least 20 minutes with the appropriate mobile phase, which covered at least 1 cm of the bottom of the chamber. Then, the TLC plate was inserted into the chamber and, the mobile phase allowed to run through the whole TLC plate. TLC plate was removed from the chamber when solvent reached 1 cm distance from the upper end of the plate. Finally, the TLC plate was dried under laminar flux and revealed with the appropriate staining. Depending on the staining, TLC plates needed to be heated for 2 to 5 min at 120ºC. The composition of mobile phases, staining, and lipids observed throughout the experiments are summarized in Table 13.

Figure 13. Mobile phases used to decipher the presence of mycobacterial lipids

Mobile Phase	TLC Stain	Heating at 120 °C	Sample	Lipids
Petroleum ether: diethyl ether (90:10)	10% Molybdatophosphoric acid hydrate (Merck) in ethanol absolute (Carlo Erba)	Yes	Superficial and Total extraction	AG, PDIM,
Chloroform:Methanol (96:4)	10% Molybdatophosphoric acid hydrate in ethanol absolute	Yes	Superficial and Total extraction	GroMM, PGL
Chloroform:Methanol:Water (30:8:1)	1% anthrone (Sigma) in sulfuric acid 95-97% (Merck)	Yes	Total Extraction	TDM, TMM
Chloroform:Methanol:Water (65:25:4)	1% anthrone in sulfuric acid 95-97%	Yes	Total Extraction	TMM, PIMs
Chloroform:Methanol:Water (65:25:4)	Molybdenum Blue Spray Reagent, 1.3 % (Sigma)	No	Total Extraction	PIMs
Chloroform:Methanol:Water (65:35:8)	1% anthrone in sulfuric acid 95-97%	Yes	Total Extraction	TMM, PIMs

Figure 14. Scheme of the main steps to decipher the total lipidic content of mycobacteria cells
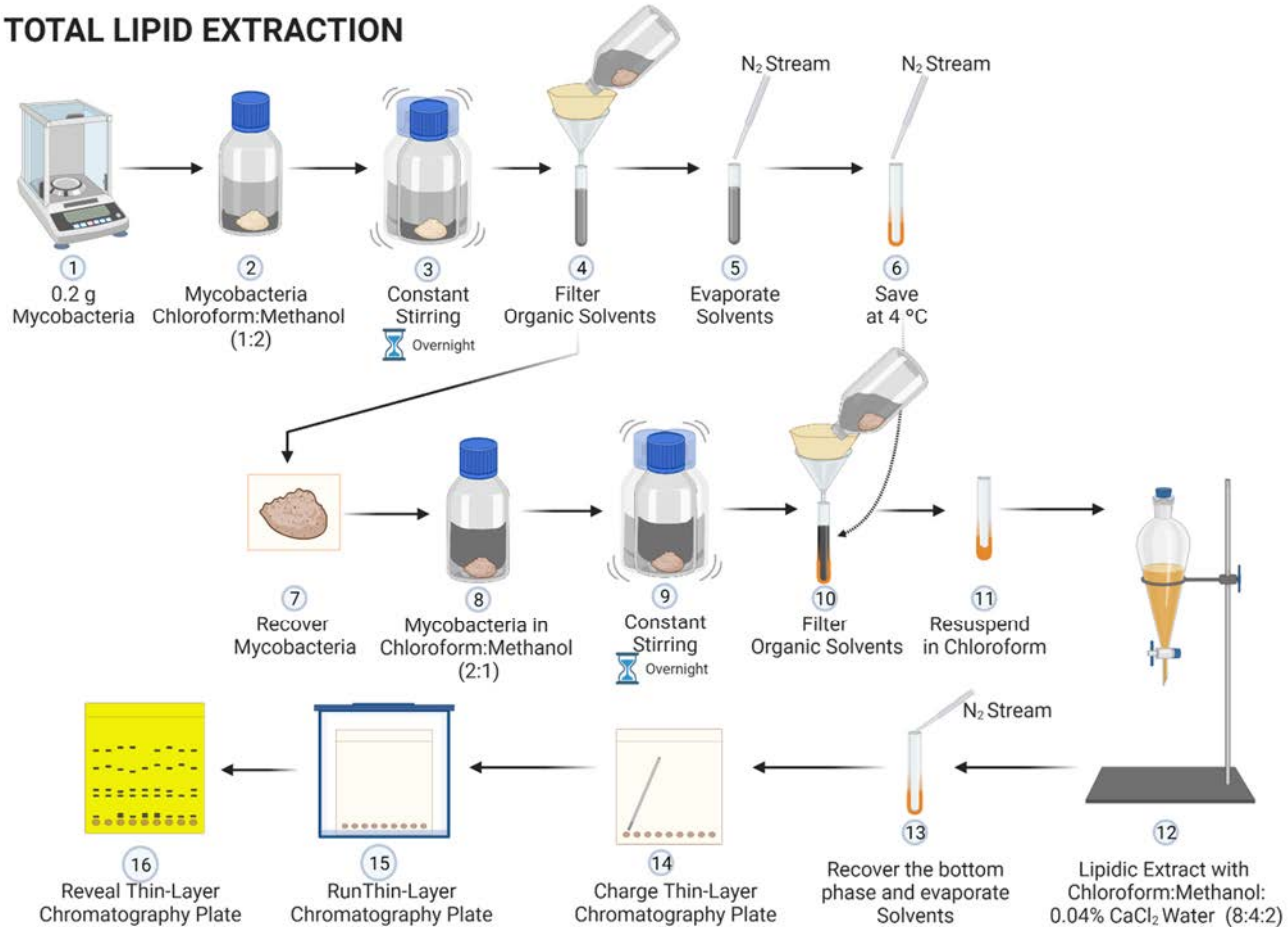
Modified from Guallar-Garrido *et al.* (2021) [324]

3.10 Lipid purification and NMR analysis

Most apolar lipids found on the surface of mycobacteria were purified and analyzed by nuclear magnetic resonance (NMR).

Lipid extract obtained after performing the superficial lipidic extraction was resuspended in 200 μL of chloroform, and 10 μL were added to a Silica Gel 60 (Merck, Germany) column stabilized with PE (60-80°C b.p). Increasing diethyl ether concentrations were used to elute the spots observed on the TLC plate eluted with petroleum ether:diethyl ether (90:10). Then, fractions containing the eluted spots were evaporated under a nitrogen stream. After corroborating the isolation of the different lipids from the initial extract by TLC, NMR analyses were performed.

A similar Silica Gel 60 column was used to isolate GroMM and PGL. Accordingly, chloroform was used to stabilize the column, and increasing methanol concentrations were required to elucidate the spots. The fractions collected were evaporated, and lipid purification was corroborated using TLC before the NMR analysis.

To identify lipid content through NMR, each purified lipid was resuspended in 600 μL of $CDCl_3$ (99.80 % D, Cortecnet, France) and transferred to a 5-mm diameter NMR tube. A Bruker Avance II 600 NMR spectrometer (Bruker Biospin, Germany) equipped with a 5 mm TBI probe with Z-gradients, operating at a 1H NMR frequency of 600.13 and 298.0 K of temperature, was used. A standard 90° pulse sequence with an acquisition time of 1.71 s and a relaxation delay of 2 s was used to acquire 1D ^{1}H NMR spectra.

Data were collected into 32 K computer data points, with a spectral width of 9590 Hz and as the sum of 1024 transients. The resulting free inductions decays (FIDs) were Fourier transformed, manually phased, and baseline corrected. In the quantitative 1D ^{1}H NMR spectrum, the relaxation delay was set to 15 s. 2D NMR experiments were performed to confirm molecular structures. 1H,1H-COSY (Correlation Spectroscopy) and ^{1}H,^{13}C-HSQC (Heteronuclear Single Quantum Coherence) were performed using standard Bruker pulse sequences and acquired under typical conditions.

All spectra were calibrated using the residual solvent signal (CHCl3,δH, 7.26 and δC, 77.0 ppm). Chemical shift data are expressed in ppm and coupling constants (J) values in Hz. The diversity of peaks is abbreviated as s (singlet), d (doublet), t (triplet), dd (doublet of doublets) and m (multiplet). Integration was performed with MestreNova 8 (Mestrelab Research S.L.) and its global spectral deconvolution (GSD) application.

RMN analysis was done at the Servei de Ressonància Magnètica Nuclear from the Autonomous University of Barcelona.

3.11 Neutral red staining

Dried mycobacteria from pellicles or mycobacteria scratched from solid media were transferred to a screw-cap tube until completely filling its bottom. Then, 5 mL of 50% methanol in distilled water were added to the tube, and mixed with mycobacteria cells. Tubes were hermetically closed and incubated for 1 h at 37 °C. Later, the solvent from the tube was carefully discarded using a Pasteur glass pipette, and 5 mL of 50% methanol in distilled water were again added to the tube to wash the cells twice. The tube was mixed, closed and incubated for 1 h at 37 °C.

Pentobarbital buffer (PB) was prepared by solving 5 g of NaCl and 1 g of Sodium 5,5 diethyl butyrate in 100 mL of de-ionized water [pH 9.8]. Then, 0.02 g of neutral red (Merck, Germany) were solved in 10 mL of PB. Lastly, 0.9 mL of PB containing the neutral red were mixed with the remaining 90 mL of PB without neutral red to achieve a final concentration of 0.002%.

After discarding the wash solvent from inside the tubes, 2 mL of PB containing neutral red were added to each tube. Tubes were incubated at room temperature in the dark. Finally, the colour reaction was read 1 hour after adding PB solution.

3.12 Evaluation of mycobacterial cell surface hydrophobicity

Mycobacteria pellicles were filtered, dried under the hood and transferred to conical tubes. Dried mycobacteria were suspended in 10 mL of phosphate urea magnesium sulphate (PUM) buffer [K_2HPO_4, 17 g/L; KH_2PO_4, 7.26 g/L; urea, 1.8 g/L; $MgSO_4 \cdot 7H_2O$, 0.2 g/L], gently disaggregated with a vortex for 10 min, and left to settle for 1-2 min to avoid clumps. The supernatant was discarded, and 10 mL of PUM buffer were added to perform the second wash. Then, 3 mL of the suspension of around OD 1-1.2 at 400 nm were transferred to two new tubes (control and test tubes). In the test tube, 2.4 mL of hexadecane were added, vortexed and incubated at 37 °C for 8 min. Two differentiated phases were obtained after 15 min at room temperature, and the bottom phase was recovered. Finally, the absorbance of 200 μL of the control suspension and bottom phase was measured at 400 nm (Infinite 100 PRO, Tecan, Switzerland). Percentage of hydrophobicity was obtained comparing the OD at 400 nm of bacterial suspension in PUM buffer alone and in the presence of n-hexadecane. Results show the mean ± Standard Deviation (SD) of at least three independent experiments.

3.13 Orthotopic model of bladder cancer and intravesical treatment

Animal experiments were executed according to procedures approved by the Ethics Animal Care Committee (CEEA) of the Autonomous University of Barcelona and Generalitat de Catalunya. The welfare of the animals was contemplated by reducing the number of animals and duration of the procedures. Animals used throughout the experiments were maintained in quarantine to guarantee healthy conditions for one week before their manipulation.

During the experiment, all animals were housed with a maximum of six animals per cage with food and water *ad libitum* in an enriched environment, in a Biosafety Level (BSL) 2 facility. Animals were weighed and examined for their appearance, behaviour, and clinical signs every day to avoid unnecessary suffering. Moreover, all experiments were carried out under inhaled anaesthesia, 1.5-2 % isoflurane in pure O_2 and eyes protected with liquid ophthalmic gel.

The orthotopic model of BC in mice was performed according to previous experiments developed in our laboratory. Eight animals per group were used to analyze the immune response triggered by mycobacteria treatments, while 10 animals per group were used to analyse tumour-bearing mice survival. C57Bl/6 female mice (6 to 8-week-old, Charles River Laboratories, Spain) per group were randomized and anaesthetized. Animals were maintained in a supine position to perform the experiment. The bladder was emptied through a superficial massage of the abdominal region. Then, chemical lesions on the urothelium of the bladder were induced by an intravesically instillation of 50 µL of Poly-L-Lysine solution (PLL, Sigma) through a 24-gauge catheter for 15 min. Then, PLL was poured out of the bladder to instillate 100 µL of DMEM without FBS containing 10^5 MB49 cells for 1 hour. Finally, the bladder was emptied, and animals recovered from the anaesthesia. The day after tumour induction, mice were anaesthetized, and the bladder was emptied. Then, animals received 100 µL of PBS, 100 µL of PBS containing 2 x 10^7 CFU of *M. brumae,* or 100 µL of PBS containing 2 x 10^6 CFU of *M. bovis* BCG grown on different culture media. Mycobacteria dose was previously optimised [314]. Treatments were repeated weekly on day 8, 15 and 22, for a total of 4 treatments, following the schedule shown in Figure 15.
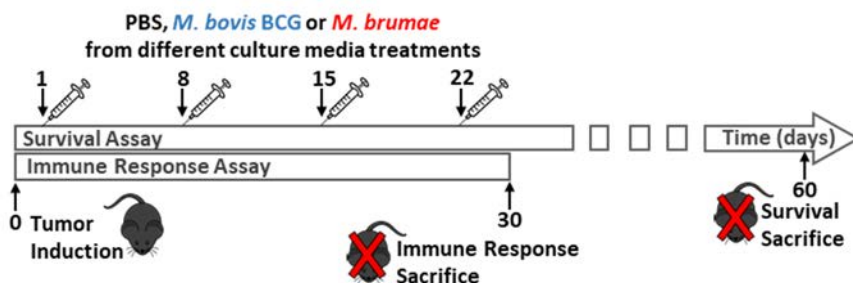
Figure 15. **Schematic schedule of *in vivo* experiments to evaluate the effect of culture media**

One set of animals were sacrificed at day 30 by cardiac puncture and cervical dislocation under isoflurane anaesthesia to analyze the systemic and local triggered immune response. Accordingly, blood, bladders and spleens were removed in aseptic conditions. Samples were conserved in ice until their analyses.

Another set of animals were used to analyze mice survival. Surviving animals were sacrificed by cervical dislocation at day 60 to obtain the bladder and spleens in aseptic conditions. Then, bladders were fixed in 10% neutral buffered formalin for histopathological evaluation. Four-micrometer paraffin-embedded sections were stained with Hematoxylin and Eosin (H&E). Otherwise, spleens were resuspended in 5 mL of PBS, disrupted with tweezers, and desegregated by passing the suspension through a 23 *g* needle. Then, serial dilutions of the homogenates were plated on Middlebrook 7H10 plates to determine and count *M. brumae* and *M. bovis* BCG's presence after 1 and 4 weeks of incubation at 37 °c, respectively. A negative (healthy mice) and a positive (non-treated tumour-bearing mice) control group were used in all the experiments. Mice from the healthy group received the PLL instillation, but PBS was used instead of either BC tumour cells or mycobacteria treatments. Otherwise, the positive control received PLL and BC tumour cells, but PBS alone was used for the intravesical treatments. Table 15 shows the established groups for the study.

Table 15.   Mice groups included in experiments to evaluate the impact of culture medium.

	Mice group	PLL	Tumour cells	Treatment
	M. brumae -A60	Yes	Yes	*M. brumae* -A60
	M. brumae -G15	Yes	Yes	*M. brumae* -G15
	M. brumae -G60	Yes	Yes	*M. brumae* -G60
	M. brumae -7H10	Yes	Yes	*M. brumae* -7H10
	M. bovis BCG-A60	Yes	Yes	*M. bovis* BCG-A60
	M. bovis BCG-G15	Yes	Yes	*M. bovis* BCG-G15
	M. bovis BCG-G60	Yes	Yes	*M. bovis* BCG-G60
	M. bovis BCG-7H10	Yes	Yes	*M. bovis* BCG-7H10
	Tumour	Yes	No	PBS
	Healthy	Yes	Yes	PBS

PLL: Poly-L-Lysine; -A60: Mycobacteria grown on Sauton A60; -G15: Mycobacteria grown on Sauton G15; -G60: Mycobacteria grown on Sauton G60; -7H10: Mycobacteria grown on Sauton 7H10; PBS: phosphate-buffered saline.

3.14 Orthotopic model of bladder cancer and intravesical treatment for vaccinated animals

Experiments to evaluate the impact of previous vaccination in the orthotopic BC model were performed following the schedule indicated in Figure 16.
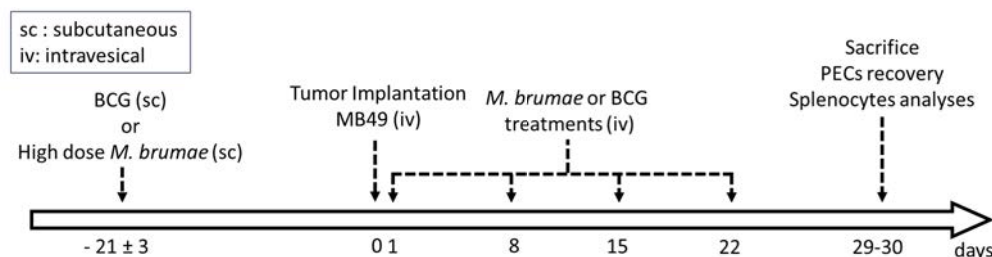
Figure 16. Schematic schedule of *in vivo* experiments to evaluate the impact of vaccination

Each group of animals consisted of eight randomized C57Bl/6 female mice. From 18 to 21 days before the tumour implantation, animals were vaccinated subcutaneously with 100 µL of PBS containing 2×10^7 CFU of *M. brumae* (low dose), 2×10^8 CFU of *M. brumae* (high dose) or 2×10^6 CFU of *M. bovis* BCG. Control groups were considered those groups without vaccination and/or treatment (see Table 16).

Table 16. Mice groups included in experiments to evaluate the impact of previous vaccination

Mice group	Vaccination	PLL	Tumour Cells	Treatment
	2×10^7 CFU of *M. brumae*	Yes	Yes	PBS
	2×10^7 CFU of *M. brumae*	Yes	Yes	*M. brumae*
	2×10^8 CFU of *M. brumae*	Yes	Yes	PBS
	2×10^8 CFU of *M. brumae*	Yes	Yes	*M. brumae*
	M. bovis BCG	Yes	Yes	PBS
	M. bovis BCG	Yes	Yes	*M. bovis* BCG
	M. bovis BCG	Yes	Yes	*M. brumae*
	PBS	Yes	Yes	*M. brumae*
	PBS	Yes	Yes	*M. bovis* BCG
	PBS	Yes	No	PBS
	PBS	No	No	PBS

PLL: Poly-L-Lysine; PBS: phosphate-buffered saline.

M. brumae used for both vaccination and treatments were grown on Sauton A60 culture medium, while *M. bovis* BCG was grown on Middlebrook 7H10. Tumour and mycobacterial intravesical instillations were performed as previously explained in Section 4.13. Animals were euthanized on day 30 by cardiac puncture and cervical dislocation under isoflurane anaesthesia. Blood, spleens, lungs and peritoneal exudate cells (PECs) were removed and collected in aseptic conditions for further experiments.

3.15 PECs recovery

After cleaning the mice abdomen with 70% ethanol, superficial scission using sterile scissors and forceps was performed over the mice's left leg, allowing the exposition of the peritoneum. Then, 5 mL of sterile PBS + 3% FBS were carefully introduced into the peritoneum cavity through a syringe with a 25-gauge needle. After vigorous massage of the mouse abdomen, PECs were collected in a 15 mL tube. PECs were maintained in ice until their use. Once in the laboratory, PECs were centrifuged for 5 min at 4 °C at 310 g, and the supernatant was discarded. Finally, cells were resuspended in FBS + 10% DMSO and frozen at -80 °C until use.

3.16 Antitumour and immunostimulatory effect of PECs

PECs were unfrozen to determine the antitumour effect on MB49. Cryovial containing 1 mL of PECs was resuspended in 1 mL of RPMI and transferred to a 15 mL tube. The tube was centrifuged for 5 min at 300 g at room temperature. Then, the supernatant was discarded to eliminate residual DMSO. Pelleted cells were resuspended in 1 mL of complete RPMI medium and transferred to 35 mm Petri dishes (Nunc, Thermo Fisher) that were previously filled with 4 mL of complete RPMI medium for at least 20 min. The presence of culture media in the plates previous to the addition of cells facilitate PECs adherence. Cells were incubated for 2 hours at 37 °C in a humidified atmosphere with 5% CO_2 to let cells adhere to the plate's bottom. Then, the supernatant was discarded, and PECs were recovered using a cell scraper in 1 - 2 mL of complete RPMI medium. PECs were counted with a Neubauer chamber and adjusted to a final concentration of 1.5 x 10^5 PECs/mL. One mL of the suspension was distributed in 24 well-plates. Plates were incubated for 24 hours at 37 °C in a humidified atmosphere with 5% CO_2. After the incubation, PECs supernatant was recovered, centrifuged to eliminate cellular debris, transferred to a new Eppendorf and kept at -80 °C for further cytokine analyses. Then, 1 mL of a suspension of MB49 cells in complete RPMI medium at a concentration of 7.5 x 10^3 MB49 cells/mL were added on PECs surface to achieve the ratio of 20:1 (effector:target) in each well. Plates were incubated for 48 hours at 37 °C in a humidified atmosphere with 5% CO_2. The attached cells were resuspended in 0.1 mL of tempered PBS to perform the counting in a Neubauer chamber. Size cells enable to differentiate into MB49 cells (big size) and PECs (small size).

3.17 Antitumour and Restimulation effect of Splenocytes

To evaluate the antitumour effect of splenocytes, 10^4 MB49 cells in 100 µL of RPMI plus 10% FBS without antibiotics were seeded in a 96-well plate the day before the sacrifice. Plates were incubated overnight at 37 °C in a humidified atmosphere with 5% CO_2

After recovering and counting, 100 µL of splenocytes resuspended in RPMI plus 10% FBS without antibiotics were added to each well. A ratio of 25:1 (splenocytes: tumour cell) was used for experiments analyzing the impact of culture media, and a ratio of 12.5:1 for experiments to decipher the effect of *M. brumae* or *M. bovis* BCG vaccination. Plates were incubated for 24 h at 37°C in a humidified atmosphere with 5% of CO_2. Then, wells were vigorously washed with 250 µL of warm PBS to eliminate any presence of splenocytes. Finally, MTT was performed to measure MB49 cells viability, as explained in Section 4.6.

Splenocytes were also adjusted to a final concentration of 3×10^6 cell/mL to evaluate its reestimulatory effect. Then, 180 µL of the suspension was added to each well and was restimulated with 20 µL of PBS (negative control), 5 µg/mL of Concanavalin A (ConA, Sigma, positive control), or 1mg/mL of *M. brumae* or *M. bovis* BCG grown on the same medium used for mouse treatment. Plates were incubated for 72 hours at 37 °C in a humidified atmosphere with 5% CO_2. After the incubation, plates were centrifuged for 10 min at 250 - 300 *g* to pellet suspended splenocytes. Supernatants were recovered, centrifuged to eliminate cellular debris, transferred to a new tube and stored at -80°C for cytokine analyses. Finally, splenocytes proliferation was measured through MTT assay.

3.18 IgG detection in sera

Blood taken from sacrificed mice was maintained at room temperature for at least 2 hours to allow coagulation. Then, the coagulum was collected through a sterile Kölle handle and discarded. The remaining liquid was centrifugated at 3500 *g* for 10 min at room temperature. Finally, supernatant that refers to serum was transferred to a new tube and frozen at -80 °C for further analysis.

To analyze IgG levels in sera, the bottom of the 96-well plate was coated overnight at room temperature with 20 µg/mL of heat-killed (HK)-*M.brumae* or HK-*M. bovis* BCG, grown on different culture medium suspended in carbonate-bicarbonate buffer at pH 9.6. HK-mycobacteria suspension was prepared in a carbonate buffer (30% of Na_2CO_3 and 70% of $NaHCO_3$ in water) and autoclaved for 30 minutes at 121°C. After overnight incubation, the plate was washed five times with Tris-buffered saline (TBS) for 5 minutes each wash. Then, wells were blocked with 100 µL of 0.5% gelatin (Sigma) in TBS for at least 2 hours. Samples were diluted at 1:20 in TBS and added to wells. Sera of each animal was exposed to mycobacteria grown on the same medium used for intravesical treatment, and to mycobacteria grown on Middlebrook 7H10. Plates were incubated for 24 hours at room temperature. The day after, plates were washed five times with 100 µL of TBS for 5 minutes.

Anti-mouse IgG alkaline phosphatase conjugate (Southern Biotech, Birmingham, AL, USA) was diluted 1/200 in TBS + 0.05% gelatin, 50 μL added to each well, and incubated for 1 hour at room temperature. Plates were washed 5 times with 100 μL / well of TBS for 5 minutes, and 100 μL of P-nitrophenyl phosphate (Sigma) were finally added to each well to develop the enzyme-substrate reaction. Absorbance was measured after 40 minutes of incubation at 405 nm using a multiscan reader (Tecan). Control or blank wells consist of wells containing sera without antigen adhered to the bottom of the well. Their absorbance was deducted to wells with sera plus antigen for each animal.

3.19   Detection of infiltrated immune cells into the bladders

The infiltration of the immune cells into the bladder was analyzed by flow cytometry. Firstly, bladders were extracted from mice in sterile conditions and transferred to a sterile tube containing RPMI maintained in ice until their analysis. Then to label the immune cells, bladders were minced using a scalpel and digested with 0.5 mg/mL collagenase II (Sigma, Spain) and 1U/mL DNAse I in RPMI medium supplemented with 5% FBS for two-three successive 30 min cycles, shaking at 37 °C. The cell suspension was filtered using a 40-μm disposable plastic strainer (Becton & Dickinson) and pelleted for staining. Immune cells were labelled with antibodies summarised in Table 17.

Table 17.   Used antibodies to analyse immune cells infiltrated into the bladder

Antibody	Clon	Company
PerCP-CD45	30F11	Biolegend
APC-Cy7-CD3	145-2c11	Biolegend
FITC-CD4	RM4-5	Biolegend
Alexa 700-CD8	53-6.7	Biolegend
APC-CD62L	MEL-14	Biolegend
BV786-CD127	A7R34	Biolegend
PE-Dazzle-CD44	IM7	Biolegend
FITC-CD45R/B220	RA3-6B2	Biolegend
Live/dead fixable Aqua Dead Cell Stain kit	-	Invitrogen

To obtain and analyze the results, morphological parameters were used to define the lymphocyte gate. Dead cells were eliminated using a live/dead stain kit (live/dead fixable Aqua Dead Cell Stain kit, Invitrogen). Immune cells infiltration acquisition was performed in a Fortessa flow cytometer (Becton & Dickinson), and the data were analyzed using FlowJo software (9.8v; TreeStar, USA). Absolute cell numbers were obtained by using Perfect-Count Microspheres (Cytognos). All analysis were done by the Tissue Virology group from the Germans Trias i Pujol Institute for Health Science Research (IGTP).

3.20 Preparation for ultrastructural Assessment of Mycobacterial Pellicles

Mycobacteria pellicles grown on different culture media were collected using a nucleopore membrane (Whatman ®Nuclepore™) and were placed over aluminium foil structures incorporated into 6-well plates (Nunc ® Thermo Scientific™). To fix the pellicles, 250 µL of 4% osmium tetraoxide (TAAB Lab, UK) were added to each well and maintained at 4 °C overnight. For Scanning Electron microscopy (SEM) analysis, fixed pellicles were deposited on stubs with carbon adhesive discs. Then, pellicles were metallized with a gold-palladium alloy in three-four minutes cycles (Emitech Au-Metallizer). EVO® MA 10 microscope (Oberkochen, Germany) was used to analyze the pellicle structure. All analysis were done at the Servei de Microscopia from the Autonomous University of Barcelona.

To analyse the length of each mycobacterial cell, 50 entire bacilli from the top of the cords were randomly chosen for each condition. Then, the length of the major axis was measured by two blind evaluators and from duplicate experiments using ImageJ software.

3.21 Statistics

All in vitro experiments were performed at least three times. The data represent the mean and the standard deviation (SD) of three independent pellicles per condition.

The student's t-test was used to assess the statistical significance of differences for biomass production in the presence of zinc sulphate in Sauton media. Analysis of variance (ANOVA) with Bonferroni post-test was used to assess the significance of amino acid source and glycerol concentration in biomass production, mycobacteria length, mycobacteria survival inside macrophages, antitumour activity on tested cell lines, cytokine production, hydrophobicity experiments and *ex vivo* experiments. Log-rank (Mantel-Cox) test was used to evaluate differences between mice survival curses. Immune infiltration data were analyzed using Mann-Whitney tests, and Spearman tests analyzed their correlations to IL-17 and IFN-ɣ.

Analyses were performed using GraphPad Prism version 6.0 or 8.0 software (San Diego, CA, USA). Statistical significance was considered at $p < 0.05$.

4 - RESULTS
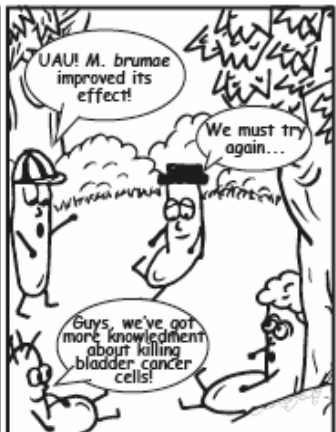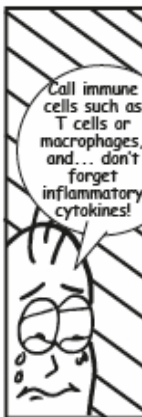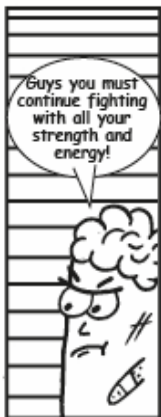
4. 1 Study to evaluate the impact of culture media composition in mycobacteria growth

4.1.1 Influence of zinc sulphate in Sauton media on *M. brumae* growth: Macroscopic appearance and lipidic and glycolipidic content

After an extensive revision of the different Sauton compositions used along through the literature to grow *M. bovis* BCG (Table 2), the source of nitrogen (L-asparagine or L-glutamate), the amount of carbon in the form of glycerol and the presence of the inorganic compound zinc sulphate, seemed to be the most changeable compounds in culture composition. Accordingly, *M. brumae* was grown on eight different conditions, with 4 g/L of L-asparagine or L-glutamate, two concentrations of glycerol (30 or 60 mL/L) in the presence or absence of zinc sulphate at 1.4 mg/L (Table 18).

Table 18.   **Composition of culture media to evaluate the influence of zinc sulphate on *M. brumae* growth.** Each medium was tested in the presence or absence (-) of $ZnSO_4$.

	L-asparagine		L-glutamate	
	A30	A60	G30	G60
L-asparagine (g/L)	4	4	-	-
L-glutamate (g/L)	-	-	4	4
Glycerol (mL/L)	30	60	30	60
Zinc sulphate (mg/L)	1.4 / -	1.4 / -	1.4 / -	1.4 / -

M. brumae pellicles were carefully grown under the same growth conditions: strict control of the temperature (37°C) in the same incubator, the addition of the same amount of liquid culture medium in the same kind of bottles with the same aeration conditions, or inoculation of the same number of cells. Additionally, all *M. brumae* cultures were grown for 11 days as *M. brumae* belongs to the rapid grower mycobacteria group. Consequently, differences observed in the mycobacteria morphologies are exclusively due to the composition of the culture medium. Firstly, the incubation time was standardized to compare the growth of the cultures according to previous knowledge from Middlebrook 7H10. While *M. brumae* requires 7 days to grow in Middlebrook 7H10 medium, it was necessary to increase the incubation time up to 11 days due to growing in culture medium based on sales, such as Sauton medium.

After an accurate daily observation of the pellicles, when *M. brumae* grown for more than 11 days on the most productive media, pellicles were very thick and, therefore, pellicles precipitated to the bottom of the bottle. However, the thick of pellicles grown on the least productive medium did not improve over time. Thus, *M. brumae* was grown for 11 days to obtaining a proper pellicle to perform further experiments.

Results: Objective 1

The macroscopic appearance of *M. brumae* pellicles was always evaluated on day 11. A daily observation let to observe that mycobacteria initially cover the surface area, and then the thick and folding of the pellicle increase whenever possible. As Figure 17 shows, when the culture medium contained L-glutamate, the addition of zinc sulphate did not provide differences in biomass production or macroscopic appearance. However, macroscopic differences were observed when zinc sulphate was added to the medium in the presence of L-asparagine as the amino acid source, accordingly to the significant increase in biomass production. Moreover, in culture media containing L-asparagine and zinc sulphate, a significant increase in biomass production was observed with increasing glycerol concentrations.

a)

b)
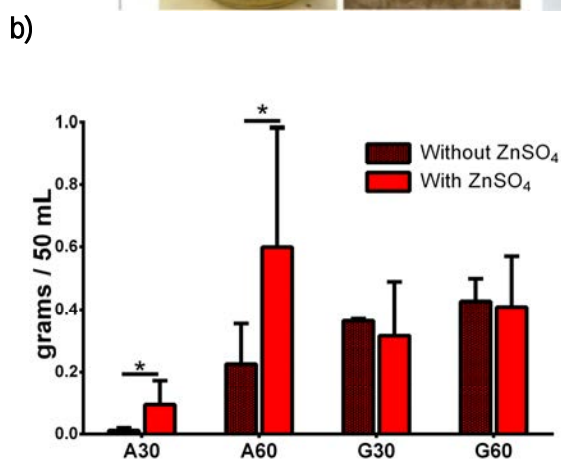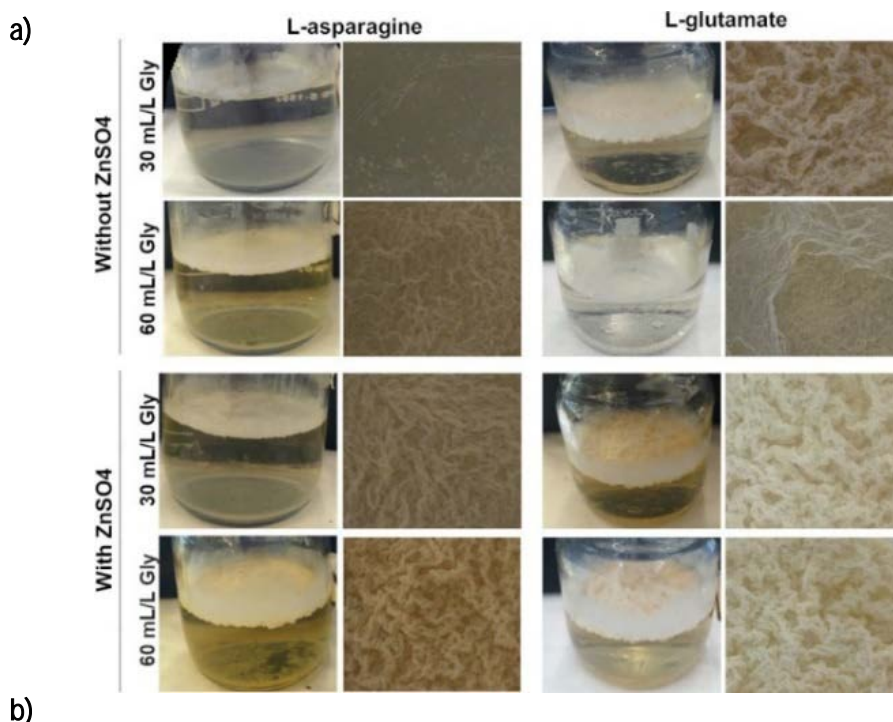
Figure 17. *M. brumae* growth in the presence or absence of ZnSO₄. a) Macroscopic appearance of *M. brumae* pellicles; b) Biomass production expressed in grams per 50 mL of culture media of *M. brumae* pellicles grown on the presence or absence of ZnSO₄

When the lipidic content of mycobacterial cells grown on pellicles was analyzed, no significant differences were found in the presence of AG, TMM or PIMs (Figure 18).
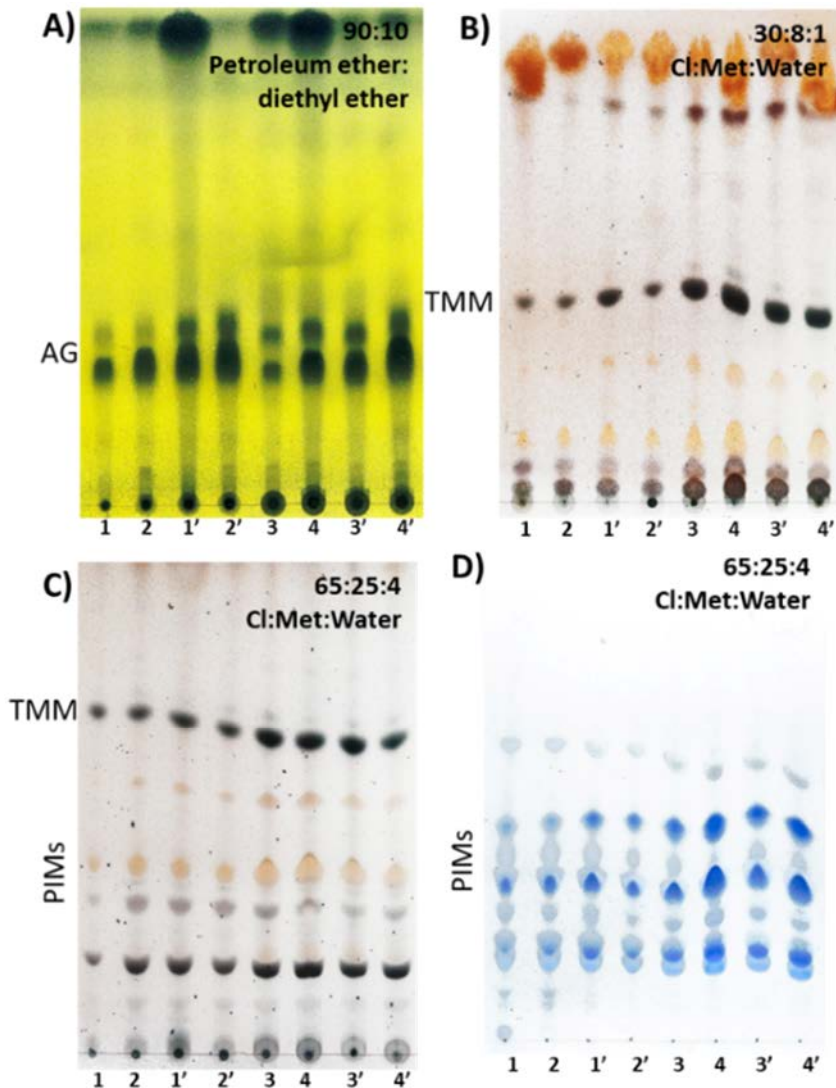
Figure 18. *M. brumae* growth in presence or absence of ZnSO₄. Thin layer chromatographies (TLC) corresponding to the total lipidic extract of *M. brumae* pellicles grown on different culture media. The results are one representative experiment out of at least three biological replicates. TLCs were developed in A) petroleum ether 60 - 80 °C:diethyl ether (90:10, v/v), B) chloroform:methanol:water (30:8:1, v/v/v) and C-D) chloroform:methanol:water (65:25:4, v/v/v). TLCs were revealed with 10% molybdatophosphoric acid in ethanol (A), 1% anthrone in sulfuric acid (B and C), and Molybdenum Blue Spray (D). *M. brumae* grown on: (1-1') L-glutamate and 30 mL/L of glycerol; (2-2') L-glutamate and 60 mL/L of glycerol; (3-3') L-asparagine and 30 mL/L of glycerol; and (4-4') L-asparagine and 60 mL/L of glycerol. *M. brumae* grown on culture media without ZnSO₄ (1-4); and *M. brumae* grown on culture media with ZnSO₄ (1'-4').

4.1.2 Influence of amino acid source and glycerol concentrations in Sauton media on *M. brumae* growth: Macroscopic appearance and lipidic and glycolipidic content

Because of the obtained results, zinc sulphate was added to media compositions, and the influence of the amino acid source and glycerol concentrations was further evaluated to analyse the growth of *M. brumae*. Nine different compositions that differ in glycerol concentration (15, 30 or 60 mL/L) and the amino acid source (L-glutamate or L-asparagine) were used. Compositions are summarised in Table 19.

Table 19. Sauton formulas used to evaluate the influence of increasing glycerol concentrations in the presence of two different amino acid sources on *M. brumae* growth

	L-asparagine			L-glutamate		
	A15	A30	A60	G15	G30	G60
L-asparagine (g/L)	4	4	4	-	-	-
L-glutamate (g/L)	-	-	-	2 / 4	2 / 4	2 / 4
Glycerol (mL/L)	15	30	60	15	30	60

As Figure 19 shows, biomass production of *M. brumae* was increased when the Sauton medium contained L-asparagine and increasing glycerol concentration, which correlates with the macroscopic appearance of pellicles.

However, *M. brumae* growth was not affected by increasing glycerol concentrations in L-glutamate-containing media. Besides, *M. brumae* grown on the Sauton composition containing 2 g/L of L-glutamate did not produce a significant amount of biomass. Accordingly, macroscopic appearance was similar in all cultures formed by L-glutamate. Later, pellicles were recovered to analyse the total lipidic content of the mycobacteria cell composition, yet no differences among all *M. brumae* cultures were found in the presence of AG, TDM, TMM or PIMs (Figure 19)

Given the previous results obtained and based on the biomass production, culture media containing L-asparagine and 60 mL/L of glycerol (A60), 4 g/L of L-glutamate plus 15 mL/L of glycerol (G15), and 4 g/L of L-glutamate plus 60 mL/L of glycerol (G60) were selected for further studies.
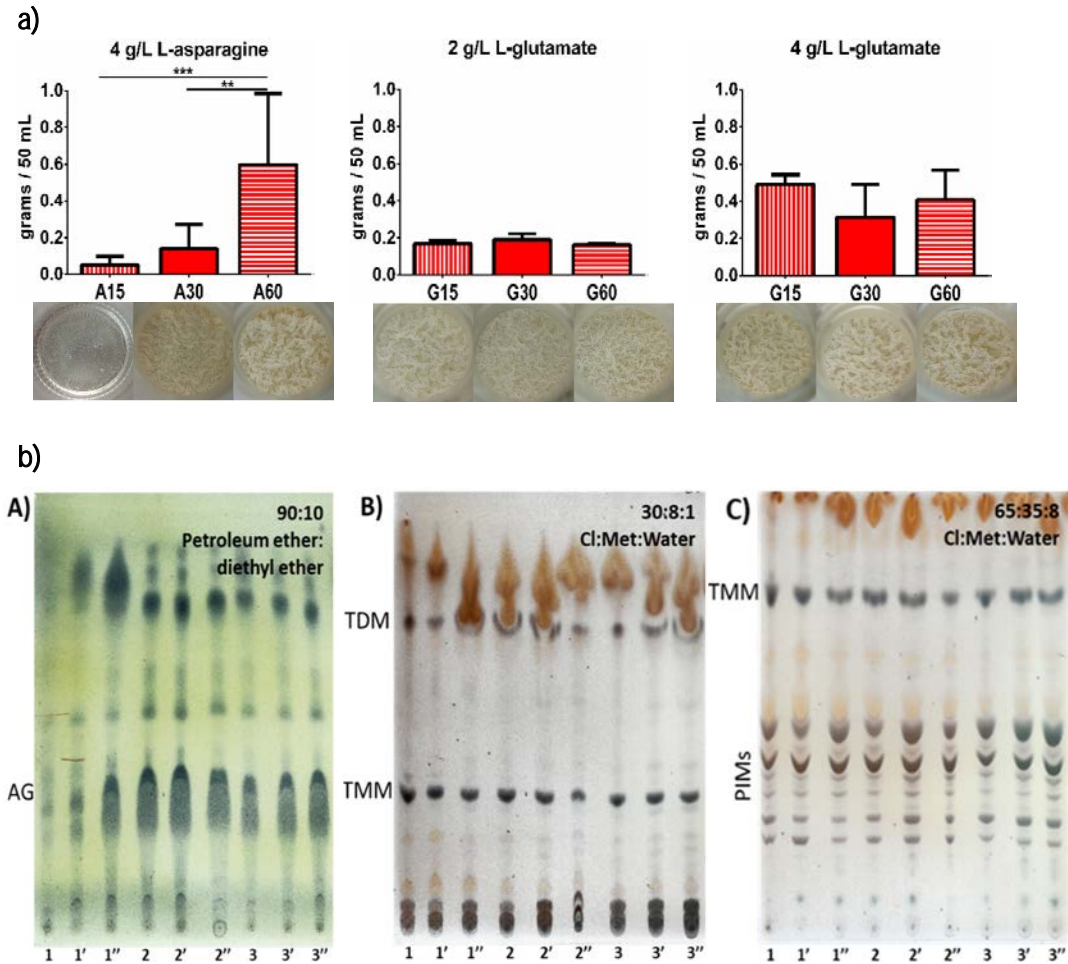
Figure 19. **M. brumae pellicles grown on culture media with L-glutamate or L-asparagine, and increasing glycerol concentrations.** a) Biomass production, expressed in grams per 50 mL of culture media, and macroscopic appearance of *M. brumae* pellicles, grown on the presence of L-asparagine or L-glutamate, and different concentrations of glycerol (30 or 60 mL/L). b) Thin layer chromatographies (TLC) corresponding to the total lipidic extracted using mixtures of chloroform and methanol of *M. brumae* pellicles grown on different culture media. The results are one representative experiment out of several biological replicates. TLCs were developed in A) petroleum ether 60 - 80 °C:diethyl ether (90:10, v/v), B) chloroform:methanol:water (30:8:1, v/v/v) and C) chloroform:methanol:water (65:35:8, v/v/v). TLCs were revealed with 10% molybdatophosphoric acid in ethanol (A), 1% anthrone in sulfuric acid (B-D). *M. brumae* grown on L-asparagine (A) and 15 (1), 30 (1') or 60 (1'') mL/L of glycerol. *M. brumae* grown on 2 g/L L-glutamate (G) and 15 (2), 30 (2') or 60 (2'') mL/L of glycerol. *M. brumae* grown on 4 g/L L-glutamate and 15 (3), 30 (3') or 60 (3'') mL/L of glycerol.

4.1.3   Study of *M. bovis* BCG and *M. brumae* growth in the optimised culture media

4.1.3.1 Macroscopic and microscopic analyses

Once obtained the most productive media for *M. brumae,* the liquid and rich medium Middlebrook 7H9 was included. The four media were also used to grow *M. bovis* BCG as a pellicle. All *M. bovis* BCG pellicles were carefully grown under the same growth conditions and incubated for 4 weeks, as it is a slow-growing mycobacterium.

When the macroscopic analysis was performed, similar pellicles were observed among *M. brumae* grown on A60, G15 and G60, and *M. bovis* BCG grown on A60. *M. bovis* BCG grown on Sauton A60 triggered thick pellicles, consistent, and contained noticeable wrinkles. However, *M. brumae* grown on Middlebrook 7H9 or *M. bovis* BCG grown on G15, G60 and Middlebrook 7H9 produced a fragile, thin, flat and easily breakable pellicle. The pellicle appearance correlated with biomass production. Remarkably, *M. bovis* BCG grown on A60 produced the highest biomass production than all conditions (Figure 20).
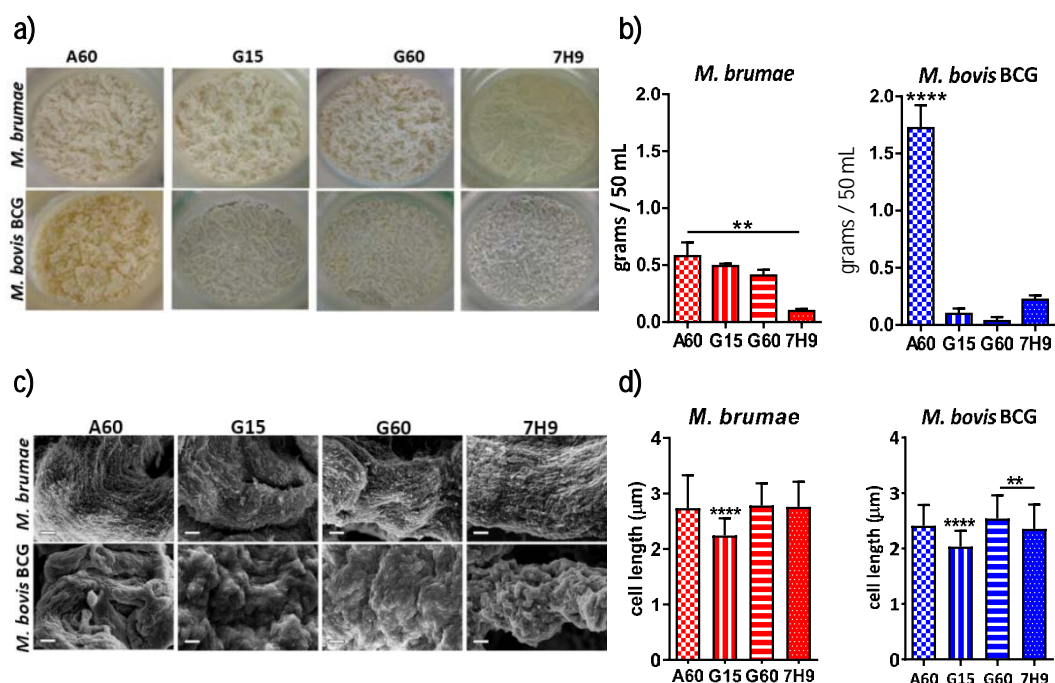
Figure 20.   ***M. brumae* and *M. bovis* BCG pellicles grown on chosen compositions.** a) Macroscopic appearance of mycobacteria pellicles; b) Mycobacteria production expressed in grams per 50 mL of culture medium; c) Representative SEM micrographs comparing mycobacteria pellicles, bar size is 30 μm. d) Mycobacteria cell length expressed in micrometres (μm). *M. brumae* and *M. bovis* BCG grown on optimized Sauton (A60, G15, G60) and Middlebrook 7H9.

M. brumae and *M. bovis* BCG pellicles grown on the four compositions were analyzed through SEM. Although the macroscopic appearance of pellicles was very different among conditions, no significant differences were observed among pellicles of *M. brumae* or pellicles of *M. bovis* BCG (Figure 20c). The length of mycobacteria cells of each pellicle was measured using the SEM micrographs obtained. Mycobacteria cells showed a different size of the major axis depending on the culture medium used for their growth. In both species, the G15 culture medium triggered shorter cells than in the rest of the conditions. Otherwise, similar length was found in the other conditions, except for *M. bovis* BCG grown on G60 or Middlebrook 7H9 (Figure 20d).

Remarkably, *M. bovis* BCG pellicles showed a thick extracellular matrix covering the surface of the pellicles, perceiving mycobacteria cells under this layer. In contrast, *M. brumae* pellicles exhibited an abundant roughness formed by free cells clustered with an apparent directionality creating folds, independently of the culture media used for *M. brumae* growth (Figure 21).
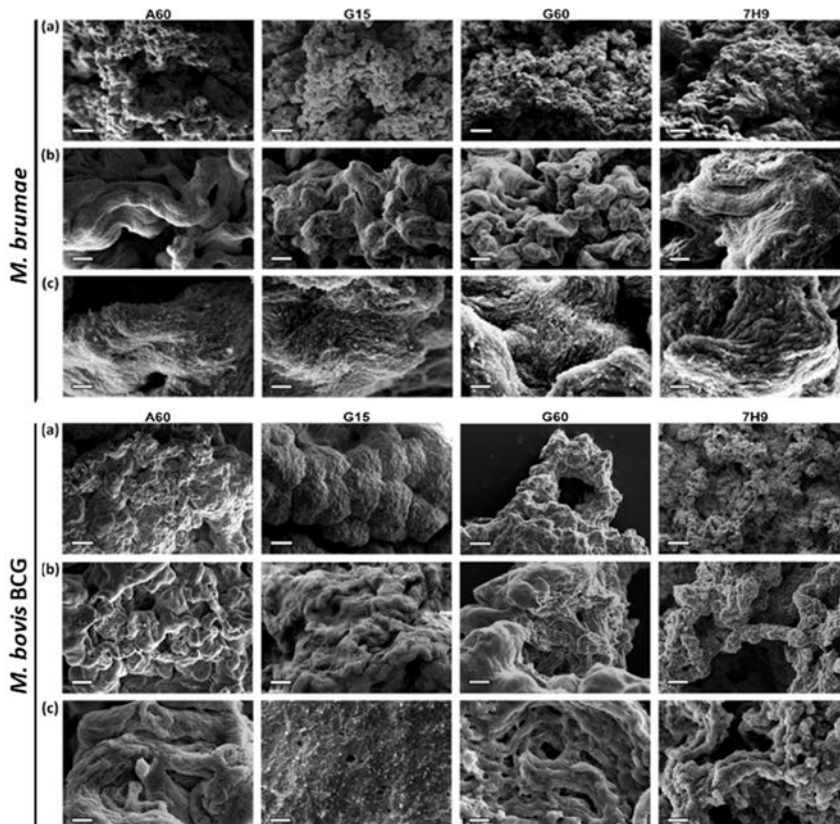
Figure 21. Representative SEM micrographs of *M. brumae* and *M. bovis* BCG pellicles grown on Sauton media and Middlebrook 7H9. a) Appearance of the general surface of the pellicles, scale bars are 130 μm. b) Appearance of structures formed by mycobacteria ordered into the pellicle, scale bars are 30 μm. c) Appearance of detailed bacilli forming part of the pellicle, scale bars are 6 μm.

109

4.1.3.2. Analyses of the total lipidic content of *M. brumae* and *M. bovis* BCG

Mycobacteria species are characterized by their complex and waxy cell wall, as explained in the Introduction section. To evaluate whether the culture medium used for growing mycobacteria modify the composition of the cell wall, *M. brumae* and *M. bovis* BCG were grown on A60, G15 and G60 Sauton media, and on the liquid formulation of Middlebrook medium (7H9) and in its solid formulation (7H10). After extracting the mycobacterial lipids using mixtures of chloroform and methanol, they were analysed by TLC. Different elution systems differing in the polarity were used to study the main described mycobacterial lipids.

The elution system formed by petroleum ether 60-80 °C:diethyl ether (90:10, v/v) was the most apolar composition used to decipher the presence of PDIM and AG. In *M. brumae*, AGs were detected in all conditions and no significant differences were observed among culture media. For *M. bovis* BCG, AGs were similarly seen in all conditions, while PDIM was present in cells grown in A60, G60 and Middlebrook media, but not in cells grown in G15 medium (Figure 22a).

Using a more polar elution system constituted by chloroform:methanol (96:4, v/v), an intense spot, corresponding to GroMM, was detected in *M. brumae* cells that were cultured in media with high glycerol concentration (A60, G60). In the *M. bovis* BCG extract, GroMM was also overproduced in those media with high glycerol concentration. Besides, PGL production was almost abolished when *M. bovis* BCG was cultured in the Sauton medium G15, in contrast to the rest of *M. bovis* BCG conditions (Figure 22b).

When chloroform:methanol:water (30:8:1, v/v/v, or 65:25:4, v/v/v) were used as elution system for further lipid analyses by TLC, the result showed that both mycobacteria species grown in different culture media synthesised TDM and TMM, similarly (Figure 22c). PIMs were detected in *M. brumae* and *M. bovis* BCG, independently of the culture medium used for their growth. However, slight few PIMs seem to be produced by mycobacteria grown in Middlebrook formulas, in contrast to mycobacteria grown in Sauton compositions (Figure 22d).
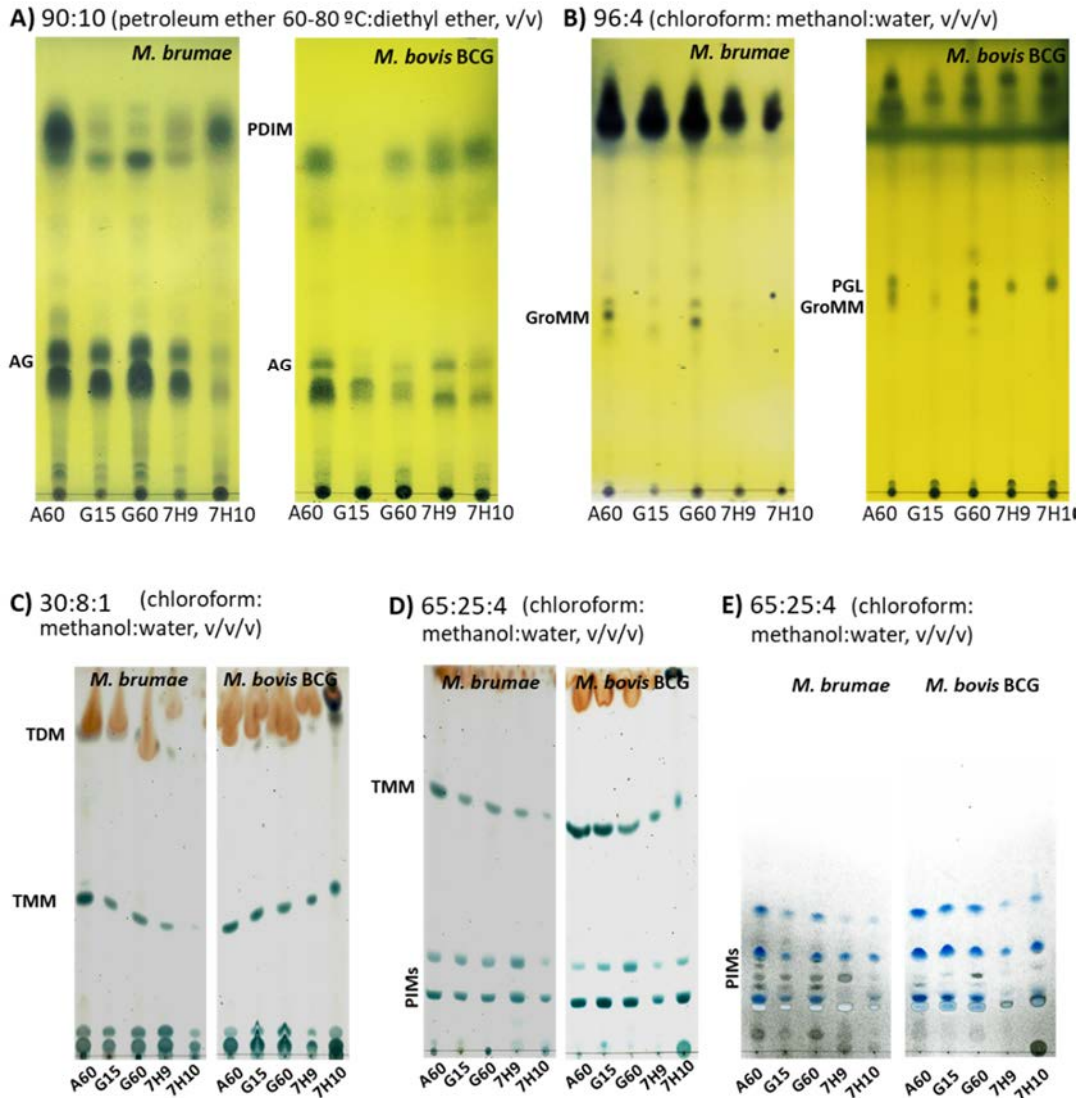
Figure 22. Thin layer chromatographies (TLC) corresponding to the total lipidic content of *M. brumae* and *M. bovis* BCG pellicles grown on different culture media. The results are one representative experiment out of at least three biological replicates. TLCs were developed in A) petroleum ether 60 - 80 °C:diethyl ether (90:10, v/v), B) chloroform:methanol (96:4, v/v), C) chloroform:methanol:water (30:8:1, v/v/v), D-E) chloroform:methanol:water (65:25:4, v/v/v). TLCs were revealed with 10% molybdatophosphoric acid in ethanol (A-B), 1% anthrone in sulfuric acid (C-D) and Molybdenum Blue Spray (E). Mycobacteria were grown in three Sauton compositions (A60, G15, G60) and Middlebrook 7H9 and 7H10. AG: Acylglycerols; GroMM: glycerol monomycolate; PGL: phenol glycolipid; TDM: trehalose dimycolate; TMM: Trehalose monomycolate; PIMs: phosphatidylinositol mannosides.

4.1.3.3. Analysis of the lipidic content and physicochemical properties of the outermost surface of *M. brumae* and *M. bovis* BCG

M. brumae and *M. bovis* BCG pellicles produced in liquid media (A60, G15, G60 and 7H9) were exposed to a superficial extraction with petroleum ether (PE) 40-60 °C for 5 min to recover the most outer lipids present on the surface of mycobacterial cells. Noticeably, the superficial lipidic extraction was not feasible when mycobacteria grew in a solid medium. Once lipidic extraction was performed, the lipidic extract was analysed similarly to the total lipidic extract by TLC (Figure 23).

Accordingly, lipidic extracts exposed to the elution system formed by PE:diethyl ether (90:10, v/v) showed that no AGs were present on the surface of *M. brumae* grown on A60. For *M. bovis* BCG, AGs were seen in all the conditions, yet being diminished in *M. bovis* BCG-7H9. Besides, PDIM was almost untraceable in *M. bovis* BCG cultured in G15, in contrast to the rest of *M. bovis* BCG conditions.

Using the elution system formed by chloroform:methanol (96:4, v/v), the presence of GroMM was detected in both species. Especifically, *M. brumae* cells only produced GroMM when cultured in A60 and G60 culture media, yet not when grown on G15 or 7H9 conditions. Otherwise, *M. bovis* BCG grown on low glycerol concentration (G15) diminished PGL and GroMM expression, compared to the lipid production triggered when *M. bovis* BCG grew in high glycerol concentrations (A60 and G60).
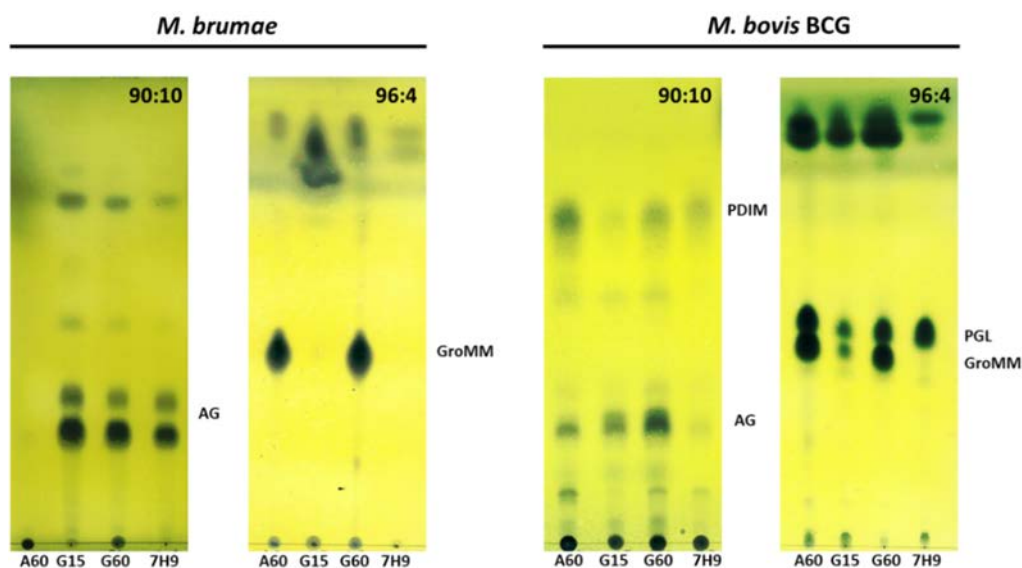
Figure 23. Thin layer chromatographies (TLC) corresponding to the superficial lipidic extract using petroleum ether on *M. brumae* and *M. bovis* BCG pellicles grown on different culture media. The results are one representative experiment out of several biological replicates. TLCs were developed in A) petroleum ether 60 - 80 °C:diethyl ether (90:10, v/v) and B) chloroform:methanol (96:4, v/v)). TLCs were revealed with 10% molybdatophosphoric acid in ethanol. AG: acylglycerols, GroMM: glycerol monomycolate, PGL: phenol glycolipid.

The four spots observed in the lipidic extract from M. brumae cells grown on G15, G60 or 7H9 when eluted with PE:diethyl ether (90:10, v/v) were purified using a Silica Gel 60 column stabilized with PE and increasing diethyl ether concentrations. Remarkably, any of them was detected on the surface of *M. brumae* cells grown on A60. When spots were analyzed by RMN, the first and upper spot corresponded to long aliphatic chains and aromatic groups; the second spot corresponded to long chains with *cis* and *trans* insaturations, while the two bottom spots were AGs.

Besides, developing a Silica Gel 60 column stabilized with chloroform and increasing methanol concentrations enable the purification of 1) GroMM of *M. brumae*, 2) GroMM of *M. bovis* BCG, and 3) PGL from *M. bovis* BCG. Those compounds were confirmed by 1D and 2D NMR experiments (1D ^{1}H, ^{1}H-^{1}H COSY and ^{1}H-^{13}C HSQC), which permitted the total ^{1}H and ^{13}C NMR molecules characterization.

In GroMM purified, typical resonances of the glycerol monosubstituted unit were identified as H1a and H1b at 4.28 and 4.24 ppm, respectively (directly bonded to C1 at 65.1 ppm via HSQC), and correlated via COSY to H2 at 3.96 ppm (bonded to C2 at 69.6 ppm). H3a and H3b resonated at 3.75 and 3.63 ppm, respectively (C3 at 63.0 ppm), and were also correlated to H2 via COSY. The typical peaks of α-mycolates were identified. Briefly, at 2.46 ppm, the α-carboxylic proton H4 (directly bonded to C4 at 51.7 ppm via HSQC) correlated via COSY to the β-carboxylic proton H6 at 3.70 ppm (bonded to C6 at 72.6 ppm) and to the β-carboxylic H5 at 1.69 ppm (bonded to C5 at 29.2 ppm). The spectrum showed typical signals corresponding to olefinic protons of trans double bonds, multiplets at 5.33 and 5.24 ppm (H10 and H11, respectively) and cis double bonds at 5.35 ppm (H9). Additionally, the protons adjacent to the double bond, H8, were identified at 1.96 ppm via COSY correlation. Methylene chains resonated at approximately 1.26 ppm (broad intense signal), and terminal methyl groups, CH3t, resonated at 0.88 ppm (t, 7.1 Hz). Therefore, peak integrations were in accordance with the structure of α-GroMM in *M. brumae* (Figure 24a, Table 20a). α-GroMM showed two different H1b signals revealed as H1b (dd at 4.242 ppm) and H1b' (dd at 4.228 ppm), which were partially overlapped. Both signals were correlated via COSY to H1a, via HSQC to C1 and via COSY to H2. Moreover, the relative integration of H1a and (H1b +H1b') signals were 1.00 to 1.03. Altogether, a mixture of the two diastereoisomers *R* and *S*, corresponding each to one H1b signal (H1b an H1b').

In the case of GroMM from *M. bovis* BCG, the NMR resonances of the monosubstituted glycerol unit matched with those previously described for α-GroMM. However, important differences were found regarding the NMR peaks of the mycolate structure (Figure 24b, Table 20a). The observed peaks were typical of the k group (H10 at 2.50 and H11 at 1.05 ppm) and cis cyclopropane (H8 at 0.65, H9a at -0.33 and H9b at 0.56 ppm) appeared. The integration of quantitative 1D ^{1}H NMR spectrum signals showed that the GroMM molecular

structure was mainly formed by k-mycolates (Figure 24b). Once *R* and *S* diastereoisomers were studied, a mixture of both was found, similarly to the previous results observed in α-GroMM. Besides, the presence of PGL in *M. bovis* BCG was also confirmed by NMR (Figure 24d, Table 20b).
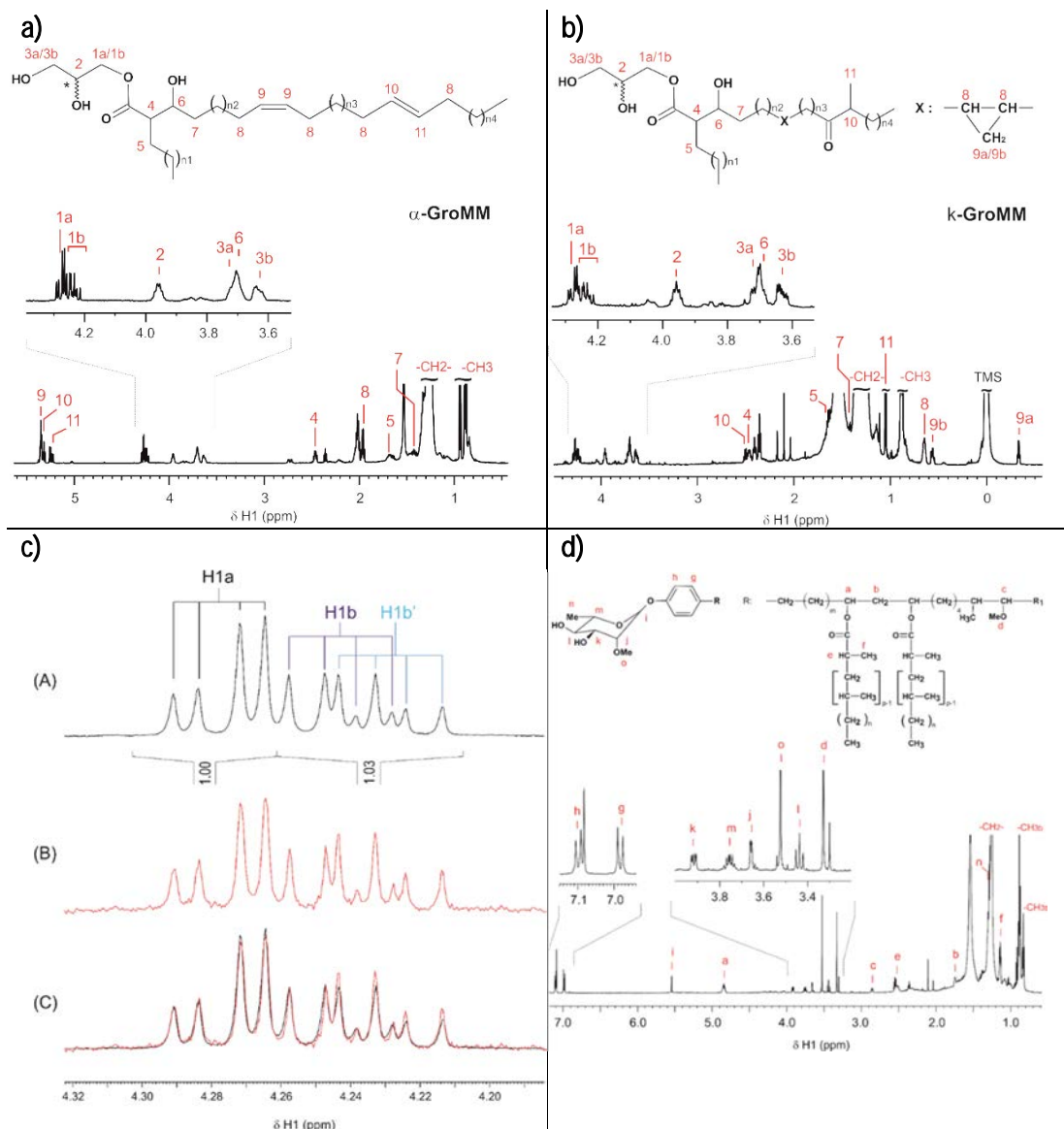
Figure 24. **¹H NMR spectra of purified lipids.** a)¹H NMR spectra of purified α-GroMM from *M. brumae;* b) ¹H NMR spectra of k-GroMM from *M. bovis* BCG; c) Enlargement of the 1H NMR spectrum region containing H1a, H1b and H1b' signals of (A) spot 1 of *M. brumae*; (B) spot C of *M. bovis* BCG and (C) both spectra overlapped. Spectra acquired at 298.0 K and at a magnetic field of 600 MHz; d) ¹H NMR spectra of PGL from *M. bovis* BCG. Spectrum obtained at 298.0 K and at a magnetic field of 600 MHz.

Table 20. Table of ¹H NMR spectra from purified lipids. Table of $^1H^{13}C$ NMR chemical shifts and ^1H-^1H J couplings of a) α-GroMM from *M. brumae* and k-GroMM from *M. bovis* BCG; b) PGL from *M. bovis* BCG.

a)

	α-GroMM			k-GroMM		
	¹H		**¹³C**	**¹H**		**¹³C**
Id	**δ (¹H)** [ppm]	**(mult.,* $^{2/3}J_{H,H}$)** [Hz]	**δ (¹³C)** [ppm]	**δ (¹H)** [ppm]	**(mult.,* $^{3/4}J_{H,H}$)** [Hz]	**δ (¹³C)** [ppm]
1a	4,278	(dd, $J_{1a,1b}$=11,6 $J_{1a,2}$=4,3)	65,04	4,278	(dd, $J_{1a,1b}$=11,6 $J_{1a,2}$=4,3)	65,16
1b	4,242	(dd, $J_{1b,1a}$=11,5 $J_{1b,2}$=6,2)	"	4,242	(dd, $J_{1b,1a}$=11,5 $J_{1b,2}$=6,2)	"
1b'	4,228	(dd, $J_{1b',1a}$=11,6 $J_{1b',2}$=6,3)	"	4,228	(dd, $J_{1b',1a}$=11,6 $J_{1b',2}$=6,3)	"
2	3,958	(m, br)	69,62	3,957	(m, br)	69,79
3a	3,753	(m, br)	63,01	3,708	(m, br)	63,05
3b	3,633	(m, br)	"	3,629	(m, br)	"
4	2,460	(m)	51,69	2,461	(m)	51,83
5	1,692	(m)	29,19	1,670	(m, ov)	29,00
6	3,698	(m, ov)	72,61	3,698	(m, ov)	72,76
7	1,438	(m, ov)	35,19	1,420	(m, ov)	-
8	1,961	(m)	32,33	0,646	(m, br)	15,53
9	5,347	(m)	129,66		-	
9a		-		-0,334	(dd, $J_{9a,9b}$=9,7 $J_{9a,8}$=5,1)	-
9b		-		0,562	(m)	"
10	5,330	(m, ov)	128,11	2,500	(m, ov)	-
11	5,237	(dd, $J_{11,10}$=15,4 $J_{11,8}$=7,8)	136,29	1,046	(d, $J_{11,10}$=7,0)	16,17
-CH2-	1,260	(br)	29,34	1,260	(br)	29,40
-CH3	0,881	(t, $J_{CH3,CH2}$=7,1)	13,87	0,881	(t, $J_{CH3,CH2}$=7,1)	13,96

* Multiplicity: d (doublet), dd (double doublet), t (triplet), m (multiplet).

** Broad signal (br), overlapped signal (ov).

b)

	PGL		
	¹H		**¹³C**
Id	**δ (¹H)** [ppm]	**(mult.,* $^{2/3}J_{H,H}$)** [Hz]	**δ (¹³C)** [ppm]
a	4,840	(m)	69,97
b	1,745	(m)	38,14
c	2,855	(m)	86,41
d	3,328	(s)	57,13
e	2,524	(m)	37,50
f	1,137	(ov)	18,07
g	6,983	(d, $J_{g,h}$=8,7)	115,88
h	7,099	(d, $J_{h,g}$=8,7)	129,04
i	5,541	(d, $J_{i,j}$=1,4)	94,59
j	3,657	(dd, $J_{j,k}$=3,7 $J_{j,i}$=1,4)	79,92
k	3,918	(dd, $J_{k,j}$=3,7 $J_{k,i}$=9,4)	71,11
l	3,437	(dd, $J_{l,k}$=9,4 $J_{l,m}$=9,4)	73,76
m	3,755	(m)	68,21
n	1,281	(ov)	17,30
o	3,524	(s)	58,73
-CH2-	1,255	(br)	29,30
-CH3b	0,880	(t, J=6,9)	19,68
-CH3t	0,826	(t, J=6,8)	14,46

* Multiplicity: d (doublet), dd (double doublet), t (triplet), m (multiplet).

** Broad signal (br), overlapped signal (ov).

4.1.3.4. Neutral red staining and hydrophobicity

After studying the different lipidic pattern present in the outermost layer of *M. brumae* and *M. bovis* BCG grown on different culture media, some physicochemical properties such as the hydrophobicity or the capacity to be stained with neutral red, were analysed.

Accordingly, *M. brumae* and *M. bovis* BCG grown on Sauton media were carefully taken, dried and exposed to neutral red staining. Considering that both mycobacteria species showed similar lipidic pattern grown on either Middlebrook 7H9 or 7H10 media (Section 4.1.3.2), mycobacteria cultured in Middlebrook 7H10 were used as a control. Although neutral red staining is yellow, compounds with reducing power on mycobacteria surface trigger a red colouration of cells. Hence, the colour shift indicates the presence of a more negative charge of the mycobacteria surface. In the case of *M. brumae,* none condition was able to reduce the staining. However, in the case of *M. bovis* BCG, differences were found among the conditions. Specifically, *M. bovis* BCG-G15 was unable to reduce the neutral-red staining compared to the rest of *M. bovis* BCG conditions, indicating a less negative charge of the surface of *M. bovis* BCG-G15 (Figure 25a).

Later, *M. brumae* and *M. bovis* BCG were exposed to suspensions with phosphate urea magnesium sulphate (PUM) buffer and n-hexadecane to determine the cell hydrophobicity. As Figure 24b shows, cell hydrophobicity is modified depending on the culture media used for the mycobacteria growth. Specifically, *M. brumae* grown on A60 or 7H10 triggered a significant less hydrophobic cell wall than *M. brumae* grown on G60. Otherwise, *M. bovis* BCG cells grown on G15 or 7H10 were less hydrophobic cell wall than cells grown on A60 or G60. Besides, *E. coli* as a negative control corroborates the high hydrophobic cell wall of mycobacteria species. Noticeable, *M. brumae* cells were less hydrophobic than *M.bovis* BCG cells, independently of the culture medium used for their growth (Figure 25b).

a)

b)
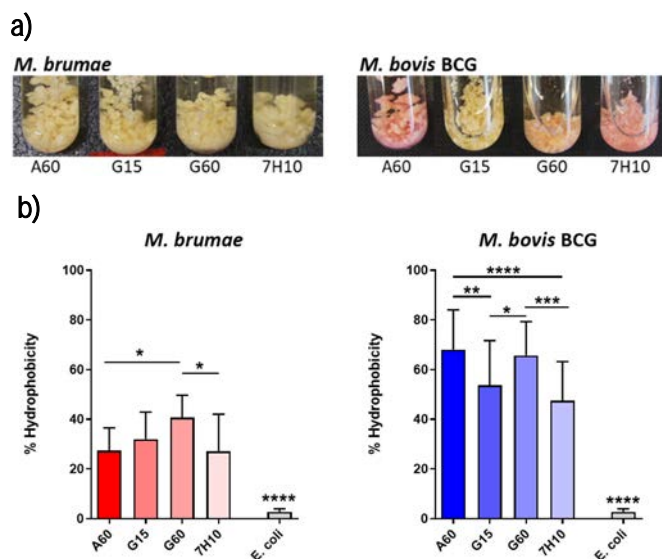
Figure 25. **Physicochemical properties of *M. brumae* and *M. bovis* BCG grown on the different culture media.** a) Neutral red staining from *M. brumae* and *M. bovis* BCG. Representative pictures from at least three independent experiments. b) Graphs show the percentage of the cell surface hydrophobicity of *M. brumae* and *M. bovis* BCG with respect to non-exposed n-hexadecane cells. Data represent the mean ± SD from three independent experiments. *$p<0.05$; **$p<0.01$; ***$p<0.001$; ****$p<0.0001$ (ANOVA test).

4.1.4 Study of physicochemical characteristics of *M. bovis* BCG substrains

4.1.4.1 Neutral red staining and hydrophobicity of *M. bovis* BCG substrains grown on different culture media

To analyze the influence of the culture media in the physicochemical and lipidic characteristics of different substrains of *M. bovis* BCG; *M. bovis* BCG-Pasteur, -Phipps, -Tice, -Glaxo and -Moreau were grown on three culture media: 1) in A60 composition as it triggered the highest biomass production; 2) in G15 composition, and 3) in Middlebrook 7H10 as control of a solid and rich medium.

As previously observed for *M. bovis* BCG Connaught, all tested BCG substrains grown on A60 medium immediately took an intense red colouration, contrary to the yellowish colour taken by BCG substrains grown on G15 medium. When neutral-red staining was applied to *M. bovis* BCG substrains grown on Middlebrook 7H10, different intensities of red colouration were reached among *M. bovis* BCG substrains. Remarkably, *M. bovis* BCG-Pasteur, -Phipps and -Tice took an intense red colour, yet *M. bovis* BCG-Glaxo, and especially *M. bovis* BCG-Moreau, the reddish colouration was extremely weak (Figure 26a).

According to the results shown in Figure 25b, cell hydrophobicity increased in correlation with the amount of glycerol added to the culture media. Therefore, *M. bovis* BCG grown on A60 culture medium showed the highest hydrophobicity for all *M. bovis* BCG substrains studied. Middlebrook 7H10, which only contains 5 mL of glycerol per litre, was the culture medium in which the lowest hydrophobicity was observed in almost all the cases. Only in *M. bovis* BCG-Tice, cell hydrophobicity when grown on G15 medium was lower than the obtained in cells grown on 7H10. Besides, cell hydrophobicity was higher in all mycobacteria cells than in *E. coli* cells (Figure 26b).

a)
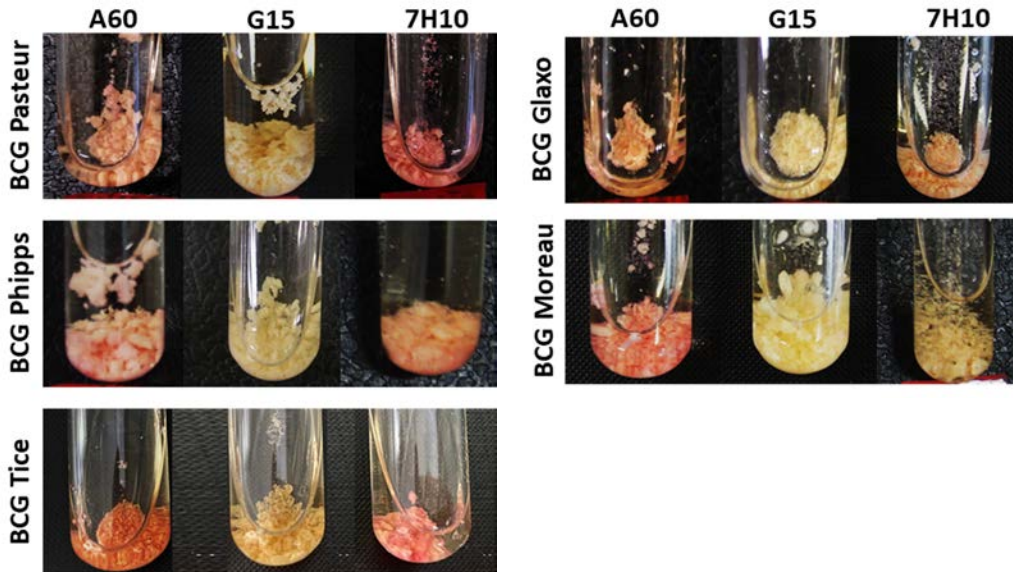
b)
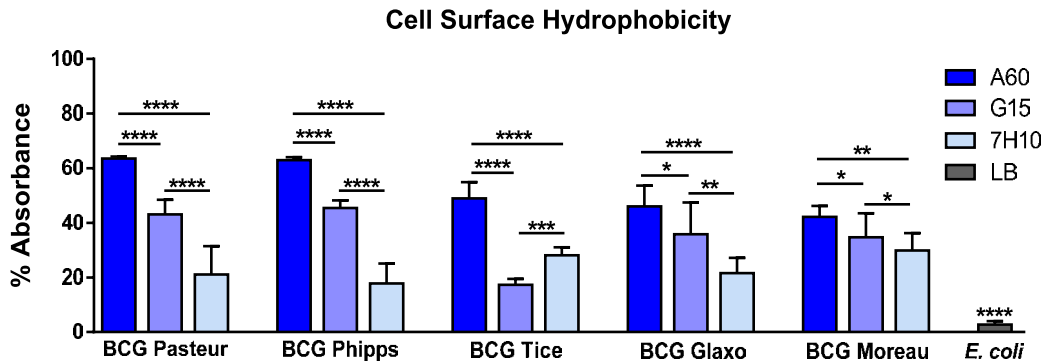
Figure 26. **Physicochemical characteristics of M. bovis BCG substrains.** a)Neutral red staining of different *M. bovis* BCG substrains. Representative pictures from at least three independent experiments. b) Cell wall hydrophobicity of different *M. bovis* BCG substrains. Graphs show the percentage of the cell surface hydrophobicity of M. brumae and M. bovis BCG with respect to non-exposed n-hexadecane cells. Data represent the mean ± SD from three independent experiments. *p<0.05; **p<0.01; ***p<0.001; ****p<0.0001 (ANOVA test).

4.1.4.2 Lipidic content of the outermost layer of different *M. bovis* BCG substrains grown on different culture media

To determine whether the differences observed on the cell hydrophobicity could be related to lipids' presence on the surface of the mycobacteria, *M. bovis* BCG-Pasteur, -Phipps, -Tice, -Glaxo and -Moreau were grown as pellicles on A60 and G15 liquid media. Once proper pellicles were obtained, superficial lipid extraction was performed as previously explained for *M. bovis* BCG Connaught.

According to previous studies of *M. bovis* BCG substrains cultured on Middlebrook 7H10, *M. bovis* BCG- Pasteur and -Phipps showed the presence of PDIM and PGL, *M. bovis* BCG-Tice only PDIM, and *M. bovis* BCG-Glaxo and -Moreau, neither PDIM nor PGL were described.

Eluting the TLC plate with PE 60-80 °C:diethyl ether (90:10, v/v), PDIM was only observed when *M. bovis* BCG-Pasteur or -Phipps were grown on A60 medium, and it was not detected in any of the other conditions. Remarkably, PDIM was non seen in *M. bovis* BCG-Tice, neither in cells grown on A60 nor in cells grown on G15 culture medium (Figure 27a). When lipidic extracts were exposed to chloroform:methanol (96:4, v/v), PGL was also only detected on *M. bovis* BCG-Pasteur or -Phipps grown on A60 medium. Additionally, and according to the previous results obtained for *M. bovis* BCG Connaught, GroMM was produced in all *M. bovis* BCG substrains grown with high glycerol availability in the culture media. Therefore, GroMM was highly expressed when mycobacteria grew in A60, and almost untraceable when grown on G15 composition (Figure 27b).
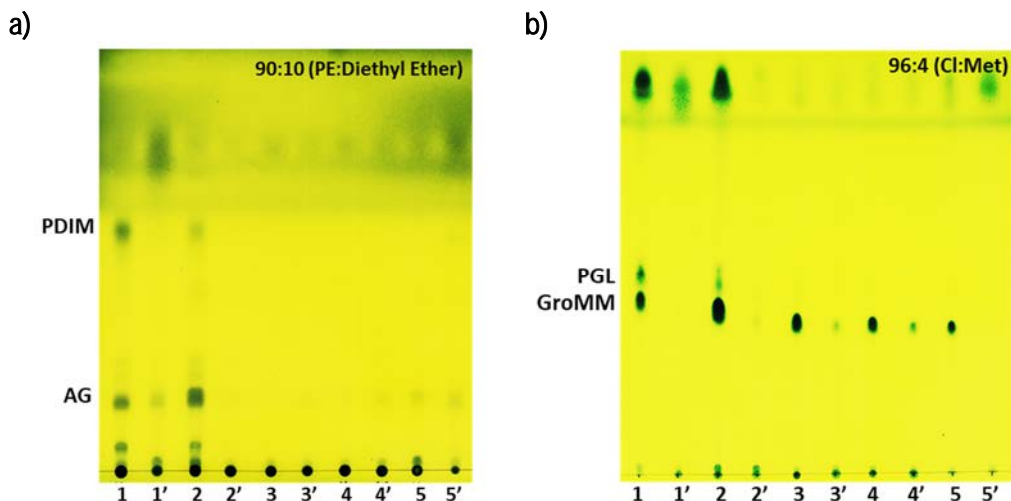
Figure 27. Thin layer chromatographies (TLC) corresponding to the superficial lipidic extract using petroleum ether on pellicles of *M. bovis* BCG substrains grown on different culture media. The results are one representative experiment out of several biological replicates. TLCs were developed in A) petroleum ether 60 - 80 °C:diethyl ether (90:10, v/v) and B) chloroform:methanol (96:4, v/v). TLCs were revealed with 10% molybdatophosphoric acid in ethanol. AG: acylglycerols, GroMM: glycerol monomycolate, PGL: phenol glycolipid.

4.2 Study to evaluate the impact of culture media composition in the antitumour and immunostimulatory effect of *M. brumae* and *M. bovis* BCG *in vitro*

4.2.1 *M. brumae* and *M. bovis* BCG survival inside macrophages and triggered cytokine release

M. brumae and *M. bovis* BCG were grown on the four liquid culture media (A60, G15, G60 and 7H9) previously evaluated, and on Middlebrook 7H10 for comparative purposes. After infecting two different cell lines of macrophages, mice macrophages (J774) and human macrophages (THP-1) at a MOI 10 for *M. brumae* and MOI 1 for *M. bovis* BCG, cells were lysed at different time points (3, 24, 48, 72, 96 and 120 hours post-infection, hpi) to evaluate mycobacterial survival. Finally, supernatants were collected to measure the cytokine and NO production by macrophages. Figure 28 shows the number of CFU/well of *M. brumae* or *M. bovis* BCG recovered from infected macrophages at the different time points after infection.

J774 macrophages were able to kill *M. brumae*, independently of the culture media used for its growth. However, *M. brumae* grown on G15 and 7H10 were killed within 72 hpi, while the rest of *M. brumae* required 120 hpi to be cleared from macrophages. No differences were reached among conditions (Figure 28).

In the case of *M. bovis* BCG, J774 macrophages could not kill *M. bovis* BCG grown on the different culture conditions. As previously described for *M. bovis* BCG grown on Middlebrook 7H10 [314], J774 macrophages could decrease one order of magnitude compared to the infection dose within the first 3 h. Then, the number of viable *M. bovis* BCG cells remained steady until the end of the experiment (Figure 28).

Although no differences were reached among the mycobacterial survival inside J774 macrophages for neither *M. brumae* nor *M. bovis* BCG, the cytokine and NO secretion by the macrophages was highly influenced by the culture media used for their growth. The production of TNF-α, IL-12 and NO by J774 macrophages induced by *M. brumae*-A60 was significantly higher than *M. brumae*-G15 and -G60, being only statistically significant in the case of the TNF-α production. *M. brumae*-7H10 triggered the highest amounts of IL-12 and NO. Otherwise, *M. bovis* BCG-G15 triggered the highest production of IL-6, TNF-α, IL-12 and IL-1β by J774 macrophages compared to *M. bovis* BCG-A60 and -G60, being significant in all cases except for IL-1β. Besides, *M. bovis* BCG grown on both Middlebrook media triggered the highest production of IL-12 and NO, compared to the rest of *M. bovis* BCG conditions (Figure 28).
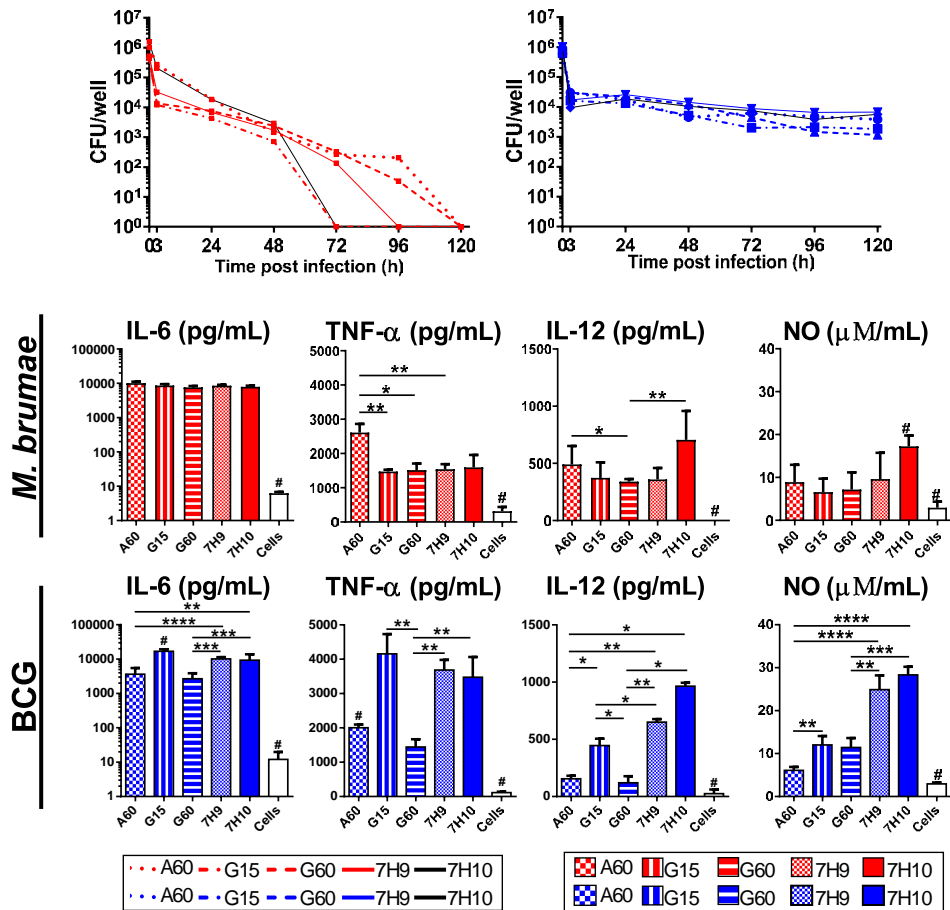
Figure 28. Mycobacterial survival rates and cytokine production in infected J774 macrophages. Macrophages were infected with *M. brumae* or *M. bovis BCG* grown on A60, G15 and G60 Sauton media, or Middlebrook 7H9 and 7H10. Mycobacteria-infected J774 were lysed at different time points, and CFUs were counted after plating serial dilutions of the lysates on Middlebrook 7H10 plates. Graphs show the mycobacterial burden and the cytokines and NO production. TNF-α, IL-12 and NO were evaluated in culture supernatants collected at 72 hours post-infection (hpi), while IL-6 and IL-1β were evaluated in the supernatants collected at 96 hpi, using commercially available ELISA tests. *M. brumae* is shown in red, and M. *bovis* BCG in blue. Data represent the mean ± standard deviation from three independent experiments. $p < 0.05$; ** $p < 0.01$; *** $p < 0.001$; ****, $p < 0.0001$ (ANOVA test).

Similar behaviour was also observed in THP-1 macrophages (Figure 29). *M. brumae*-G15 was killed within the first 72 hpi, while the rest of *M. brumae* conditions were killed within 120 hpi. In contrast, *M. bovis* BCG grown on any of the culture media remained inside human macrophages until the end of the experiments. In *M. brumae* cultures, *M. brumae*-A60 induced the highest production of cytokines, being statistically significant for IL-6, IL-12 and IL-1β production. In the case of *M. bovis* BCG, *M. bovis* BCG-G15 was once again the

condition in which higher production of IL-6, TNF-α and IL-12 was detected, despite not being statistically significant (Figure 29).
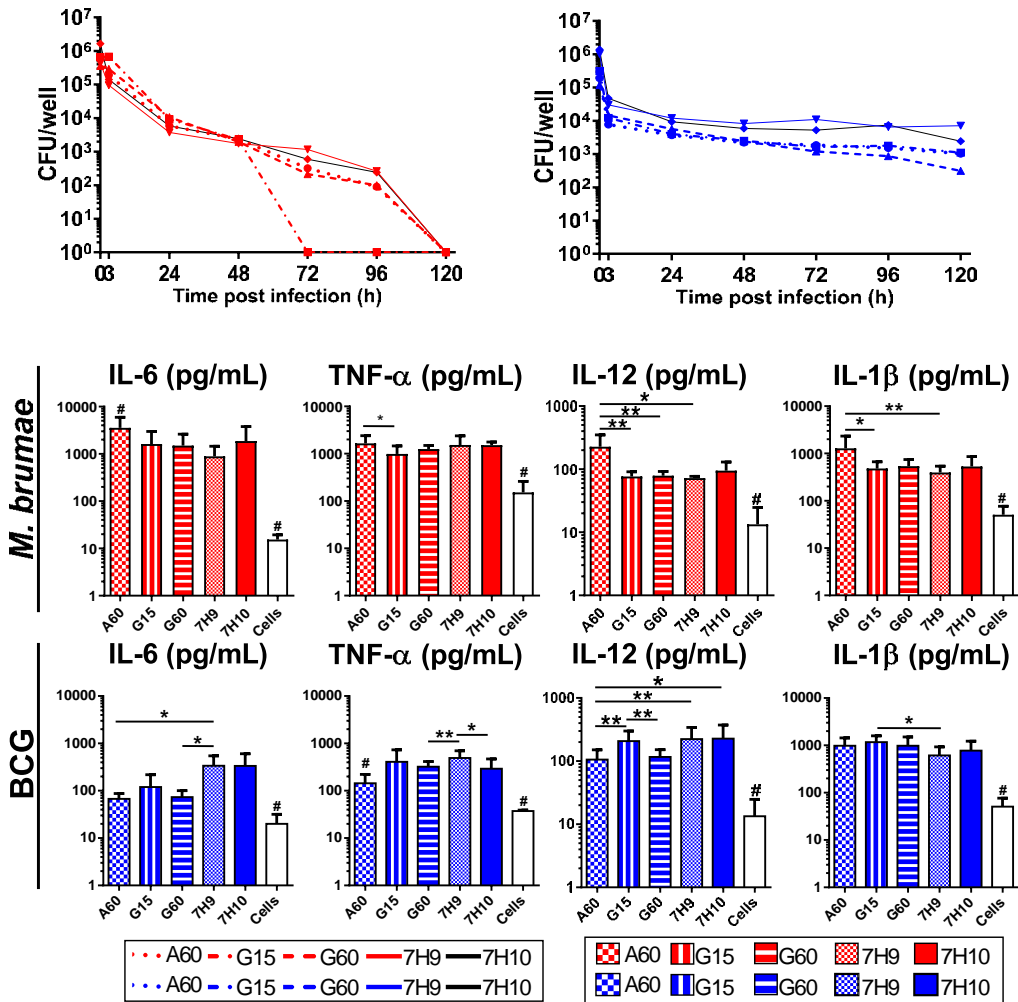
Figure 29. Mycobacterial survival rates and cytokine production in infected THP-1 macrophages. Macrophages were infected with *M. brumae* or *M. bovis BCG* grown on A60, G15 and G60 Sauton media, or Middlebrook 7H9 and 7H10. Mycobacteria-infected THP-1 were lysed at different time points, and CFUs were counted after plating serial dilutions of the lysates on Middlebrook 7H10 plates. Graphs show the mycobacterial burden and the cytokines and NO production. TNF-α, IL-12 and NO were evaluated in culture supernatants collected at 72 hours post-infection (hpi), while IL-6 and IL-1β were evaluated in the supernatants collected at 96 hpi, using commercially available ELISA tests. *M. brumae* is shown in red, and M. *bovis* BCG in blue. Data represent the mean ± standard deviation from three independent experiments. p < 0.05; ** p < 0.01; *** p < 0.001; ****, p < 0.0001 (ANOVA test).

4.2.2   *M. brumae* and *M. bovis* BCG proliferative activity against BC cells

The antiproliferative activity of *M. brumae* and *M. bovis* BCG grown on different culture media was tested against four different BC cell lines. As shown in Figure 30 and 31, there is a different effect of *M. bovis* BCG or *M. brumae* depending on the culture medium's composition.

M. brumae-A60 showed the highest antitumour capacity than the rest of *M. brumae* cultures, although statistical differences were only observed for the T24 cell line. When cytokine production was analysed on culture supernatants, *M. brumae*-A60 induced the highest cytokine release in all cell lines tested. Both IL-6 and CXCL-8/IL-8 production was significantly higher when *M. brumae* was grown on A60 than in the rest of *M. brumae* conditions. Among *M. bovis* BCG conditions, *M. bovis* BCG-G15 tend to inhibit BC cells more than *M. bovis* BCG in the rest of the conditions, except for MB49 cell cultures. However, the IL-6, CXCL-8/ IL-8 cytokine release by infected BC cells after the infection with *M. bovis* BCG-G15 was highly superior compared to those produced by cultures infected with *M. bovis* BCG grown on A60, G60, 7H9 or 7H10. IL-6 production was similar among all *M. bovis* BCG conditions only in the case of 5637 BC cells.
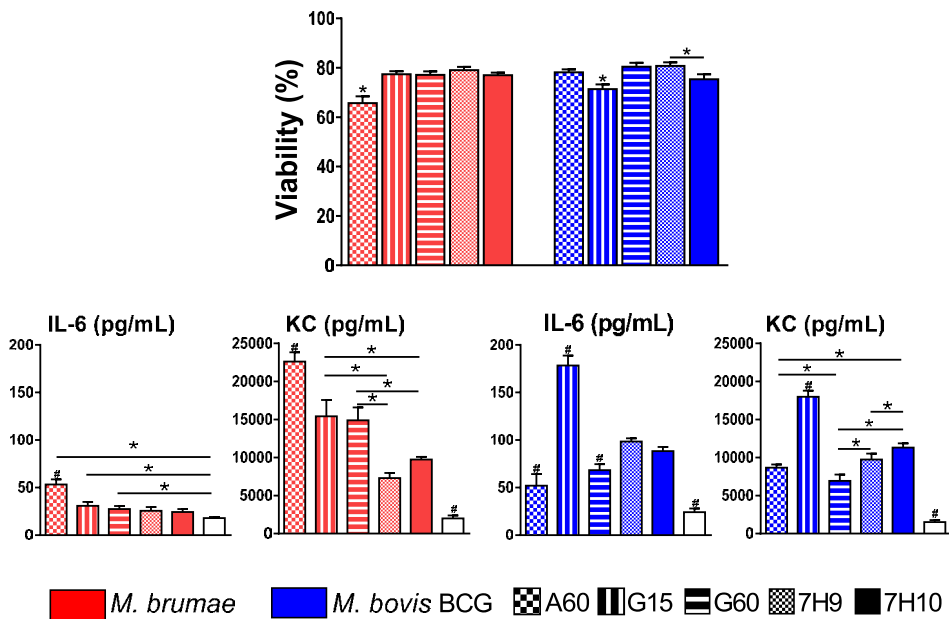
Figure 30. **Cell growth inhibition and cytokine production by *M. brumae* and *M. bovis BCG*-infected MB49 bladder cancer (BC) cell line.** The antitumour effect of *M. brumae* is shown in red, and *M. bovis* BCG in blue grown on different culture media was evaluated on murine (MB49) BC cell lines. Graphs show the percentage of growth inhibition with respect to non-infected cells using the 3-(4,5-dimethylthiazol-2-yl)-2,5-diphenyltetrazolium bromide (MTT) colourimetric assay. Cytokine production in cell culture supernatants collected 72 h after mycobacterial infection was evaluated using ELISA tests. Data represent the mean ± SD from at least three independent experiments. *$p < 0.05$; **$p < 0.01$; ***$p < 0.001$; ****$p < 0.0001$ (ANOVA test).
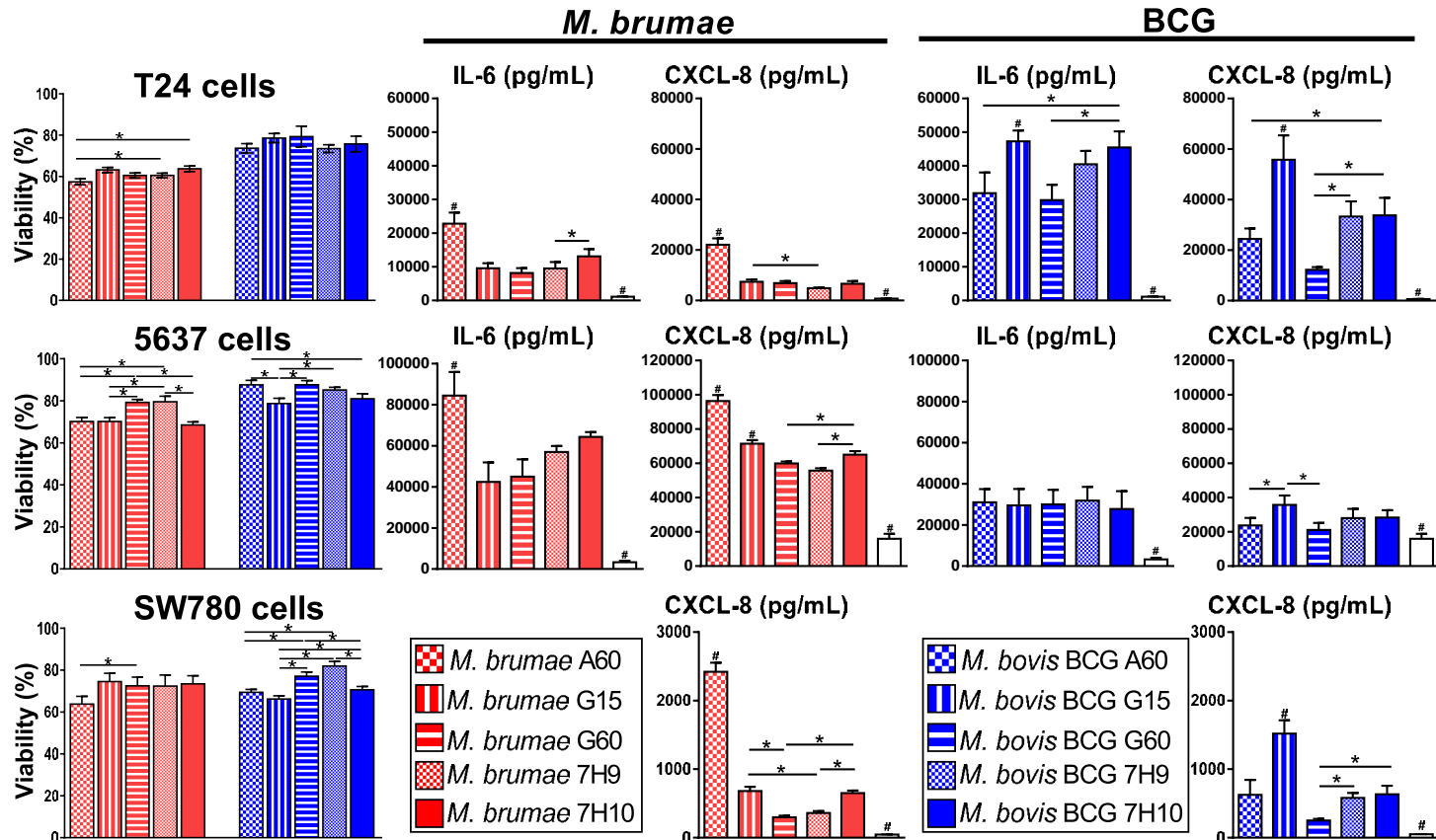
Figure 31. Cell growth inhibition and cytokine production by *M. brumae* and *M. bovis* BCG-infected bladder cancer (BC) cell lines. The antitumour effect of *M. brumae* is shown in red, and *M. bovis* BCG in blue grown on different culture media was evaluated on human (T24, 5637, and SW780) BC cell lines. Graphs show the percentage of growth inhibition with respect to non-infected cells using the 3-(4,5-dimethylthiazol-2-yl)-2,5-diphenyltetrazolium bromide (MTT) colourimetric assay. Cytokine production in cell culture supernatants collected 72 h after mycobacterial infection was evaluated using ELISA tests. Data represent the mean ± SD from at least three independent experiments. *$p < 0.05$; **$p < 0.01$; ***$p < 0.001$; ****$p < 0.0001$ (ANOVA test).

4.3 Study *in vivo* to evaluate the impact of culture media composition in the antitumour and immunostimulatory effect of *M. brumae* and *M. bovis* BCG

4.3.1 Survival analyses of tumour-bearing mice treated with *M. brumae* and *M. bovis* BCG grown on different culture media

After observing differences in the antiproliferative activity of *M. brumae* and *M. bovis* BCG grown on different culture media on BC cells, their effect was further evaluated in the orthotopic syngeneic mice model of BC. Mycobacteria grown on A60, G15 and G60 were used for *in vivo* experiments. Considering that the antiproliferative and immunostimulatory activity triggered by both mycobacteria grown on Middlebrook 7H9 and 7H10 was similar; that Middlebrook 7H9 and 7H10 contain animal-derived components, and that previous data from our lab was done with mycobacteria grown on Middlebrook 7H10 [314,323]; *M. brumae* and *M. bovis* BCG grown on Middlebrook 7H10 were also used with comparative porpuses. Besides, the elimination of mycobacteria grown on Middlebrook 7H9 enables minimizing the number of animals used per experiment.

Experiments were performed according to the treatment schedule shown in the Material and Methods Section (Figure 15). Firstly, hematuria was observed on day 10-12, demonstrating the establishment of the tumour. According to previous studies, present results in the orthotopic mice model of BC confirmed that *M. brumae* and *M. bovis* BCG prolonged the survival in tumour-bearing mice. While the whole control group of tumour-bearing mice treated with PBS needed to be sacrificed before day 30 after carefully checking different clinical parameters to avoid unnecessary suffering, 100 % of tumour-bearing mice treated with *M. brumae*-A60 survived at day 40. Besides, 89 % of *M. brumae*-A60 treated mice survived at day 60, the end of the experiment. Otherwise, tumour-bearing mice treated with *M. brumae* grown on G15, G60, or 7H10 prolonged the survival of around 70 % of mice. Therefore, *M. brumae*-A60 was the most successful treatment among all *M. brumae*-treated animals, despite no significant differences were reached among groups (Figure 32).
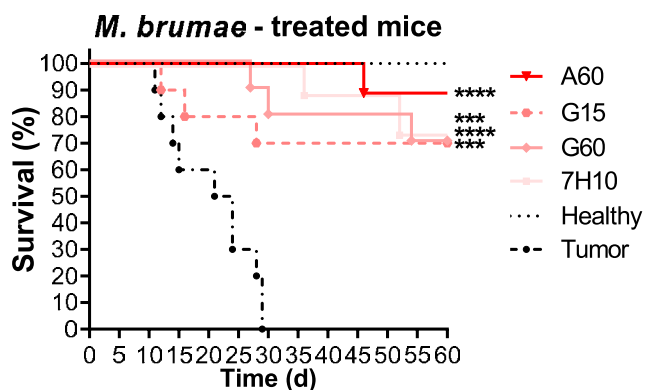
Figure 32. *In vivo* antitumour capacity of *M. brumae.* Kaplan-Meier analysis of healthy and tumour-bearing mice survival after intravesical instillation with PBS or *M. brumae* grown on different culture media. ***$p < 0.001$; ****$p < 0.0001$ versus PBS group, log-Rank (Mantel-Cox) test (N=10).

For *M. bovis* BCG-treated mice, the group that showed higher survival rates among *M. bovis* BCG conditions was *M. bovis* BCG-G15. *M. bovis* BCG-G15 prolonged mice survival in 78 % of mice at day 40 and this survival was maintained until the end of the experiment. When tumour-bearing mice were treated with the *M. bovis* BCG grown on A60, G60 or Middlebrook 7H10, similar survival was reached among groups, being around 55 % of mice. Hence, *M. bovis* BCG-G15 was superior to the rest of *M. bovis* BCG culture conditions, although without statistical significance (Figure 33).

Besides, It is worth mentioning that tumour-bearing mice treated with *M. brumae* conditions obtained in all cases better survival rates than tumour-bearing mice treated with any condition of *M. bovis* BCG. These results confirmed the previous results obtained in the *in vitro* studies that showed that *M. brumae*-A60 and *M. bovis* BCG-G15 were the most successful treatments among the rest of the conditions for each mycobacterium.
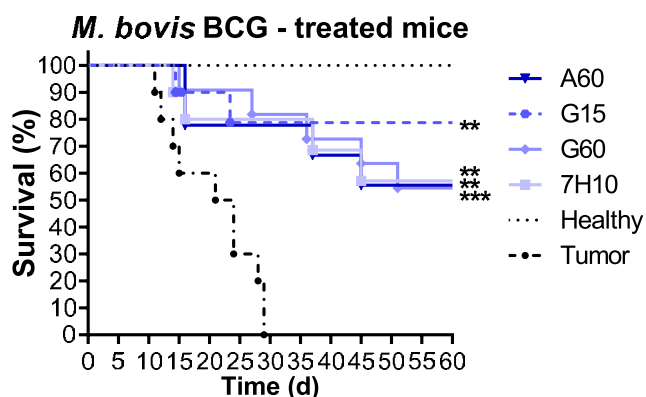
Figure 33. *In vivo* antitumour capacity of *M. bovis* BCG. Kaplan-Meier analysis of healthy and tumour-bearing mice survival after intravesical instillation with PBS or *M. bovis* BCG grown on different culture media. ***$p < 0.001$; ****$p < 0.0001$ versus PBS group, log-Rank (Mantel-Cox) test (N=10).

After evaluating the capacity of mycobacteria to inhibit the tumour growth *in vivo*, the immune response triggered by intravesical instillations of both mycobacteria grown on different culture media was analysed in tumour-bearing mice. Accordingly, both local and systemic immune response triggered by intravesical treatments is explained in the following sections.

4.3.2 Detection of IgG antibodies against mycobacteria in tumour-bearing mice sera.

The presence of IgG against mycobacteria in sera was studied in blood samples collected from mice sacrificed at day 30 after tumour induction. Specifically, serum from each animal was exposed to *M. brumae* or *M. bovis* BCG grown on the same conditions used for mice treatment. Moreover, each serum was also exposed to *M. brumae* and *M. bovis* BCG grown on Middlebrook 7H10 to evaluate antigen specificity.

Overall, tumour-bearing mice treated with *M. brumae* presented higher IgG levels than tumour-bearing mice treated with *M. bovis* BCG (Figure 34a). No differences were observed in IgG levels among *M. brumae*-treated groups. In the case of *M. bovis* BCG, statistical differences were only reached when IgG anti-*M. bovis* BCG-7H10 was compared with IgG anti-*M. bovis* BCG-A60 and -G15 levels.

Regarding cross-reaction, no differences among treatments were found when cross-reactivity was analyzed. Similar to the previous IgG reactivity, higher antibody levels were found in *M. brumae* treatments than *M. bovis* BCG treatments (Figure 34b). Remarkably, the IgG levels obtained in *M. brumae*-treated mice was higher against mycobacteria grown on Middlebrook 7H10 than those obtained in the same culture medium used for the intravesical treatment.
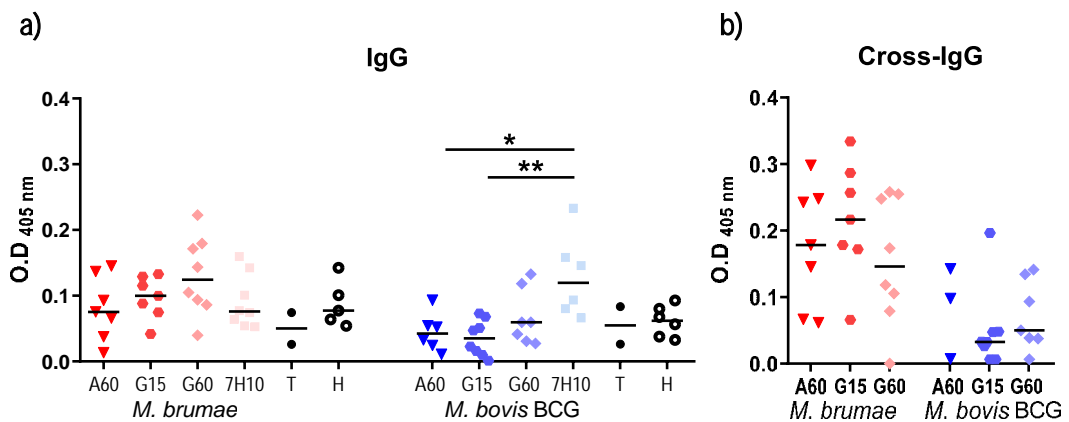
Figure 34. Mycobacteria-specific IgG antibodies detected in sera from mice. Levels of specific IgG anti-*M. brumae* are shown in red and IgG anti-*M. bovis* BCG in blue. Sera from each animal was exposed to mycobacteria grown on a) the same medium used for mice treatment (IgG) and in b) Middlebrook 7H10 (Cross-IgG). Levels of IgG anti-*M. brumae* or *M. bovis* BCG grown on 7H10 found in non-treated tumour-bearing mice (T) is represented in full black dots. Levels of IgG anti-*M. brumae* or *M. bovis* BCG grown on 7H10 found in healthy (H) mice are shown as empty black dots. Data represents the mean, *$p < 0.05$; **$p < 0.01$ (ANOVA test) (N=8).

4.3.3 Proliferation, cytokine production and direct antitumour effect on MB49 cells of splenocytes from tumour-bearing mice

Spleens collected in aseptic conditions from animals sacrificed at day 30 after tumour induction were used to analyze 1) the cytotoxicity against the MB49 BC cell line, and 2) the systemic immune response triggered after mycobacteria instillations.

4.3.3.1 Cytotoxic activity triggered by splenocytes

Splenocytes from each animal were co-cultured with the MB49 cell line at a ratio of 25 splenocytes per tumour cell for 24 hours (25:1). Then, the viability of MB49 cells was determined by the MTT assay. Splenocytes from animals treated with *M. brumae*-A60 triggered the highest inhibition of MB49 cells proliferation compared to the rest of *M. brumae* conditions, being statistically different in the case of *M. brumae*-G60 (Figure 35). A similar cytotoxic effect was observed among *M. bovis* BCG treatments. Control groups (non-treated tumour-bearing mice and healthy animals) triggered the lowest cytotoxicity on MB49 cells.
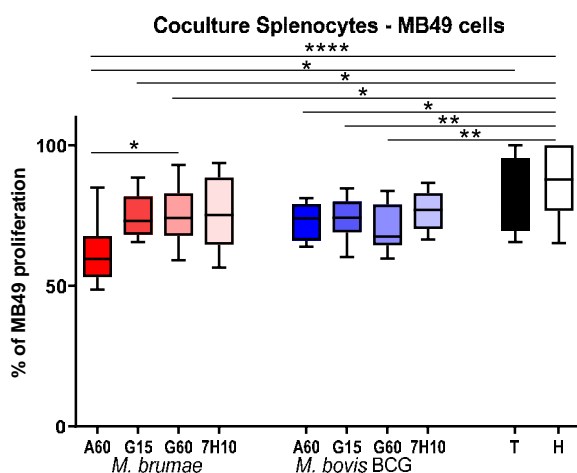
Figure 35. **Cytotoxic activity triggered by splenocytes.** MB49 cell inhibition triggered by splenocytes from *M. brumae* treated tumour-bearing mice shown in red, *M. bovis* BCG in blue, non-treated tumour bearing mice in grey, and healthy mice in white. Ratio 25:1 (splenocytes: MB49 cells) Data represent the mean ± SD. *p < 0.05; **p < 0.01;****p < 0.0001 (ANOVA test). (N=8)

4.3.3.2 Splenocytes proliferation and cytokine production

Splenocytes from each animal were incubated for 72 hours together with 1) a positive control (Concanavaline A, ConA), 2) negative control (PBS), 3) heat-killed (HK) cells of mycobacteria used for the treatment of each animal, or 4) HK cells of mycobacteria grown on Middlebrook 7H10 to analyze antigen specificity. The proliferation ratio obtained from stimulating splenocytes with HK-mycobacteria with respect to non-stimulated splenocytes (basal restimulation) was expressed as the index of restimulation.

Splenocytes proliferation with ConA was induced in all groups. When splenocytes were restimulated with the same mycobacteria used for mice treatment, *M. brumae*-A60 showed the highest proliferation ratio among all *M. brumae* treatments, being statistically significant

when *M. brumae*-A60 was compared with *M.* brumae-G60 or *M. brumae*-7H10. Besides, the restimulation index from *M. brumae*-A60, -G15 and -G60 was statistically higher than the restimulation index produced by splenocytes from non-treated tumour-bearing mice restimulated with *M. brumae*-7H10. In the case of *M. bovis* BCG, *M. bovis* BCG-G15 triggered a significant highest proliferation ratio among the rest of *M. bovis* BCG treatments, splenocytes from non-treated tumour-bearing mice restimulated with *M. bovis* BCG-7H10 or splenocytes from healthy mice restimulated with *M. bovis* BCG-7H10.

When splenocytes from mice treated with *M. brumae* or *M. bovis* BCG grown on A60, G15 or G60 culture media were exposed to the same mycobacteria, yet grown on Middlebrook 7H10, the restimulation index of all conditions tended to be lower than the observed with mycobacteria grown on the same media used for intravesical treatments, although it was not statistically significant in any case. However, the restimulation index from *M.brumae*-A60, -G15 or -G60 was significantly higher than non-treated tumour-bearing mice restimulated with *M. bovis* BCG-7H10. Moreover, cross-restimulation of splenocytes from *M. bovis* BCG treated with *M. bovis* BCG-7H10 showed similar restimulation of splenocytes from *M. bovis* BCG-G15 than non-treated tumour mice, contrary to the rest of conditions in which less proliferation was found. In all cases, the restimulation response triggered by healthy animals was different to the rest of the conditions, except for splenocytes from *M. brumae*-A60 or -G15 treated mice (Figure 36).
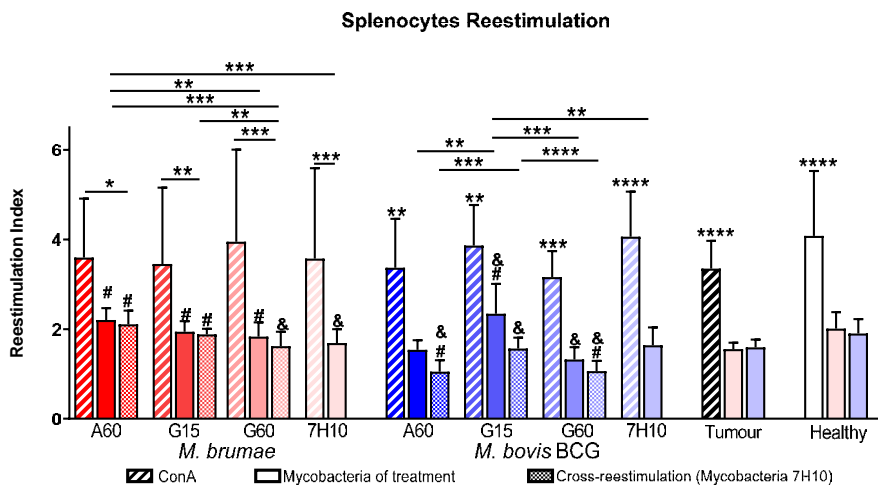
Figure 36. Proliferation of mycobacteria-restimulated splenocytes. Data represent the restimulation index of restimulated splenocytes over non-reestimulated splenocytes. Splenocytes were reestimulated with Concanavaline A (ConA) shown as linear bars, mycobacteria used for mice treatment shown as solid bars, or mycobacteria used for mice treatment grown on Middlebrook 7H10 shown as checkered bar. Data represent the mean ± SD. *$p < 0.05$; **$p < 0.01$; ***$p < 0.001$; ****$p < 0.0001$; # $p < 0.05$ respect the non-treated tumour-bearing mice; and & $p < 0.05$ respect the healthy animals(ANOVA test) (N=8).

129

Supernatants from restimulated splenocytes were collected. Production of IFN-ɣ, IL-4 and IL-17 production was analysed to observe a Th1, Th2, or Th17 response triggered after mycobacteria intravesical treatment

IFN-ɣ and IL-17 were present in all culture supernatants from splenocytes restimulated ConA, but not IL-4 (data not shown). Besides, IFN-ɣ and IL-17 were also detected in all culture supernatants from splenocytes that were specifically restimulated with mycobacteria. IL-4 was not detected in any culture supernatant, being all the values under the limit of detection of the kit. Besides, any cytokine was found on the culture supernatant of non-restimulated splenocytes.

Differences were found in the production of IFN-ɣ and IL-17 by splenocytes from mice that were intravesically treated with mycobacteria.

As shown in Figure 37, IL-17 production was higher in splenocytes supernatants from mice treated with *M. brumae,* independently of the culture used for the growth, compared to culture supernatants from mice treated with *M. bovis* BCG treatments. When the production of IL-17 was compared among *M. brumae* or *M. bovis* BCG treatments, culture supernatant of splenocytes from mice treated with *M. brumae*-A60 showed the highest production of IL-17, being significant in all the cases. No differences were found among *M. bovis* BCG conditions. Besides, IL-17 released by splenocytes from all mycobacteria-treated tumour-bearing mice was significantly higher than the IL-17 released by splenocytes from healthy mice restimulated with either *M. brumae* or *M. bovis* BCG. However, only splenocytes from tumour-bearing animals treated with *M. brumae*-A60 or -G15 conditions triggered more IL-17 production than non-treated tumour-bearing mice (Figure 37a).

Otherwise, supernatants of splenocytes from tumour-bearing mice treated with *M. bovis* BCG showed higher IFN-ɣ production than those treated with *M. brumae,* independently of the culture media used for mycobacterial growth. In fact, the amount of IFN-ɣ produced in splenocytes supernatants from *M. bovis* BCG-treated mice was even one log superior to those obtained in cultures from *M. brumae*-treated mice. In *M. brumae*, the production of IFN-ɣ was statistically higher in supernatants from splenocytes of *M. brumae*-A60-treated mice, compared to *M. brumae*-G60 or 7H10- treated mice. For *M. bovis* BCG, the detection of IFN-ɣ was significantly superior in splenocytes supernatants from animals treated with *M. bovis* BCG-G15, compared to the rest of the conditions. Remarkably, only splenocytes from *M. brumae*-A60 and -G60, and *M. bovis* BCG-G15 and -G60 triggered significantly higher production of IFN-ɣ than non-treated tumour-bearing mice or healthy animals (Figure 37b).

Finally, splenocytes from animals treated with *M. brumae* or *M. bovis* BCG grown on A60, G15 or G60 were restimulated with the same mycobacteria but grown on Middlebrook 7H10. IL-17 production was still significant in *M. brumae*-A60 supernatants compared to *M. brumae*-G15 or -G60 conditions. Besides, IL-17 production was also significantly superior in splenocytes supernatants from *M. bovis* BCG-G15 compared to *M. bovis* BCG-A60 and *M.*

bovis BCG-G60 (Figure 37c). However, IFN-ɣ production was the same in all *M. brumae* and *M. bovis* BCG conditions (Figure 37d).
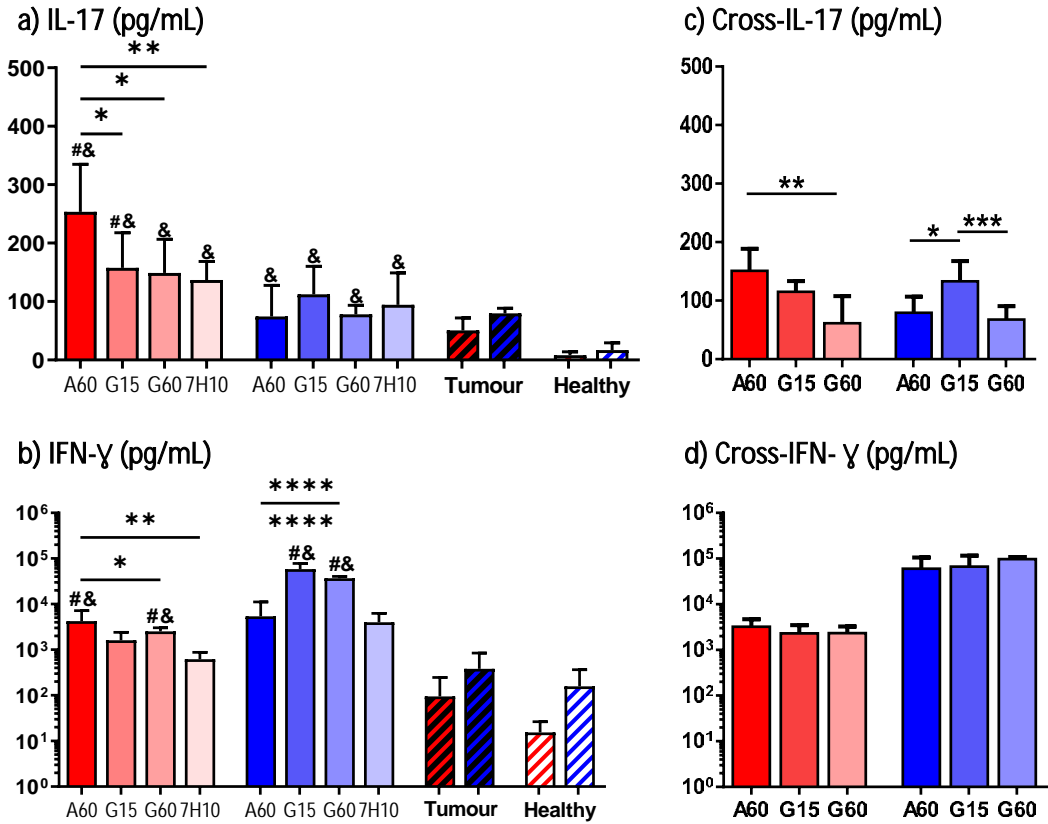
Figure 37. IFN-ɣ and IL-17 cytokine detection in culture supernatants from restimulated splenocytes. IFN-ɣ and IL-17 detection in culture supernatants from restimulated splenocytes. Splenocytes restimulated with heat-killed *M. brumae* are shown in red, while splenocytes restimulated with heat-killed *M. bovis* BCG are in blue. Mycobacteria were grown on the same culture media used for treating tumour-bearing mice (a and b); or with mycobacteria grown on Middlebrook 7H10 culture medium (c and d). Data represent the mean ± SD. *p < 0.05; **p < 0.01; ****p < 0.0001; # p< 0.05 respect the non-treated tumour-bearing mice; and & p< 0.05 respect the healthy animals (ANOVA test) (N=8).

4.3.4 Viable mycobacteria in spleens from mycobacteria-treated tumour-bearing mice

In previous results shown in section 4.2.1, *M. brumae* was cleared from the J774 murine macrophage cell line and THP-1 human macrophage cell line. At the same time, *M. bovis* BCG remained steady and persisted along through the experiment *in vitro*. To corroborate the capacity to survive or not, the presence of viable mycobacteria was studied in spleens from animals treated with *M. brumae* or *M. bovis* BCG grown on different culture conditions.

In *M.* brumae, culture media in which mycobacteria were grown did not affect the persistence of the bacteria as none *M. brumae* cells were detected in any spleen from treated mice. Otherwise, the results showed similar levels of *M. bovis* BCG cells detected in spleens from *M. bovis* BCG-treated mice, independent of the culture media used to grow the mycobacterium (Figure 38).
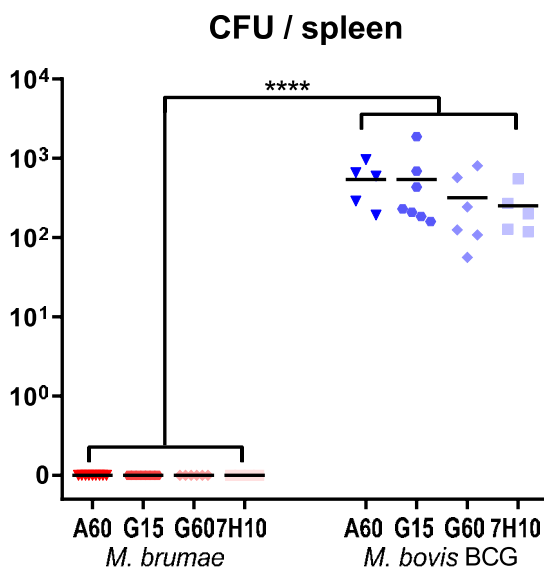
Figure 38. Colony-forming units (CFU) of spleens from mycobacteria-treated tumour-bearing mice. Colony-forming units (CFU) of spleens of tumour-bearing mice treated with *M. brumae* are shown in red, while tumour-bearing mice treated with *M. bovis* BCG are in blue. Mycobacteria counts from each spleen are represented by a dot; the line identifies the median for each group. *p<0.05 Kruskal-Wallis test, Dunn's multiple comparison test (N=8).

4.3.5 Local immune response induced in mycobacteria-treated tumour-bearing mice

Bladder from sacrificed animals at day 30 was analyzed by flow cytometry to determine the immune cell infiltration. Figure 39 shows the used gating strategy to identify a wide range of lymphocyte cells, defined as CD45+. Inside this phenotype, different populations were differentiated: ILCs defined as CD3−CD127+, B cells defined as CD3−B220+, NK cells defined as CD3−NK1.1+ or T cells defined as CD3+. T cells were also divided into CD8+ and CD4+ T cells. Besides, CD4+ T$_{EM}$ cells defined as CD62L−CD44+ were analyzed from the CD4+ T cells subset.
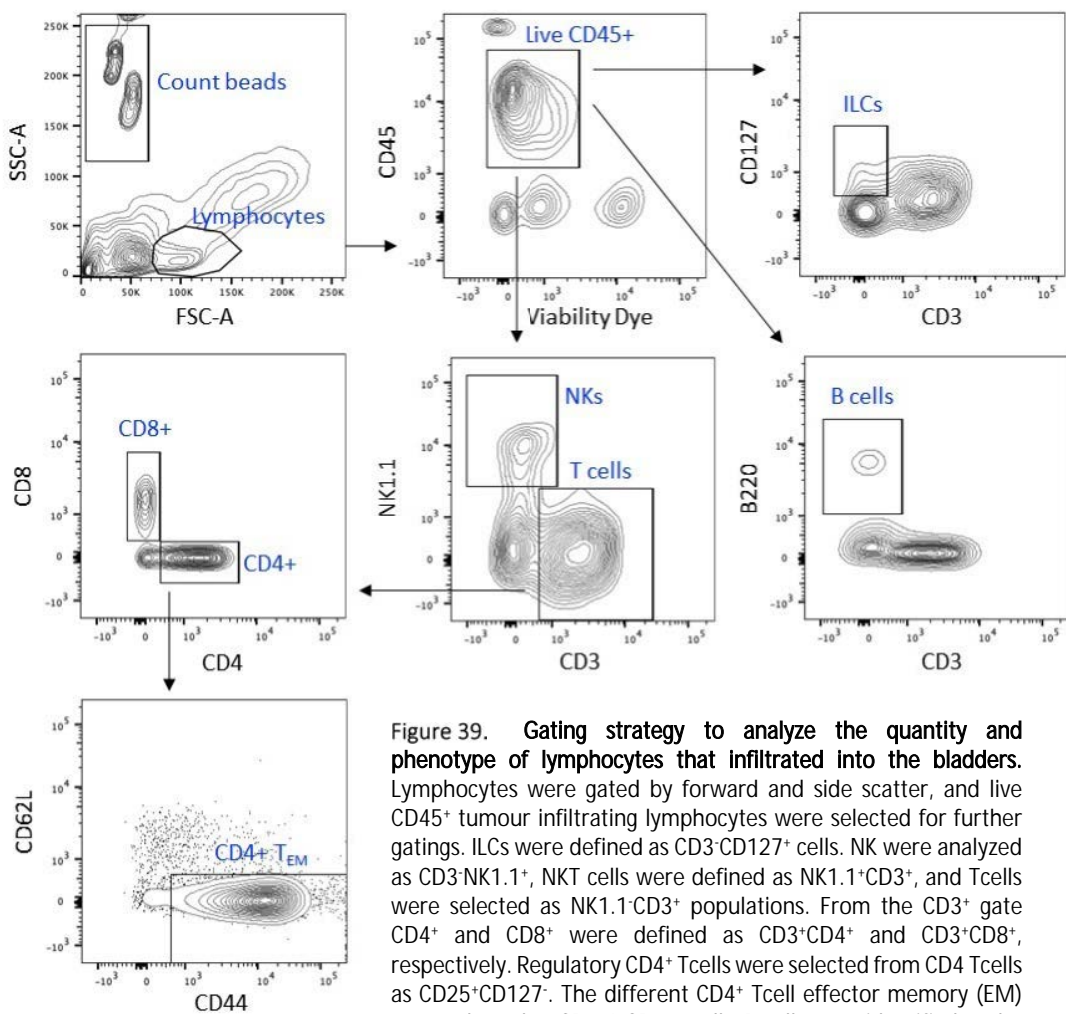
Figure 39. Gating strategy to analyze the quantity and phenotype of lymphocytes that infiltrated into the bladders. Lymphocytes were gated by forward and side scatter, and live CD45+ tumour infiltrating lymphocytes were selected for further gatings. ILCs were defined as CD3−CD127+ cells. NK were analyzed as CD3−NK1.1+, NKT cells were defined as NK1.1+CD3+, and Tcells were selected as NK1.1−CD3+ populations. From the CD3+ gate CD4+ and CD8+ were defined as CD3+CD4+ and CD3+CD8+, respectively. Regulatory CD4+ Tcells were selected from CD4 Tcells as CD25+CD127−. The different CD4+ Tcell effector memory (EM) were selected as CD62L−CD44+ cells. B cells were identified as the B220+ population gated from CD3- cells.

Firstly, all *M. bovis* BCG or *M. brumae* treatments were pulled together to increase the N of both mycobacteria to differentiate between the infiltration of the immune cells triggered after *M. brumae* or *M. bovis* BCG instillations.

M. bovis BCG treatments triggered a robust infiltration of lymphocytes CD45$^+$ into the bladder of tumour-bearing mice, including CD3+, CD4+ and CD8+ T NK and B cells, when compared with *M. brumae* intravesical treatments or control groups (non-treated tumour-bearing mice and healthy mice). Besides, *M. brumae* intravesical treatments also trigger higher infiltration of CD4$^+$ and CD8$^+$ T cells, NK and B cells into the bladder of tumour-bearing mice than healthy mice (Figure 40).

Then, differences among the infiltrated cells when comparing *M. brumae* and *M. bovis* BCG treatments were also assessed (Figure 41 and 42). When CD45$^+$, CD3$^+$, CD4$^+$ and CD8$^+$ T cells, or B and NK cells are shown together, an evident massive immune cell infiltration is triggered by intravesical treatments of both mycobacteria grown on Sauton G15 (Figure 41).

The absolute number of lymphocytes described as CD45$^+$, CD3$^+$, CD8$^+$ and NK were significantly less infiltrated into bladders of tumour-bearing mice treated with *M. brumae*-A60 than in the rest of the conditions, being statistically significant for all *M. bovis* BCG treatments. No differences were observed among *M. bovis* BCG treatments, except for CD4$^+$ that where highly infiltration was observed in *M. bovis* BCG-G15 treated-mice than in *M. bovis* BCG-A60 treated-mice (Figure 42c).

When CD8$^+$ were analysed, low infiltration was found in tumour-bearing mice treated with *M. brumae*-A60 compared to the other *M. brumae* treatments, although not reaching statistical differences. Besides, CD8$^+$ infiltrated into the bladder of tumour-bearing mice treated with *M. bovis* BCG-G15 was significantly superior to animals treated with *M. brumae*-A60, -G60 and -7H10 (Figure 42d).

Regarding B cells, significant low infiltration was found into the bladder of tumour-bearing mice treated with *M. brumae*-A60 compared to *M. brumae*-G15 condition, or *M. bovis* BCG-A60 and *M. bovis* BCG-G60 (Figure 42e).
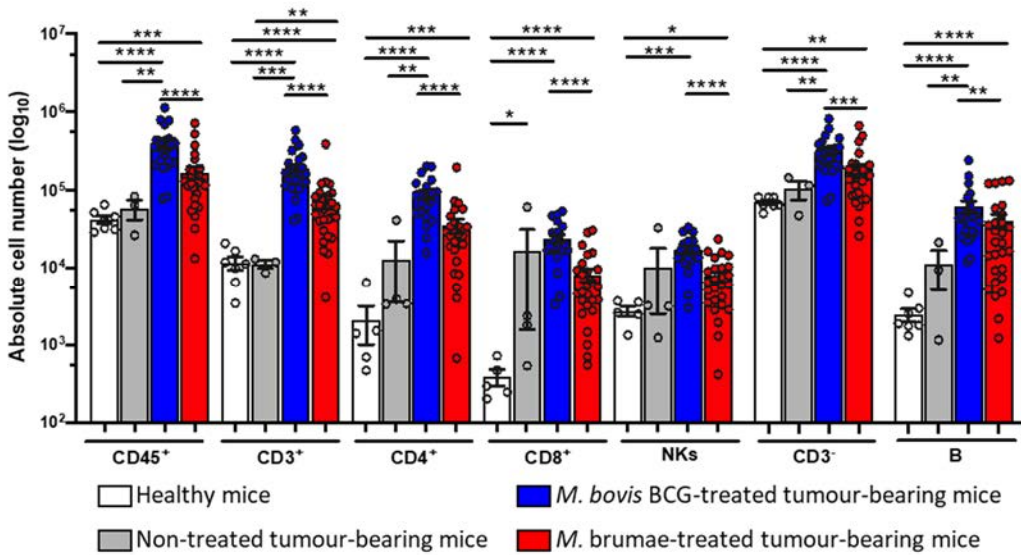
Figure 40. Robust infiltration of immune cells into the bladder after mycobacteria treatment. Absolute counts of total live CD45+ cells, CD3+ T cells, CD4+ and CD8+ T cells, NK+ cells (CD3-NK1.1+), CD3- cells and B cells (CD3-B220+) were quantified by flow cytometry after bladder digestion of untreated healthy mice (white bars), non-treated tumour-bearing mice (grey bars), pooled tumour-bearing mice treated with *M. bovis* BCG treatments (blue bars) or *M. brumae* treatments (red bars), independently of the culture media used for their growth. Data represent the mean ± Standard error of the mean (error bars), and each dot represents a separate animal. Mann-Whitney U nonparametric test. *$p \leq 0.05$; **$p \leq 0.01$; ***$p \leq 0.001$; ****$p \leq 0.0001$.
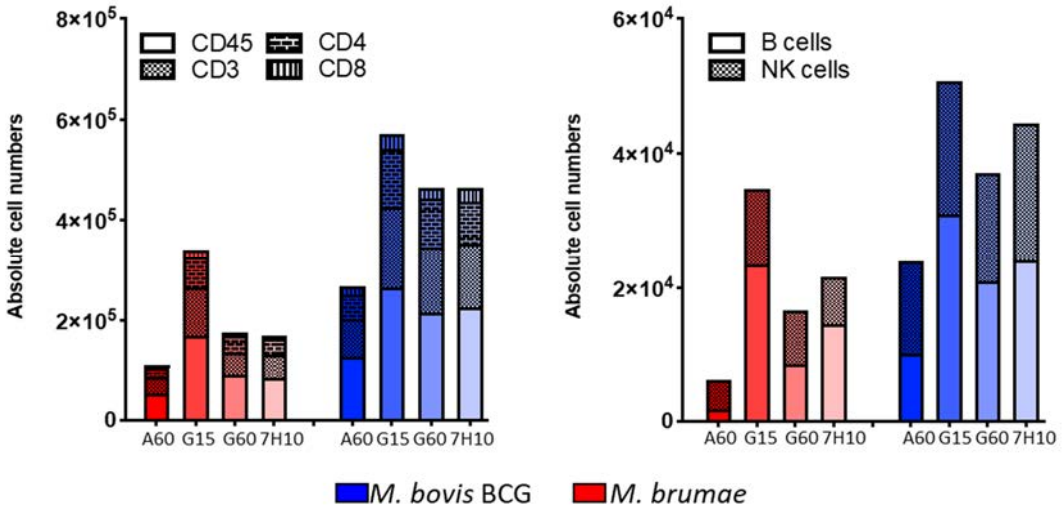
Figure 41. Immune cell infiltration into the bladder of mycobacteria-treated tumour-bearing mice. Immune cell infiltration into the bladder of mycobacteria-treated tumour-bearing mice, either *M. brumae* or *M. bovis* BCG grown on different culture media. Absolute numbers of infiltrating CD45+, CD3+, CD4+ and CD8+ T cells (left graph) and B and NK cells (right graph).

135
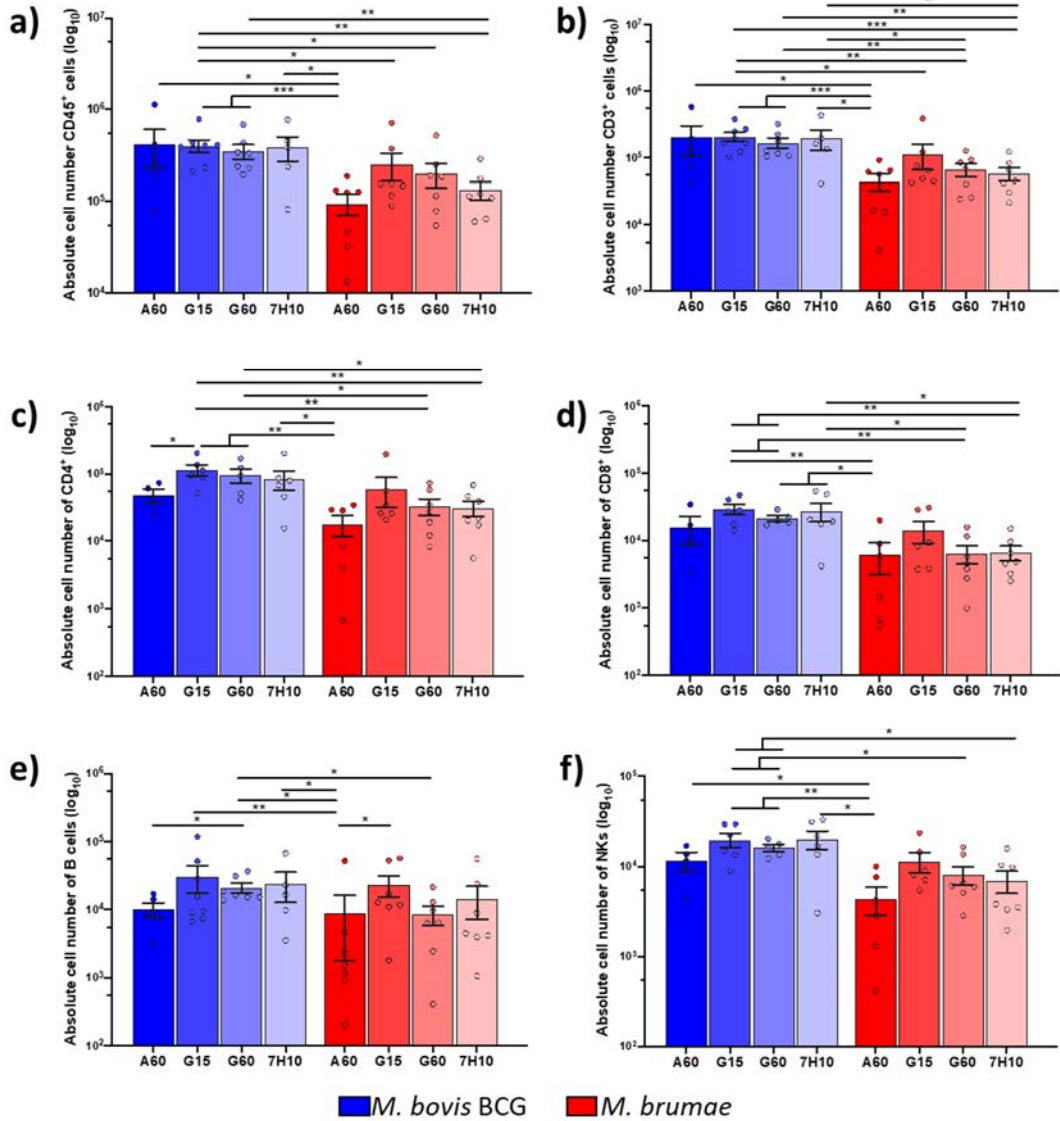
Figure 42. **Robust infiltration of immune cells into the bladder triggered by mycobacteria grown on different culture media.** Absolute counts of total live CD45+ cells, CD3+ T cells, CD4+ and CD8+ T cells, NK+ cells (CD3-NK1.1+), CD3- cells and B cells (CD3-B220+) were quantified by flow cytometry after bladder digestion. *M. bovis* BCG treatments are shown in blue, and *M. brumae* treatments in red. Data represent the mean ± Standard error of the mean (error bars), and each dot represents a separate animal. Mann-Whitney U nonparametric test. *p≤ 0.05; **p ≤ 0.01; ***p ≤ 0.001.

After analysing the most common immune cell population infiltrated into the bladder of mycobacteria-treated tumour-bearing mice, other populations were analysed to correlate the local and the systemic immune response observed in splenocytes.

Considering the high production of IL-17 secreted by splenocytes from *M. brumae*-treated mice restimulated with *M. brumae*, specifically *M. brumae*-A60, ILC and CD4$^+$ T$_{EM}$ were analyzed as IL-17 producers' cells. Remarkably, despite the low number of infiltrated immune cells induced by *M. brumae*-A60, a significant high infiltration of CD4$^+$ T$_{EM}$ was observed into the bladder of tumour-bearing mice treated with *M. brumae*-A60 in comparison to the rest of treatments, even among *M. bovis* BCG treatments. Additionally, ILC also showed high infiltration in bladders from *M.* brumae-A60 treated tumour-bearing mice compared to all the other treatments (Figure 43).
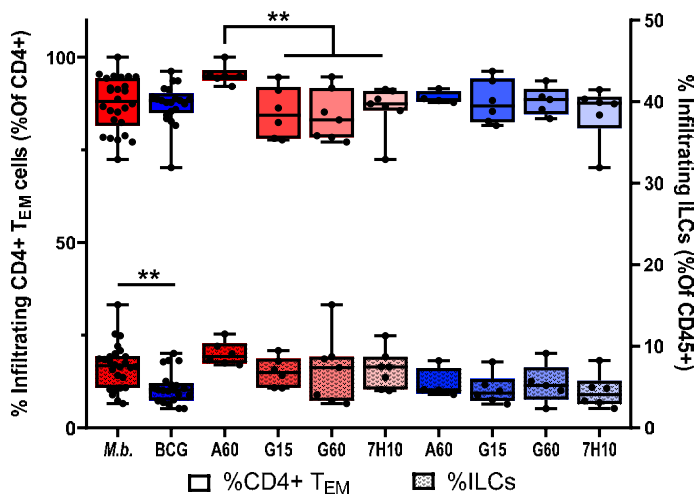
Figure 43. **CD4$^+$ T$_{EM}$ cells and ILCs infiltrating into the bladder.** Frequency of CD4$^+$ T$_{EM}$ cells and ILCs infiltrating bladder tissue from healthy or tumour-bearing mice, treated with *M. brumae* or *M. bovis* BCG grown on different culture media. Mean ± SD values are given, with dots representing individual mice. Mann-Whitney U nonparametric test **p ≤ 0.01

To decipher whether ILC and CD4$^+$ T$_{EM}$ these immune cell populations had a relation with the cytokine levels produced by splenocytes, all values of these immune cells from *M. brumae* or *M. bovis* BCG treatments were pulled together. For *M. brumae,* a positive correlation was found between IL-17 production and ILC, and IL-17 production and CD4$^+$ T$_{EM.}$ Otherwise, no correlation was found for *M. bovis* BCG-treated mice (Figure 44 a and b).

As explained before, *M. brumae* and *M. bovis* BCG induced a high production of IFN-ɣ by restimulated splenocytes, especially *M. bovis* BCG. The IFN-ɣ produced by splenocytes positively correlated to the frequency of CD3$^+$, CD4$^+$, CD8$^+$ and CD4$^+$ T$_{EM}$, immune cells described as IFN-ɣ producers. As Figure 44 shows, a positive correlation was found for both mycobacteria treatments, although the levels of IFN-ɣ produced by splenocytes of *M. bovis* BCG-treated mice were notably higher than *M. brumae*-treated mice. No correlation was found in healthy animals or non-treated tumour-bearing mice.
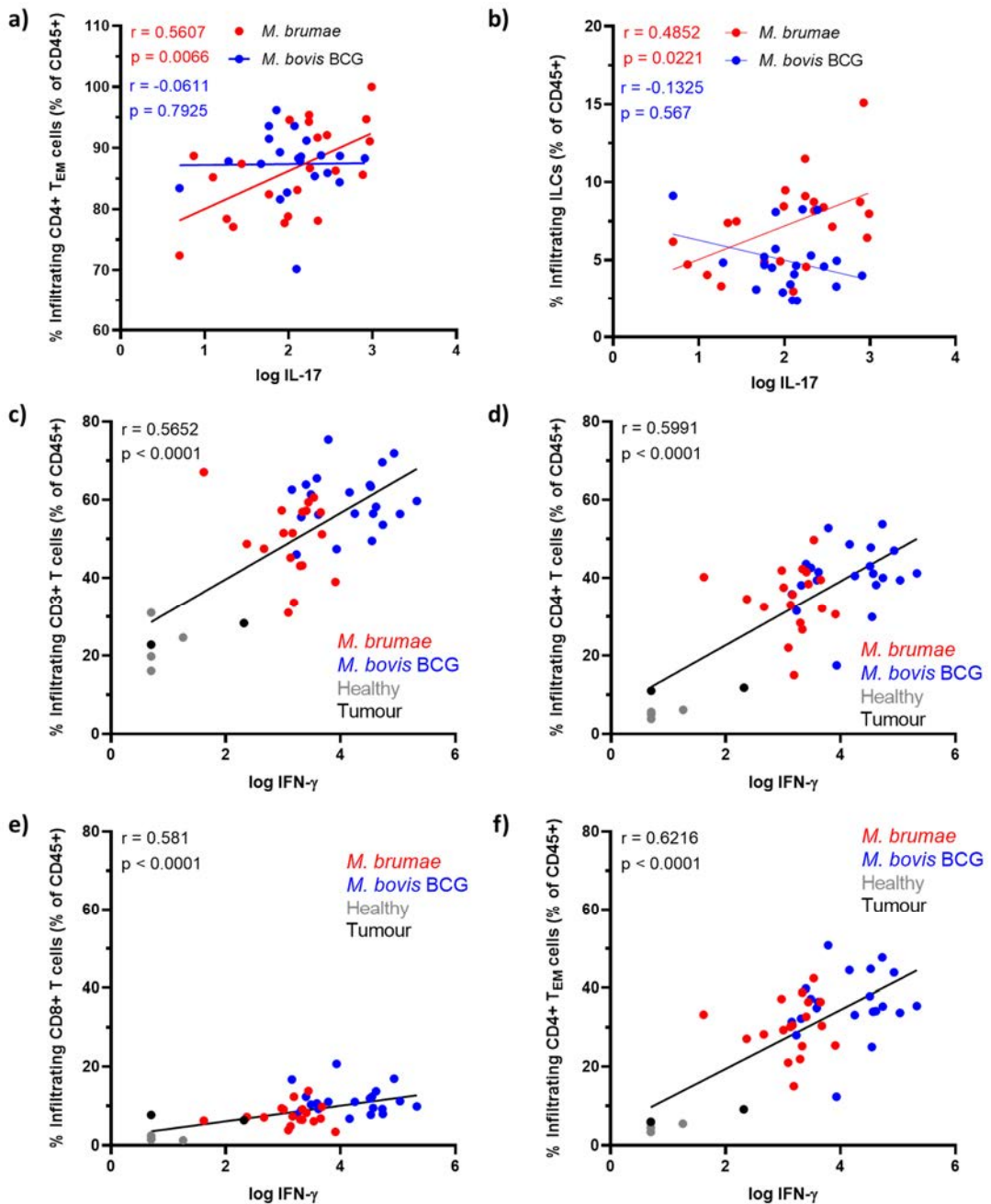
Figure 44. Correlation between immune cells infiltrated into the bladder and cytokine released by splenocytes. Secretion of IL-17 by restimulated splenocytes significantly correlates to a) the frequency of CD4$^+$ T$_{EM}$ cells and b) the frequency of innate lymphoid cells (ILCs). Secretion of IFN-ɣ produced by restimulated splenocytes significantly correlates c) CD3+, d) CD4+, e) CD8+ T, and f)CD4+ effector memory (TEM). Each dot represents one mouse. *M. brumae*-treated mice are shown in red, *M.bovis* BCG is shown in blue. Pearson *r* and *p* values are indicated.

4.3.6 Histological analysis of bladders from mycobacteria-treated tumour-bearing mice

Bladders from animals were collected, fixed and processed to perform a histopathological analysis. A solid mass inside the bladder lumen infiltrating under the *lamina propria* of the bladders was observed in bladders from non-treated tumour-bearing mice, indicating an intense lymphoplasmacytic infiltration. In the case of mycobacteria-treated mice, the majority of bladders showed a tumour clearance. Diffuse tumour cells or solid tumours were only observed in some cases. However, mild to moderate infiltrations were observed in all the mice. No differences were observed among *M. brumae* or *M. bovis* BCG conditions. Remarkably, lymphoplasmacytic infiltration was more intense among treatment conditions of *M. bovis* BCG than among *M. brumae* groups. It is worth mentioning that a granulomatous inflammation, which implies the chronic accumulation of macrophages, was observed in two animals treated with *M. bovis* BCG-G15, and two animals treated with *M. bovis* BCG-G60 (Figure 45).
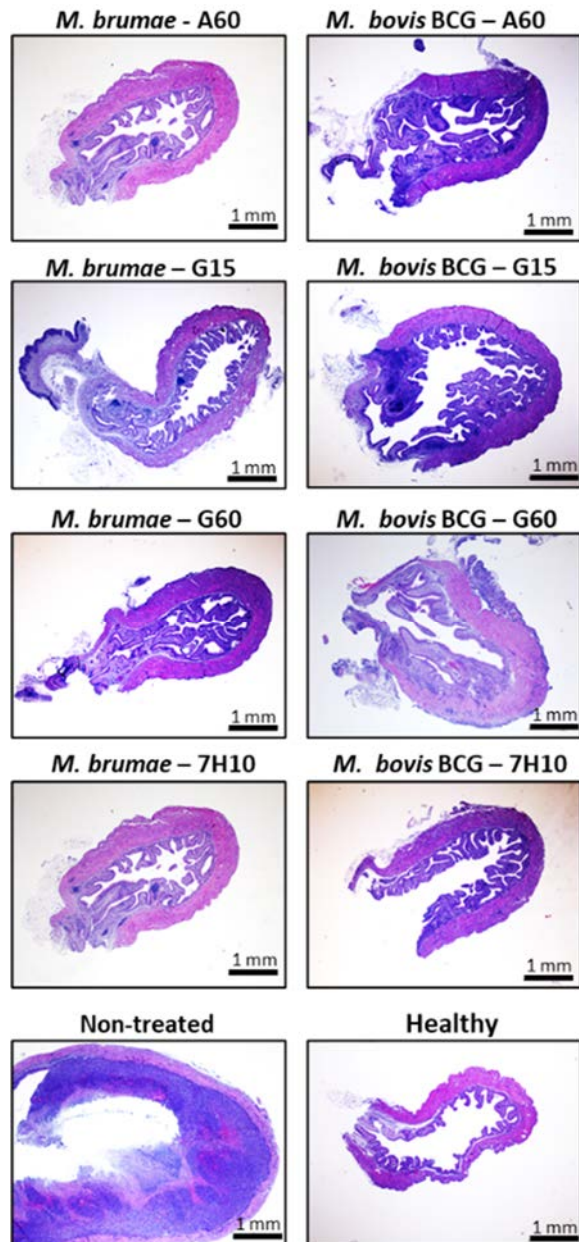
Figure 45. **Histological analysis of bladders from mycobacteria-treated tumour-bearing mice.** Representative histological images (hematoxylin-eosin staining) of bladder sections from non-treated (PBS), M. brumae-treated, and M. bovis BCG-treated tumour-bearing mice. Scale refers to 1mm.

139

4.4 Study *in vivo* to evaluate the effect of a previous mycobacteria vaccination to improve the antitumour effect of mycobacteria intravesical treatments

The effect of previous vaccination with *M. bovis* BCG is considered a plausible option to improve the response to later intravesical instillations with the same mycobacterium. Accordingly, sets of experiments were performed in the orthotopic BC mouse model to evaluate the effect of *M. brumae* and *M. bovis* BCG. Besides, a cross-immunostimulating reaction, which means a subcutaneous vaccination with *M. bovis* BCG plus intravesical instillations with *M. brumae,* was also evaluated.

M. brumae grown on A60 culture media was selected to perform the vaccination experiments since it showed the most favourable immunostimulatory effect for antitumour activity. However, *M. bovis* BCG was grown on Middlebrook 7H10 for comparative purposes as more data are available. The dose of subcutaneous vaccination with *M. bovis* BCG in the literature ranges from 5 x 10^6 CFU to a maximum of 1 x 10^7 CFU, being the order of 10^6 CFU the most repeated vaccination dose. Accordingly, animals were subcutaneously vaccinated with 2 x 10^6 CFU of *M. bovis* BCG. In *M. brumae*, two different doses were used (2 x 10^7 CFU and 2 x 10^8 CFU) as none study is published in the literature. The complete schedule is shown in Figure 16. Briefly, 20-22 days after subcutaneous vaccination, BC was induced, and animals received a weekly intravesical treatment for a total of 4 weeks.

4.4.1 Proliferation and cytokine production of splenocytes recovered from tumour-bearing mice previously vaccinated with *M. brumae*

4.4.1.1 Antitumour effect on MB49 cells of splenocytes from tumour-bearing mice previously vaccinated with *M. brumae*

Splenocytes from each animal were cultured together with the MB49 cell line at a ratio of 12.5 splenocytes per tumour cell for 24 hours, contrary to the previous experiment showed in Section 4.3.3.1, where the used ratio was 25:1. Then, the viability of MB49 cells was determined by the MTT assay. No significant differences were observed between the groups (Figure 46).

Coculture Splenocytes - MB49 cells
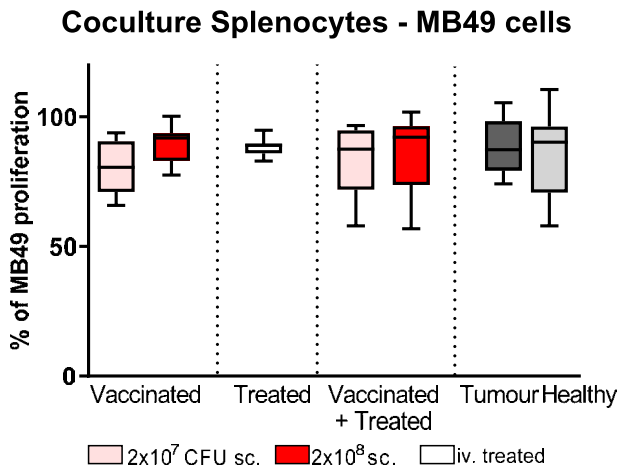
Figure 46. **Cytotoxic activity triggered by splenocytes.** MB49 cell inhibition triggered by splenocytes from mice that were only subcutaneously (sc) vaccinated with 2 x 10⁷ CFU of *M. brumae* (pink) or vaccinated with 2 x 10⁸ CFU of *M. brumae* (red), only intravesically treated (iv, white), or vaccinated and treated. Non-vaccinated non-treated tumour bearing mice (black) and healthy animals (grey). Data represent the mean ± SD. N=8.

4.4.1.2   Splenocytes proliferation and cytokine production

Spleens from animals vaccinated with the two different doses of *M. brumae* were collected at day 30 after tumour induction to study the systemic immune response triggered by the vaccination and/or the intravesical treatments. The splenocytes were cultured in the presence of 1) ConA as a positive control, 2) HK-*M. brumae* grown on A60 medium and 3) PBS to establish the basal level of either splenocytes proliferation and cytokine production. After 72 h of incubation at 37°C in the presence of 5% of CO_2, cell proliferation was determined by MTT. Supernatants were collected to analyse the presence of IL-2 produced by T cells proliferation, and the production of IFN-ɣ, IL-4 and IL-17 to observe whether the combination of vaccination and intravesical treatment induced a Th1, Th2 or Th17 response, respectively.

Splenocytes proliferation with ConA was induced in all groups. When splenocytes were exposed to HK-*M. brumae,* significant differences in splenocytes proliferation were achieved between only intravesically-treated mice compared to healthy or tumour animals. Moreover, restimulation of only intravesically-treated mice was also superior to the restimulation triggered by the splenocytes from vaccinated animals with the lowest dose of *M. brumae.* Remarkably, the restimulation produced by any of the vaccinated groups was not significantly different to the control groups (Figure 47).

When the presence of cytokines (IL-2, IL-4, IL-17 and IFN-ɣ) was analyzed in splenocyte culture supernatants at 72 h, the levels of all cytokines triggered by ConA were higher than those obtained by splenocytes exposed to HK-*M. brumae.* Moreover, none cytokines were detectable on culture supernatants of splenocytes exposed to PBS (data not shown).
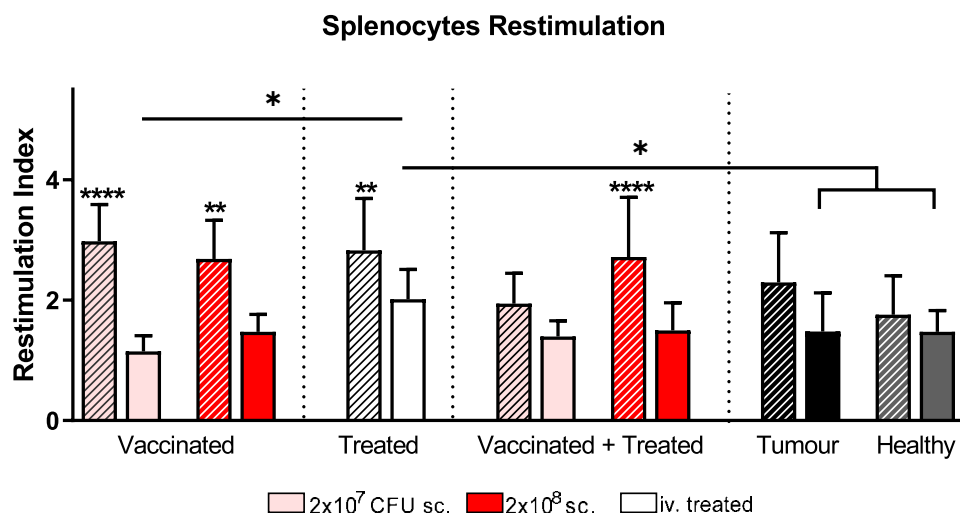
Figure 47. **Proliferation of *M. brumae*-restimulated splenocytes.** Data represent the restimulation index of restimulated splenocytes over non-restimulated splenocytes. Splenocytes were restimulated with Concanavalin A (ConA) shown as linear bars or *M. brumae* shown as solid bars. Mice were only subcutaneously (sc) vaccinated with 2 x 10⁷ CFU of *M. brumae* (pink) or vaccinated with 2 x 10⁸ CFU of *M. brumae* (red), only intravesically treated (iv, white), or vaccinated and treated. Non-vaccinated non-treated tumour bearing mice (black) and healthy animals (grey). Data represent the mean ± SD. *p < 0.05; ****p < 0.0001 (ANOVA test) N=8.

Regarding the production of IL-2 after specific restimulation with HK-*M. brumae*, all mice that were vaccinated, treated, or vaccinated + treated with *M. brumae* produce IL-2, while in control groups (healthy or non-treated tumour-bearing mice), the IL-2 response was undetectable. Once focused on the two doses of subcutaneous vaccination of *M. brumae*, the subcutaneous vaccination with 2×10^8 CFU induced higher production of IL-2 in comparison to the subcutaneous vaccination with 2×10^7 CFU, independently of being the animal treated or not. Moreover, splenocytes from mice that were not vaccinated produced significantly lesser IL-2 than mice that were vaccinated or vaccinated + treated with the high dose of *M. brumae* (Figure 48a).

Only the splenocytes from tumour-bearing mice that were vaccinated with the high dose of *M. brumae* and intravesically treated triggered significantly higher levels of IFN-ɣ than the rest of the conditions. Moreover, splenocytes from tumour-bearing mice that were only intravesically treated produced the lowest production of IFN-ɣ, despite not being significantly different (Figure 48b).

Despite an apparent tendency to produce IL-17 depending on the dose used for the mice vaccination, significant differences were only achieved for vaccinated and treated tumour-bearing mice with the high dose of *M. brumae* (Figure 48c).

Finally, IL-4 production was also analyzed on the spleen supernatants. When IL-4 production was studied in splenocytes specifically restimulated with *M. brumae*, no significant differences between the groups were observed (Figure 48d).
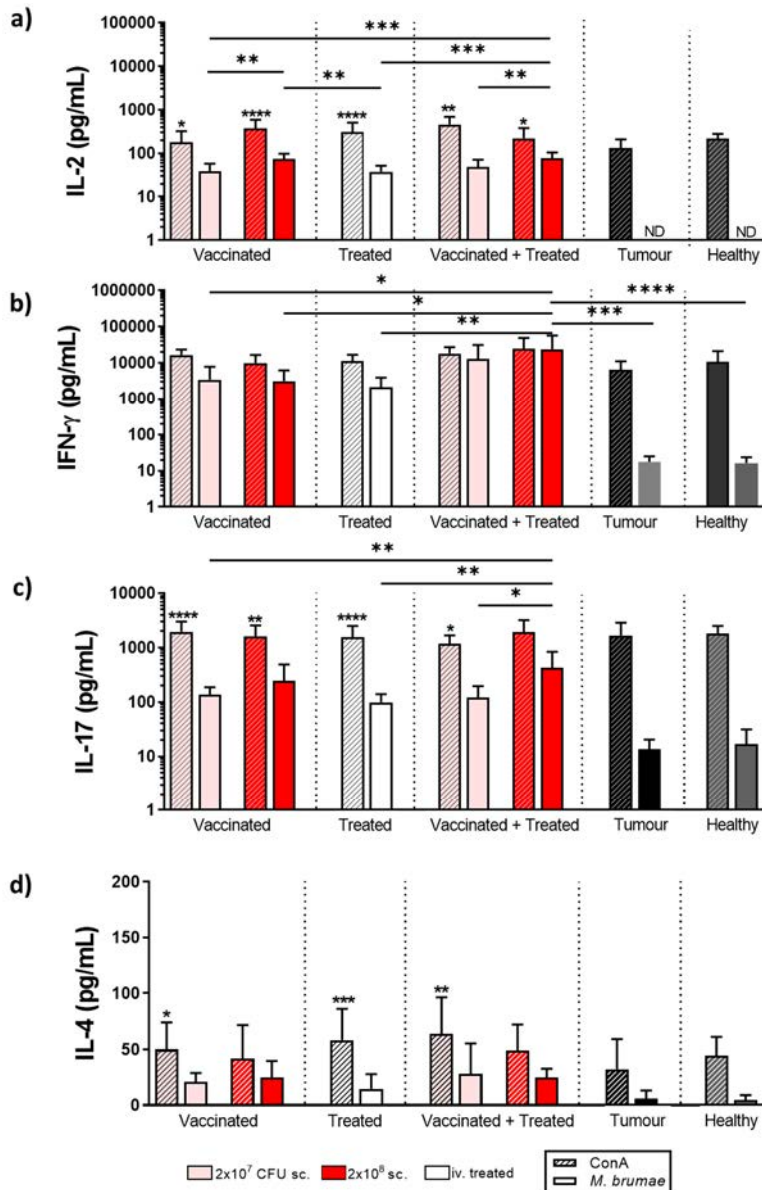
Figure 48. Cytokine detection in culture supernatants from restimulated splenocytes. IL-2, IFN-ɣ, IL-17 and IL-4 detection in culture supernatants from restimulated splenocytes. Splenocytes were restimulated with Concanavalin A (ConA) shown as linear bars, or *M. brumae* shown as solid bars. Mice were only subcutaneously (sc) vaccinated with 2×10^7 CFU of *M. brumae* (pink) or vaccinated with 2×10^8 CFU of *M. brumae* (red), only intravesically treated (iv, white), or vaccinated and treated. Non-vaccinated non-treated tumour bearing mice (black) and healthy animals (grey). Data represent the mean ± SD. *$p < 0.05$; **$p < 0.01$;****$p < 0.0001$ (ANOVA test) N=8.

4.4.2 Detection of viable mycobacteria in organs from tumour-bearing mice previously vaccinated with *M. brumae*

Spleens and lungs were carefully extracted from sacrificed mice to determine the presence of viable bacteria. Before processing the spleen, the spleen's size was also measured. Measurement of spleen size revealed that spleens from healthy animals were smaller than the rest of the groups. No differences were found among only vaccinated, only treated, or vaccinated + treated animals. However, spleens from only intravesically treated animals seemed to be smaller than those that were vaccinated, or vaccinated and treated (Figure 49). Nevertheless, non-statistical significances were observed among groups. When CFUs were counted, the results showed that no mycobacteria were detected in mice's spleens or lungs from any of the conditions of *M. brumae.*
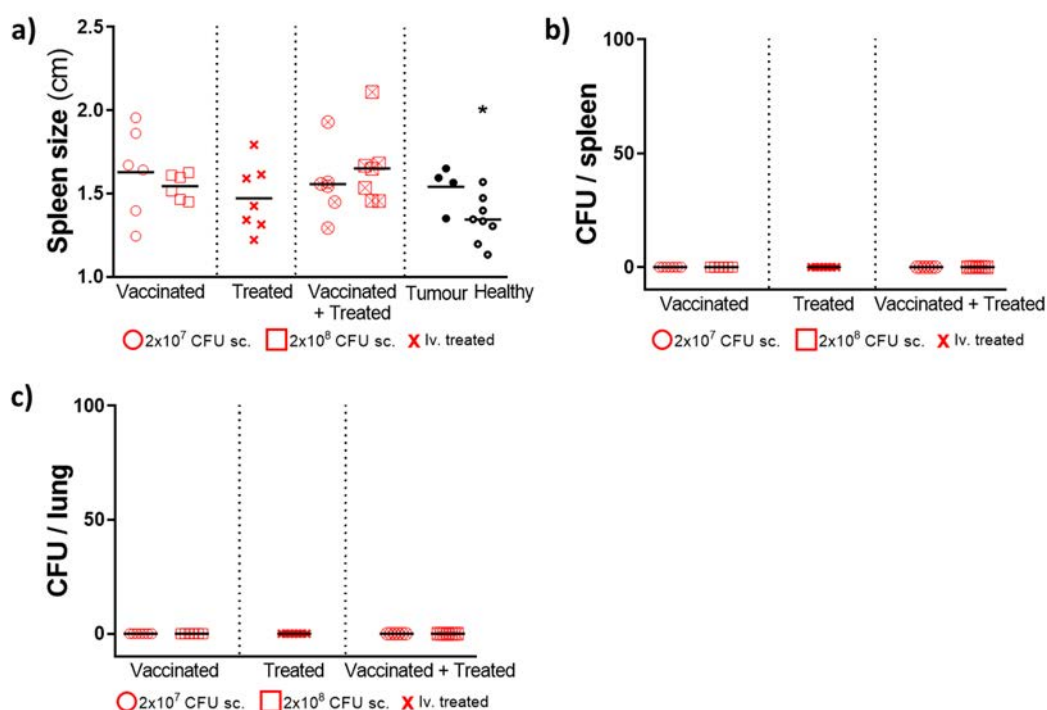
Figure 49. Detection of viable *M. brumae* in organs. a) Spleen size expressed in cm. b) Colony-forming units (CFU) of spleens from *M. brumae*-vaccinated or -treated tumour-bearing mice. c) Colony-forming units (CFU) of lungs from *M. brumae*-vaccinated or -treated tumour-bearing mice. Each animal is represented by a dot; the line identifies the median for each group. Mice were only subcutaneously (sc) vaccinated with 2 x 10^7 CFU of *M. brumae* (empty red dot) or vaccinated with 2 x 10^8 CFU of *M. brumae* (empty red square), only intravesically treated (iv, red cross), vaccinated with 2 x 10^7 CFU of *M. brumae* and treated (cross red dot) or vaccinated with 2 x 10^8 CFU of *M. brumae* and treated (cross red square). Non-vaccinated and non-treated tumour-bearing mice (full black dot), healthy animals (empty black dot).

4.4.3 Detection of IgG in sera of tumour-bearing mice previously vaccinated with *M. brumae*

The systemic humoral immune response was assessed in the sera of blood samples obtained at day 30. In all tumour-bearing mice, significant IgG levels against *M. brumae* were found in comparison to healthy mice. However, no significant differences were found among groups, as shown in Figure 50.

Figure 50. ***M. brumae*-specific IgG antibodies detected in sera from mice.** Levels of specific IgG anti-*M. brumae* are shown. Each animal is represented by a dot; the line identifies the median for each group. Mice were only subcutaneously (sc) vaccinated with 2×10^7 CFU of *M. brumae* (empty red dot) or vaccinated with 2×10^8 CFU of *M. brumae* (empty red square), only intravesically treated (iv, red cross), vaccinated with 2×10^7 CFU of *M. brumae* and treated (cross red dot) or vaccinated with 2×10^8 CFU of *M. brumae* and treated (cross red square). Non-vaccinated and non-treated tumour-bearing mice (full black dot), healthy animals (empty black dot). Data represent the mean *$p < 0.05$ (ANOVA test)
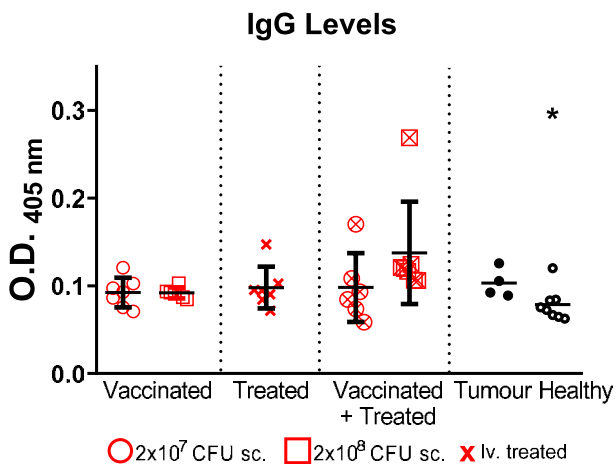
4.4.4 Antitumour effect on MB49 cells and cytokine release of PECs from tumour-bearing mice previously vaccinated with *M. brumae*

PECs were recovered from mice after performing a vigorous massage of the mice abdomen. Then, PECs were counted and cultured for 24 hours. At that time point, supernatants were collected, and MB49 cells were added to the wells for 48 hours to measure the inhibition of BC proliferation triggered by PECs.

Regarding the inhibition of tumour cells by PECs, no significant differences were observed between the groups. Despite these results, the production of cytokines in PECs cultures supernatants showed different immune response among groups. Firstly, no production of IL-2 was detected in any condition (Figure 51).

When IL-6 was analysed, its detection was significantly lower in the supernatants of PECs from tumour-bearing mice that were subcutaneously vaccinated with the low dose of *M. brumae*, compared to vaccinated + treated animals, independently of the dose. Surprisingly,

145

high IL-6 levels were found in only treated mice compared to the rest of the groups, although no significant differences were found (Figure 51).

Regarding the production of TNF-α, vaccination with a high dose of *M. brumae* seemed to induce higher levels of TNF-α in the culture supernatants of PECs, despite not reaching statistically differences. Remarkably, differences were found in tumour-bearing mice compared to the two groups vaccinated with the low dose of *M. brumae.* However, conclusions can not be performed due to the low number of non-treated tumour-bearing mice (Figure 51).
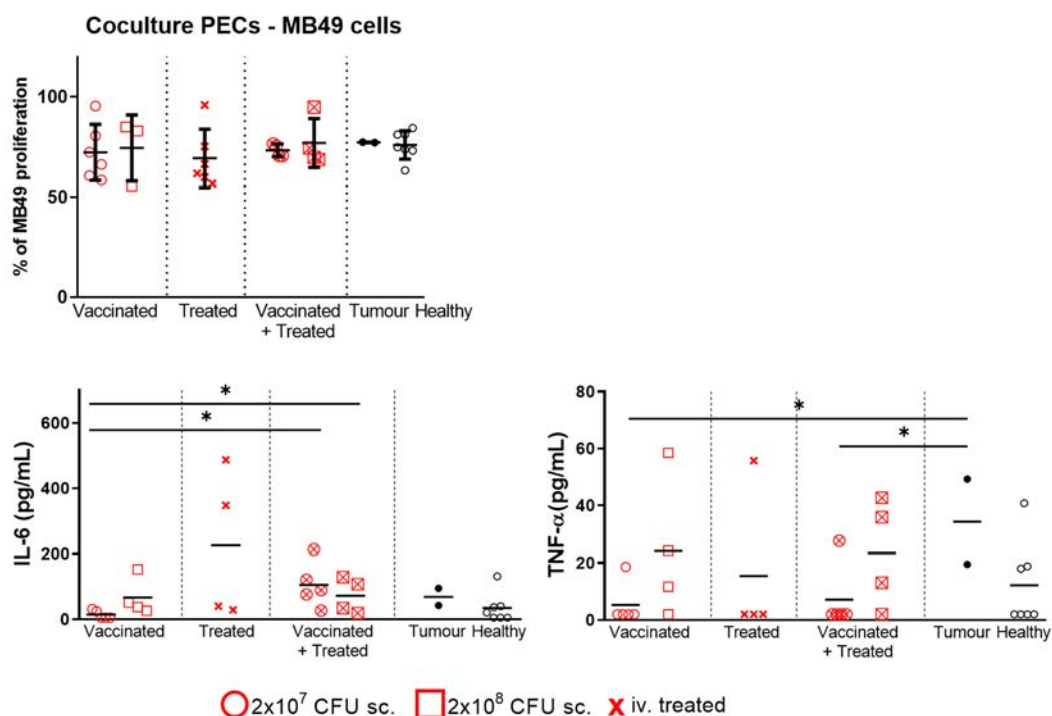
Figure 51. Cytotoxic activity triggered by peritoneal exudate cells (PECs). MB49 cell inhibition triggered by PECs from mice. Each animal is represented by a dot; the line identifies the mean for each group. Mice were only subcutaneously (sc) vaccinated with 2 x 10^7 CFU of *M. brumae* (empty red dot) or vaccinated with 2 x 10^8 CFU of *M. brumae* (empty red square), only intravesically treated (iv, red cross), vaccinated with 2 x 10^7 CFU of *M. brumae* and treated (cross red dot) or vaccinated with 2 x 10^8 CFU of *M. brumae* and treated (cross red square). Non-vaccinated and non-treated tumour-bearing mice (full black dot), healthy animals (empty black dot). Data represent the mean *$p < 0.05$; ANOVA test. Cytokine analyses were measured in PECs supernatants at 24h before adding MB49 cells.

Considering that prior vaccination with a high dose of *M. brumae* triggered a systemic immune response, mainly observed in splenocytes, those results were used to compare the effect of *M. brumae* and *M. bovis* BCG vaccination.

4.4.5 Proliferation and cytokine production of splenocytes recovered from tumour-bearing mice previously vaccinated with *M. brumae* or *M. bovis* BCG

4.4.5.1 Antitumour effect on MB49 cells of PECs from tumour-bearing mice previously vaccinated with *M. brumae* or *M. bovis* BCG

As previously explained, splenocytes from each animal were cultured together with the MB49 cell line at a ratio of 12.5 splenocytes per tumour cell for 24 hours. Splenocytes from *M. bovis* BCG-vaccinated mice treated with *M. brumae* triggered significant higher inhibition of MB49 proliferation than the rest of the conditions, except those that were only *M. bovis* BCG-vaccinated or vaccinated and treated with *M. brumae* (Figure 52).

	Vaccinated		Treated		Vaccinated + Treated		Cross Reaction	Tumour	Healthy
Vaccination	M	B	∅	∅	M	B	B	∅	∅
Tumour	✔	✔	✔	✔	✔	✔	✔	✔	∅
Treatment	∅	∅	M	B	M	B	M	∅	∅
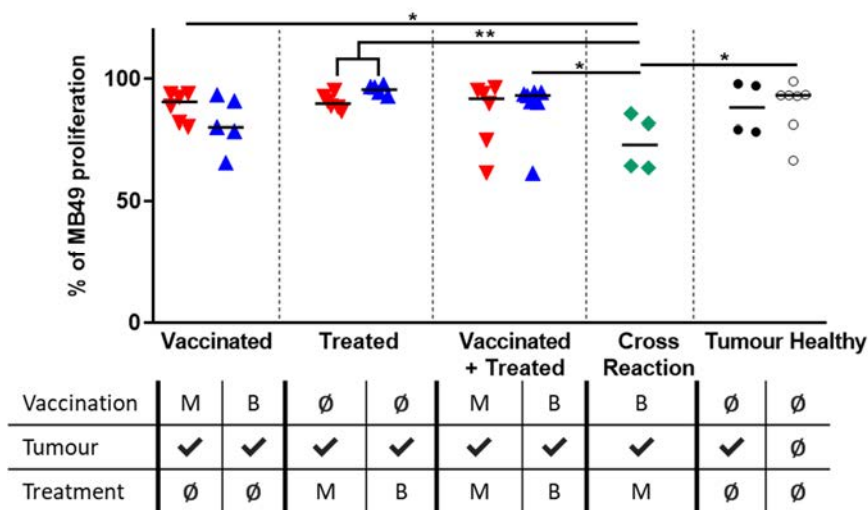
Figure 52. **Cytotoxic activity triggered by splenocytes.** MB49 cell inhibition triggered by splenocytes from tumour-bearing mice (✓) that were only subcutaneously vaccinated with *M. brumae* (M) or vaccinated with *M. bovis* BCG (B), only intravesically treated with *M. brumae* or *M. bovis* BCG, vaccinated and treated with *M. brumae*, vaccinated and treated with *M. bovis* BCG, vaccinated with *M. bovis* BCG and treated with *M. brumae*, or non-vaccinated (∅) and non-treated (∅) (full black dot). *M. brumae* in red, *M. bovis* BCG in blue. Healthy animals (empty dot). Line represents the mean ± SD. *$p < 0.05$; **$p < 0.01$, ANOVA test.

4.4.5.2 Splenocytes proliferation and cytokine production

Proliferation index and cytokine release of spleens from animals vaccinated with the high dose of *M. brumae*, treated with *M. brumae*, or vaccinated with the high dose + treated with *M. brumae* were compared with spleens from animals vaccinated with *M. bovis* BCG, treated with *M. bovis* BCG, or vaccinated + treated with *M. bovis* BCG. All conditions were listed in Table 16. Splenocytes were cultured in the presence of 1) ConA as a positive control; 2) HK-

M. brumae grown on A60 medium or HK-*M. bovis* BCG grown on Middlebrook 7H10 depending on the mycobacteria used for the vaccination and treatment; and 3) PBS to establish the basal level of either splenocytes proliferation or cytokine production. Besides, splenocytes from control groups (healthy and non-treated tumour-bearing mice) and those animals *M. bovis* BCG-vaccinated and *M. brumae*-treated were exposed to both, HK-*M. brumae* and HK-*M. bovis* BCG. After 72 h of incubation at 37°C in the presence of 5% of CO_2, cell proliferation in response to the antigens was determined by MTT. Supernatants were collected to analyze the presence of IL-2, IFN-ɣ, IL-4 and IL-17 cytokines.

Accordingly, to the previous results observed in *M. brumae*, all splenocytes were nonspecifically restimulated with ConA. When splenocytes were exposed specifically to mycobacteria, no differences were reached among conditions (Figure 53).
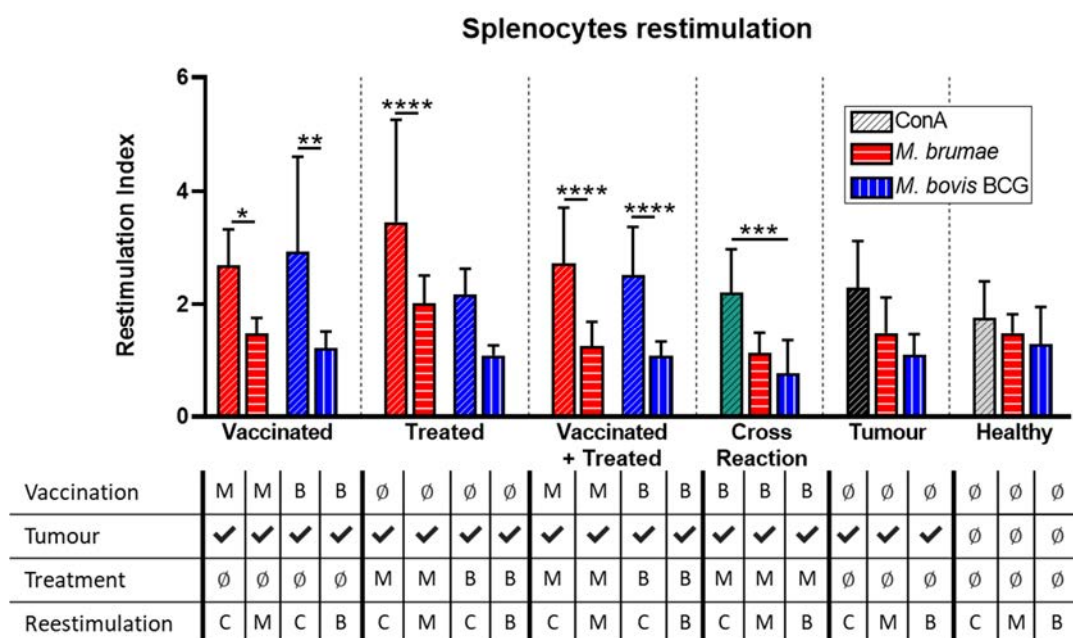
Figure 53. Proliferation of mycobacteria-restimulated splenocytes. Data represent the restimulation index of restimulated splenocytes over non-restimulated splenocytes. Splenocytes were restimulated with Concanavalin A (ConA, C) shown as oblique line bars, *M. brumae* shown as horizontal line bars solid bars, or *M. bovis* BCG shown as vertical line bars. Mice were subcutaneously vaccinated with *M. brumae* (M) or vaccinated with *M. bovis* BCG (B), only intravesically treated with *M. brumae* or *M. bovis* BCG, vaccinated and treated with *M. brumae*, vaccinated and treated with *M. bovis* BCG, vaccinated with *M. bovis* BCG and treated with *M. brumae* (green), or non-vaccinated (∅) and non-treated (∅) shown in black. *M. brumae* in red, *M. bovis* BCG in blue, and healthy animals in grey. Line represents the mean ± SD. *$p < 0.05$; **$p < 0.01$, ***$p < 0.001$; ****$p < 0.0001$ ANOVA test. N=8.

When the presence of IL-2, IL-4, IL-17 and IFN-ɣ was analyzed in splenocyte culture supernatants at 72h, the levels of cytokines triggered by concanavalin A were higher than those obtained by splenocytes exposed to HK-mycobacteria. Moreover, any cytokines were detectable on culture supernatants of splenocytes exposed to PBS.

Regarding the production of IL-2 after specific restimulation with HK-mycobacteria, all mice that were vaccinated, or vaccinated + treated with *M. bovis* BCG produced statistically significant more IL-2 in comparison to vaccinated or vaccinated + treated with *M. brumae.* IL-2 production by splenocytes from tumour-bearing mice that were vaccinated + intravesically treated with *M. bovis* BCG triggered the highest production of IL-2, being statistically significant in comparison to the rest of the conditions, except for spleens from mice where the cross-reaction was tested. Remarkably, vaccination with *M. bovis* BCG followed by intravesical treatments with *M. brumae* diminished the production of IL-2 when exposed to both HK-*M. brumae* or HK-*M. bovis* BCG, achieving similar levels to the conditions of *M. brumae* (Figure 54a).

Once focused on the production of IFN-γ, ConA triggered unspecific IFN-γ production in all splenocytes. However, splenocytes from *M. bovis* BCG-vaccinated or *M. bovis* BCG-treated mice triggered statistically significant higher amounts of IFN-γ, in comparison to splenocytes from *M. brumae*-vaccinated or *M. brumae*-treated tumour-bearing mice. Noticeably, the vaccination followed by the intravesical treatment with *M. brumae* triggered an increase of the IFN-γ production. In the case of *M. bovis* BCG, the vaccination followed by the intravesical treatment triggered a significant decrease in the production of IFN-γ. Otherwise, when the IFN-γ release by splenocytes of cross-immunogenicity mice group was evaluated, significant low production of IFN-γ was detected when splenocytes were exposed to either HK-*M. brumae* or HK-*M. bovis* BCG, compared to splenocytes from only vaccinated or only treated *M. bovis* BCG mice (Figure 54b). Similarly to the IL-2 response, the cross-immunogenicity produced similar levels of cytokines than *M. brumae* treatments.

The production of IL-17 was also evaluated in splenocytes exposed specifically to mycobacteria. In general, vaccination with *M. bovis* BCG, independently of being later treated with *M. bovis* BCG or not, produced significantly higher levels of IL-17 on spleen cultures, compared to results obtained from animals that were vaccinated or vaccinated + treated with *M. brumae*. Moreover, that production was significantly higher than the observed in spleen cultures from mice only treated with *M. brumae* or *M. bovis* BCG (Figure 54c). Remarkably, the only situation in which the IL-17 production was higher in *M. brumae* condition than in *M. bovis* BCG was observed when animals were only intravesically treated. Finally, splenocytes from the cross-immunogenicity mice group triggered significantly lower production of IL-17 than *M. bovis* BCG-vaccinated animals, independently of being treated or not, or independently of restimulated cultures with HK-*M. brumae* or to HK-*M. bovis* BCG.

Similar levels of IL-4 were found among all conditions, being only significantly higher in those cultures obtained from mice that were only subcutaneous vaccinated with *M. bovis* BCG, compared to only treated animals, cross-reaction restimulated with *M. bovis* BCG, or control groups (Figure 54d).

Figure 54. Cytokine detection in culture supernatants from restimulated splenocytes. IL-2, IFN-ɣ, IL-17 and IL-4 detection in culture supernatants from restimulated splenocytes. . Splenocytes were restimulated with Concanavalin A (ConA, C), shown as oblique line bars, *M. brumae* shown as horizontal line bars solid bars, or *M. bovis* BCG shown as vertical line bars. Mice were subcutaneously vaccinated with *M. brumae* (M) or vaccinated with *M. bovis* BCG (B), only intravesically treated with *M. brumae* or *M. bovis* BCG, vaccinated and treated with *M. brumae*, vaccinated and treated with *M. bovis* BCG, vaccinated with *M. bovis* BCG and treated with *M. brumae* (green), or non-vaccinated (Ø) and non-treated (Ø) shown in black. *M. brumae* in red, *M. bovis* BCG in blue, and healthy animals in grey. Line represents the mean ± SD. *$p < 0.05$; **$p < 0.01$, ***$p < 0.001$; ****$p < 0.0001$ ANOVA test. N=8.

	Vaccinated				Treated				Vaccinated + Treated				Cross Reaction			Tumour			Healthy		
Vaccination	M	M	B	B	Ø	Ø	Ø	Ø	M	M	B	B	B	B	B	Ø	Ø	Ø	Ø	Ø	Ø
Tumour	✓	✓	✓	✓	✓	✓	✓	✓	✓	✓	✓	✓	✓	✓	✓	✓	✓	✓	Ø	Ø	Ø
Treatment	Ø	Ø	Ø	Ø	M	M	B	B	M	M	B	B	M	M	M	Ø	Ø	Ø	Ø	Ø	Ø
Reestimulation	C	M	C	B	C	M	C	B	C	M	C	B	C	M	B	C	M	B	C	M	B

4.4.6 Detection of viable mycobacteria in organs from tumour-bearing mice previously vaccinated with *M. brumae* or M. bovis BCG

Spleens were carefully collected from mice to be measured. Then, spleens were disrupted to count viable mycobacteria on them. Lungs were also collected and plated to count CFUs.

Spleens of animals that were intravesically treated with *M. bovis* BCG were significantly bigger than spleens from mice intravesically treated with *M. brumae* or healthy animals. Spleens from animals in which cross-reaction was tested were also significantly bigger than the spleen's size of healthy animals. When CFUs were counted in spleens, mice that were only intravesically treated with *M. bovis* BCG contained higher CFU levels than the rest of the conditions, even those that were vaccinated and treated with *M. bovis* BCG (Figure 55a). No viable CFUs were found in the spleens of vaccinated mice with *M. bovis* BCG that were not treated, or were intravesically treated with *M. brumae* (Figure 55b).
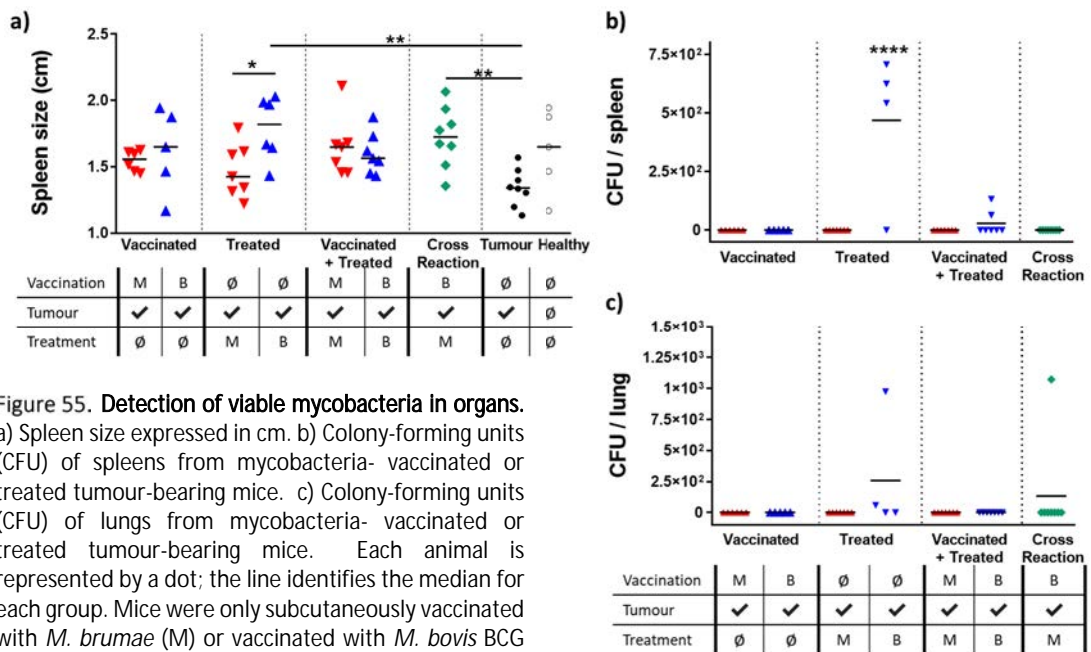
Figure 55. Detection of viable mycobacteria in organs. a) Spleen size expressed in cm. b) Colony-forming units (CFU) of spleens from mycobacteria- vaccinated or treated tumour-bearing mice. c) Colony-forming units (CFU) of lungs from mycobacteria- vaccinated or treated tumour-bearing mice. Each animal is represented by a dot; the line identifies the median for each group. Mice were only subcutaneously vaccinated with *M. brumae* (M) or vaccinated with *M. bovis* BCG (B), only intravesically treated with *M. brumae* or *M. bovis* BCG, vaccinated and treated with *M. brumae*, vaccinated and treated with *M. bovis* BCG, vaccinated with *M. bovis* BCG and treated with *M. brumae* (green), or non-vaccinated (Ø) and non-treated (Ø) (full black dot). *M. brumae* in red, *M. bovis* BCG in blue. Healthy animals (empty dot). *$p < 0.05$; **$p < 0.01$, ****$p < 0.0001$ ANOVA test.

Otherwise, the CFU count performed in the lungs deciphered viable mycobacteria in vaccinated and/or treated mice. Only CFUs were found in *M. bovis* BCG-treated mice. Furthermore, only colonies of *M. bovis* BCG were observed in one spleen from the cross-reaction mice group (Figure 55c).

4.4.7 Detection of IgG in sera of tumour-bearing mice previously vaccinated with *M. brumae* or *M. bovis BCG*

Significant IgG levels were found in sera samples from tumour-bearing mice subcutaneously vaccinated with *M. bovis* BCG and treated with *M. brumae* when exposed to HK-*M. brumae* or HK-*M. bovis* BCG, in comparison to control groups. However, no differences in IgG levels were found among the rest of the groups (Figure 56).
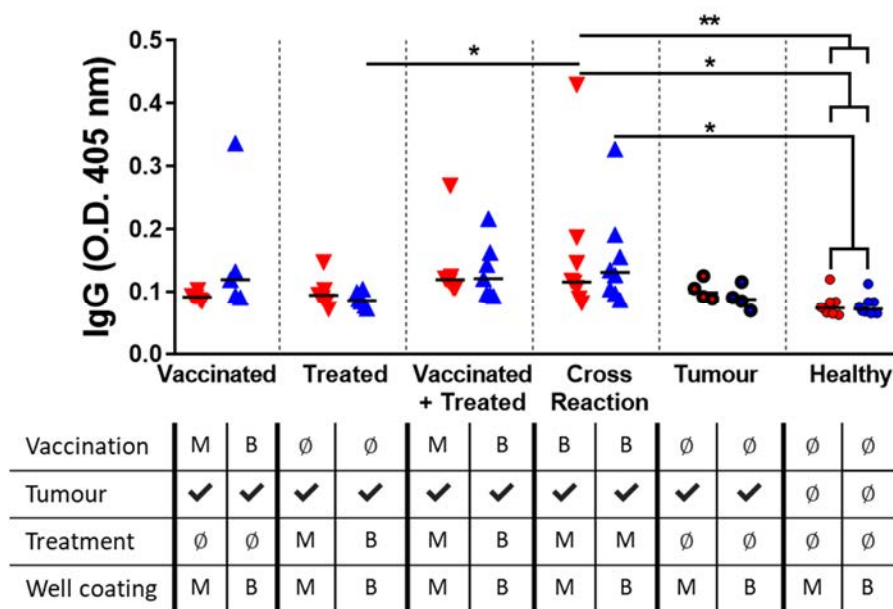
Figure 56. Mycobacteria-specific IgG antibodies detected in sera from mice. Levels of specific IgG anti-*M. brumae* or anti-*M. bovis* BCG is shown. Each animal is represented by a dot; the line identifies the median for each group. Mice were only subcutaneously vaccinated with *M. brumae* (M) or vaccinated with *M. bovis* BCG (B), only intravesically treated with *M. brumae* or *M. bovis* BCG, vaccinated and treated with *M. brumae*, vaccinated and treated with *M. bovis* BCG, vaccinated with *M. bovis* BCG and treated with *M. brumae*, or non-vaccinated (∅) and non-treated (∅). *M. brumae* in red, *M. bovis* BCG in blue. $*p < 0.05$; $**p < 0.01$, ANOVA test.

4.4.8 Antitumour effect on MB49 cells and cytokine release of PECs from tumour-bearing mice previously vaccinated with *M. brumae* or *M. bovis* BCG

4.4.8.1 Cytotoxic activity triggered by PECs

Values obtained from PECs of animals vaccinated with the high dose of *M. brumae* were compared with the results obtained from PECs of animals vaccinated, treated or vaccinated and treated with *M. bovis* BCG. As previously observed in the comparative study analysing the effect of different doses of *M. brumae* (Figure 51), no significant differences were observed between the groups regarding the inhibition of tumour cells by PECs (Figure 57).
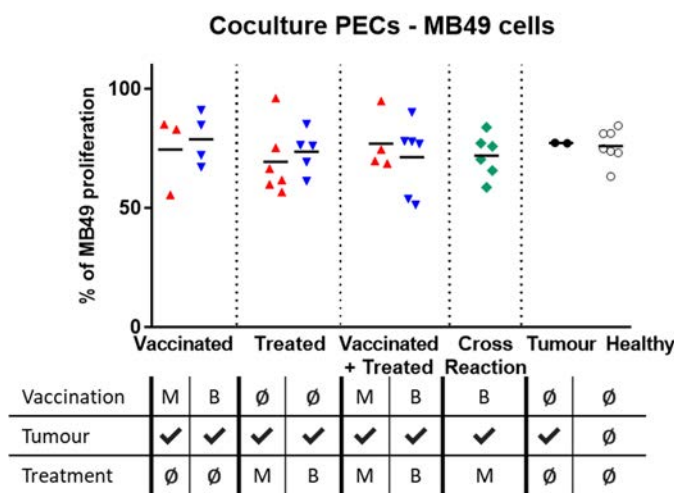
	Vaccinated		Treated		Vaccinated + Treated		Cross Reaction	Tumour	Healthy
Vaccination	M	B	ø	ø	M	B	B	ø	ø
Tumour	✓	✓	✓	✓	✓	✓	✓	✓	ø
Treatment	ø	ø	M	B	M	B	M	ø	ø

Figure 57. Cytotoxic activity triggered by peritoneal exudate cells (PECs). MB49 cell inhibition triggered by Peritoneal Exudate Cells (PECs) from tumour-bearing mice that were only subcutaneously vaccinated with *M. brumae* (M) or vaccinated with *M. bovis* BCG (B), only intravesically treated with *M. brumae* or *M. bovis* BCG, vaccinated and treated with *M. brumae*, vaccinated and treated with *M. bovis* BCG, vaccinated with *M. bovis* BCG and treated with *M. brumae*, or non-vaccinated (ø) and non-treated (ø). *M. brumae* in red, *M. bovis* BCG in blue, non-treated and non-vaccinated tumour bearing mice in black, healthy mice in white.

4.4.8.2 Cytokine production triggered by PECs

When the production of TNF-α by PECs was studied, similar values were obtained among all the tested groups. Moreover, no significant differences were neither observed among groups when IL-6 was analyzed. Remarkably, vaccination seems to be related to an increased production of TNF-α by PECs, which is further increased when intravesical instillations are performed, independently of the mycobacteria used (Figure 58).
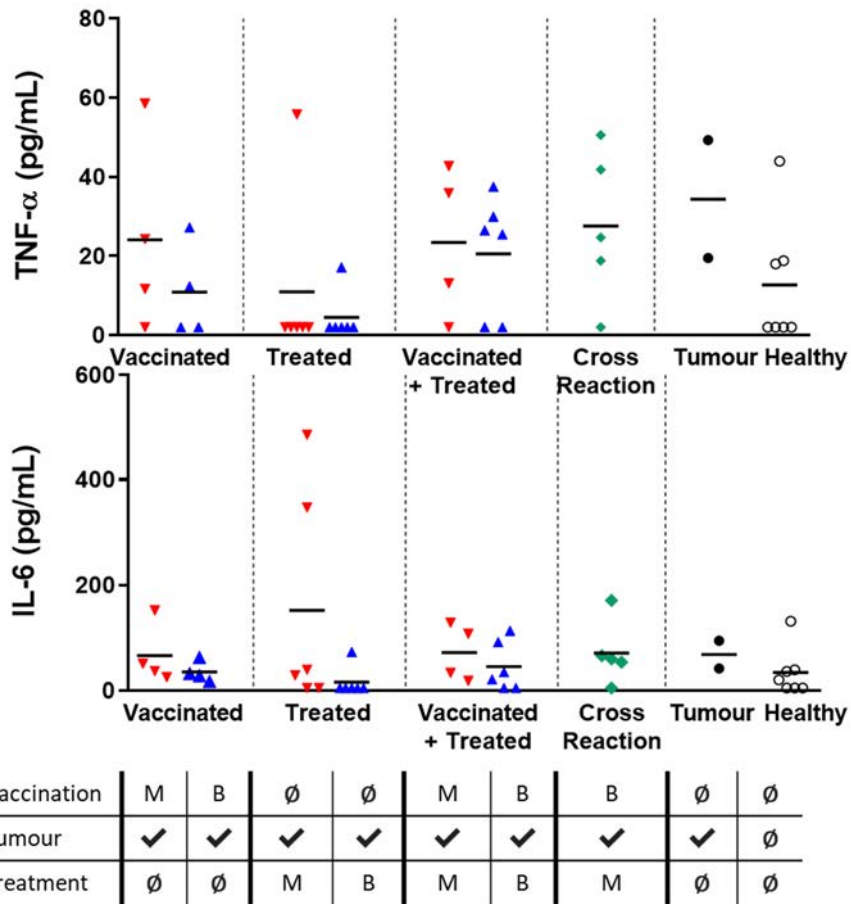
Figure 58. Cytotoxic activity triggered by peritoneal exudate cells (PECs). MB49 cell inhibition triggered by PECs from mice. Each animal is represented by a dot; the line identifies the mean for each group. Only subcutaneously vaccinated with *M. brumae* (M) or vaccinated with *M. bovis* BCG (B), only intravesically treated with *M. brumae* or *M. bovis* BCG, vaccinated and treated with *M. brumae*, vaccinated and treated with *M. bovis* BCG, vaccinated with *M. bovis* BCG and treated with *M. brumae*, or non-vaccinated (Ø) and non-treated (Ø). *M. brumae* in red, *M. bovis* BCG in blue, non-treated and non-vaccinated tumour bearing mice in black, healthy mice in white. Cytokine analyses were measured in PECs supernatants at 24h before adding MB49 cells.

154

5 - DISCUSSION

M. bovis BCG is the preferred treatment for NMIBC patients, being the only live microorganism authorized as an immunotherapeutic agent [325].

Although *M. bovis* BCG therapy is the most efficient treatment for NMBC patients, mild to several adverse effects are described in a high percentage of patients [263]. Therefore, some patients need to abandon intravesical therapy due to mycobacterium toxicity. Moreover, a small percentage of NMIBC patients do not respond to *M. bovis* BCG treatment [297]. Both situations are two of the main concerns due to the absence of alternative therapy for those patients. Then, several alternatives are described along through the literature to improve or substitute the current treatment. For instance, genetically modified *M. bovis* BCG, administration of specific molecules including lipids and/or proteins, modifications of the intravesical schedule, or the use of other mycobacteria or bacteria [278,303,305,326]. In that sense, the antitumour and immunostimulatory effect of the environmental *M. brumae* has been described *in vitro*, *in vivo* and *ex vivo* [286,314,320].

All mycobacteria species are characterized by having a complex and waxy cell wall composed of a wide range of lipids. After *M. bovis* BCG was originated in the Pasteur Institute in 1921, it was distributed worldwide. Sequential passages in different culture media in the receiving countries over the years evoke spontaneous mutations that triggered *M. bovis* BCG substrains, displaying different characteristics [327,328]. Nowadays, *M. bovis* BCG substrains are indistinctly used to vaccinate for preventing TB; or to treat NMIBC patients.

It is not necessary to sub-culture mycobacteria for years to induce the expression of different characteristics. Mycobacteria characters can also be altered when growing in different culture media in few passages. For instance, differences between smooth and rough morphotypes of *M. vaccae* are observed when it is cultured in TSA, but not in other media such as Middlebrook 7H10 or Sauton [129]. Similarly, it has been already demonstrated that the growth of *M. bovis* BCG in Middlebrook or Sauton media modifies its antigenic profile, affecting its protective role for TB infection in mice models [132].

Because of the exposed data, the main purpose of the present thesis was to investigate the influence of culture media composition on the therapeutic effect of both mycobacteria, *M. brumae* and *M. bovis* BCG in the context of BC. While Middlebrook media is the most used culture media in research laboratories in either its solid or liquid form (7H10/7H11 or 7H9, respectively), Sauton medium is selected to massively produce *M. bovis* BCG due to the lack of animal-derived components. Tens of compositions can be found in the literature referring to the Sauton medium because it has been commonly made in-house. Therefore, the therapeutic effect of *M. brumae* and *M. bovis* BCG species was compared in several compositions of Sauton medium and Middlebrook media in their liquid and solid formulation.

Discussion

Optimization of Sauton culture medium

After carefully reviewing the literature, several Sauton medium compositions were found to grow mycobacteria, mainly to culture *M. bovis* BCG or *M. tuberculosis.* The most common discrepancies among the compositions (Table 2) remain on the type of amino acid source (L-asparagine or L-glutamate), the amount of carbon (normally glycerol) and the addition of some inorganic compounds such as zinc sulphate. As none previous work has been done to optimize the growth of *M. brumae* in Sauton medium, different compositions were made to find the medium composition that leads to the maximum biomass production of *M. brumae*.

Firstly, the impact of zinc sulphate was addressed in *M. brumae* cultures. *M. brumae* grown with zinc sulphate and L-asparagine improved its growth, but not when *M. brumae* was grown with zinc sulphate and L-glutamate (Figure 17). Probably because the aspartate transaminase enzyme requires zinc to transform the L-asparagine hydrolysis product (aspartate) to L-glutamate [75]. The addition of zinc sulphate is also needed for other mycobacteria species. For instance, zinc sulphate leads to large pellicles of *M. bovis* BCG or increase the biomass production of *M. tuberculosis* when growing in media containing L-asparagine [123,133]. Therefore, zinc sulphate was included in the Sauton composition to evaluate the influence of other compounds.

Then, a set of compositions were performed to evaluate the impact of increasing glycerol concentrations in the growth of *M. brumae* in the presence of either L-asparagine or L-glutamate as amino acids source. While similar growth of *M. brumae* was achieved among L-glutamate conditions, *M. brumae* growth was highly increased in the presence of high glycerol concentration (Figure 19). Hence, three Sauton media compositions (A60, G15 and G60) were chosen for further experiments according to biomass production.

Because of the results obtained for *M. brumae,* the growth of *M. bovis* BCG Connaught was compared in the three Sauton compositions and in the liquid medium Middlebrook 7H9. Remarkably, *M. bovis* BCG growth was highly enlarged in a culture medium containing L-asparagine (Figure 20), according to some studies indicating that mycobacteria species prefer asparagine over other compounds [44,88,90]. In fact, the best biomass productivity of *M. bovis* BCG Moreau cultured in bioreactors was achieved with L-asparagine and high glycerol concentration [125]. However, the nitrogen metabolism of mycobacteria is complex and poorly known. For instance, *M. tuberculosis*, which is the most studied mycobacterium, can use the 20 amino acids. But when *M. tuberculosis* growth was compared to the growth of *M. smegmatis* cultured with various amino acid sources, variations in biomass production at the end of the experiment was observed, suggesting the presence of different amino acid regulators among mycobacteria species [91]. For instance, surface sensors that could control and modify the amino acid uptake differentially by mycobacteria species, or sensing mechanisms, previously described in *M. tuberculosis* and other mycobacteria species responsible for amino acid assimilation [76,94,329–332]. Besides, central mycobacterial

metabolism is highly influenced by carbon availability. For instance, *M. bovis* BCG can use L-glutamate as an amino acid or a carbon source when culture media contain glycerol [333].

Therefore, the present thesis highlights the importance of selecting the most appropriate culture medium meticulously to grow each mycobacterium species.

Mycobacteria characteristics

Characteristics of *M. brumae* and *M. bovis* BCG cells were modified depending on the culture media used for their growth. Not only in terms of biomass production, as previously discussed, but also other characteristics such as cell length, lipidic composition or cell wall hydrophobicity. Therefore, it is essential to evaluate these mycobacterial changes as they can influence the triggered immune response when mycobacteria are used as an immunostimulatory agent.

It is known that the central metabolism of mycobacteria is modified depending on the source of carbon [78,94]. In the present experiments, glycerol as a carbon source was the compound with a more considerable influence on mycobacteria characteristics than the rest of the compounds evaluated. Glycerol can be easily incorporated into mycobacteria via membrane diffusion. Then, it can be used to produce energy or to synthesise new molecules such as mycolic acids or AG [334–336]. The balance between anabolism and catabolism depends on several factors: state of cell growth, nutrients availability or oxygen conditions, among others [12,74,82]. When mycobacterial cells characteristics were analysed, *M. brumae* and *M. bovis* BCG grown on low glycerol concentration (Sauton G15) showed a reduced cell length compared to the rest of the culture conditions (Figure 20). According to previous studies, culture media with high glycerol concentration triggered longer mycobacterial cells than media with low glycerol concentration [337,338].

Moreover, glycerol was crucial in remodelling the lipidic content of the mycobacterial cell wall. Genus-specific lipids may form the cell wall of each mycobacterium. However, all mycobacteria species share a common skeleton formed by arabinogalactan, peptidoglycan, mycolic acids and some noncovalent lipids such as PIM, TMM, TDM or AG. Consequently, the cell wall composition of *M. brumae* is significantly different to the cell wall of *M. bovis* BCG. When both species were grown on different culture media and the lipidic was analysed, lipids such as TDM, TMM, AG or PIMS were found in all mycobacterial cells, independently of the culture media used for their growth. However, the expression of other lipids, such as GroMM in *M. brumae* or GroMM, PDIM and PGL in *M. bovis* BCG, was diminished when both mycobacteria were cultured in a culture medium containing low-glycerol concentration (G15) (Figure 22). The diminished expression of mycobacterial lipids when are grown on a glycerol-poor medium is in accordance with other studies of *M. phlei* or *M. avium* subsp.

159

hominissuis that showed a relation between low lipid content in mycobacterial cell walls and low presence of glycerol [74,83].

Considering that the first interaction between BC and/or immune cells and intravesical mycobacteria could be crucial for achieving a good antitumor effect, the outermost layer of *M. brumae* and *M. bovis* BCG was analysed. Interestingly, a different lipidic pattern was observed on the surface of *M. brumae* grown on A60 and *M. bovis* BCG grown on G15, compared to the rest of *M. brumae* or *M. bovis* BCG conditions (Figure 23). *M. brumae*-A60 showed a cell wall surface with GroMM, yet devoiding AGs, while *M. bovis* BCG grown on G15 showed a cell wall surface with few amounts of GroMM, PDIM and PGL. Therefore, the GroMM in the surface of both *M. brumae* and *M. bovis* BCG was associated with a high glycerol concentration in the medium, as previously observed by Hattori *et al.* [44]. GroMM, which is an immunostimulatory molecule formed by a glycerol esterified with one mycolic acid, has been previously described in other species such as *M. tuberculosis* or *M. bovis* BCG [41]. *M. brumae* can only synthesize α-mycolate, and hence, α-GroMM was produced by *M. brumae*. However, *M. bovis* BCG, which can produce α- and k- mycolates, GroMM was only formed by k-mycolate (Figure 24). It could be associated with the higher stability acquired by k- mycolates than α-mycolates [41]. Because of published data describing that *cis*-conformation of GroMM was associated with a pro-inflammatory response [46], further analyses were carried out in the lipids purified from both *M. brumae* and *M. bovis* BCG grown as a pellicle in the surface of the Sauton media. However, a mix of both conformations in GroMM was found in both mycobacterial species.

Regarding *M. brumae*, the surface of *M. brumae* grown on A60 lacked AGs, contrary to the total lipidic profile in which AG were present. AG can be transported and accumulated on the cell wall surface, or be accumulated into mycobacterial cytoplasm, forming ILIs [339]. Those functions have been described in *M. tuberculosis* and also in nontuberculous mycobacteria [340,341]. Besides *M. tuberculosis* release of AG into the culture medium to resist in the host immune environment due to the overexpression of an efflux pump and the membrane lipoprotein LprG/Rv1410 [85,342]. Although the function of AG on the surface of nontuberculous mycobacteria, such as *M. brumae*, is still unknown, it could be hypothesized that the absence of AG in *M. brumae*- A60 could favour the interaction of PAMPs with host receptors. However, further studies are required to reveal AG roles.

Otherwise, the few lipidic expression observed in *M. bovis* BCG grown on G15 can be related to the diminished availability of glycerol in the culture medium. The highly apolar lipids PDIM and PGL are only produced by some mycobacterial species such as *M. tuberculosis* or *M. marinum* [20,30], and their presence varies among *M. bovis* BCG substrains [343]. Their expression has been related to increased cell wall hydrophobicity, the ability to inhibit phagosome maturation, or triggering a masking phenomenon between mycobacteria PAMPs and host cells [20,24,30].

In the present thesis, *M. bovis* BCG Connaught substrain was used in all experiments, which previously showed PDIM and PGL expression in its cell surface when grown on Middlebrook 7H10 [217]. However, because the lipid expression varies depending on the culture media used for *M. bovis* BCG Connaught growth, it was considered noteworthy to unravel whether the described lipidic pattern was also reproduced by other *M. bovis* BCG substrains grown on the different culture media. Overall, the lipidic pattern observed in *M. bovis* BCG Connaught was repeated in the rest of *M. bovis* BCG substrains (-Pasteur, -Phipps, -Tice, -Glaxo and -Moreau). GroMM expression was induced in the presence of high glycerol concentrations in all the studied substrains, and PDIM and/or PGL were diminished when *M. bovis* BCG substrains were cultured in low glycerol concentration (G15) (Figure 27).

Then, considering the lipidic differences observed on the surface of both mycobacteria species, physicochemical characteristics of mycobacterial cells were evaluated. Regarding their hydrophobicity, *M. brumae* cells were less hydrophobic than *M. bovis* BCG cells (Figure 25). Besides, differences in hydrophobicity were found among *M. brumae* and *M. bovis* BCG conditions. *M. brumae* cultured either in A60 in which AGs are not exposed in the outmost layer or in Middlebrook 7H10 in which GroMM is not synthesised, cells were less hydrophobic, compared to *M. brumae* cultured in G60 which express GroMM and AG. Similarly, all *M. bovis* BCG substrains with diminished expression of GroMM, PDIM and PGL showed a reduced cell wall hydrophobicity. A marked difference was observed in *M. bovis* BCG grown on Middlebrook 7H10, in which low hydrophobicity was found in their cell wall compared to the rest of *M. bovis* BCG cells grown on the rest of conditions, despite expressing PDIM and PGL. The absence of GroMM in mycobacteria grown on Middlebrook 7H10 indicates the strong influence of GroMM in cell wall hydrophobicity, both in *M. brumae* and *M. bovis* BCG. Therefore, lipid accumulation on the cell wall surface of mycobacteria leads to an increased hydrophobic cell wall, which can be intimately related to their interaction with both the environment and/or host cells. In fact, differences in culture media have been associated with different cell permeability and protein release [344–346]. It is worth mentioning that mycobacterial cell hydrophobicity has a further impact on the use of mycobacteria as immunomodulatory agents since hydrophobicity leads to mycobacteria clump formation in aqueous solutions hampering the obtention of a stable and homogenous suspension [347].

Then, it was interesting to determine whether the differences observed in the lipid composition of *M. brumae* and *M. bovis* BCG grown on different culture media could modify the response to neutral red staining. Neutral red cytochemical staining has been described as a helpful technique to discriminate between the virulent strain of *M. tuberculosis* H37Rv that can fix neutral red in an alkaline aqueous environment and became red, and the attenuated strain of *M. tuberculosis* H37a that remain unstained [348]. When the cell wall

161

components responsible for the positive neutral red reaction were studied, a positive correlation was observed between the staining and the presence of mycobacterial lipids such as SL, PAT, PDIM and PGL[348–350]. However, the neutral red positive reaction has not been yet associated with one compound specifically. The present results showed that *M. brumae* remained unstained, independently of the culture media used for its growth (Figure 25). At the same time, *M. bovis* BCG with diminished production of PDIM/PGL could not take the neutral red stain in its anionic form, contrary to the rest of *M. bovis* BCG conditions, indicating a less negative charge on their cell wall, which could be an advantage when interacting with BC cells. (Figure 25 and Figure 26). As previously explained in the Introduction section, BC cells contain few GAGs compared to normal cells, making the BC cell surface less negatively charged. Hence, *M. bovis* BCG-G15 could properly attach to BC cells. Moreover, it is plausible that the exposure of fibronectin-binding proteins implicated in the interactions between mycobacteria and BC cells could be altered as a role of the mycobacterial surface lipidome[320].

Altogether the results demonstrate that culture medium composition modifies the mycobacteria cell surface triggering a different lipidic pattern. Besides, the minor presence of apolar lipids in the cell wall leads to a reduced hydrophobicity and a modification of the charge of the mycobacterial surface in the case of *M. bovis* BCG.

In vitro antitumour effect of mycobacteria grown on different culture media

M. brumae was described as a new agent for cancer treatment in previous experiments performed in our laboratory [286,314,323]. In all these studies, both *M. brumae* and *M. bovis* BCG were cultured on Middlebrook 7H10. Here, after studying the growth and the physiological effects of culturing mycobacteria in different compositions, the antitumour effect of *M. brumae* and *M. bovis* BCG grown on different culture media was assayed firstly *in vitro*, followed by *in vivo* experiments.

Results from *in vitro* experiments showed that *M. brumae* grown on A60 and *M. bovis* BCG grown on G15 triggered the best antiproliferative effect on four different BC cell lines of different degree of differentiation (Figure 30 and Figure 31). Although not reaching statistical differences in all BC cells, a clear tendency was observed for empowering *M. brumae*-A60 and *M. bovis* BCG-G15 as antiproliferative agents. Differences found on mycobacteria ability to inhibit BC cell proliferation depending on the culture media used for their growth are in accordance with a previous study in which *M. bovis* BCG grown on a Sauton media was more effective in inhibiting apoptosis of infected cells than *M. bovis* BCG grown on Middlebrook 7H9 medium when used as a vaccine against TB [132].

Regarding the pro-inflammatory response induced *in vitro*, *M. brumae* and *M. bovis* BCG grown on A60 and G15, respectively, clearly elicited the release of the highest amounts of tested cytokines (IL-6 and CXCL-8/KC) compared to the rest of mycobacteria conditions in

the majority of tumour cell lines (Figure 30 and Figure 31). IL-6 and CXCL-8 are two important proinflammatory cytokines that trigger the activation and attraction of immune cells such as macrophages or lymphocytes to solve the tumour [229]. Moreover, *M. brumae* and *M. bovis* BCG grown on different culture media induce several proinflammatory cytokines release in both mice and human macrophages. Remarkably, *M.brumae*-A60 and *M. bovis* BCG-G15 induced the production of the highest cytokines levels among all *M. brumae* and *M. bovis* BCG conditions. Proinflammatory cytokine release is essential to differentiate lymphocytes and, in turn, produce further pro-inflammatory cytokines evoking a cascade of cytokines and the infiltration of immune cells modifying the tumour microenvironment [144].

In vivo antitumour effect of mycobacteria grown on different culture media

Both the antigenic profile and the results of the *in vitro* experiments point out *M. brumae*-A60 and *M. bovis* BCG-G15 as the most interesting conditions to be compared with the strains grown on Middlebrook 7H10 in the orthotopic murine model of the disease. As mentioned before, mycobacteria grown on Middlebrook 7H10 had been the only condition evaluated *in vitro* and *in vivo* in previous reports [314,323,351]. However, this thesis provides an exciting opportunity to unravel whether there were differences in the mechanism of action against BC triggered by different mycobacteria culture conditions. Therefore, the *in vivo* experiments were done using mycobacteria grown on the three Sauton compositions and grown on Middlebrook 7H10 medium.

The most efficacious treatment for tumour-bearing mice was *M. brumae* grown on A60, which prolong the survival of 89% of tumour-bearing mice compared to the least effective treatment (*M. brumae*-G60) which prolongs the survival of 67% of the animals. Remarkably, 100% of the animals treated with *M.brumae*-A60 survived until day 40 of the experiment (Figure 32). Otherwise, *M. bovis* BCG-G15 treatment was the most effective condition, with 78% of the mice surviving at the end of the experiment (Figure 33). Any statistical differences were reached among treatments, probably due to the low number of animals used in the experiments. However, considering the tendency observed in *M. brumae*-A60 and *M. bovis* BCG-G15, further analysis of the immune response triggered, either systemically or locally into the bladder, was performed to decipher differences among mycobacteria treatments.

When splenocytes from treated animals were exposed to the MB49 BC cell line, splenocytes from *M. brumae*-A60-treated tumour-bearing mice triggered the highest cytotoxic activity against tumour cells compared to the rest of the conditions. However, no significant differences were found among *M. bovis* BCG conditions (Figure 35).

Discussion

Then, the cytokine release by splenocytes exposed to HK-mycobacterial antigens was analysed *ex vivo*. IFN-γ was significantly overproduced in splenocytes of tumour-bearing mice treated with *M. bovis* BCG, specifically *M. bovis* BCG-G15. However, splenocytes from tumour-bearing mice treated with *M. brumae*, specifically *M. brumae*-A60, triggered the highest production of IL-17 among all treatments. IFN-γ was also produced in *M. brumae*-treated mice (Figure 37). Remarkably, IL-4 was not detected in any condition. The production of IFN-γ by splenocytes after being specifically restimulated with both mycobacteria implies that memory cells are present in the spleen [352], leading to the Th1 response necessary to obtain successful therapy outcomes [229,320]. Besides, the effect of IL-17 in immunotherapy is still being studied, yet its beneficial effect seems clear in a BC context. After analysing the tumour microenvironment of BC patients, a higher number of IL-17+ cells were related to improved survival rates. IL-17 induce the expression of IL-6 and IL-8 that can directly inhibit BC cells and trigger neutrophil infiltration into the bladder after *M. bovis* BCG instillations. Altogether had led to propose the detection of IL-17 in the tumour microenvironment as a biomarker for positive prognostic in NMIBC patients [233,235]. Therefore, these results could indicate that both mycobacteria treatments trigger a Th1 response, yet *M. brumae* also induce a Th17 response.

Besides, *M. brumae* treatments induced higher IgG levels than *M. bovis* BCG treatments. No differences were observed in IgG levels among *M. brumae*-treated groups. However, levels of IgG anti-*M. bovis* BCG-7H10 was significantly different to IgG anti-*M. bovis* BCG-A60 and -G15 levels, meaning antigen specificity depending on the culture media used for mycobacterial growth (Figure 34).

After analysing the systemic immune response triggered in tumour-bearing mice treated with *M. brumae* or *M. bovis* BCG grown on different culture media, the immune cell infiltration into the bladder was assessed. The first observed result was that both mycobacteria species grown on G15 culture medium triggered a robust infiltration of CD45+, CD3+, CD4+ and CD8+ T cells, NK and B cells than the rest of *M. brumae* or *M. bovis* BCG treatments (Figure 41). Then, the high production by splenocytes of 1) IL-17 in *M. brumae* treatments, particularly *M. brumae*-A60, and 2) IFN-γ in both mycobacterial treatments; were considered to decipher whether their expression could be related to specific immune cell populations infiltrated into the bladder. Accordingly, two IL-17 producers' cells were analysed, CD4+ T_{EM} cells and ILC cells. Although *M.* brumae-A60 triggered a low immune cells infiltration into the bladder of tumour-bearing mice, both immune cell populations were higher infiltrated in *M.* brumae-A60-treated mice compared to the rest of the conditions (Figure 43). Additionally, a positive correlation was observed between both immune cells and IL-17 produced by splenocytes from *M. brumae*-treated mice (Figure 44). T_{EM} cells are a subset of differentiated T cells that migrate to the site of infection, which are characterised by long-term survival [353]. Moreover, three types of ILC have been described along through the literature, being the innate homologues for a Th1, Th2 and Th17 responses. The presence of type 2 ILC in the urine of BC patients during mycobacteria instillations induced

164

the secretion of IL-13 and was associated with tumour recurrence[353]. Therefore, after observing the high production of IL-17 triggered in *M. brumae*-treated mice, especially *M. brumae*-A60, type 3 ILC is expected to be the subset infiltrated into bladders of *M. brumae* groups. Remarkably, no positive correlation was found between T_{EM} cells and ILC cells and *M. bovis* BCG treatments.

In all *M. bovis* BCG treatments, increased production of IFN-ɣ by splenocytes was observed, especially in *M. bovis* BCG-G15, demonstrating a strong activation of a Th1 response. Typical IFN-ɣ producers' cells are CD4$^+$ and CD8$^+$ T cells, whose infiltration into the bladder correlated positively with the IFN-ɣ produced by splenocytes (Figure 44). Besides, a positive correlation was also observed in *M. brumae* treated animals. *In vivo* results demonstrated that *M. bovis* BCG-G15 prolonged survival of the tumour-bearing mice and triggered the highest immune cell infiltration into the bladder of tumour-bearing mice among *M. bovis* BCG conditions. The hypothesis that an elevated immune response produces a more efficacious treatment has been highly discussed. For instance, a low local immune response is related to a treatment failure [354], yet a high systemic immune response has also been related to moderate and severe systemic adverse effects [144]. However, the activation of a Th1 response to successfully solve the tumour is widely accepted. In fact, some proposed alternatives for *M. bovis* BCG non-responders BC patients consist of empowering the Th1 response [353].

Overall, the results demonstrate that the mechanism of *M. brumae* is highly different to the triggered by *M. bovis* BCG. *M. brumae*-A60 triggered the highest survival rate of tumour-bearing mice, not only among the other *M. brumae* treatments but also among all *M. bovis* BCG treatments, indicating that a massive immune cell infiltration into the bladder is not necessary to produce an efficient response against BC. While in the case of *M. bovis* BCG, the massive infiltration induces tumour reduction. Accordingly, some immune cells, such as ILCs or CD4$^+$ T_{EM} cells, can modify the tumour microenvironment more efficiently than CD4$^+$, CD8$^+$ T cells, NK or B cells. In conclusion, culture medium composition has an impact on immunostimulatory activity triggered by mycobacteria.

<u>The effect of a boosting strategy</u>

Considering the apparent beneficial effect triggered by subcutaneous immunization with *M. bovis* BCG a few weeks before the mycobacterial intravesical treatment [273], it was considered highly interesting to decipher the impact of subcutaneous vaccination with a non-pathogenic mycobacterium, such as *M. brumae.* To evaluate the possible advantage of subcutaneous vaccination, two doses of *M. brumae* were tested with or without later intravesical treatment with *M. brumae* in tumour-bearing mice. To perform the experiments, *M. brumae*-A60, which showed the best antitumor results, was selected. All

treatments showed a systemic immune response regarding cytokine release by splenocytes and PECs. Cytokines released by splenocytes tend to be increased in vaccinated tumour-bearing mice, followed by intravesical instillation compared to non-vaccinated mice. The present data showed that subcutaneous vaccination with a high dose of *M. brumae* resulted in systemic changes, increasing the amount of released cytokines such as IL-2, IFN-ɣ or IL-17 (Figure 48).

Otherwise, subcutaneous vaccination with *M. bovis* BCG with or without intravesical *M. bovis* BCG was also assessed. A previous study showed that vaccination with *M. bovis* BCG or *M. tuberculosis* mutants resulted in a robust Th1 cytokines release such as IFN-ɣ, TNF-α or IL-2, and the Th17 cytokine, IL-17, in a TB context [355]. In our orthotopic BC mice model, subcutaneous vaccination with *M. bovis* BCG triggered a high release of IL-2 and IL-17 by restimulated splenocytes, independently of being intravesical treated or not. Noticeably, the IFN-ɣ production was surprisingly decreased in vaccinated and treated mice (Figure 54). Therefore, a subcutaneous vaccination previous to intravesical treatment could favour the balance of a Th17 response over a Th1 response.

Considering that *M. bovis* BCG is typically administered subcutaneously in many countries, it was deemed to be interesting to test the immune reaction obtained by subcutaneous *M. bovis* BCG followed by *M. brumae* in tumour-bearing mice. Surprisingly, few amounts of all tested cytokines were produced by splenocytes, despite splenocytes triggered the highest direct inhibition of the proliferation growth of MB49 cells *ex vivo*.

When Dr Morales considered a boosting strategy to improve the BC treatment outcomes, it consisted of inoculating *M. bovis* BCG subcutaneous and intravesical simultaneously. However, because none benefit was observed in patients, the idea was discarded [269]. Several years later, Biot *et al.* demonstrated that vaccination with *M. bovis* BCG previous to the intravesical treatment triggered a favourable boosting of the immune system that might accelerate T cell recruitment into the bladder and, consequently, improve the host antitumour response [273]. Therefore, vaccinating before intravesical treatments may be crucial considering that the adaptive immune response requires few days to be effective [237]. Nevertheless, as mentioned before, many researchers emphasize that a high immune response is not always correlated with an improved outcome. In fact, both a poor or an exacerbated local immune response has been associated with therapy failure [354]. Therefore, what seems important is the type of immune response triggered, which is related to the infiltration of the immune cells induced after a boosting therapy. Hence, given the present results in which different balance between the types of immune response is produced depending on the mycobacteria treatment, further experiments are required to decipher whether subcutaneous vaccination could be beneficial, especially for *M. bovis* BCG non-responders BC patients who are one of the main concerns by physicians.

Pathogenicity

As explained in the Introduction section of this thesis, *M. brumae* was mainly studied due to their safety profile compared to *M. bovis* BCG. In previous experiments, safety, in terms of mycobacteria survival, was studied both in *in vitro* cultures of different cell types and in different animal models *in vivo* [322,351]. In all cases, *M. brumae* was always grown on Middlebrook 7H10 medium.

In the present experiments, the ability of *M. brumae* or *M. bovis* BCG grown on different culture media to survive inside mouse or human macrophages was analysed. Contrary to all *M. brumae* conditions, *M. bovis* BCG grown on all tested media could persist inside mice and human macrophages until the end of the experiment (Figure 28 and Figure 29).

In vivo experiments performed in the BC tumour-bearing mice model, *M. brumae* was not found in any mice spleen, independently of the culture media used for their growth (Figure 38). Otherwise, one of the main limitations of *M. bovis* BCG instillations is the persistence of the mycobacterium and its associated infections. Accordingly, *M. bovis* BCG was found in spleens of *M. bovis* treated mice, independently of the culture media used for their production (Figure 38). Similar to a previous study by Venkataswamy *et al.* that do not observe any difference in the CFU counts after *M. bovis* BCG grown on Sauton or Middlebrook medium [132].

Besides, *M. brumae* was not found when animals were subcutaneously vaccinated neither in spleens or lungs (Figure 49). Those results are in accordance with none human or animal infection with clinical relevance associated with *M. brumae.* Regarding *M. bovis* BCG, CFUs were recovered from spleens or lungs in those animals that were intravesical treated, yet the CFU burden notably decreased in those animals that had been previously vaccinated (Figure 55).

The present experiments demonstrate that culture media do not modify the pathogenicity of both mycobacteria. *M. bovis* BCG enters into cells and persists in them, while *M. brumae* enters into cells but is killed.

General discussion

Culture media affects mycobacteria characteristics that, in turn, trigger different antitumour and immunostimulatory effect *in vitro* and *in vivo*. However, the observed differences cannot be directly associated with the specific lipids observed on the surface of both mycobacteria.

Discussion

The main characteristic of mycobacteria species relies on their highly waxy and hydrophobic cell wall. Although the expression of some specific lipids, such as GroMM, AG, PDIM and/or PGL, can be related to a direct antitumour effect, the mechanism of action could go much further. For instance, 1) the presence/absence of some lipids can block the interaction with immunomodulatory receptors present in the cell wall, modifying the indirect antitumour effect triggered by mycobacteria; 2) changes on the hydrophobicity and charge of the mycobacteria cell wall can alter the interaction of mycobacteria-tumour cell; or 3) differences on mycobacterial cell wall composition can interfere on the release of antitumour and immunostimulatory proteins important to solve the tumour.

Therefore, culture media composition must be carefully designed to improve the treatment for NMIBC patients.

6 - CONCLUSIONS

1. Sauton composition with zinc sulphate together with L-asparagine as amino acid source enhances *M. brumae* growth. Sauton composition with L- asparagine and high glycerol concentration favours *M. bovis* BCG growth.

2. *M. brumae* grown on A60 Sauton medium and *M. bovis* BCG grown on G15 Sauton medium induce a higher release of proinflammatory cytokines by macrophages and BC cells in *in vitro* cultures than both mycobacteria grown on the rest of the culture conditions.

3. Culture media composition modifies the lipidic content of *M. brumae* and different *M. bovis* BCG substrains. High glycerol concentration in Sauton media triggers the production of GroMM in both mycobacteria species. The mycobacterial cell wall surface of *M. brumae* grown on A60 medium contains α-GroMM, yet does not have TAGs, differing from the other *M. brumae* conditions. *M. bovis* BCG Connaught grown on G15 medium present a diminished production of apolar lipids such as PDIM, PGL and κ-GroMM, contrary to the other *M. bovis* BCG conditions.

4. *M. brumae* does not survive inside human (THP-1) or mouse (J774) macrophages, independently of the culture media used for its growth. *M. bovis* BCG persists inside THP-1 and J774 macrophages, independently of the culture media used for its production.

5. Intravesical instillation of *M. brumae*-A60 in tumour-bearing mice enhances the best survival rate among all *M. brumae* and *M. bovis* BCG treatments. *M. bovis* BCG-G15 trigger the highest survival rate among all *M. bovis* BCG intravesical treatments.

6. Intravesical instillation with *M. brumae*-A60 induces a reduced infiltration of immune cells into the bladder, compared to the rest of *M. brumae* treatments. This infiltration is characterized by a high number of ILCs and CD4$^+$ T$_{EM}$ cells. Intravesical instillation with *M. bovis* BCG-G15 induces a massive infiltration of immune cells into the bladder, mainly CD4$^+$ and CD8$^+$ T cells, NK and B cells, compared to the rest of *M. bovis* BCG treatments.

7. *M. brumae*-A60 intravesical treatment triggers a systemic immune response based on IFN-γ and IL-17 release, while *M. bovis* BCG-G15 treatment triggers a systemic immune response characterized by a massive release of IFN-γ.

8. Based on the observed local and systemic immune response induced by the intravesical instillations of *M. brumae* or *M. bovis* BCG, the antitumour mechanism triggered by each mycobacterium is notably different.

9. Subcutaneous vaccination with *M. brumae* in tumour-bearing mice enhances the systemic immune response in a dose-dependent manner.

10. Subcutaneous vaccination with the high dose of *M. brumae* previous to intravesical treatment with *M. brumae* triggered the highest systemic release of proinflammatory cytokines, compared to only vaccinated or only treated mice. Subcutaneous vaccination with *M. bovis* BCG, followed or not by intravesical treatment with *M. bovis* BCG, induces higher secretion of IL-17 compared to only intravesically treated mice.

11. Splenocytes from mice vaccinated with *M. bovis* BCG followed by intravesical instillation with *M. brumae* trigger the highest inhibition of MB49 cell proliferation *in vitro* among all conditions.

7 - REFERENCES

1. Gupta, R.S.; Lo, B.; Son, J. Phylogenomics and comparative genomic studies robustly support division of the genus Mycobacterium into an emended genus Mycobacterium and four novel genera. *Front. Microbiol.* **2018**, *9*, 1–41, doi:10.3389/fmicb.2018.00067.
2. Pereira, A.C.; Ramos, B.; Reis, A.C.; Cunha, M. V. Non-tuberculous mycobacteria: Molecular and physiological bases of virulence and adaptation to ecological niches. *Microorganisms* **2020**, *8*, 1–49, doi:10.3390/microorganisms8091380.
3. Percival, S.L.; Williams, D.W. Mycobacterium. In *Microbiology of Waterborne Diseases: Microbiological Aspects and Risks: Second Edition*; Elsevier Ltd., 2013; pp. 177–207 ISBN 9780124158467.
4. Krieg, A.M. CpG motifs in bacterial DNA and their immune effects. *Annu. Rev. Immunol.* **2002**, *20*, 709–760, doi:10.1146/annurev.immunol.20.100301.064842.
5. Saviola, B.; Bishai, W. The Genus Mycobacterium-Medical. In *The Prokaryotes*; Springer New York, 2006; pp. 919–933.
6. Pfyffer, G.E. Mycobacterium: General Characteristics, Laboratory Detection, and Staining Procedures. In *Manual of Clinical Microbiology, 11th Edition*; American Society of Microbiology, 2015; pp. 536–569.
7. van der Werf, M.J.; Ködmön, C.; Katalinic-Jankovic, V.; Kummik, T.; Soini, H.; Richter, E.; Papaventsis, D.; Tortoli, E.; Perrin, M.; van Soolingen, D.; et al. Inventory study of non-tuberculous mycobacteria in the European Union. *BMC Infect. Dis.* **2014**, *14*, 62, doi:10.1186/1471-2334-14-62.
8. Bachmann, N.L.; Salamzade, R.; Manson, A.L.; Whittington, R.; Sintchenko, V.; Earl, A.M.; Marais, B.J. Key Transitions in the Evolution of Rapid and Slow Growing Mycobacteria Identified by Comparative Genomics. *Front. Microbiol.* **2020**, *10*, 1–12, doi:10.3389/fmicb.2019.03019.
9. RUNYON, E.H. Anonymous mycobacteria in pulmonary disease. *Med. Clin. North Am.* **1959**, *43*, 273–290, doi:10.1016/S0025-7125(16)34193-1.
10. Seth-Smith, H.M.B.; Imkamp, F.; Tagini, F.; Cuénod, A.; Hömke, R.; Jahn, K.; Tschacher, A.; Grendelmeier, P.; Bättig, V.; Erb, S.; et al. Discovery and characterization of Mycobacterium basiliensesp. nov., a nontuberculous mycobacterium isolated from human lungs. *Front. Microbiol.* **2019**, *10*, doi:10.3389/fmicb.2018.03184.
11. Chiaradia, L.; Lefebvre, C.; Parra, J.; Marcoux, J.; Burlet-Schiltz, O.; Etienne, G.; Tropis, M.; Daffé, M. Dissecting the mycobacterial cell envelope and defining the composition of the native mycomembrane OPEN. *Sci. Rep.* **2017**, *7*, doi:10.1038/s41598-017-12718-4.
12. Zeng, S.; Constant, P.; Yang, D.; Baulard, A.; Lefèvre, P.; Daffé, M.; Wattiez, R.; Fontaine, V. Cpn60.1 (GroEL) contributes to mycobacterial crabtree effect: Implications for biofilm formation. *Front. Microbiol.* **2019**, *10*, 1–15, doi:10.3389/fmicb.2019.01149.
13. Daffé, M.; Marrakchi, H. Unraveling the Structure of the Mycobacterial Envelope. *Microbiol. Spectr.* **2019**, *7*, doi:10.1128/microbiolspec.gpp3-0027-2018.
14. Marrakchi, H.; Lanéelle, M.-A.; Daffé, M. Mycolic Acids: Structures, Biosynthesis, and Beyond. *Chem. Biol.* **2014**, *21*, 67–85, doi:10.1016/j.chembiol.2013.11.011.
15. Jackson, M. The Mycobacterial Cell Envelope-Lipids. *Cold Spring Harb. Perspect. Med.* **2014**, *4:a021105*, 1–36, doi:10.1101/cshperspect.a021105.
16. Minnikin, D.E.; Brennan, P.J. Lipids of Clinically Significant Mycobacteria. *Heal. Consequences Microb. Interact. with Hydrocarb. Oils, Lipids* **2020**, 33–108, doi:10.1007/978-3-030-15147-8_7.
17. Steck, P.A.; Schwartz, B.A.; Rosendahl, M.S.; Gray, G.R. Mycolic acids. A reinvestigation. *J. Biol. Chem.* **1978**, *253*, 5625–5629, doi:10.1016/s0021-9258(17)30312-5.
18. Minnikin, D.E. Complex lipids, their chemistry biosynthesis and roles. *Biol. Mycobact.* **1982**, *1*, 95–184.
19. Ly, A.; Liu, J. Mycobacterial virulence factors: Surface-exposed lipids and secreted proteins. *Int. J. Mol. Sci.* **2020**, *21*, doi:10.3390/ijms21113985.
20. Quigley, J.; Hughitt, V.K.; Velikovsky, C.A.; Mariuzza, R.A.; El-Sayed, N.M.; Briken, V. The cell wall lipid PDIM contributes to phagosomal escape and host cell exit of Mycobacterium tuberculosis. *MBio* **2017**, *8*, 1–12.
21. Camacho, L R, P Constant, C Raynaud, M A Laneelle, J A Triccas, B Gicquel, M Daffe, C.G. Analysis of the phthiocerol dimycocerosate locus of Mycobacterium tuberculosis. Evidence that this lipid is involved in the cell wall permeability barrier. *J. Biol. Chem.* **2001**, *8*.
22. Augenstreich, J.; Arbues, A.; Simeone, R.; Haanappel, E.; Wegener, A.; Sayer, F.; Le Chevalier, F.; Chalut, C.; Malaga, W.; Guilhot, C.; et al. ESX - 1 and phthiocerol dimycocerosates of Mycobacterium tuberculosis act

in concert to cause phagosomal rupture and host cell apoptosis. *Cell. Microbiol.* **2017**, *e12726*, 1–19, doi:10.1111/cmi.12726.

23. Augenstreich, J.; Haanappel, E.; Sayes, F.; Simeone, R.; Guillet, V.; Mazeres, S.; Chalut, C.; Mourey, L.; Brosch, R.; Guilhot, C.; et al. Phthiocerol Dimycocerosates From Mycobacterium tuberculosis Increase the Membrane Activity of Bacterial Effectors and Host Receptors. *Front. Cell. Infect. Microbiol.* **2020**, *10*, 420, doi:10.3389/fcimb.2020.00420.

24. Cardenal-Muñoz, E.; Barisch, C.; Lefrançois, L.H.; López-jiménez, A.T.; Soldati, T. When Dicty met Myco, a (Not So) romantic story about one amoeba and its intracellular pathogen. *Front. Cell. Infect. Microbiol.* **2018**, *7*, 1–20, doi:10.3389/fcimb.2017.00529.

25. Cambier, C.; Banik, S.M.; Buonomo, J.A.; Bertozzi, C.R. Spreading of a mycobacterial cell surface lipid into host epithelial membranes promotes infectivity. *eLife Sci.* **2020**, *9*.

26. Rousseau, C.; Winter, N.; Privert, E.; Bordat, Y.; Neyrolles, O.; Avé, P.; Huerre, M.; Gicquel, B.; Jackson, M. Production of phthiocerol dimycocerosates protects Mycobacterium tuberculosis from the cidal activity of reactive nitrogen intermediates produced by macrophages and modulates the early immune response to infection. *Cell. Microbiol.* **2004**, *6*, 277–287, doi:10.1046/j.1462-5822.2004.00368.x.

27. Cambier, C.J.; Takaki, K.K.; Larson, R.P.; Hernandez, R.E.; Tobin, D.M.; Urdahl, K.B.; Cosma, C.L.; Ramakrishnan, L. Mycobacteria manipulate macrophage recruitment through coordinated use of membrane lipids. *Nature* **2014**, *505*, 218–222, doi:10.1038/nature12799.

28. Garcia-Vilanova, A.; Chan, J.; Torrelles, J.B. Underestimated Manipulative Roles of Mycobacterium tuberculosis Cell Envelope Glycolipids During Infection. *Front. Immunol.* **2019**, *10*, doi:10.3389/fimmu.2019.02909.

29. Tabouret, G.; Astarie-Dequeker, C.; Demangel, C.; Malaga, W.; Constant, P.; Ray, A.; Honoré, N.; Bello, N.F.; Perez, E.; Daffé, M.; et al. Mycobacterium leprae Phenolglycolipid-1 Expressed by Engineered M. bovis BCG modulates early interaction with human phagocytes. *PLoS Pathog.* **2010**, *6*, doi:10.1371/journal.ppat.1001159.

30. Yu, J.; Tran, V.; Li, M.; Huang, X.; Niu, C.; Wang, D.; Zhu, J.; Wang, J.; Gao, Q.; Liu, J. Both Phthiocerol Dimycocerosates and Phenolic Glycolipids Are Required for Virulence of Mycobacterium marinum. *Infect. Immun.* **2012**, *80*, 1381–1389, doi:10.1128/IAI.06370-11.

31. Torrelles, J.B.; Knaup, R.; Kolareth, A.; Slepushkina, T.; Kaufman, T.M.; Kang, P.; Hill, P.J.; Brennan, P.J.; Chatterjee, D.; Belisle, J.T.; et al. Identification of Mycobacterium tuberculosis clinical isolates with altered phagocytosis by human macrophages due to a truncated lipoarabinomannan. *J. Biol. Chem.* **2008**, *283*, 31417–31428, doi:10.1074/jbc.M806350200.

32. Arbués, A.; Malaga, W.; Constant, P.; Guilhot, C.; Prandi, J.; Astarie-Dequeker, C.; Arbués, A.A.; Malaga, W.; Constant, P.; Guilhot, C.; et al. Trisaccharides of Phenolic Glycolipids Confer Advantages to Pathogenic Mycobacteria through Manipulation of Host-Cell Pattern-Recognition Receptors. *ACS Chem. Biol.* **2016**, *11*, 2865–2875, doi:10.1021/acschembio.6b00568.

33. Domingo-Gonzalez, R.; Das, S.; Griffiths, K.L.; Ahmed, M.; Bambouskova, M.; Gopal, R.; Gondi, S.; Muñoz-Torrico, M.; Salazar-Lezama, M.A.; Cruz-Lagunas, A.; et al. Interleukin-17 limits hypoxia-inducible factor 1α and development of hypoxic granulomas during tuberculosis. *JCI Insight* **2017**, *2*, doi:10.1172/jci.insight.92973.

34. Tran, V.; Ahn, S.K.; Ng, M.; Li, M.; Liu, J. Loss of Lipid Virulence Factors Reduces the Efficacy of the BCG Vaccine. *Sci. Rep.* **2016**, *6*, doi:10.1038/srep29076.

35. Su, C.C.; Klenotic, P.A.; Bolla, J.R.; Purdy, G.E.; Robinson, C. V.; Yu, E.W. MmpL3 is a lipid transporter that binds trehalose monomycolate and phosphatidylethanolamine. *Proc. Natl. Acad. Sci. U. S. A.* **2019**, *166*, 11241–11246, doi:10.1073/pnas.1901346116.

36. Fiolek, T.J.; Banahene, N.; Kavunja, H.W.; Holmes, N.J.; Rylski, A.K.; Pohane, A.A.; Siegrist, M.S.; Swarts, B.M. Engineering the Mycomembrane of Live Mycobacteria with an Expanded Set of Trehalose Monomycolate Analogues. *ChemBioChem* **2019**, *20*, 1282–1291, doi:10.1002/cbic.201800687.

37. Sueoka, E.; Nishiwaki, S.; Okabe, S.; Iida, N.; Suganuma, M.; Yano, I.; Aoki, K.; Fujiki, H. Activation of Protein Kinase C by Mycobacterial Cord Factor, Trehalose 6-Monomycolate, Resulting in Tumor Necrosis Factor-α Release in Mouse Lung Tissues. *Japanese J. Cancer Res.* **1995**, *86*, 749–755, doi:10.1111/j.1349-7006.1995.tb02464.x.

38. Indrigo, J.; Hunter, R.L.; Actor, J.K. Influence of trehalose 6,6′-dimycolate (TDM) during mycobacterial infection of bone marrow macrophages. *Microbiology* **2017**, *1412*, 1991–1998.

39. Linares, C.; Bernabéu, A.; Luquin, M.; Valero-Guillén, P.L. Cord factors from atypical mycobacteria (Mycobacterium alvei, Mycobacterium brumae) stimulate the secretion of some pro-inflammatory

cytokines of relevance in tuberculosis. *Microbiol. (United Kingdom)* **2012**, *158*, 2878–2885, doi:10.1099/mic.0.060681-0.

40. Rao, V.; Gao, F.; Chen, B.; Jacobs, W.R.; Glickman, M.S. Trans-cyclopropanation of mycolic acids on trehalose dimycolate suppresses Mycobacterium tuberculosis-induced inflammation and virulence. *J. Clin. Invest.* **2006**, *116*, 1660–1667, doi:10.1172/JCI27335.

41. Layre, E.; Collmann, A.; Bastian, M.; Mariotti, S.; Czaplicki, J.; Prandi, J.; Mori, L.; Stenger, S.; De Libero, G.; Puzo, G.; et al. Mycolic Acids Constitute a Scaffold for Mycobacterial Lipid Antigens Stimulating CD1-Restricted T Cells. *Chem. Biol.* **2009**, *16*, 82–92, doi:10.1016/j.chembiol.2008.11.008.

42. Andersen, C.A.S.; Rosenkrands, I.; Olsen, A.W.; Nordly, P.; Christensen, D.; Lang, R.; Kirschning, C.; Gomes, J.M.; Bhowruth, V.; Minnikin, D.E.; et al. Novel Generation Mycobacterial Adjuvant Based on Liposome-Encapsulated Monomycoloyl Glycerol from Mycobacterium bovis Bacillus Calmette-Guerin. *J. Immunol.* **2009**, *183*, 2294–2302, doi:10.4049/jimmunol.0804091.

43. Benedictus, L.; Steinbach, S.; Holder, T.; Bakker, D.; Vrettou, C.; Morrison, W.I.; Vordermeier, M.; Connelley, T. Hydrophobic Mycobacterial Antigens Elicit Polyfunctional T Cells in Mycobacterium bovis Immunized Cattle: Association With Protection Against Challenge? *Front. Immunol.* **2020**, *11*, 1, doi:10.3389/fimmu.2020.588180.

44. Hattori, Y.; Matsunaga, I.; Komori, T.; Urakawa, T.; Nakamura, T.; Fujiwara, N.; Hiromatsu, K.; Harashima, H.; Sugita, M. Glycerol monomycolate, a latent tuberculosis-associated mycobacterial lipid, induces eosinophilic hypersensitivity responses in guinea pigs. *Biochem. Biophys. Res. Commun.* **2011**, *409*, 304–307, doi:10.1016/j.bbrc.2011.04.146.

45. Andersen, C.S.; Agger, E.M.; Rosenkrands, I.; Gomes, J.M.; Bhowruth, V.; Gibson, K.J.C.; Petersen, R. V.; Minnikin, D.E.; Besra, G.S.; Andersen, P. A Simple Mycobacterial Monomycolated Glycerol Lipid Has Potent Immunostimulatory Activity. *J. Immunol.* **2009**, *182*, 424–432, doi:10.4049/jimmunol.182.1.424.

46. Groenewald, W.; Baird, M.S.; Verschoor, J.A.; Minnikin, D.E.; Croft, A.K. Differential spontaneous folding of mycolic acids from Mycobacterium tuberculosis. *Chem. Phys. Lipids* **2014**, *180*, 15–22, doi:10.1016/j.chemphyslip.2013.12.004.

47. Jackson, M.; Stadthagen, G.; Gicquel, B. Long-chain multiple methyl-branched fatty acid-containing lipids of Mycobacterium tuberculosis: Biosynthesis, transport, regulation and biological activities. *Tuberculosis* **2007**, *87*, 78–86, doi:10.1016/j.tube.2006.05.003.

48. Blanc, L.; Gilleron, M.; Prandi, J.; Song, O. ryul; Jang, M.S.; Gicquel, B.; Drocourt, D.; Neyrolles, O.; Brodin, P.; Tiraby, G.; et al. Mycobacterium tuberculosis inhibits human innate immune responses via the production of TLR2 antagonist glycolipids. *Proc. Natl. Acad. Sci. U. S. A.* **2017**, *114*, 11205–11210, doi:10.1073/pnas.1707840114.

49. Rousseau, C.; Neyrolles, O.; Bordat, Y.; Giroux, S.; Sirakova, T.D.; Prevost, M.-C.; Kolattukudy, P.E.; Gicquel, B.; Jackson, M. Deficiency in mycolipenate- and mycosanoate-derived acyltrehaloses enhances early interactions of Mycobacterium tuberculosis with host cells. *Cell. Microbiol.* **2003**, *5*, 405–415, doi:10.1046/j.1462-5822.2003.00289.x.

50. Saavedra, R.; Segura, E.; Leyva, R.; Esparza, L.A.; López-Marín, L.M. Mycobacterial Di-O-acyl-trehalose inhibits mitogen- and antigen-induced proliferation of murine T cells in vitro. *Clin. Diagn. Lab. Immunol.* **2001**, *8*, 1081–1088, doi:10.1128/CDLI.8.6.1-91-1088.2001.

51. Daffé, M.; Crick, D.C.; Jackson, M. Genetics of Capsular Polysaccharides and Cell Envelope (Glyco)lipids. *Microbiol. Spectr.* **2014**, *2*, doi:10.1128/microbiolspec.MGM2-0021-2013.

52. Ren, H.; Dover, L.G.; Islam, S.T.; Alexander, D.C.; Chen, J.M.; Besra, G.S.; Liu, J. Identification of the lipooligosaccharide biosynthetic gene cluster from Mycobacterium marinum. *Mol. Microbiol.* **2007**, *63*, 1345–1359, doi:10.1111/j.1365-2958.2007.05603.x.

53. Van Der Woude, A.D.; Sarkar, D.; Bhatt, A.; Sparrius, M.; Raadsen, S.A.; Boon, L.; Geurtsen, J.; Van Der Sar, A.M.; Luirink, J.; Houben, E.N.G.; et al. Unexpected link between lipooligosaccharide biosynthesis and surface protein release in Mycobacterium marinum. *J. Biol. Chem.* **2012**, *287*, 20417–20429, doi:10.1074/jbc.M111.336461.

54. Batt, S.M.; Minnikin, D.E.; Besra, G.S. The thick waxy coat of mycobacteria, a protective layer against antibiotics and the host's immune system. *Biochem. J.* **2020**, *447*, 1983–2006, doi:10.1042/BCJ20200194.

55. Etienne, G.; Villeneuve, C.; Billman-Jacobe, H.; Astarie-Dequeker, C.; Dupont, M.A.; Daffé, M. The impact of the absence of glycopeptidolipids on the ultrastructure, cell surface and cell wall properties, and

References

phagocytosis of Mycobacterium smegmatis. *Microbiology* **2002**, *148*, 3089–3100, doi:10.1099/00221287-148-10-3089.

56. Fujiwara, N.; Ohara, N.; Ogawa, M.; Maeda, S.; Naka, T.; Taniguchi, H.; Yamamoto, S.; Ayata, M. Glycopeptidolipid of Mycobacterium smegmatis J15cs Affects Morphology and Survival in Host Cells. *PLoS One* **2015**, *10*, doi:10.1371/journal.pone.0126813.

57. Howard, S.T.; Rhoades, E.; Recht, J.; Pang, X.; Alsup, A.; Kolter, R.; Lyons, C.R.; Byrd, T.F. Spontaneous reversion of Mycobacterium abscessus from a smooth to a rough morphotype is associated with reduced expression of glycopeptidolipid and reacquisition of an invasive phenotype. *Microbiology* **2006**, *152*, 1581–1590, doi:10.1099/mic.0.28625-0.

58. Catherinot, E.; Clarissou, J.; Etienne, G.; Ripoll, F.; Emile, J.F.; Daffé, M.; Perronne, C.; Soudais, C.; Gaillard, J.L.; Rottman, M. Hypervirulence of a rough variant of the Mycobacterium abscessus type strain. *Infect. Immun.* **2007**, *75*, 1055–1058, doi:10.1128/IAI.00835-06.

59. Barrow, W.W.; Davis, T.L.; Wright, E.L.; Labrousse, V.; Bachelet, M.; Rastogi, N. Immunomodulatory spectrum of lipids associated with Mycobacterium avium serovar 8. *Infect. Immun.* **1995**, *63*, 126–133, doi:10.1128/iai.63.1.126-133.1995.

60. Quesniaux, V.J.; Nicolle, D.M.; Torres, D.; Kremer, L.; Guérardel, Y.; Nigou, J.; Puzo, G.; Erard, F.; Ryffel, B. Toll-Like Receptor 2 (TLR2)-Dependent-Positive and TLR2-Independent-Negative Regulation of Proinflammatory Cytokines by Mycobacterial Lipomannans. *J. Immunol.* **2004**, *172*, 4425–4434, doi:10.4049/jimmunol.172.7.4425.

61. Tran, T.; Bonham, A.J.; Chan, E.D.; Honda, J.R. A paucity of knowledge regarding nontuberculous mycobacterial lipids compared to the tubercle bacillus. *Tuberculosis* **2019**, *115*, 96–107, doi:10.1016/j.tube.2019.02.008.

62. Guérardel, Y.; Maes, E.; Briken, V.; Chirat, F.; Leroy, Y.; Locht, C.; Strecker, G.; Kremer, L. Lipomannan and lipoarabinomannan from a clinical isolate of Mycobacterium kansasii: Novel structural features and apoptosis-inducing properties. *J. Biol. Chem.* **2003**, *278*, 36637–36651, doi:10.1074/jbc.M305427200.

63. Khoo, K.H.; Dell, A.; Morris, H.R.; Brennan, P.J.; Chatterjee, D. Inositol phosphate capping of the nonreducing termini of lipoarabinomannan from rapidly growing strains of Mycobacterium. *J. Biol. Chem.* **1995**, *270*, 12380–12389, doi:10.1074/jbc.270.21.12380.

64. Correia-Neves, M.; Sundling, C.; Cooper, A.; Källenius, G. Lipoarabinomannan in Active and Passive Protection Against Tuberculosis. *Front. Immunol.* **2019**, *10*, doi:10.3389/fimmu.2019.01968.

65. Noguera-Ortega, E.; Guallar-Garrido, S.; Julián, E. Mycobacteria-based vaccines as immunotherapy for non-urological cancers. *Cancers (Basel).* **2020**, *12*, 1–25, doi:10.3390/cancers12071802.

66. Secanella Fandos, S.P.; Luquín Fernández, M.; Barcelona., U.A. de Funcionalitat dels micobacteris ambientals de creixement ràpid com a agents antitumorals. **2013**.

67. Mathew, R.; Kruthiventi, A.K.; Prasad, J. V.; Kumar, S.P.; Srinu, G.; Chatterji, D. Inhibition of Mycobacterial Growth by Plumbagin Derivatives. *Chem. Biol. Drug Des.* **2010**, *76*, 34–42, doi:10.1111/j.1747-0285.2010.00987.x.

68. Thorson, L.M.; Doxsee, D.; Scott, M.G.; Wheeler, P.; Stokes, R.W. Effect of mycobacterial phospholipids on interaction of Mycobacterium tuberculosis with macrophages. *Infect. Immun.* **2001**, *69*, 2172–2179, doi:10.1128/IAI.69.4.2172-2179.2001.

69. Vergne, I.; Fratti, R.A.; Hill, P.J.; Chua, J.; Belisle, J.; Deretic, V. Mycobacterium tuberculosis Phagosome Maturation Arrest: Mycobacterial Phosphatidylinositol Analog Phosphatidylinositol Mannoside Stimulates Early Endosomal Fusion. *Mol. Biol. Cell* **2004**, *15*, 751–760, doi:10.1091/mbc.E03-05-0307.

70. Court, N.; Rose, S.; Bourigault, M.L.; Front, S.; Martin, O.R.; Dowling, J.K.; Kenny, E.F.; O'Neill, L.; Erard, F.; Quesniaux, V.F.J. Mycobacterial PIMs inhibit host inflammatory responses through CD14-dependent and CD14-independent mechanisms. *PLoS One* **2011**, *6*, doi:10.1371/journal.pone.0024631.

71. Goldman, D.S. Enzyme systems in the mycobacteria. Xv. Initial steps in the metabolism of glycerol. *J. Bacteriol.* **1963**, *86*, 30–7.

72. Wedum, A.G. Glycerol and Carbohydrate utilization by Mycobacterium tuberculosis. *J. Bacteriol.* **1936**, *32*, 599–611.

73. Edward E, S.; Jann, G.J. Utilization of Carbohydrates and Polyhydric Alcohols by Mycobacterium tuberculosis. *J. Bacteriol.* **1962**, *84*.

74. Baughn, A.D.; Rhee, K.Y. Metabolomics of Central Carbon Metabolism in Mycobacterium tuberculosis. *Microbiol. Spectr.* **2014**, *2*, doi:10.1128/microbiolspec.mgm2-0026-2013.

75. Ojha, A.K.; Baughn, A.D.; Sambandan, D.; Hsu, T.; Trivelli, X.; Guerardel, Y.; Alahari, A.; Kremer, L.; Jr, W.R.J.; Hatfull, G.F. Growth of Mycobacterium tuberculosis biofilms containing free mycolic acids and harbouring

drug-tolerant bacteria. *Mol. Microbiol.* **2008**, *69*, 164–174, doi:10.1111/j.1365-2958.2008.06274.x.

76. Cook, G.M.; Berney, M.; Gebhard, S.; Heinemann, M.; Robert, A.; Danilchanka, O.; Niederweis, M. Physiology of Mycobacteria. *Adv. Microb. Physiol.* **2013**, *2911*, doi:10.1016/S0065-2911(09)05502-7.Physiology.

77. And, E. Turnover of Acylglucose, Acyltrehalose and Free Trehalose during Growth of Mycobacterium smegmatis on Glucose. *Microbiology* **1972**, *73*, 539–546.

78. Shi, L.; Sohaskey, C.D.; Pfeiffer, C.; Datta, P.; Parks, M.; Mcfadden, J.; North, R.J.; Gennaro, M.L. Carbon flux rerouting during Mycobacterium tuberculosis growth arrest. *Mol. Microbiol.* **2010**, *78*, 1199–1215, doi:10.1111/j.1365-2958.2010.07399.x.

79. De Carvalho, L.P.S.; Fischer, S.M.; Marrero, J.; Nathan, C.; Ehrt, S.; Rhee, K.Y. Metabolomics of mycobacterium tuberculosis reveals compartmentalized co-catabolism of carbon substrates. *Chem. Biol.* **2010**, *17*, 1122–1131, doi:10.1016/j.chembiol.2010.08.009.

80. Rittmann, D.; Lindner, S.N.; Wendisch, V.F. Engineering of a glycerol utilization pathway for amino acid production by Corynebacterium glutamicum. *Appl. Environ. Microbiol.* **2008**, *74*, 6216–6222, doi:10.1128/AEM.00963-08.

81. Keating, L.A.; Wheeler, P.R.; Mansoor, H.; Inwald, J.K.; Dale, J.; Hewinson, R.G.; Gordon, S. V The pyruvate requirement of some members of the Mycobacterium tuberculosis complex is due to an inactive pyruvate kinase : implications for in vivo growth. *Mol. Microbiol.* **2005**, *56*, 163–174, doi:10.1111/j.1365-2958.2005.04524.x.

82. Nigou, J.; Besra, G.S. Cytidine diphosphate-diacylglycerol synthesis in *Mycobacterium smegmatis. Biochem. J.* **2002**, *367*, 157–162.

83. Morita, Y.S.; Fukuda, T.; Sena, C.B.C.; Yamaryo-Botte, Y.; McConville, M.J.; Kinoshita, T. Inositol lipid metabolism in mycobacteria: Biosynthesis and regulatory mechanisms. *Biochim. Biophys. Acta - Gen. Subj.* **2011**, *1810*, 630–641, doi:10.1016/j.bbagen.2011.03.017.

84. Jain, M.; Cox, J.S. Interaction between polyketide synthase and transporter suggests coupled synthesis and export of virulence lipid in M. tuberculosis. *PLoS Pathog.* **2005**, *1*, 0012–0019, doi:10.1371/journal.ppat.0010002.

85. Maurya, R.K.; Bharti, S.; Krishnan, M.Y. Triacylglycerols: Fuelling the Hibernating Mycobacterium tuberculosis. *Front. Cell. Infect. Microbiol.* **2019**, *8*, 450, doi:10.3389/fcimb.2018.00450.

86. K., P.; Luo, C.-Y.; S., Y. Metabolism of Plasma Membrane Lipids in Mycobacteria and Corynebacteria. In *Lipid Metabolism*; InTech, 2013.

87. Stokas, H.; Rhodes, H.L.; Purdy, G.E. Modulation of the M. tuberculosis cell envelope between replicating and non-replicating persistent bacteria. *Tuberculosis* **2020**, *125*, 102007, doi:10.1016/j.tube.2020.102007.

88. Agapova, A.; Serafini, A.; Petridis, M.; Hunt, D.M.; Garza-Garcia, A.; Sohaskey, C.D.; de Carvalho, L.P.S. Flexible nitrogen utilisation by the metabolic generalist pathogen Mycobacterium tuberculosis. *Elife* **2019**, *8*, doi:10.7554/eLife.41129.

89. Petridis, M.; Benjak, A.; Cook, G.M. Defining the nitrogen regulated transcriptome of Mycobacterium smegmatis using continuous culture. *BMC Genomics* **2015**, *16*, 1–13, doi:10.1186/s12864-015-2051-x.

90. Rieck, B.; Degiacomi, G.; Zimmermann, M.; Cascioferro, A.; Boldrin, F.; Lazar-adler, N.R.; Bottrill, R.; Chevalier, F.; Frigui, W.; Bellinzoni, M.; et al. *PknG senses amino acid availability to control metabolism and virulence of Mycobacterium tuberculosis*; 2017; ISBN 1111111111.

91. Viljoen, A.J.; Kirsten, C.J.; Baker, B.; Van Helden, P.D.; Wiid, I.J.F. The role of glutamine oxoglutarate aminotransferase and glutamate dehydrogenase in nitrogen metabolism in Mycobacterium bovis BCG. *PLoS One* **2013**, *8*, 1–9, doi:10.1371/journal.pone.0084452.

92. Gallant, J.L.; Viljoen, A.J.; Van Helden, P.D.; Wiid, I.J.F. Glutamate dehydrogenase is required by mycobacterium bovis BCG for resistance to cellular stress. *PLoS One* **2016**, *11*, doi:10.1371/journal.pone.0147706.

93. Barisch, C.; Paschke, P.; Hagedorn, M.; Maniak, M.; Soldati, T. Lipid droplet dynamics at early stages of *M ycobacterium marinum* infection in *D ictyostelium. Cell. Microbiol.* **2015**, *17*, 1332–1349, doi:10.1111/cmi.12437.

94. Murphy, D.J. The biogenesis and functions of lipid bodies in animals, plants and microorganisms. *Prog. Lipid Res.* **2001**, *40*, 325–438.

95. Daniel, J.; Deb, C.; Dubey, V.S.; Sirakova, T.D.; Abomoelak, B.; Morbidoni, H.R.; Kolattukudy, P.E.; Al, D.E.T.

References

Induction of a Novel Class of Diacylglycerol Acyltransferases and Triacylglycerol Accumulation in Mycobacterium tuberculosis as It Goes into a Dormancy-Like State in Culture. *J. Bacteriol.* **2004**, *186*, 5017–5030, doi:10.1128/JB.186.15.5017.

96. Garton, N.J.; Christensen, H.; Minnikin, D.E.; Adegbola, R.A.; Barer, M.R. Intracellular lipophilic inclusions of mycobacteria in vitro and in sputum. *Microbiology* **2018**, *148*, 2951–2958.

97. Hammond, R.J.H.; Baron, V.O.; Oravcova, K.; Lipworth, S.; Gillespie, S.H. Phenotypic resistance in mycobacteria: Is it because I am old or fat that I resist you? *J. Antimicrob. Chemother.* **2015**, *70*, 2823–2827, doi:10.1093/jac/dkv178.

98. Kai, L.L.; Rao, P.S.S.; Shui, G.; Bendt, A.K.; Pethe, K.; Dick, T.; Wenk, M.R. Triacylglycerol utilization is required for regrowth of in vitro hypoxic nonreplicating Mycobacterium bovis bacillus Calmette-Guerin. *J. Bacteriol.* **2009**, *191*, 5037–5043, doi:10.1128/JB.00530-09.

99. Wältermann, M.; Hinz, A.; Robenek, H.; Troyer, D.; Reichelt, R.; Malkus, U.; Galla, H.; Kalscheuer, R.; Stöveken, T.; Landenberg, P. Von; et al. Mechanism of lipid-body formation in prokaryotes : how bacteria fatten up. *Mol. Microbiol.* **2005**, *55*, 750–763, doi:10.1111/j.1365-2958.2004.04441.x.

100. van Wyk, R.; van Wyk, M.; Mashele, S.S.; Nelson, D.R.; Syed, K. Comprehensive comparative analysis of cholesterol catabolic genes/proteins in mycobacterial species. *Int. J. Mol. Sci.* **2019**, *20*, doi:10.3390/ijms20051032.

101. Wältermann, M.; Steinbüchel, A. MINIREVIEW Neutral lipid Bodies in Prokaryotes: Recent Insights into Structure, Formation, and Relationship to Eukaryotic Lipid Depots. *J. Bacteriol.* **2005**, *187*, 3607–3619, doi:10.1128/JB.187.11.3607–3619.2005.

102. Bacon, J.; Alderwick, L.J.; Allnutt, J.A.; Gabasova, E.; Watson, R.; Hatch, K.A.; Clark, S.O.; Jeeves, R.E.; Marriott, A.; Rayner, E.; et al. Non-Replicating Mycobacterium tuberculosis Elicits a Reduced Infectivity Profile with Corresponding Modifications to the Cell Wall and Extracellular Matrix. *PLoS One* **2014**, doi:10.1371/journal.pone.0087329.

103. Wright, C.C.; Hsu, F.F.; Arnett, E.; Dunaj, J.L.; Davidson, P.M.; Pacheco, S.A.; Harriff, M.J.; Lewinsohn, D.M.; Schlesinger, L.S.; Purdy, G.E. The Mycobacterium tuberculosis MmpL11 cell wall lipid transporter is important for biofilm formation, intracellular growth, and nonreplicating persistence. *Infect. Immun.* **2017**, *85*, doi:10.1128/IAI.00131-17.

104. Lovewell, R.R.; Sassetti, C.M.; VanderVen, B.C. Chewing the fat: Lipid metabolism and homeostasis during M. tuberculosis infection. *Curr. Opin. Microbiol.* **2016**, *29*, 30–36, doi:10.1016/j.mib.2015.10.002.

105. Dulberger, C.L.; Rubin, E.J.; Boutte, C.C. The mycobacterial cell envelope — a moving target. *Nat. Rev. Microbiol.* **2019**, doi:10.1038/s41579-019-0273-7.

106. Galagan, J.E.; Minch, K.; Peterson, M.; Lyubetskaya, A.; Azizi, E.; Sweet, L.; Gomes, A.; Rustad, T.; Dolganov, G.; Glotova, I.; et al. The Mycobacterium tuberculosis regulatory network and hypoxia. *Nature* **2013**, *499*, 178–183, doi:10.1038/nature12337.

107. Eoh, H.; Wang, Z.; Layre, E.; Rath, P.; Morris, R.; Branch Moody, D.; Rhee, K.Y. Metabolic anticipation in Mycobacterium tuberculosis. *Nat. Microbiol.* **2017**, *2*, 1–7, doi:10.1038/nmicrobiol.2017.84.

108. Briken, V.; Porcelli, S.A.; Besra, G.S.; Kremer, L. Mycobacterial lipoarabinomannan and related lipoglycans: From biogenesis to modulation of the immune response. *Mol. Microbiol.* **2004**, *53*, 391–403, doi:10.1111/j.1365-2958.2004.04183.x.

109. McKinney, J.D.; Höner Zu Bentrup, K.; Muñoz-Elias, E.J.; Miczak, A.; Chen, B.; Chan, W.T.; Swenson, D.; Sacchettini, J.C.; Jacobs, W.R.; Russell, D.G. Persistence of Mycobacterium tuberculosis in macrophages and mice requires the glyoxylate shunt enzyme isocitrate lyase. *Nature* **2000**, *406*, 735–738, doi:10.1038/35021074.

110. Muñoz-Elías, E.J.; Upton, A.M.; Cherian, J.; McKinney, J.D. Role of the methylcitrate cycle in Mycobacterium tuberculosis metabolism, intracellular growth, and virulence. *Mol. Microbiol.* **2006**, *60*, 1109–1122, doi:10.1111/j.1365-2958.2006.05155.x.

111. Dos Santos, A.C.D.; Marinho, V.H.D.S.; Silva, P.H.D.A.; MacChi, B.D.M.; Arruda, M.S.P.; Silva, E.O. Da; Do Nascimento, J.L.M.; Sena, C.B.C. De Microenvironment of Mycobacterium smegmatis Culture to Induce Cholesterol Consumption Does Cell Wall Remodeling and Enables the Formation of Granuloma-Like Structures. *Biomed Res. Int.* **2019**, *2019*, doi:10.1155/2019/1871239.

112. Ojha, A.; Anand, M.; Bhatt, A.; Kremer, L.; Jacobs, W.R.; Hatfull, G.F. GroEL1: A dedicated chaperone involved in mycolic acid biosynthesis during biofilm formation in mycobacteria. *Cell* **2005**, *123*, 861–873, doi:10.1016/j.cell.2005.09.012.

113. Allen, B.W. Mycobacteria. General culture methodology and safety considerations. *Methods Mol. Biol.* **1998**, *101*, 15–30, doi:10.1385/0-89603-471-2:15.

114. Koch, R. Die Aetiologie der Tuberculose. (Nach einem in der physiologischen Gesellschaft zu Berlin am 24. März er, gehaltenen Vortrage). *Berhner Khnzsche Wochenschrft* **1882**, *19*, 221–230.

115. Allen, B.W.; Hinkes, W.F. Koch's cultivation of tubercle bacilli . *Med. Lab. Sci.* **1983**, *40*, 85–87.

116. Middlebrook, G.; Cohn, M.L. Bacteriology of tuberculosis: laboratory methods. *Am. J. Public Health* **1958**, *48*, 844–853, doi:10.2105/ajph.48.7.844.

117. Dubos, R.J.; Middlebrook, G. Media for tubercle bacilli . *Am. Rev. Tuberc.* **1947**, *56*, 334–345.

118. Goude, R.; Parish, T.; Goude, R. *Mycobacteria Protocols. Methods in Molecular Biology*; 2008; Vol. 465; ISBN 0896034712.

119. Guallar-Garrido, S.; Campo-Pérez, V.; Sánchez-Chardi, A.; Luquin, M.; Julián, E. Each Mycobacterium Requires a Specific Culture Medium Composition for Triggering an Optimized Immunomodulatory and Antitumoral Effect. *Microorganisms* **2020**, *8*, 734, doi:10.3390/microorganisms8050734.

120. Prados-Rosales, R.; Carreño, L.J.; Weinrick, B.; Batista-Gonzalez, A.; Glatman-Freedman, A.; Xu, J.; Chan, J.; Jacobs, W.R.; Porcelli, S.A.; Casadevall, A. The Type of Growth Medium Affects the Presence of a Mycobacterial Capsule and Is Associated with Differences in Protective Efficacy of BCG Vaccination Against Mycobacterium tuberculosis. *J. Infect. Dis.* **2016**, *214*, 426–437, doi:10.1093/infdis/jiw153.

121. Leisching, G.; Pietersen, R.-D.; Wiid, I.; Baker, B. Virulence, biochemistry, morphology and host-interacting properties of detergent-free cultured mycobacteria: An update. *Tuberculosis* **2016**, *100*, 53–60, doi:10.1016/j.tube.2016.07.002.

122. Abou-Zeid, C.; Rook, G.A.W.; Minnikin, D.E.; Parlett, J.H.; Osbornt, T.W.; Grangets, J.M. Effect of the method of preparation of Bacille Calmette-Guérin (BCG) vaccine on the properties of four daughter strains. *J. Appl. Bacteriol.* **1987**, *63*, 449–453, doi:10.1111/j.1365-2672.1987.tb04867.x.

123. Osborn, T.W. Some effects of nutritional components on the morphology of BCG colonies. *Dev. Biol. Stand.* **1986**, *58*, 79–94.

124. Florio, W.; Batoni, G.; Esin, S.; Bottai, D.; Maisetta, G.; Favilli, F.; Brancatisano, F.L.; Campa, M. Influence of culture medium on the resistance and response of Mycobacterium bovis BCG to reactive nitrogen intermediates. *Microbes Infect.* **2006**, *8*, 434–441, doi:10.1016/j.micinf.2005.07.013.

125. Leal, M.B.B.; Baruque-Ramos, J.; Hiss, H.; Paz, M.F. da; Sakai, M.C.; Vassoler, U.M.; Arauz, L.J. de; Raw, I.; Betania Batista Leal, M.; Baruque-Ramos, J.; et al. Influence of initial L-asparagine and glycerol concentrations on the batch growth kinetics of Mycobacterium bovis BCG. *Brazilian J. Microbiol.* **2004**, *35*, 337–344, doi:10.1590/S1517-83822004000300013.

126. Cox, R.A.; Garcia, M.J. Adaptation of Mycobacteria to Growth Conditions: A Theoretical Analysis of Changes in Gene Expression Revealed by Microarrays. *PLoS One* **2013**, *8*, doi:10.1371/journal.pone.0059883.

127. Petricevich, V.; Ueda, C.; Alves, R.; da Silva, M.; Moreno, C.; Melo, A.; Dias da Silva, W.; Dias da Silva, C.W.; Butantan, F. A single strain of Mycobacterium bovis bacillus Calmette-Guérin (BCG) grown in two different media evokes distinct humoral immune responses in mice. *Braz J Med Biol ResGuérin Brazilian J. Med. Biol. Res.* **2001**, *34*, 81–92.

128. Gago, G.; Diacovich, L.; Gramajo, H. Lipid metabolism and its implication in mycobacteria-host interaction. *Curr. Opin. Microbiol.* **2019**, 36–42, doi:10.1016/j.mib.2017.11.020.Lipid.

129. Rodríguez-Güell, E.; Agustí, G.; Corominas, M.; Cardona, P.-J.; Casals, I.; Parella, T.; Sempere, M.-A.; Luquin, M.; Julián, E. The production of a new extracellular putative long-chain saturated polyester by smooth variants of Mycobacterium vaccae interferes with Th1-cytokine production. *Antonie Van Leeuwenhoek* **2006**, *90*, 93–108, doi:10.1007/s10482-006-9062-1.

130. Bai, G.; Schaak, D.D.; Mcdonough, K.A. cAMP levels within Mycobacterium tuberculosis and Mycobacterium bovis BCG increase upon infection of macrophages: RESEARCH ARTICLE. *FEMS Immunol. Med. Microbiol.* **2009**, *55*, 68–73, doi:10.1111/j.1574-695X.2008.00500.x.

131. Sani, M.; Houben, E.N.G.; Geurtsen, J.; Pierson, J.; de Punder, K.; van Zon, M.; Wever, B.; Piersma, S.R.; Jiménez, C.R.; Daffé, M.; et al. Direct Visualization by Cryo-EM of the Mycobacterial Capsular Layer: A Labile Structure Containing ESX-1-Secreted Proteins. *PLoS Pathog.* **2010**, *6*, e1000794, doi:10.1371/journal.ppat.1000794.

132. Venkataswamy, M.M.; Goldberg, M.F.; Baena, A.; Chan, J.; Jacobs, W.R.; Porcelli, S.A. In vitro culture medium influences the vaccine efficacy of Mycobacterium bovis BCG. *Vaccine* **2012**, *30*, 1038–1049, doi:10.1016/j.vaccine.2011.12.044.

133. Tepper, B.S.; Hopkins-Leonard, J. Differences in the Utilization of Glycerol and Glucose-by Mycobacterium

References

phlei Downloaded from. *J. Bacteriol.* **1968**, *95*, 1713–1717.

134. Totani, T.; Nishiuchi, Y.; Tateishi, Y.; Yoshida, Y.; Kitanaka, H.; Niki, M.; Kaneko, Y.; Matsumoto, S. Effects of nutritional and ambient oxygen condition on biofilm formation in Mycobacterium avium subsp. hominissuis via altered glycolipid expression. *Sci. Rep.* **2017**, *7*, 41775, doi:10.1038/srep41775.

135. Bellerose, M.M.; Baek, S.-H.; Huang, C.-C.; Moss, C.E.; Koh, E.-I.; Proulx, M.K.; Smith, C.M.; Baker, R.E.; Lee, J.S.; Eum, S.; et al. Common Variants in the Glycerol Kinase Gene Reduce Tuberculosis Drug Efficacy. *MBio* **2019**, *10*, doi:10.1128/mBio.00663-19.

136. Piddington, D.L.; Kashkouli, A.L.I.; Buchmeier, N.A. Growth of Mycobacterium tuberculosis in a Defined Medium Is Very Restricted by Acid pH and Mg 2 ε Levels. **2000**, *68*, 4518–4522.

137. Van De Weerd, R.; Boot, M.; Maaskant, J.; Sparrius, M.; Verboom, T.; Van Leeuwen, L.M.; Burggraaf, M.J.; Paauw, N.J.; Dainese, E.; Manganelli, R.; et al. Inorganic phosphate limitation modulates capsular polysaccharide composition in mycobacteria. *J. Biol. Chem.* **2016**, *291*, 11787–11799, doi:10.1074/jbc.M116.722454.

138. Dawson, D.J.; Jennis, F. Mycobacteria with a Growth Requirement for Ferric Ammonium Citrate, Identified as Mycobacterium haemophilum Downloaded from. *J. Clin. Microbiol.* **1980**, *11*, 190–192.

139. Velayati, A.A.; Farnia, P. *Atlas of Mycobacterium Tuberculosis*; Academic Press 2017, 2017;

140. WHO *GLOBAL TUBERCULOSIS REPORT 2020*; 2020; ISBN 9789240013131.

141. Degiacomi, G.; Sammartino, J.C.; Chiarelli, L.R.; Riabova, O.; Makarov, V.; Pasca, M.R. Mycobacterium abscessus, an emerging and worrisome pathogen among cystic fibrosis patients. *Int. J. Mol. Sci.* **2019**, *20*, doi:10.3390/ijms20235868.

142. Nontuberculous Mycobacteria (NTM) Infections | HAI | CDC.

143. WHO WHO | Global Leprosy Strategy 2016–2020: Accelerating towards a leprosy-free world. *WHO* **2017**.

144. Pettenati, C.; Ingersoll, M.A. Mechanisms of BCG immunotherapy and its outlook for bladder cancer. *Nat. Rev. Urol.* **2018**, *15*, 615–625, doi:10.1038/s41585-018-0055-4.

145. Verma, I.; Grover, A. Antituberculous vaccine development: a perspective for the endemic world. *Expert Rev. Vaccines* **2009**, *8*, 1547–1553, doi:10.1586/erv.09.111.

146. Wiseman, C.L. Inflammatory breast cancer: 10-year follow-up of a trial of surgery, chemotherapy, and allogeneic tumor cell/BCG immunotherapy. *Cancer Invest.* **1995**, *13*, 267–71.

147. Montesinos, J.C.H.; Romero, H.O.G. Autologous tumor lysate / Bacillus Calmette – Gue ´rin immunotherapy as an adjuvant to conventional breast cancer therapy. *Clin. Transl. Oncol.* **2015**, 3–6, doi:10.1007/s12094-015-1320-0.

148. Chung, M.A.; Luo, Y.; O'Donnell, M.; Rodriguez, C.; Heber, W.; Sharma, S.; Chang, H.R. Development and preclinical evaluation of a Bacillus Calmette-Guérin-MUC1-based novel breast cancer vaccine. *Cancer Res.* **2003**, *63*, 1280–7.

149. Yuan, S.; Shi, C.; Ling, R.; Wang, T.; Wang, H.; Han, W. Immunization with two recombinant Bacillus Calmette-Guérin vaccines that combine the expression of multiple tandem repeats of mucin-1 and colony stimulating-factor suppress breast tumor growth in mice. *J. Cancer Res. Clin. Oncol.* **2010**, *136*, 1359–1367, doi:10.1007/s00432-010-0787-x.

150. Yuan, S.; Shi, C.; Lv, Y.; Wang, T.; Wang, H.; Han, W. A Novel *Bacillus Calmette-Guérin* -based Breast Cancer Vaccine that Coexpresses Multiple Tandem Repeats of MUC1 and CD80 Breaks the Immune Tolerance and Inhibits MUC1-Positive Breast Cancer Growth. *Cancer Biother. Radiopharm.* **2009**, *24*, 607–613, doi:10.1089/cbr.2009.0622.

151. Popiela, T.; Kulig, J.; Czupryna, A.; Szczepanik, A.M.; Zembala, M. Efficiency of adjuvant immunochemotherapy following curative resection in patients with locally advanced gastric cancer. *Gastric Cancer* **2004**, *7*, 240–5, doi:10.1007/s10120-004-0299-y.

152. Zhang, Q.; Ni, W.; Zhao, X.; Wang, F.; Gao, Z.; Tai, G. Synergistic antitumor effects of Escherichia coli maltose binding protein and Bacillus Calmette-Guerin in a mouse lung carcinoma model. *Immunol. Lett.* **2011**, *136*, 108–113, doi:10.1016/j.imlet.2010.12.005.

153. Abei, M.; Okumura, T.; Fukuda, K.; Hashimoto, T.; Araki, M.; Ishige, K.; Hyodo, I.; Kanemoto, A.; Numajiri, H.; Mizumoto, M.; et al. A phase I study on combined therapy with proton-beam radiotherapy and in situ tumor vaccination for locally advanced recurrent hepatocellular carcinoma. *Radiat. Oncol.* **2013**, *8*, 239, doi:10.1186/1748-717X-8-239.

154. Yi, H.; Rong, Y.; Yankai, Z.; Wentao, L.; Hongxia, Z.; Jie, W.; Rongyue, C.; Taiming, L.; Jingjing, L. Improved efficacy of DNA vaccination against breast cancer by boosting with the repeat beta-hCG C-terminal peptide carried by mycobacterial heat-shock protein HSP65. *Vaccine* **2006**, *24*, 2575–2584, doi:10.1016/j.vaccine.2005.12.030.

155. Pavlenko, M.; Roos, A.-K.; Leder, C.; Hansson, L.-O.; Kiessling, R.; Levitskaya, E.; Pisa, P. Comparison of PSA-specific CD8+ CTL responses and antitumor immunity generated by plasmid DNA vaccines encoding PSA-HSP chimeric proteins. *Cancer Immunol. Immunother.* **2004**, *53*, 1085–92.

156. Li, D.; Li, H.; Zhang, P.; Wu, X.; Wei, H.; Wang, L.; Wan, M.; Deng, P.; Zhang, Y.; Wang, J.; et al. Heat shock fusion protein induces both specific and nonspecific anti-tumor immunity. *Eur. J. Immunol.* **2006**, *36*, 1324–1336, doi:10.1002/eji.200535490.

157. Yang, M.; Yan, Y.; Fang, M.; Wan, M.; Wu, X.; Zhang, X.; Zhao, T.; Wei, H.; Song, D.; Wang, L.; et al. MF59 formulated with CpG ODN as a potent adjuvant of recombinant HSP65-MUC1 for inducing anti-MUC1+ tumor immunity in mice. *Int. Immunopharmacol.* **2012**, *13*, 408–416, doi:10.1016/j.intimp.2012.05.003.

158. Daniel, D.; Chiu, C.; Giraudo, E.; Inoue, M.; Mizzen, L.A.; Chu, N.R.; Hanahan, D. CD4+ T Cell-Mediated Antigen-Specific Immunotherapy in a Mouse Model of Cervical Cancer. *Cancer Res.* **2005**, *65*, 2018–2025, doi:10.1158/0008-5472.CAN-04-3444.

159. Roman, L.D.; Wilczynski, S.; Muderspach, L.I.; Burnett, A.F.; O'Meara, A.; Brinkman, J.A.; Kast, W.M.; Facio, G.; Felix, J.C.; Aldana, M.; et al. A phase II study of Hsp-7 (SGN-00101) in women with high-grade cervical intraepithelial neoplasia. *Gynecol. Oncol.* **2007**, *106*, 558–66, doi:10.1016/j.ygyno.2007.05.038.

160. Yoo, Y.C.; Hata, K.; Lee, K.B.; Azuma, I. Inhibitory effect of BCG cell-wall skeletons (BCG-CWS) emulsified in squalane on tumor growth and metastasis in mice. *Arch. Pharm. Res.* **2002**, *25*, 522–7.

161. Kashiwazaki, Y.; Murata, M.; Sato, T.; Miyauchi, M.; Nakagawa, M.; Fukushima, A.; Chiba, N.; Azuma, I.; Yamaoka, T. Injection of cell-wall skeleton of Mycobacterium bovis BCG draining to a sentinel lymph node eliminates both lymph node metastases and the primary transplanted tumor. *Drug Discov Ther* **2008**, *2*, 168–177.

162. Nakajima, H.; Kawasaki, K.; Oka, Y.; Tsuboi, A.; Kawakami, M.; Ikegame, K.; Hoshida, Y.; Fujiki, F.; Nakano, A.; Masuda, T.; et al. WT1 peptide vaccination combined with BCG-CWS is more efficient for tumor eradication than WT1 peptide vaccination alone. *Cancer Immunol. Immunother.* **2004**, *53*, 617–624, doi:10.1007/s00262-003-0498-0.

163. Murata, M. Activation of Toll-like receptor 2 by a novel preparation of cell wall skeleton from Mycobacterium bovis BCG Tokyo (SMP-105) sufficiently enhances immune responses against tumors. *Cancer Sci.* **2008**, *99*, 1435–1440, doi:10.1111/j.1349-7006.2008.00832.x.

164. Masuda, H.; Nakamura, T.; Noma, Y.; Harashima, H. *Application of BCG-CWS as a Systemic Adjuvant by Using Nanoparticulation Technology*; 2018; Vol. 15; ISBN 8111706391.

165. MacEwen, E.G.; Kurzman, I.D.; Vail, D.M.; Dubielzig, R.R.; Everlith, K.; Madewell, B.R.; Rodriguez, C.O.; Phillips, B.; Zwahlen, C.H.; Obradovich, J.; et al. Adjuvant therapy for melanoma in dogs: results of randomized clinical trials using surgery, liposome-encapsulated muramyl tripeptide, and granulocyte macrophage colony-stimulating factor. *Clin. Cancer Res.* **1999**, *5*, 4249–58.

166. Meyers, P.A.; Chou, A.J. Muramyl tripeptide-phosphatidyl ethanolamine encapsulated in liposomes (L-MTP-PE) in the treatment of osteosarcoma. *Adv. Exp. Med. Biol.* **2014**, *804*, 307–321, doi:10.1007/978-3-319-04843-7_17.

167. Biteau, K.; Guiho, R.; Chatelais, M.; Taurelle, J.; Chesneau, J.; Corradini, N.; Heymann, D.; Redini, F. L-MTP-PE and zoledronic acid combination in osteosarcoma: preclinical evidence of positive therapeutic combination for clinical transfer. *Am. J. Cancer Res.* **2016**, *6*, 677–89.

168. Lou, Y.; Groves, M.J.; Klegerman, M.E. In-vivo and in-vitro targeting of a murine sarcoma by gelatin microparticles loaded with a glycan (PS1). *J. Pharm. Pharmacol.* **1994**, *46*, 863–6.

169. Ito, T.; Hirahara, K.; Onodera, A.; Koyama-Nasu, R.; Yano, I.; Nakayama, T. Anti-tumor immunity via the superoxide-eosinophil axis induced by a lipophilic component of Mycobacterium lipomannan. *Int. Immunol.* **2017**, *29*, 411–421, doi:10.1093/intimm/dxx051.

170. Lee, S.Y.; Yang, S. Bin; Choi, Y.M.; Oh, S.J.; Kim, B.J.; Kook, Y.H.; Kim, B.J. Heat-killed Mycobacterium paragordonae therapy exerts an anti-cancer immune response via enhanced immune cell mediated oncolytic activity in xenograft mice model. *Cancer Lett.* **2020**, *472*, 142–150, doi:10.1016/j.canlet.2019.12.028.

171. Jian, W.; Li, X.; Kang, J.; Lei, Y.; Bai, Y.; Xue, Y. Antitumor effect of recombinant Mycobacterium smegmatis expressing MAGEA3 and SSX2 fusion proteins. *Exp. Ther. Med.* **2018**, *16*, 2160–2166, doi:10.3892/etm.2018.6425.

172. Kuhn, S.; Hyde, E.J.; Yang, J.; Rich, F.J.; Harper, J.L.; Kirman, J.R.; Ronchese, F. Increased Numbers of

References

Monocyte-Derived Dendritic Cells during Successful Tumor Immunotherapy with Immune-Activating Agents. *J. Immunol.* **2013**, *191*, 1984–1992, doi:10.4049/jimmunol.1301135.

173. Fowler, D.; Dalgleish, A.; Liu, W. A heat-killed preparation of mycobacterium obuense can reduce metastatic burden in vivo. *J. Immunother. Cancer* **2014**, *2*, P54, doi:10.1186/2051-1426-2-S3-P54.

174. Stebbing, J.; Dalgleish, A.; Gifford-Moore, A.; Martin, A.; Gleeson, C.; Wilson, G.; Brunet, L.R.; Grange, J.; Mudan, S. An intra-patient placebo-controlled phase I trial to evaluate the safety and tolerability of intradermal IMM-101 in melanoma. *Ann. Oncol. Off. J. Eur. Soc. Med. Oncol.* **2012**, *23*, 1314–9, doi:10.1093/annonc/mdr363.

175. Bazzi, S.; Modjtahedi, H.; Mudan, S.; Achkar, M.; Akle, C.; Bahr, G.M. Immunomodulatory effects of heat-killed Mycobacterium obuense on human blood dendritic cells. *Innate Immun.* **2017**, *23*, 592–605, doi:10.1177/1753425917727838.

176. Bilyard, H.; Mines, C.; Brunet, L.; Dalgleish, A.; Macintosh, F. IMM-101, an immunotherapeutic agent in clinical development as an adjunctive treatment for pancreatic cancer. *J. Immunother. Cancer* **2014**, *2*, P83, doi:10.1186/2051-1426-2-S3-P83.

177. Woodlock, T.J.; Sahasrabudhe, D.M.; Marquis, D.M.; Greene, D.; Pandya, K.J.; McCune, C.S. Active specific immunotherapy for metastatic colorectal carcinoma: phase I study of an allogeneic cell vaccine plus low-dose interleukin-1 alpha. *J. Immunother.* **1999**, *22*, 251–9.

178. Korbelik, M.; Cecic, I. Enhancement of tumour response to photodynamic therapy by adjuvant mycobacterium cell-wall treatment. *J. Photochem. Photobiol. B Biol.* **1998**, *44*, 151–158, doi:10.1016/S1011-1344(98)00138-9.

179. Ahmad, F.; Mani, J.; Kumar, P.; Haridas, S.; Upadhyay, P.; Bhaskar, S. Activation of anti-tumor immune response and reduction of regulatory T cells with Mycobacterium indicus pranii (MIP) therapy in tumor bearing mice. *PLoS One* **2011**, *6*, e25424, doi:10.1371/journal.pone.0025424.

180. Kumar, P.; Das, G.; Bhaskar, S. Mycobacterium indicus pranii therapy induces tumor regression in MyD88- and TLR2-dependent manner. *BMC Res. Notes* **2019**, *12*, 1–5, doi:10.1186/s13104-019-4679-0.

181. Halder, K.; Banerjee, S.; Ghosh, S.; Bose, A.; Das, S.; Chowdhury, B.P.; Majumdar, S. *Mycobacterium indicus pranii* (*Mw*) inhibits invasion by reducing matrix metalloproteinase (MMP-9) via AKT/ERK-1/2 and PKCα signalling: a potential candidate in melanoma cancer therapy. *Cancer Biol. Ther.* **2015**, 00–00, doi:10.1080/15384047.2015.1078024.

182. Rakshit, S.; Ponnusamy, M.; Papanna, S.; Saha, B.; Ahmed, A.; Nandi, D. Immunotherapeutic efficacy of Mycobacterium indicus pranii in eliciting anti-tumor T cell responses: critical roles of IFNγ. *Int. J. Cancer* **2012**, *130*, 865–75, doi:10.1002/ijc.26099.

183. Sur, P.K.; Dastidar, A.G. Role of mycobacterium w as adjuvant treatment of lung cancer (non-small cell lung cancer). *J. Indian Med. Assoc.* **2003**, *101*, 118, 120.

184. Belani, C.P.; Chakraborty, B.; Desai, D.; Khamar, B.M. Randomized multicenter phase ii clinical trial of a toll like receptor-2 (TLR-2) agonist mycobacterium w (CADI-05) in combination with paclitaxel plus cisplatin versus paclitaxel plus cisplatin in advanced nonsmall cell lung cancer (NSCLC). *J. Thorac. Oncol.* **2011**, *6*, S468–S469.

185. Garg, H.; Gupta, J.C.; Talwar, G.P.; Dubey, S. Immunotherapy approach with recombinant survivin adjuvanted with alum and MIP suppresses tumor growth in murine model of breast cancer. *Prep. Biochem. Biotechnol.* **2018**, *48*, 264–269, doi:10.1080/10826068.2018.1425710.

186. Subramaniam, M.; Arshad, N.M.; Mun, K.S.; Malagobadan, S. Anti-Cancer E ff ects of Synergistic Drug – Bacterium Combinations on Induced Breast Cancer in BALB / c Mice. *Biomolecules* **2019**, *9*, doi:10.3390/biom9100626.

187. Juin, S.K.; Ghosh, S.; Majumdar, S. Glycyrrhizic acid facilitates anti-tumor immunity by attenuating Tregs and MDSCs: An immunotherapeutic approach. *Int. Immunopharmacol.* **2020**, *88*, 106932, doi:10.1016/j.intimp.2020.106932.

188. Subramaniam, M.; In, L.L.A.; Kumar, A.; Ahmed, N.; Nagoor, N.H. Cytotoxic and apoptotic effects of heat killed Mycobacterium indicus pranii (MIP) on various human cancer cell lines. *Sci. Rep.* **2016**, *6*, 19833, doi:10.1038/srep19833.

189. Sharma, C.; Khan, M.A.; Mohan, T.; Shrinet, J.; Latha, N.; Singh, N. A synthetic chimeric peptide harboring human papillomavirus 16 cytotoxic T lymphocyte epitopes shows therapeutic potential in a murine model of cervical cancer. *Immunol. Res.* **2014**, *58*, 132–138, doi:10.1007/s12026-013-8447-2.

190. Saqib, M.; Khatri, R.; Singh, B.; Gupta, A.; Bhaskar, S. Cell wall fraction of Mycobacterium indicus pranii shows potential Th1 adjuvant activity. *Int. Immunopharmacol.* **2019**, *70*, 408–416, doi:10.1016/j.intimp.2019.02.049.

180

191. O'Brien, M.E.R.; Anderson, H.; Kaukel, E.; O'Byrne, K.; Pawlicki, M.; Von Pawel, J.; Reck, M.; SR-ON-12 Study Group SRL172 (killed Mycobacterium vaccae) in addition to standard chemotherapy improves quality of life without affecting survival, in patients with advanced non-small-cell lung cancer: phase III results. *Ann. Oncol. Off. J. Eur. Soc. Med. Oncol.* **2004**, *15*, 906–14.

192. Stanford, J.L.L.; Stanford, C.A.A.; O'Brien, M.E.R.; Grange, J.M.M.; O'Brien, M.E.R.; Grange, J.M.M. Successful immunotherapy with Mycobacterium vaccae in the treatment of adenocarcinoma of the lung. *Eur. J. Cancer* **2008**, *44*, 224–227, doi:10.1016/j.ejca.2007.08.021.

193. Harper-Wynne, C.L.; Sumpter, K.; Ryan, C.; Priest, K.; Norton, A.; Ross, P.; Ford, H.E.R.; Johnson, P.; O'Brien, M.E.R. Addition of SRL 172 to standard chemotherapy in small cell lung cancer (SCLC) improves symptom control. *Lung Cancer* **2005**, *47*, 289–290, doi:10.1016/j.lungcan.2004.08.013.

194. Maraveyas, A.; Baban, B.; Kennard, D.A.; Rook, G.A.W.; Westby, M.; Grange, J.M.; Lydyard, P.; Stanford, J.L.; Jones, M.; Selby, P.J.; et al. Possible improved survival of patients with stage IV AJCC melanoma receiving SRL 172 immunotherapy: Correlation with induction of increased levels of intracellular interleukin-2 in peripheral blood lymphocytes. *Ann. Oncol.* **1999**, *10*, 817–824, doi:10.1023/A:1008307821189.

195. O'Brien, M.E.R.E.R.; Saini, A.; Smith, I.E.; Webb, A.; Gregory, K.; Mendes, R.; Ryan, C.; Priest, K.; Bromelow, K. V; Palmer, R.D.; et al. A randomized phase II study of SRL172 (Mycobacterium vaccae) combined with chemotherapy in patients with advanced inoperable non-small-cell lung cancer and mesothelioma. *Br. J. Cancer* **2000**, *83*, 853–857, doi:10.1054/bjoc.2000.1401.

196. Mendes, R.; O'Brien, M.E.R.; Mitra, A.; Norton, A.; Gregory, R.K.; Padhani, A.R.; Bromelow, K. V; Winkley, A.R.; Ashley, S.; Smith, I.E.; et al. Clinical and immunological assessment of Mycobacterium vaccae (SRL172) with chemotherapy in patients with malignant mesothelioma. *Br. J. Cancer* **2002**, *86*, 336–341, doi:10.1038/sj.bjc.6600063.

197. Nicholson, S.; Guile, K.; John, J.; Clarke, I.A.; Diffley, J.; Donnellan, P.; Michael, A.; Szlosarek, P.; Dalgleish, A.G. A randomized phase II trial of SRL172 (Mycobacterium vaccae) +/- low-dose interleukin-2 in the treatment of metastatic malignant melanoma. *Melanoma Res.* **2003**, *13*, 389–93, doi:10.1097/01.cmr.0000056252.56735.1a.

198. Cananzi, F.C.M.; Mudan, S.; Dunne, M.; Belonwu, N.; Dalgleish, A.G. Long-term survival and outcome of patients originally given Mycobacterium vaccae for metastatic malignant melanoma. *Hum. Vaccin. Immunother.* **2013**, *9*, 2427–33.

199. Altundag, K.; Mohamed, A.-S.; Altundag, O.; Silay, Y.S.; Gunduz, E.; Demircan, K. SRL172 (killed Mycobacterium vaccae) may augment the efficacy of trastuzumab in metastatic breast cancer patients. *Med. Hypotheses* **2005**, *64*, 248–251, doi:10.1016/j.mehy.2004.07.016.

200. Tian, X.X.; Li, A.; Zhou, W.; Farrugia, I. V; Groves, M.J. Isolation and biological activities of an antineoplastic protein- polysaccharide complex (PS4A) obtained from Mycobacterium vaccae. *Anticancer Res.* **1999**, *19*, 237–243.

201. Kim, D.H.; Moon, C.; Oh, S.-S.; Park, S.; Jeong, J.-W.; Kim, S.; Lee, H.G.; Kwon, H.-J.; Kim, K.D. Liposome-Encapsulated CpG Enhances Antitumor Activity Accompanying the Changing of Lymphocyte Populations in Tumor via Intratumoral Administration. *Nucleic Acid Ther.* **2015**, *25*, 95–102, doi:10.1089/nat.2014.0509.

202. Hayashi, Y.; Sasaki, H.; Emori, Y.; Nomoto, K. The effect of combination therapy of radiation and Z-100, an arabinomannan on tumor growth in mice. *Biotherapy* **1993**, *7*, 63–9.

203. Sasaki, H.; Schmitt, D.A.; Kobayashi, M.; Hayashi, Y.; Pollard, R.B.; Suzuki, F. Prolongation of concomitant antitumor immunity in mice treated with Z-100, an arabinomannan extracted from Mycobacterium tuberculosis. *Nat Immun* **1993**, *12*, 152–164.

204. He, X.; Wang, J.; Zhao, F.; Yu, F.; Chen, D.; Cai, K.; Yang, C.; Chen, J.; Dou, J. Antitumor efficacy of viable tumor vaccine modified by heterogenetic ESAT-6 antigen and cytokine IL-21 in melanomatous mouse. *Immunol. Res.* **2012**, *52*, 240–249, doi:10.1007/s12026-012-8332-4.

205. He, X.; Wang, J.; Zhao, F.; Chen, D.; Chen, J.; Zhang, H.; Yang, C.; Liu, Y.; Dou, J. ESAT-6-gpi DNA Vaccine Augmented the Specific Antitumour Efficacy Induced by the Tumour Vaccine B16F10-ESAT-6-gpi/IL-21 in a Mouse Model. *Scand. J. Immunol.* **2013**, *78*, 69–78, doi:10.1111/sji.12074.

206. Koyama, Y.; Yoshihara, C.; Ito, T. Novel Antitumor Strategy Utilizing a Plasmid Expressing a Mycobacterium tuberculosis Antigen as a "Danger Signal" to Block Immune Escape of Tumor Cells. *Pharmaceutics* **2015**, *7*, 165–174, doi:10.3390/pharmaceutics7030165.

207. Vo, M.-C.; Lee, H.-J.; Kim, J.-S.; Hoang, M.-D.; Choi, N.-R.; Rhee, J.H.; Lakshmanan, V.-K.; Shin, S.-J.; Lee, J.-J.

References

Dendritic cell vaccination with a toll-like receptor agonist derived from mycobacteria enhances anti-tumor immunity. *Oncotarget* **2015**, *6*, 33781–90, doi:10.18632/oncotarget.5281.

208. Shi, Y.-L.; Bao, L.; Shang, Z.-L.; Yao, S.-X. RelE toxin protein of Mycobacterium tuberculosis induces growth inhibition of lung cancer A-549 cell. *Sichuan Da Xue Xue Bao. Yi Xue Ban* **2008**, *39*, 368–72.

209. Li, X.-L.; Zhao, C.-L.; Dong, Q.; Sun, L.-R. Enhancement of immunogenicity of murine lymphocytic leukemia cells by transfection with BCG heat shock protein 70 gene. *Int. Immunopharmacol.* **2013**, *15*, 1–5, doi:10.1016/j.intimp.2012.11.010.

210. Borges, T.J.; Porto, B.N.; Teixeira, C.A.; Rodrigues, M.; Machado, F.D.; Ornaghi, A.P.; de Souza, A.P.D.; Maito, F.; Pavanelli, W.R.; Silva, J.S.; et al. Prolonged survival of allografts induced by mycobacterial Hsp70 is dependent on CD4+CD25+ regulatory T cells. *PLoS One* **2010**, *5*, e14264, doi:10.1371/journal.pone.0014264.

211. Xu, M.; Zhou, L.; Zhang, Y.; Xie, Z.; Zhang, J.; Guo, L.; Wang, C.; Yang, X. A Fixed Human Umbilical Vein Endothelial Cell Vaccine With 2 Tandem Repeats of Microbial HSP70 Peptide Epitope 407-426 As Adjuvant for Therapy of Hepatoma in Mice. *J. Immunother.* **2015**, *38*, 276–284, doi:10.1097/CJI.0000000000000091.

212. Zeng, S.; Liu, Q.; Wang, S.; Peng, X.; Zhang, J.; Zhang, J. Intratumor injection of recombinant attenuated salmonella carrying Mycobacterium tuberculosis heat shock protein 70 and herpes simplex virus thymidine kinase genes to suppress murine melanoma growth. *Nan Fang Yi Ke Da Xue Xue Bao* **2012**, *32*, 101–5.

213. Liso, A.; Benedetti, R.; Fagioli, M.; Mariano, A.; Falini, B. Modulatory effects of mycobacterial heat-shock protein 70 in DNA vaccination lymphoma. *Haematologica* **2005**, *90*, 60–65.

214. Karyampudi, L.; Ghosh, S.K. Mycobacterial HSP70 as an adjuvant in the design of an idiotype vaccine against a murine lymphoma. *Cell. Immunol.* **2008**, *254*, 74–80, doi:10.1016/j.cellimm.2008.07.003.

215. Yu, W.; Qu, H.; Cao, G.; Liu, C.; Deng, H.; Zhang, Z. MtHsp70-CLIC1-pulsed dendritic cells enhance the immune response against ovarian cancer. *Biochem. Biophys. Res. Commun.* **2017**, *494*, 13–19, doi:10.1016/j.bbrc.2017.10.094.

216. Zong, J.; Peng, Q.; Wang, Q.; Zhang, T.; Fan, D.; Xu, X. Human HSP70 and modified HPV16 E7 fusion DNA vaccine induces enhanced specific CD8+ T cell responses and anti-tumor effects. *Oncol. Rep.* **2009**, *22*, 953–61.

217. Secanella-Fandos, S.; Luquin, M.; Julián, E. Connaught and russian strains showed the highest direct antitumor effects of different bacillus calmette-guérin substrains. *J. Urol.* **2013**, *189*, 711–718, doi:10.1016/j.juro.2012.09.049.

218. Secanella-Fandos, S.; Noguera-Ortega, E.; Olivares, F.; Luquin, M.; Julián, E. Killed but metabolically active Mycobacterium bovis bacillus Calmette-Guérin retains the antitumor ability of live bacillus Calmette-Guérin. *J. Urol.* **2014**, *191*, 1422–8, doi:10.1016/j.juro.2013.12.002.

219. Unda-urzaiz, M.; Cozar-olmos, J.M.; Miñana-Lopez, B.; Camarero-Jimenez, J.; Brugarolas-Rossello, X.; Zubiaur-Libano, C.; Ribal-Caparros, M.J.; Suarez-Charneco, A.J.; Rodriguez-Tesedo, V.; Chantada-Abal, V.; et al. Safety and efficacy of various strains of bacille Calmette-Guérin in the treatment of bladder tumors in standard clinical practice. *Actas Urológicas Españolas* **2018**, *42*, 238–248, doi:10.1016/j.acuroe.2018.03.004.

220. Del Giudice, F.; Busetto, G.M.; Gross, M.S.; Maggi, M.; Sciarra, A.; Salciccia, S.; Ferro, M.; Sperduti, I.; Flammia, S.; Canale, V.; et al. Efficacy of three BCG strains (Connaught, TICE and RIVM) with or without secondary resection (re-TUR) for intermediate/high-risk non-muscle-invasive bladder cancers: results from a retrospective single-institution cohort analysis. *J. Cancer Res. Clin. Oncol.* **2021**, doi:10.1007/s00432-021-03571-0.

221. Rentsch, C.A.; Birkhäuser, F.D.; Biot, C.; Gsponer, J.R.; Bisiaux, A.; Wetterauer, C.; Lagranderie, M.; Marchal, G.; Orgeur, M.; Bouchier, C.; et al. Bacillus calmette-guérin strain differences have an impact on clinical outcome in bladder cancer immunotherapy. *Eur. Urol.* **2014**, *66*, 677–688, doi:10.1016/j.eururo.2014.02.061.

222. Guerrero-Ramos, F.; Lara-Isla, A.; Justo-Quintas, J.; Duarte-Ojeda, J.M.M.; de la Rosa-Kehrmann, F.; Villacampa-Aubá, F. Adjuvant intravesical treatment for non-muscle invasive bladder cancer: The importance of the strain and maintenance. *Actas Urológicas Españolas (English Ed.* **2017**, *41*, 590–595, doi:10.1016/j.acuroe.2017.08.008.

223. Krajewski, W.; Matuszewski, M.; Poletajew, S.; Grzegrzółka, J.; Zdrojowy, R.; Kołodziej, A. Are there differences in toxicity and efficacy between various Bacillus Calmette-Guerin strains in bladder cancer patients? Analysis of 844 Patients. *Urol. Int.* **2018**, *101*, 277–284, doi:10.1159/000492722.

224. D'Andrea, D.; Soria, F.; Gontero, P.; Machado, A.T.; Waksman, R.; Shariat, S.F.; Chade*, D.C. Pd13-01 Comparative Effectiveness of Intravesical Bcg-Tice and Bcg-Moreau in Patients With Non-Muscle Invasive

Bladder Cancer. *J. Urol.* **2019**, *201*, doi:10.1097/01.ju.0000555381.73832.50.

225. Miyazaki, J.; Onozawa, M.; Takaoka, E.; Yano, I. Bacillus Calmette–Guérin strain differences as the basis for immunotherapies against bladder cancer. *Int. J. Urol.* **2018**, *25*, 405–413, doi:10.1111/iju.13538.

226. Secanella-Fandos, S.; Luquin, M.; Julián, E. Connaught and Russian strains showed the highest direct antitumor effects of different Bacillus Calmette-Guérin substrains. *J. Urol.* **2013**, *189*, 711–8, doi:10.1016/j.juro.2012.09.049.

227. Low, L.S.; Scholtz, D.; Leyland, J.; Nair, S.M. A severe complication of intravesical bacillus Calmette-Guerin: An effect of different strains. *Urol. Case Reports* **2021**, *36*, 101592, doi:10.1016/j.eucr.2021.101592.

228. Lacerda Mariano, L.; Ingersoll, M.A. The immune response to infection in the bladder. *Nat. Rev. Urol.* **2020**, *17*, 439–458, doi:10.1038/s41585-020-0350-8.

229. Redelman-Sidi, G.; Glickman, M.S.; Bochner, B.H. The mechanism of action of BCG therapy for bladder cancer-A current perspective. *Nat. Rev. Urol.* **2014**, *11*, 153–162, doi:10.1038/nrurol.2014.15.

230. Han, J.; Gu, X.; Li, Y.; Wu, Q. Mechanisms of BCG in the treatment of bladder cancer-current understanding and the prospect. *Biomed. Pharmacother.* **2020**, *129*, doi:10.1016/j.biopha.2020.110393.

231. Bevers, R.F.; Boer, E.C. de; Kurth, K.; Schamhart, D. BCG-induced interleukin-6 upregulation and BCG internalization in well and poorly differentiated human bladder cancer cell lines. *Eur. Cytokine Netw.* **1998**.

232. Antonelli, A.C.; Binyamin, A.; Hohl, T.M.; Glickman, M.S.; Redelman-Sidi, G. Bacterial immunotherapy for cancer induces CD4-dependent tumor-specific immunity through tumor-intrinsic interferon-γ signaling. *Proc. Natl. Acad. Sci. U. S. A.* **2020**, *117*, 18627–18637, doi:10.1073/pnas.2004421117.

233. Shan, G.; Tang, T.; Qian, H.; Xia, Y. Certain BCG-reactive responses are associated with bladder cancer prognosis. *Cancer Immunol. Immunother.* **2018**, *67*, 797–803, doi:10.1007/s00262-018-2127-y.

234. Bakhru, P.; Sirisaengtaksin, N.; Soudani, E.; Mukherjee, S.; Khan, A.; Jagannath, C. BCG vaccine mediated reduction in the MHC-II expression of macrophages and dendritic cells is reversed by activation of Toll-like receptors 7 and 9. *Cell. Immunol.* **2014**, *287*, 53–61, doi:10.1016/j.cellimm.2013.11.007.

235. Pichler, R.; Fritz, J.; Zavadil, C.; Schäfer, G.; Culig, Z.; Brunner, A. Tumor-infiltrating immune cell subpopulations influence the oncologic outcome after intravesical bacillus calmette-guérin therapy in bladder cancer. *Oncotarget* **2016**, *7*, 39916–39930, doi:10.18632/oncotarget.9537.

236. Akan, S.; Ediz, C.; Sahin, A.; Tavukcu, H.H.; Urkmez, A.; Horasan, A.; Yilmaz, O.; Verit, A. Can the systemic immune inflammation index be a predictor of BCG response in patients with high-risk non-muscle invasive bladder cancer? *Int. J. Clin. Pract.* **2020**, 1–9, doi:10.1111/ijcp.13813.

237. Wang, H.; Wang, D.; Feng, Y.; Zhai, J.; Lu, C. Improved antitumor efficacy of neutrophils stimulated by bacillus Calmette-Guérin. *Mol. Med. Rep.* **2019**, *20*, 2909–2915, doi:10.3892/mmr.2019.10532.

238. Liu, K.; Sun, E.; Lei, M.; Li, L.; Gao, J.; Nian, X.; Wang, L. BCG-induced formation of neutrophil extracellular traps play an important role in bladder cancer treatment. *Clin. Immunol.* **2019**, *201*, 4–14, doi:10.1016/j.clim.2019.02.005.

239. Yuk, H.D.; Jeong, C.W.; Kwak, C.; Kim, H.H.; Ku, J.H. Elevated neutrophil to lymphocyte ratio predicts poor prognosis in non-muscle invasive bladder cancer patients: Initial intravesical bacillus Calmette-Guerin treatment after transurethral resection of bladder tumor setting. *Front. Oncol.* **2019**, *9*, 1–8, doi:10.3389/fonc.2018.00642.

240. Vartolomei, M.D.; Ferro, M.; Cantiello, F.; Lucarelli, G.; Di Stasi, S.; Hurle, R.; Guazzoni, G.; Busetto, G.M.; De Berardinis, E.; Damiano, R.; et al. Validation of Neutrophil-to-lymphocyte Ratio in a Multi-institutional Cohort of Patients With T1G3 Non–muscle-invasive Bladder Cancer. *Clin. Genitourin. Cancer* **2018**, *16*, 445–452, doi:10.1016/j.clgc.2018.07.003.

241. Joseph, M.; Enting, D. Immune Responses in Bladder Cancer-Role of Immune Cell Populations, Prognostic Factors and Therapeutic Implications. *Front. Oncol.* **2019**, *9*, 1–15, doi:10.3389/fonc.2019.01270.

242. Krpina, K.; Babarović, E.; Đordević, G.; Markić, D.; Maricić, A.; Jonjić, N. Impact of NK cell count on bladder cancer recurrence. *Urologia* **2014**, *81*, 233–236, doi:10.5301/uro.5000063.

243. Brandau, S.; Riemensberger, J.; Jacobsen, M.; Kemp, D.; Zhao, W.; Zhao, X.; Jocham, D.; Ratliff, T.L.; Böhleböhle, A. NK cells are essential for effective BCG immunotherapy. *Int. J. Cancer* **2001**, *92*, 697–702, doi:10.1002/1097-0215.

244. Mukherjee, N.; Ji, N.; Hurez, V.; Curiel, T.J.; Montgomery, M.O.; Braun, A.J.; Nicolas, M.; Aguilera, M.; Kaushik, D.; Liu, Q.; et al. Intratumoral CD56bright natural killer cells are associated with improved survival in bladder cancer. *Oncotarget* **2018**, *9*, 36492–36502, doi:10.18632/oncotarget.26362.

183

References

245. Ghaedi, M.; Ohashi, P.S. ILC transdifferentiation: roles in cancer progression. *Cell Res.* **2020**, *30*, 562–563, doi:10.1038/s41422-020-0326-5.

246. Chevalier, M.F.; Trabanelli, S.; Racle, J.; Salomé, B.; Cesson, V.; Gharbi, D.; Bohner, P.; Domingos-Pereira, S.; Dartiguenave, F.; Fritschi, A.S.; et al. ILC2-modulated T cell-to-MDSC balance is associated with bladder cancer recurrence. *J. Clin. Invest.* **2017**, *127*, 2916–2929, doi:10.1172/JCI89717.

247. Puttmann, K.; Duggan, M.; Mortazavi, A.; Diaz, D.A.; Carson, W.E.; Sundi, D. The Role of Myeloid Derived Suppressor Cells in Urothelial Carcinoma Immunotherapy. *Bl. Cancer* **2019**, *5*, 103–114, doi:10.3233/BLC-190219.

248. M. Ibrahim, O.; K Pandey, R.; Chatta, G.; Kalinski, P. Role of tumor microenvironment in the efficacy of BCG therapy. *Trends Res.* **2020**, *3*, 8–12, doi:10.15761/tr.1000170.

249. Miyake, M.; Tatsumi, Y.; Gotoh, D.; Ohnishi, S.; Owari, T.; Iida, K.; Ohnishi, K.; Hori, S.; Morizawa, Y.; Itami, Y.; et al. Regulatory T cells and tumor-associated macrophages in the tumor microenvironment in non-muscle invasive bladder cancer treated with intravesical bacille calmette-guérin: A long-term follow-up study of a Japanese cohort. *Int. J. Mol. Sci.* **2017**, *18*, doi:10.3390/ijms18102186.

250. Lim, C.J.; Nguyen, P.H.D.; Wasser, M.; Kumar, P.; Lee, Y.H.; Nasir, N.J.M.; Chua, C.; Lai, L.; Hazirah, S.N.; Loh, J.J.H.; et al. Immunological Hallmarks for Clinical Response to BCG in Bladder Cancer. *Front. Immunol.* **2021**, *11*, doi:10.3389/fimmu.2020.615091.

251. Annels, N.E.; Simpson, G.R.; Pandha, H. Modifying the Non-muscle Invasive Bladder Cancer Immune Microenvironment for Optimal Therapeutic Response. *Front. Oncol.* **2020**, *10*, doi:10.3389/fonc.2020.00175.

252. Chugh, S.; Anand, V.; Swaroop, L.; Sharma, M.; Seth, A.; Sharma, A. Involvement of Th17 cells in patients of urothelial carcinoma of bladder. *Hum. Immunol.* **2013**, *74*, 1258–1262, doi:10.1016/j.humimm.2013.06.032.

253. Ji, N.; Mukherjee, N.; Reyes, R.M.; Gelfond, J.; Javors, M.; Meeks, J.J.; McConkey, D.J.; Shu, Z.J.; Ramamurthy, C.; Dennett, R.; et al. Rapamycin enhances BCG-specific 3δT cells during intravesical BCG therapy for non-muscle invasive bladder cancer: A randomized, double-blind study. *J. Immunother. Cancer* **2021**, *9*, doi:10.1136/jitc-2020-001941.

254. Ji, N.; Mukherjee, N.; Morales, E.E.; Tomasini, M.E.; Hurez, V.; Curiel, T.J.; Abate, G.; Hoft, D.F.; Zhao, X.R.; Gelfond, J.; et al. Percutaneous BCG enhances innate effector antitumor cytotoxicity during treatment of bladder cancer: a translational clinical trial. *Oncoimmunology* **2019**, *8*, doi:10.1080/2162402X.2019.1614857.

255. Tanaka, Y. Cancer immunotherapy harnessing γδ T cells and programmed death-1. *Immunol. Rev.* **2020**, *298*, 237–253, doi:10.1111/imr.12917.

256. Fuge, O.; Vasdev, N.; Allchorne, P.; Green, J.S. Immunotherapy for bladder cancer. *Res. reports Urol.* **2015**, *7*, 65–79, doi:10.2147/RRU.S63447.

257. Bevers, R.F.M.; Kurth, K.-H.; Schamhart, D.H.J. Role of urothelial cells in BCG immunotherapy for superficial bladder cancer. *Br. J. Cancer* **2004**, *91*, 607–12, doi:10.1038/sj.bjc.6602026.

258. Zangouei, A.S.; Hamidi, A.A.; Rahimi, H.R.; Saburi, E.; Mojarrad, M.; Moghbeli, M. Chemokines as the critical factors during bladder cancer progression: an overview. *Int. Rev. Immunol.* **2021**, *16*, 1–15, doi:10.1080/08830185.2021.1877287.

259. Takeuchi, A.; Dejima, T.; Yamada, H.; Shibata, K.; Nakamura, R.; Eto, M.; Nakatani, T.; Naito, S.; Yoshikai, Y. IL-17 production by γδ T cells is important for the antitumor effect of Mycobacterium bovis bacillus Calmette-Guérin treatment against bladder cancer. *Eur. J. Immunol.* **2011**, *41*, 246–251, doi:10.1002/eji.201040773.

260. Dowell, A.C.; Cobby, E.; Wen, K.; Devall, A.J.; During, V.; Anderson, J.; James, N.D.; Cheng, K.K.; Zeegers, M.P.; Bryan, R.T.; et al. Interleukin-17-positive mast cells influence outcomes from BCG for patients with CIS: Data from a comprehensive characterisation of the immune microenvironment of urothelial bladder cancer. *PLoS One* **2017**, *12*, doi:10.1371/journal.pone.0184841.

261. Murphy, C.; Rettedal, E.; Lehouritis, P.; Devoy, C.; Tangney, M. Intratumoural production of TNFα by bacteria mediates cancer therapy. *PLoS One* **2017**, *12*, 1–13, doi:10.1371/journal.pone.0180034.

262. Langle, Y.V.; Balarino, N.P.; Belgorosky, D.; Cresta Morgado, P.D.; Sandes, E.O.; Marino, L.; Bilbao, E.R.; Zambrano, M.; Lodillinsky, C.; Eiján, A.M. Effect of nitric oxide inhibition in Bacillus Calmette-Guerin bladder cancer treatment. *Nitric Oxide - Biol. Chem.* **2020**, *98*, 50–59, doi:10.1016/j.niox.2020.03.003.

263. Brausi, M.; Oddens, J.; Sylvester, R.; Bono, A.; Van De Beek, C.; Van Andel, G.; Gontero, P.; Turkeri, L.; Marreaud, S.; Collette, S.; et al. Side effects of bacillus calmette-guérin (BCG) in the treatment of intermediate- and high-risk Ta, T1 papillary carcinoma of the bladder: Results of the EORTC genito-urinary

cancers group randomised phase 3 study comparing one-third dose with full dose an. *Eur. Assoc. Urol.* **2014**, *65*, 69–76, doi:10.1016/j.eururo.2013.07.021.

264. Wells, B.Y.H.; Harris, M. Bladder cancer: where are we with intravesical therapies? *Urol. News* **2016**, *20*, 20–23.

265. Racioppi, M.; DI Gianfrancesco, L.; Ragonese, M.; Palermo, G.; Sacco, E.; Bassi, P.F. ElectroMotive drug administration (EMDA) of Mitomycin C as first-line salvage therapy in high risk "bCG failure" non muscle invasive bladder cancer: 3 years follow-up outcomes. *BMC Cancer* **2018**, *18*, doi:10.1186/s12885-018-5134-7.

266. Di Stasi, S.M.; Valenti, M.; Verri, C.; Liberati, E.; Giurioli, A.; Leprini, G.; Masedu, F.; Ricci, A.R.; Micali, F.; Vespasiani, G. Electromotive instillation of mitomycin immediately before transurethral resection for patients with primary urothelial non-muscle invasive bladder cancer: A randomised controlled trial. *Lancet Oncol.* **2011**, *12*, 871–879, doi:10.1016/S1470-2045(11)70190-5.

267. Gan, C.; Amery, S.; Chatterton, K.; Khan, M.S.; Thomas, K.; O'Brien, T. Sequential bacillus Calmette-Guérin/Electromotive Drug Administration of Mitomycin C as the Standard Intravesical Regimen in High Risk Nonmuscle Invasive Bladder Cancer: 2-Year Outcomes. *J. Urol.* **2016**, *195*, 1697–1703, doi:10.1016/j.juro.2016.01.103.

268. Grimberg, D.C.; Shah, A.; Inman, B.A. Overview of Taris GemRIS, a Novel Drug Delivery System for Bladder Cancer. *Eur. Urol. Focus* **2019**, 2019–2021, doi:10.1016/j.euf.2019.09.006.

269. Morales, A. BCG: A throwback from the stone age of vaccines opened the path for bladder cancer immunotherapy. *Can. J. Urol.* **2017**, *24*, 8788–8793.

270. Lamm, D.L.; DeHaven, J.I.; Shriver, J.; Sarosdy, M.F. Prospective randomized comparison of intravesical with percutaneous bacillus Calmette-Guerin versus intravesical bacillus Calmette-Guerin in superficial bladder cancer. *J. Urol.* **1991**, *145*, 738–40, doi:10.1016/s0022-5347(17)38439-2.

271. Lüftenegger, W.; Ackermann, D.K.; Futterlieb, A.; Kraft, R.; Minder, C.E.; Nadelhaft, P.; Studer, U.E. Intravesical versus intravesical plus intradermal bacillus Calmette-Guerin: A prospective randomized study in patients with recurrent superficial bladder tumors. *J. Urol.* **1996**, *155*, 483–487, doi:10.1016/S0022-5347(01)66427-9.

272. Witjes, J.A.; Fransen, M.P.H.; van der Meijden, A.P.M.; Doesburg, W.H.; Debruyne, F.M.J. Use of Maintenance Intravesical Bacillus Calmette-Guérin (BCG), with or without Intradermal BCG, in Patients with Recurrent Superficial Bladder Cancer. *Urol. Int.* **1993**, *51*, 67–72, doi:10.1159/000282516.

273. Biot, C.; Rentsch, C.A.; Gsponer, J.R.; Birkhäuser, F.D.; Jusforgues-Saklani, H.; Lemaître, F.; Auriau, C.; Bachmann, A.; Bousso, P.; Demangel, C.; et al. Preexisting BCG-specific T cells improve intravesical immunotherapy for bladder cancer. *Sci. Transl. Med.* **2012**, *4*, 137ra72, doi:10.1126/scitranslmed.3003586.

274. Rousseau, M.; O'Brien, C.J.O.; Antequera, E.; Zdimerova, H.; Cansever, D.; Canton, T.; Scharff, A.Z.; Ingersoll, M.A. Identification of sex differences in tumor-specific T cell infiltration in bladder tumor-bearing mice treated with BCG immunotherapy. *bioRxiv* **2020**, 2020.06.19.161554, doi:10.1101/2020.06.19.161554.

275. Packiam, V.T.; Werntz, R.P.; Steinberg, G.D. Current Clinical Trials in Non-muscle-Invasive Bladder Cancer: Heightened Need in an Era of Chronic BCG Shortage. *Curr. Urol. Rep.* **2019**, *20*, 1–11, doi:10.1007/s11934-019-0952-y.

276. Taylor, J.; Becher, E.; Steinberg, G.D. Review Update on the guideline of guidelines : non- muscle-invasive bladder cancer. **2019**, doi:10.1111/bju.14915.

277. Svatek, R.S.; Tangen, C.; Delacroix, S.; Lowrance, W.; Lerner, S.P. Background and Update for S1602 "A Phase III Randomized Trial to Evaluate the Influence of BCG Strain Differences and T Cell Priming with Intradermal BCG Before Intravesical Therapy for BCG-naïve High-grade Non-muscle-invasive Bladder Cancer. *Eur. Urol. Focus* **2018**, *4*, 522–524, doi:10.1016/j.euf.2018.08.015.

278. Chen, S.; Zhang, N.; Shao, J.; Wang, X. Maintenance versus non-maintenance intravesical Bacillus Calmette-Guerin instillation for non-muscle invasive bladder cancer: A systematic review and meta-analysis of randomized clinical trials. *Int. J. Surg.* **2018**, *52*, 248–257, doi:10.1016/j.ijsu.2018.02.045.

279. Kanno, A.I.; Goulart, C.; Leite, L.C.C.; Pagliarone, A.C.; Nascimento, I.P. A bivalent recombinant mycobacterium bovis BCG expressing the S1 subunit of the pertussis toxin induces a polyfunctional CD4 + T cell immune response. *Biomed Res. Int.* **2019**, *2019*, doi:10.1155/2019/9630793.

280. Rodriguez, D.; Goulart, C.; Pagliarone, A.C.; Silva, E.P.; Cunegundes, P.S.; Nascimento, I.P.; Borra, R.C.; Dias, W.O.; Tagliabue, A.; Boraschi, D.; et al. In vitro Evidence of Human Immune Responsiveness Shows the

References

Improved Potential of a Recombinant BCG Strain for Bladder Cancer Treatment. *Front. Immunol.* **2019**, *10*, 1–9, doi:10.3389/fimmu.2019.01460.

281. Singh, A.K.; Praharaj, M.; Lombardo, K.A.; Yoshida, T.; Matoso, A.; Baras, A.S.; Zhao, L.; Prasad, P.; Powell, J.D.; Kates, M.; et al. Recombinant BCG overexpressing a STING agonist elicits trained immunity and improved antitumor efficacy in non-muscle invasive bladder cancer. *bioRxiv* **2020**, doi:10.1101/2020.04.25.061531.

282. Nieuwenhuizen, N.E.; Kulkarni, P.S.; Shaligram, U.; Cotton, M.F.; Rentsch, C.A.; Eisele, B.; Grode, L.; Kaufmann, S.H.E. The recombinant bacille Calmette-Guérin vaccine VPM1002: Ready for clinical efficacy testing. *Front. Immunol.* **2017**, *8*, 1–9, doi:10.3389/fimmu.2017.01147.

283. Cho, M.J.; Kim, M.J.; Kim, K.; Choi, Y.W.; Lee, S.J.; Whang, Y.M.; Chang, I.H. The immunotherapeutic effects of recombinant Bacillus Calmette-Guérin resistant to antimicrobial peptides on bladder cancer cells. *Biochem. Biophys. Res. Commun.* **2019**, *509*, 167–174, doi:10.1016/j.bbrc.2018.12.097.

284. Whang, Y.M.; Yoon, D.H.; Hwang, G.Y.; Yoon, H.; Park, S.I.; Wook Choi, Y.; Chang, I.H. Liposome-Encapsulated Bacillus Calmette–Guérin Cell Wall Skeleton Enhances Antitumor Efficiency for Bladder Cancer In Vitro and In Vivo via Induction of AMP-Activated Protein Kinase. *Cancers (Basel).* **2020**, *3679*, doi:10.3390/cancers12123679.

285. Julián, E.; Noguera-Ortega, E. Bacteria-derived alternatives to live *Mycobacterium bovis* Bacillus Calmette-Guerin for nonmuscle invasive bladder cancer treatment. *Microb. Infect. Cancer Ther. Recent Adv.* **2019**, *1*, 123–188.

286. Noguera-Ortega, E.; Rabanal, R.M.; Secanella-Fandos, S.; Torrents, E.; Luquin, M.; Julián, E. γ Irradiated Mycobacteria Enhance Survival in Bladder Tumor Bearing Mice Although Less Efficaciously than Live Mycobacteria. *J. Urol.* **2016**, *195*, 198–205, doi:10.1016/j.juro.2015.07.011.

287. Mangsbo, S.M.; Ninalga, C.; Essand, M.; Loskog, A.; Tötterman, T.H. CpG therapy is superior to BCG in an orthotopic bladder cancer model and generates CD4+ T-cell immunity. *J. Immunother.* **2008**, *31*, 34–42, doi:10.1097/CJI.0b013e3181587d29.

288. Kato, T.; Bilim, V.; Yuuki, K.; Naito, S.; Yamanobe, T.; Nagaoka, A.; Yano, I.; Akaza, H.; Tomita, Y. Bacillus Calmette-Guerin and BCG cell wall skeleton suppressed viability of bladder cancer cells in vitro - PubMed. *Anticancer Res.* **2010**, *30*, 4089–4096.

289. Miyazaki, J.; Kawai, K.; Kojima, T.; Oikawa, T.; Joraku, A.; Shimazui, T.; Nakaya, A.; Yano, I.; Nakamura, T.; Harashima, H.; et al. The liposome-incorporating cell wall skeleton of Mycobacterium bovis bacillus Calmette-Guéin can directly enhance the susceptibility of cancer cells to lymphokine-activated killer cells through up-regulation of natural-killer group 2, member D ligands. *BJU Int.* **2011**, *108*, 1520–1526, doi:10.1111/j.1464-410X.2010.10056.x.

290. Wang, T.; Yuan, H.; Diao, W.; Yang, R.; Zhao, X.; Guo, H. Comparison of gemcitabine and anthracycline antibiotics in prevention of superficial bladder cancer recurrence. **2019**, 1–5.

291. Steinberg, R.L.; Thomas, L.J.; O'Donnell, M.A. Combination Intravesical Chemotherapy for Non–muscle-invasive Bladder Cancer. *Eur. Urol. Focus* **2018**, *4*, 503–505, doi:10.1016/j.euf.2018.07.005.

292. Thomas, L.; Steinberg, R.; Nepple, K.G.; O'Donnell, M.A. Sequential intravesical gemcitabine and docetaxel in the treatment of BCG-naive patients with non-muscle invasive bladder cancer. *J. Clin. Oncol.* **2019**, *37*, 469–469, doi:10.1200/jco.2019.37.7_suppl.469.

293. Huang, D.; Jin, Y.H.; Weng, H.; Huang, Q.; Zeng, X.T.; Wang, X.H. Combination of intravesical bacille calmette-guérin and chemotherapy vs. Bacille calmette-guérin alone in non-muscle invasive bladder cancer: A meta-analysis. *Front. Oncol.* **2019**, *9*, doi:10.3389/fonc.2019.00121.

294. FDA grants priority review to Merck's Supplemental Biologics License Application (sBLA) for KEYTRUDA® (pembrolizumab) in certain patients with high-risk, Non-Muscle Invasive Bladder Cancer (NMIBC).

295. Annels, N.E.; Mansfield, D.; Arif, M.; Ballesteros-Merino, C.; Simpson, G.R.; Denyer, M.; Sandhu, S.S.; Melcher, A.A.; Harrington, K.J.; Davies, B.; et al. Phase I trial of an ICAM-1-targeted immunotherapeutic-coxsackievirus A21 (CVA21) as an oncolytic agent against non muscle-invasive bladder cancer. *Clin. Cancer Res.* **2019**, *25*, 5818–5831, doi:10.1158/1078-0432.CCR-18-4022.

296. Portal, D.E.; Weiss, R.E.; Wojtowicz, M.; Mansour, A.; Monken, C.; Mehnert, J.M.; Aisner, J.A.; Kane, M.; Nishioka, J.; Aisner, S.; et al. Phase I neoadjuvant study of intravesical recombinant fowlpox-GM-CSF (rF-GM-CSF) or fowlpox-TRICOM (rF-TRICOM) in patients with bladder carcinoma. *Cancer Gene Ther.* **2019**, *20*, doi:10.1038/s41417-019-0112-z.

297. Tse, J.; Singla, N.; Ghandour, R.; Lotan, Y.; Margulis, V. Current advances in BCG-unresponsive non-muscle invasive bladder cancer. *Expert Opin. Investig. Drugs* **2019**, *28*, 757–770, doi:10.1080/13543784.2019.1655730.

298. Guallar-Garrido, S.; Julián, E. Bacillus Calmette-Guérin (BCG) Therapy for Bladder Cancer : An Update Available online: https://www.businesswire.com/news/ home/20191202005300/en/FDA-Grants-Priority-Review-Merck's- Supplemental-Biologics (accessed on Dec 18, 2019).

299. Ronquillo Pangilinan, C.; Lee, C.H. Salmonella-based targeted cancer therapy: Updates on a promising and innovative tumor immunotherapeutic strategy. *Biomedicines* **2019**, *7*, doi:10.3390/biomedicines7020036.

300. Domingos-Pereira, S.; Sathiyanadan, K.; La Rosa, S.; Polák, L.; Chevalier, M.F.; Martel, P.; Hojeij, R.; Derré, L.; Haefliger, J.-A.; Jichlinski, P.; et al. Intravesical Ty21a vaccine promotes dendritic cells and T cell–mediated tumor regression in the MB49 bladder cancer model. *Cancer Immunol. Res.* **2019**, *7*, 621–629, doi:10.1158/2326-6066.CIR-18-0671.

301. Feyisetan, O.; Tracey, C.; Hellawell, G.O. Probiotics, dendritic cells and bladder cancer. *BJU Int.* **2012**, *109*, 1594–1597, doi:10.1111/j.1464-410X.2011.10749.x.

302. Seow, S.W.; Cai, S.; Rahmat, J.N.; Bay, B.H.; Lee, Y.K.; Chan, Y.H.; Mahendran, R. Lactobacillus rhamnosus GG induces tumor regression in mice bearing orthotopic bladder tumors. *Cancer Sci.* **2010**, *101*, 751–758, doi:10.1111/j.1349-7006.2009.01426.x.

303. Codolo, G.; Fassan, M.; Munari, F.; Volpe, A.; Bassi, P.; Rugge, M.; Pagano, F.; D'Elios, M.M.; De Bernard, M. HP-NAP inhibits the growth of bladder cancer in mice by activating a cytotoxic Th1 response. *Cancer Immunol. Immunother.* **2012**, *61*, 31–40, doi:10.1007/s00262-011-1087-2.

304. Han, C.; Hao, L.; Chen, M.; Hu, J.; Shi, Z.; Zhang, Z.; Dong, B.; Fu, Y.; Pei, C.; Wu, Y. Target expression of Staphylococcus enterotoxin A from an oncolytic adenovirus suppresses mouse bladder tumor growth and recruits CD3+ T cell. *Tumor Biol.* **2013**, *34*, 2863–2869, doi:10.1007/s13277-013-0847-3.

305. Reis, L.O.; Ferreira, U.; Billis, A.; Cagnon, V.H.A.; Fávaro, W.J. Anti-angiogenic effects of the superantigen staphylococcal enterotoxin B and bacillus Calmette-Guérin immunotherapy for nonmuscle invasive bladder cancer. *J. Urol.* **2012**, *187*, 438–445, doi:10.1016/j.juro.2011.10.022.

306. Sakano, S.; Shimabukuro, T.; Ohmoto, Y.; Naito, K. Cytokine-mediated antitumor effect of OK-432 on urinary bladder tumor cells in vitro. *Urol. Res.* **1997**, *25*, 239–245, doi:10.1007/BF00942092.

307. Tian, Y.F.; Tang, K.; Guan, W.; Yang, T.; Xu, H.; Zhuang, Q.Y.; Ye, Z.Q. OK-432 suppresses proliferation and metastasis by tumor associated macrophages in bladder cancer. *Asian Pacific J. Cancer Prev.* **2015**, *16*, 4537–4542, doi:10.7314/APJCP.2015.16.11.4537.

308. Vicinium Treatment for Subjects With Non-muscle Invasive Bladder Cancer Previously Treated With BCG.

309. Sänger, C.; Busche, A.; Bentien, G.; Spallek, R.; Jonas, F.; Böhle, A.; Singh, M.; Brandau, S. Immunodominant PstSI antigen of mycobacterium tuberculosis is a potent biological response modifier for the treatment of bladder cancer. *BMC Cancer* **2004**, *4*, doi:10.1186/1471-2407-4-86.

310. Prabir, C.; Mukhopadhyay, S. Bladder preserving approach for muscle invasive bladder cancer--role of mycobacterium w - PubMed. *J. Indian Med. Assoc.* **2003**, *101*, 559–560.

311. Filion, M.C.; Phillips, N.C. Therapeutic potential of mycobacterial cell wall-DNA complexes. *Expert Opin. Investig. Drugs* **2001**, *10*, 2157–2165, doi:10.1517/13543784.10.12.2157.

312. Li, R.; Amrhein, J.; Cohen, Z.; Champagne, M.; Kamat, A.M. Efficacy of mycobacterium phlei cell wall-nucleic acid complex (MCNA) in BCG-unresponsive patients. *J. Clin. Oncol.* **2017**, *35*, 342–342, doi:10.1200/jco.2017.35.6_suppl.342.

313. Morales, A.; Chin, J.L.; Ramsey, E.W. Mycobacterial cell wall extract for treatment of carcinoma in situ of the bladder. *J. Urol.* **2001**, *166*, 1633–1638.

314. Noguera-Ortega, E.; Secanella-Fandos, S.; Eraña, H.; Gasión, J.; Rabanal, R.M.; Luquin, M.; Torrents, E.; Julián, E. Nonpathogenic *Mycobacterium brumae* Inhibits Bladder Cancer Growth In Vitro, Ex Vivo, and In Vivo. *Eur. Urol. Focus* **2015**, *2*, 1-67–76, doi:10.1016/j.euf.2015.03.003.

315. Baran, J.; Baj-Krzyworzeka, M.; Węglarczyk, K.; Ruggiero, I.; Zembala, M. Modulation of monocyte-tumour cell interactions by Mycobacterium vaccae. *Cancer Immunol. Immunother.* **2004**, *53*, 1127–1134, doi:10.1007/s00262-004-0552-6.

316. Young, S.L.; Murphy, M.; Zhu, X.W.; Harnden, P.; O'Donnell, M.A.; James, K.; Patel, P.M.; Selby, P.J.; Jackson, A.M. Cytokine-modified Mycobacterium smegmatis as a novel anticancer immunotherapy. *Int. J. Cancer* **2004**, *112*, 653–660, doi:10.1002/ijc.20442.

317. Kuromatsu, I.; Matsuo, K.; Takamura, S.; Kim, G.; Takebe, Y.; Kawamura, J.; Yasutomi, Y. Induction of effective antitumor immune responses in a mouse bladder tumor model by using DNA of an α antigen from mycobacteria. *Cancer Gene Ther.* **2001**, *8*, 483–490, doi:10.1038/sj.cgt.7700330.

References

318. Zhang, P.; Wang, J.; Wang, D.; Wang, H.; Shan, F.; Chen, L.; Hou, Y.; Wang, E.; Lu, C.L. Dendritic cell vaccine modified by Ag85A gene enhances anti-tumor immunity against bladder cancer. *Int. Immunopharmacol.* **2012**, *14*, 252–260, doi:10.1016/j.intimp.2012.07.014.

319. Luquin, M.; Ausina, V.; Vincent-Lévy-Frébault, V.; Lanéelle, M.A.; Belda, F.; García-Barceló, M.; Prats, G.; Daffe, M. Mycobacterium brumae sp. nov., a Rapidly Growing, Nonphotochromogenic Mycobacterium. *Int. J. Syst. Bacteriol.* **1993**, *43*, 405–413.

320. Noguera-Ortega, E.; Blanco-Cabra, N.; Rabanal, R.M.R.M.; Sánchez-Chardi, A.; Roldán, M.; Guallar-Garrido, S.; Torrents, E.; Luquin, M.; Julián, E. Mycobacteria emulsified in olive oil-in-water trigger a robust immune response in bladder cancer treatment. *Sci. Rep.* **2016**, *6*, doi:10.1038/srep27232.

321. Noguera-Ortega, E.; Rabanal, R.M.; Gómez-Mora, E.; Cabrera, C.; Luquin, M.; Julián, E. Intravesical *Mycobacterium brumae* triggers both local and systemic immunotherapeutic responses against bladder cancer in mice. *Sci. Rep.* **2018**, *8*, doi:10.1038/s41598-018-33253-w.

322. Bach-Griera, M.; Campo-Pérez, V.; Barbosa, S.; Traserra, S.; Guallar-Garrido, S.; Moya-Andérico, L.; Herrero-Abadía, P.; Luquin, M.; Rabanal, R.M.; Torrents, E.; et al. Mycolicibacterium brumae is a safe and non-toxic immunomodulatory agent for cancer treatment. *Vaccines* **2020**, *8*, 2–17, doi:10.3390/vaccines8020198.

323. Noguera-Ortega, E.; Rabanal, R.M.; Gómez-Mora, E.; Cabrera, C.; Luquin, M.; Julián, E. Intravesical *Mycobacterium brumae* triggers both local and systemic immunotherapeutic responses against bladder cancer in mice. *Sci. Rep.* **2018**, *8*, doi:10.1038/s41598-018-33253-w.

324. Guallar-Garrido, S.; Luquin, M.; Julián, E. Analysis of the Lipid Composition of Mycobacteria by Thin Layer Chromatography. *J. Vis. Exp.* **2021**, 1–17, doi:10.3791/62368.

325. Gontero, P.; Bohle, A.; Malmstrom, P.-U.; O'Donnell, M.A.; Oderda, M.; Sylvester, R.; Witjes, F. The role of bacillus Calmette-Guérin in the treatment of non-muscle-invasive bladder cancer. *Eur. Urol.* **2010**, *57*, 410–29, doi:10.1016/j.eururo.2009.11.023.

326. Morales, A.; Herr, H.; Steinberg, G.; Given, R.; Cohen, Z.; Amrhein, J.; Kamat, A.M. Efficacy and safety of MCNA in patients with nonmuscle invasive bladder cancer at high risk for recurrence and progression after failed treatment with bacillus Calmette-Guérin. *J. Urol.* **2015**, *193*, 1135–1143, doi:10.1016/j.juro.2014.09.109.

327. Brosch, R.; Gordon, S. V; Garnier, T.; Eiglmeier, K.; Frigui, W.; Valenti, P.; Garcia-pelayo, C.; Inwald, J.K.; Santos, S. Dos; Hewinson, R.G.; et al. Genome plasticity of BCG and impact on vaccine efficacy. **2007**, 1–6.

328. Zhang, L.; Ru, H.W.; Chen, F.Z.; Jin, C.Y.; Sun, R.F.; Fan, X.Y.; Guo, M.; Mai, J.T.; Xu, W.X.; Lin, Q.X.; et al. Variable virulence and efficacy of BCG vaccine strains in mice and correlation with genome polymorphisms. *Mol. Ther.* **2016**, *24*, 398–405, doi:10.1038/mt.2015.216.

329. Gallant, J.L.; Viljoen, A.J.; Van Helden, P.D.; Wiid, I.J.F. Glutamate Dehydrogenase Is Required by Mycobacterium bovis BCG for Resistance to Cellular Stress. **2016**, doi:10.1371/journal.pone.0147706.

330. Ward, S.K.; Heintz, J.A.; Albrecht, R.M.; Talaat, A.M. Single-Cell Elemental Analysis of Bacteria: Quantitative Analysis of Polyphosphates in Mycobacterium tuberculosis. *Front. Cell. Infect. Microbiol.* **2012**, *2*, 63, doi:10.3389/fcimb.2012.00063.

331. Lyon, R.H.; Rogers, P.; Hall, W.H.; Lichstein, H.C. Inducible Glutamate Transport in Mycobacteria and Its Relation to Glutamate Oxidation '. **1967**, *94*, 92–100.

332. Chen, J.M.; Alexander, D.C.; Behr, M.A.; Liu, J. Mycobacterium bovis BCG vaccines exhibit defects in alanine and serine catabolism. *Infect. Immun.* **2003**, *71*, 708–716, doi:10.1128/IAI.71.2.708-716.2003.

333. O'Hare, H.M.; Durán, R.; Cerveñansky, C.; Bellinzoni, M.; Wehenkel, A.M.; Pritsch, O.; Obal, G.; Baumgartner, J.; Vialaret, J.; Johnsson, K.; et al. Regulation of glutamate metabolism by protein kinases in mycobacteria. *Mol. Microbiol.* **2008**, *70*, 1408–1423, doi:10.1111/j.1365-2958.2008.06489.x.

334. Fakas, S.; Makri, A.; Bellou, S.; Aggelis, G. Pathways to aerobic glycerol catabolism and their regulation. In *Microbial Conversions of Raw Glycerol*; 2009; pp. 9–18 ISBN 9781606923924.

335. Geisel, R.E.; Sakamoto, K.; Russell, D.G.; Rhoades, E.R. In Vivo Activity of Released Cell Wall Lipids of Mycobacterium bovis Bacillus Calmette-Guérin Is Due Principally to Trehalose Mycolates. *J. Immunol.* **2005**, *174*, 5007–5015, doi:10.4049/jimmunol.174.8.5007.

336. Ojha, A.K.; Baughn, A.D.; Sambandan, D.; Hsu, T.; Trivelli, X.; Guerardel, Y.; Alahari, A.; Kremer, L.; Jacobs, W.R.; Hatfull, G.F. Growth of Mycobacterium tuberculosis biofilms containing free mycolic acids and harbouring drug-tolerant bacteria. *Mol. Microbiol.* **2008**, *69*, 164–174, doi:10.1111/j.1365-2958.2008.06274.x.

337. Osborn, T.W. Some effects of nutritional components on the morphology of BCG colonies. *Dev. Biol. Stand.* **1986**, *58 (Pt A)*, 79–94.

338. Tepper, B.S. Differences in the utilization of glycerol and glucose by Mycobacterium phlei. *J. Bacteriol.* **1968**,

95, 1713–1717.

339. Christensen, H.; Garton, N.J.; Horobin, R.W.; Minnikin, D.E.; Barer, M.R. Lipid domains of mycobacteria studied with fluorescent molecular probes. *Mol. Microbiol.* **1999**, *31*, 1561–1572, doi:10.1046/j.1365-2958.1999.01304.x.

340. Bansal-Mutalik, R.; Nikaido, H. Mycobacterial outer membrane is a lipid bilayer and the inner membrane is unusually rich in diacyl phosphatidylinositol dimannosides. *Proc. Natl. Acad. Sci. U. S. A.* **2014**, *111*, 4958–4963, doi:10.1073/pnas.1403078111.

341. Ortalo-Magné, A.; Lemassu, A.; Lanéelle, M.A.; Bardou, F.; Silve, G.; Gounon, P.; Marchal, G.; Daffé, M. Identification of the surface-exposed lipids on the cell envelopes of Mycobacterium tuberculosis and other mycobacterial species. *J. Bacteriol.* **1996**, *178*, 456–461, doi:10.1128/jb.178.2.456-461.1996.

342. Martinot, A.J.; Farrow, M.; Bai, L.; Layre, E.; Cheng, T.-Y.; Tsai, J.H.; Iqbal, J.; Annand, J.W.; Sullivan, Z.A.; Hussain, M.M.; et al. Mycobacterial Metabolic Syndrome: LprG and Rv1410 Regulate Triacylglyceride Levels, Growth Rate and Virulence in Mycobacterium tuberculosis. *PLOS Pathog.* **2016**, *12*, e1005351, doi:10.1371/journal.ppat.1005351.

343. Secanella-Fandos, S.; Luquin, M.; Julián, E. Connaught and Russian Strains Showed the Highest Direct Antitumor Effects of Different Bacillus Calmette-Guérin Substrains. *J. Urol.* **2013**, *189*, 711–718, doi:10.1016/j.juro.2012.09.049.

344. Abou-Zeid, C.; Rook, G.A.W.; Minnikin, D.E.; Parlett, J.H.; Osbornt, T.W.; Grangets, J.M. Effect of the method of preparation of Bacille Calmette-Guérin (BCG) vaccine on the properties of four daughter strains. *J. Appl. Bacteriol.* **1987**, *63*, 449–453, doi:10.1111/j.1365-2672.1987.tb04867.x.

345. Petricevich, V.; Ueda, C.; Alves, R.; da Silva, M.; Moreno, C.; Melo, A.; Dias da Silva, W. A single strain of Mycobacterium bovis bacillus Calmette-Guérin (BCG) grown in two different media evokes distinct humoral immune responses in mice. *Brazilian J. Med. Biol. Res.* **2001**, *34*, 81–92, doi:10.1590/S0100-879X2001000100010.

346. Venkataswamy, M.M.; Goldberg, M.F.; Baena, A.; Chan, J.; Jacobs, W.R.; Porcelli, S.A. In vitro culture medium influences the vaccine efficacy of Mycobacterium bovis BCG. *Vaccine* **2012**, *30*, 1038–1049, doi:10.1016/j.vaccine.2011.12.044.

347. Noguera-Ortega, E.; Blanco-Cabra, N.; Rabanal, R.M.; Sánchez-Chardi, A.; Roldán, M.; Guallar-Garrido, S.; Torrents, E.; Luquin, M.; Julián, E. Mycobacteria emulsified in olive oil-in-water trigger a robust immune response in bladder cancer treatment. *Sci. Rep.* **2016**, *6*, 27232, doi:10.1038/srep27232.

348. Soto, C.Y.; Andreu, N.; Gibert, I.; Luquin, M. Simple and Rapid Differentiation of Mycobacterium tuberculosis H37Ra from M. tuberculosis Clinical Isolates through Two Cytochemical Tests Using Neutral Red and Nile Blue Stains. *J. Clin. Microbiol.* **2002**, *40*, 3021–3024, doi:10.1128/JCM.40.8.3021-3024.2002.

349. Asensio, J.G.; Maia, C.; Ferrer, N.L.; Barilone, N.; Laval, F.; Soto, C.Y.; Winter, N.; Daffe, M.; Gicquel, B.; Martín, C.; et al. The virulence-associated two-component PhoP-PhoR system controls the biosynthesis of polyketide-derived lipids in Mycobacterium tuberculosis. *J. Biol. Chem.* **2006**, *281*, 1313–1316, doi:10.1074/jbc.C500388200.

350. Cardona, P.J.; Soto, C.Y.; Martín, C.; Giquel, B.; Agustí, G.; Guirado, E.; Sirakova, T.; Kolattukudy, P.; Julián, E.; Luquin, M. Neutral-red reaction is related to virulence and cell wall methyl-branched lipids in Mycobacterium tuberculosis. *Microbes Infect.* **2006**, *8*, 183–190, doi:10.1016/j.micinf.2005.06.011.

351. Noguera-Ortega, E.; Blanco-Cabra, N.; Rabanal, R.M.; Sánchez-Chardi, A.; Roldán, M.; Guallar-Garrido, S.; Torrents, E.; Luquin, M.; Julián, E. Mycobacteria emulsified in olive oil-in-water trigger a robust immune response in bladder cancer treatment. *Sci. Rep.* **2016**, *6*, doi:10.1038/srep27232.

352. O'Donnell, M.A.; Luo, Y.; Chen, X.; Szilvasi, A.; Hunter, S.E.; Clinton, S.K. Role of IL-12 in the Induction and Potentiation of IFN-γ in Response to Bacillus Calmette-Guérin. *J. Immunol.* **1999**, *163*.

353. Dowell, A.C.; Cobby, E.; Wen, K.; Devall, A.J.; During, V.; Anderson, J.; James, N.D.; Cheng, K.K.; Zeegers, M.P.; Bryan, R.T.; et al. Interleukin-17-positive mast cells influence outcomes from BCG for patients with CIS: Data from a comprehensive characterisation of the immune microenvironment of urothelial bladder cancer. *PLoS One* **2017**, *12*, doi:10.1371/journal.pone.0184841.

354. Alexandroff, A.B.; Nicholson, S.; Patel, P.M.; Jackson, A.M. Recent advances in bacillus Calmette-Guerin immunotherapy in bladder cancer. *Immunotherapy* **2010**, *2*, 551–560, doi:10.2217/imt.10.32.

355. Hedhli, D.; Denis, O.; Barkan, D.; Daffé, M.; Glickman, M.S.; Huygen, K. M.tuberculosis Mutants Lacking Oxygenated Mycolates Show Increased Immunogenicity and Protective Efficacy as Compared to M. bovis

References

BCG Vaccine in an Experimental Mouse Model. *PLoS One* **2013**, *8*, 1–13, doi:10.1371/journal.pone.0076442.

356. Babjuk, M.; Burger, M.; Zigeuner, R.; Shariat, S.F.; van Rhijn, B.W.G.; Compérat, E.; Sylvester, R.J.; Kaasinen, E.; Böhle, A.; Palou Redorta, J.; et al. EAU guidelines on non-muscle-invasive urothelial carcinoma of the bladder: Update 2013. *Eur. Urol.* **2013**, *64*, 639–53, doi:10.1016/j.eururo.2013.06.003.

357. Sfakianos, J.P.; Salome, B.; Daza, J.; Farkas, A.; Bhardwaj, N.; Horowitz, A. Bacillus Calmette-Guerin (BCG): Its fight against pathogens and cancer. *Urol. Oncol. Semin. Orig. Investig.* 2020, *39*, 121–129.

358. Ratliffe, T.L.; Kavoussi, L.R.; Catalona, W.J. Role of fibronectin in intravesical BCG therapy for superficial bladder cancer. *J. Urol.* **1988**, *139*, 410–414, doi:10.1016/s0022-5347(17)42445-1.

359. Saluja, M.; Gilling, P. Intravesical bacillus Calmette–Guérin instillation in non-muscle-invasive bladder cancer: A review. *Int. J. Urol.* **2018**, *25*, 18–24, doi:10.1111/iju.13410.

360. Tham, S.M.; Ng, K.H.; Pook, S.H.; Esuvaranathan, K.; Mahendran, R. Tumor and Microenvironment Modification during Progression of Murine Orthotopic Bladder Cancer. *Clin. Dev. Immunol.* **2011**, *2011*, 11, doi:10.1155/2011/865684.

361. Smith, S.G.; Baltz, J.L.; Koppolu, B.P.; Ravindranathan, S.; Nguyen, K.; Zaharoff, D.A. Immunological mechanisms of intravesical chitosan/interleukin-12 immunotherapy against murine bladder cancer. *Oncoimmunology* **2017**, *6*, e1259050, doi:10.1080/2162402X.2016.1259050.

362. Kapoor, R.; Vijjan, V.; Singh, P. Bacillus Calmette-Guerin in the management of superficial bladder cancer. *Indian J. Urol.* **2008**, *24*, 72–76, doi:10.4103/0970-1591.38608.

363. Hobbs, C.; Bass, E.; Crew, J.; Mostafid, H. Intravesical BCG: where do we stand? Past, present and future. *J. Clin. Urol.* **2019**, *12*, 425–435, doi:10.1177/2051415818817120.

364. Kwak, C.; Ku, J.H.; Park, J.Y.; Lee, E.; Lee, S.E.; Lee, C. Initial tumor stage and grade as a predictive factor for recurrence in patients with stage T1 grade 3 bladder cancer. *J. Urol.* **2004**, *171*, 149–152, doi:10.1097/01.ju.0000099825.98542.a8.

365. Sylvester, R.J.; Van Der Meijden, A.P.M.; Oosterlinck, W.; Witjes, J.A.; Bouffioux, C.; Denis, L.; Newling, D.W.W.; Kurth, K. Predicting recurrence and progression in individual patients with stage Ta T1 bladder cancer using EORTC risk tables: A combined analysis of 2596 patients from seven EORTC trials. *Eur. Urol.* **2006**, *49*, 466–477, doi:10.1016/j.eururo.2005.12.031.

366. Dagogo-Jack, I.; Shaw, A.T. Tumour heterogeneity and resistance to cancer therapies. *Nat. Rev. Clin. Oncol.* 2018, *15*, 81–94.

367. Wei, H.; Kamat, A.; Chen, M.; Ke, H.L.; Chang, D.W.; Yin, J.; Grossman, H.B.; Dinney, C.P.; Wu, X. Association of polymorphisms in oxidative stress genes with clinical outcomes for Bladder cancer treated with bacillus Calmette-Guérin. *PLoS One* **2012**, *7*, 38533, doi:10.1371/journal.pone.0038533.

368. Lima, L.; Oliveira, D.; Ferreira, J.A.; Tavares, A.; Cruz, R.; Medeiros, R.; Santos, L. The role of functional polymorphisms in immune response genes as biomarkers of bacille Calmette-Guérin (BCG) immunotherapy outcome in bladder cancer: establishment of a predictive profile in a Southern Europe population. *BJU Int.* **2015**, *116*, 753–763, doi:10.1111/bju.12844.

369. Choi, W.; Porten, S.; Kim, S.; Willis, D.; Plimack, E.R.; Hoffman-Censits, J.; Roth, B.; Cheng, T.; Tran, M.; Lee, I.L.; et al. Identification of Distinct Basal and Luminal Subtypes of Muscle-Invasive Bladder Cancer with Different Sensitivities to Frontline Chemotherapy. *Cancer Cell* **2014**, *25*, 152–165, doi:10.1016/j.ccr.2014.01.009.

370. Kim, Y.J.; Ha, Y.S.; Kim, S.K.; Yoon, H.; Lym, M.S.; Kim, M.J.; Moon, S.K.; Choi, Y.H.; Kim, W.J. Gene signatures for the prediction of response to Bacillus Calmette-Guérin immunotherapy in primary pT1 bladder cancers. *Clin. Cancer Res.* **2010**, *16*, 2131–2137, doi:10.1158/1078-0432.CCR-09-3323.

371. Kim, S.K.; Park, S.H.; Kim, Y.U.; Byun, Y.J.; Piao, X.M.; Jeong, P.; Kim, K.; Lee, H.Y.; Seo, S.P.; Kang, H.W.; et al. A molecular signature determines the prognostic and therapeutic subtype of non-muscle-invasive bladder cancer responsive to intravesical bacillus calmette-guérin therapy. *Int. J. Mol. Sci.* **2021**, *22*, 1–16, doi:10.3390/ijms22031450.

372. Monfardini, S.; Morlino, S.; Valdagni, R.; Catanzaro, M.; Tafa, A.; Bortolato, B.; Petralia, G.; Bonetto, E.; Villa, E.; Picozzi, S.; et al. Follow-up of elderly patients with urogenital cancers: Evaluation of geriatric care needs and related actions. *J. Geriatr. Oncol.* **2017**, *8*, 289–295, doi:10.1016/j.jgo.2017.02.011.

373. Shao, Y.; Hu, X.; Yang, Z.; Lia, T.; Yang, W.; Wu, K.; Ren, S.; Xiong, S.; Dou, W.; Feng, S.; et al. Prognostic factors of non-muscle invasive bladder cancer: a study based on next-generation sequencing. *Cancer Cell Int.* **2021**, *21*, 1–10, doi:10.1186/s12935-020-01731-9.

374. Yuan, Y.; Leet, R.E.; Besrat, G.S.; Belislet, J.T.; Iii, C.E.B. *Identification of a gene involved in the biosynthesis of cyclopropanated mycolic acids in Mycobacterium tuberculosis*; 1995; Vol. 92;.

375. Watanabe, M.; Ohta, A.; Sasaki, S.I.; Minnikin, D.E. Structure of a new glycolipid from the *Mycobacterium avium-Mycobacterium intracellulare* complex. *J. Bacteriol.* **1999**, *181*, 2293–2297.

376. Brambilla, C.; Sá Nchez-Chardi, A.; Pé Rez-Trujillo, M.; Juliá, E.; Luquin, M. Cyclopropanation of a-mycolic acids is not required for cording in Mycobacterium brumae and Mycobacterium fallax., doi:10.1099/mic.0.057919-0.

377. Huet, G.; Constant, P.; Malaga, W.; Lanéelle, M.-A.; Kremer, K.; van Soolingen, D.; Daffé, M.; Guilhot, C. A Lipid Profile Typifies the Beijing Strains of Mycobacterium tuberculosis Identification of a mutations responsible for a modification of the structures phthiocerol dimycocerosates and phenolic glycolipids. **2009**, doi:10.1074/jbc.M109.041939.

378. Secanella-Fandos, S.; Luquin, M.; Pérez-Trujillo, M.; Julián, E. Revisited mycolic acid pattern of Mycobacterium confluentis using thin-layer chromatography. *J. Chromatogr. B* **2011**, *879*, 2821–2826, doi:10.1016/j.jchromb.2011.08.001.

379. MANKIEWICZ, E. The action of lipidolytic enzymes of larvae of Galleria melonella on virulent Mycobacterium tuberculosis. *Can. J. Med. Sci.* **1952**, *30*, 106–112, doi:10.1139/cjms52-013.

380. Spits, H.; Artis, D.; Colonna, M.; Diefenbach, A.; Di Santo, J.P.; Eberl, G.; Koyasu, S.; Locksley, R.M.; McKenzie, A.N.J.; Mebius, R.E.; et al. Innate lymphoid cells-a proposal for uniform nomenclature. *Nat. Rev. Immunol.* **2013**, *13*, 145–149, doi:10.1038/nri3365.

381. Takatori, H.; Kanno, Y.; Watford, W.T.; Tato, C.M.; Weiss, G.; Ivanov, I.I.; Littman, D.R.; O ' Shea, J.J. Lymphoid tissue inducer – like cells are an innate source of IL-17 and IL-22. *J. Exp. Med.* **2009**, *206*, 35–41, doi:10.1084/jem.20072713.

382. Ercolano, G.; Falquet, M.; Vanoni, G.; Trabanelli, S.; Jandus, C. ILC2s: New Actors in Tumor Immunity. *Front. Immunol.* 2019, *10*.

383. Crinier, A.; Vivier, E.; Bléry, M. Helper-like innate lymphoid cells and cancer immunotherapy. *Semin. Immunol.* 2019, *41*.

384. Bruchard, M.; Ghiringhelli, F. Deciphering the roles of innate lymphoid cells in cancer. *Front. Immunol.* 2019, *10*.

385. Allan, D.S.J.; Cerdeira, A.S.; Ranjan, A.; Kirkham, C.L.; Aguilar, O.A.; Tanaka, M.; Childs, R.W.; Dunbar, C.E.; Strominger, J.L.; Kopcow, H.D.; et al. Transcriptome analysis reveals similarities between human blood CD3 – CD56 bright cells and mouse CD127 + innate lymphoid cells. *Sci. Rep.* **2017**, *7*, doi:10.1038/s41598-017-03256-0.

386. García-Cuesta, E.M.; Esteso, G.; Ashiru, O.; López-Cobo, S.; Álvarez-Maestro, M.; Linares, A.; Ho, M.M.; Martínez-Piñeiro, L.; Garc ıa-Cuesta, E.M.; opez-Cobo, S.L.; et al. Characterization of a human anti-tumoral NK cell population expanded after BCG treatment of leukocytes. **2017**, doi:10.1080/2162402X.2017.1293212.

387. Kamat, A.M.; Flaig, T.W.; Grossman, H.B.; Konety, B.; Lamm, D.; O'donnell, M.A.; Uchio, E.; Efstathiou, J.A.; Taylor, J.A. Expert consensus document: Consensus statement on best practice management regarding the use of intravesical immunotherapy with BCG for bladder cancer. *Nat. Rev.* **2015**, *12*, 225–235, doi:10.1038/nrurol.2015.58.

388. Ortalo-Magné, A.; Dupont, M.-A.; Lemassu, A.; Ander~en, A.B.; Gounon4, P.; Daff@, M. *Molecular composition of the outermost capsular material of the tubercle bacillus*; 1995; Vol. 141;.

389. Llorens-Fons, M.; Pérez-Trujillo, M.; Julián, E.; Brambilla, C.; Alcaide, F.; Byrd, T.F.; Luquin, M. Trehalose polyphleates, external cell wall lipids in Mycobacterium abscessus, are associated with the formation of clumps with cording morphology, which have been associated with virulence. *Front. Microbiol.* **2017**, *8*, doi:10.3389/fmicb.2017.01402.

390. Hattori, Y.; Morita, D.; Fujiwara, N.; Mori, D.; Nakamura, T.; Harashima, H.; Yamasaki, S.; Sugita, M. Glycerol monomycolate is a novel ligand for the human, but not mouse macrophage inducible C-type lectin, Mincle. *J. Biol. Chem.* **2014**, *289*, 15405–12, doi:10.1074/jbc.M114.566489.

391. Ojha, A.K.; Trivelli, X.; Guerardel, Y.; Kremer, L.; Hatfull, G.F. Enzymatic hydrolysis of trehalose dimycolate releases free mycolic acids during mycobacterial growth in biofilms. *J. Biol. Chem.* 2010, *285*, 17380–9, doi:10.1074/jbc.M110.112813.

392. Clifton E, B.; Lee, R.E.; Mdluli, K.; Sampson, A.E.; Schroeder, B.G.; Slayden, R.A.; Yuan, Y. *Mycolic acids: Structure, Biosynthesis and physiological functions*;

393. Medjahed, H.; Gaillard, J.-L.; Reyrat, J.-M.; Brennan, P.J.; Nikaido, H.; Britton, W.J.; Triccas, J.A.; Daffé, M.;

References

Draper, P.; Gokhale, R.S.; et al. Mycobacterium abscessus: a new player in the mycobacterial field. *Trends Microbiol.* **2010**, *18*, 117–123, doi:10.1016/j.tim.2009.12.007.

394. Vander Beken, S.; Al Dulayymi, J.R.; Naessens, T.; Koza, G.; Maza-Iglesias, M.; Rowles, R.; Theunissen, C.; De Medts, J.; Lanckacker, E.; Baird, M.S.; et al. Molecular structure of the Mycobacterium tuberculosis virulence factor, mycolic acid, determines the elicited inflammatory pattern. *Eur. J. Immunol.* **2011**, *41*, 450–460, doi:10.1002/eji.201040719.

395. Sambandan, D.; Dao, D.N.; Weinrick, B.C. Keto mycolic acid dependent pellicle formation confers tolerance to drug sensitive mycobacterium tuberculosis. *MBio* **2013**, *4*, 1–10, doi:10.1128/mBio.00222-13.Editor.

396. Richardson, M.B.; Williams, S.J.; Agostino, M.; Zwirner, N.W. MCL and Mincle: C-type lectin receptors that sense damaged self and pathogen-associated molecular patterns. **2014**, doi:10.3389/fimmu.2014.00288.

397. Lee, W. Bin; Kang, J.S.; Choi, W.Y.; Zhang, Q.; Kim, C.H.; Choi, U.Y.; Kim-Ha, J.; Kim, Y.J. Mincle-mediated translational regulation is required for strong nitric oxide production and inflammation resolution. *Nat. Commun.* **2016**, *7*, 1–14, doi:10.1038/ncomms11322.

398. Patin, E.C.; Willcocks, S.; Orr, S.; Ward, T.H.; Lang, R.; Schaible, U.E. Mincle-mediated anti-inflammatory IL-10 response counter-regulates IL-12 in vitro. *Innate Immun.* **2016**, *22*, 181–185, doi:10.1177/1753425916636671.

399. Ali, O.T.; Sahb, M.M.; Al Dulayymi, J.R.; Baird, M.S. Glycerol mycolates from synthetic mycolic acids. *Carbohydr. Res.* **2017**, *448*, 67–73, doi:10.1016/j.carres.2017.04.023.

400. Iizasa, E.; Chuma, Y.; Uematsu, T.; Kubota, M.; Kawaguchi, H.; Umemura, M.; Toyonaga, K.; Kiyohara, H.; Yano, I.; Colonna, M.; et al. Contrasting roles of the innate receptors TREM2 versus Mincle in the recognition and response of macrophages to mycolic acid-containing lipids in mycobacterial cell walls. **2020**, doi:10.21203/rs.3.rs-37581/v1.

401. Viljoen, A.; Blaise, M.; de Chastellier, C.; Kremer, L. *MAB_3551c* encodes the primary triacylglycerol synthase involved in lipid accumulation in *M ycobacterium abscessus. Mol. Microbiol.* **2016**, *102*, 611–627, doi:10.1111/mmi.13482.

402. Osma, M.M.; Paga, A.J.; Shanaha, J.K.; Ramakrishnan, L. Mycobacterium marinum phthiocerol dimycocerosates enhance macrophage phagosomal permeabilization and membrane damage. *PLoS One* **2020**, *15*, doi:10.1371/journal.pone.0233252.

403. Camacho, L.R.; Ensergueix, D.; Perez, E.; Gicquel, B.; Guilhot, C. Identification of a virulence gene cluster of Mycobacterium tuberculosis by signature-tagged transposon mutagenesis. *Mol. Microbiol.* **1999**, *34*, 257–267, doi:10.1046/j.1365-2958.1999.01593.x.

404. Cox, J.S.; Chess, B.; McNeil, M.; Jacobs, W.R. Complex lipid determines tissue-specific replication of Mycobacterium tuberculosis in mice. *Nature* **1999**, *402*, 79–83, doi:10.1038/47042.

405. Passemar, C.; Arbués, A.; Malaga, W.; Mercier, I.; Moreau, F.; Lepourry, L.; Neyrolles, O.; Guilhot, C.; Astarie-Dequeker, C. Multiple deletions in the polyketide synthase gene repertoire of *Mycobacterium tuberculosis* reveal functional overlap of cell envelope lipids in host-pathogen interactions. *Cell. Microbiol.* **2014**, *16*, 195–213, doi:10.1111/cmi.12214.

406. Robinson, N.; Kolter, T.; Wolke, M.; Rybniker, J.; Hartmann, P.; Plum, G. Mycobacterial Phenolic Glycolipid Inhibits Phagosome Maturation and Subverts the Pro-inflammatory Cytokine Response. *Traffic* **2008**, *9*, 1936–1947, doi:10.1111/j.1600-0854.2008.00804.x.

407. Augenstreich, J.; Haanappel, E.; Ferré, G.; Czaplicki, G.; Jolibois, F.; Destainville, N.; Guilhot, C.; Milon, A.; Astarie-Dequeker, C.; Chavent, M. The conical shape of DIM lipids promotes Mycobacterium tuberculosis infection of macrophages. *Proc. Natl. Acad. Sci. U. S. A.* **2019**, *116*, 25649–25658, doi:10.1073/pnas.1910368116.

408. Astarie-Dequeker, C.; Le Guyader, L.; Malaga, W.; Seaphanh, F.-K.; Chalut, C.; Lopez, A.; Guilhot, C. Phthiocerol Dimycocerosates of M. tuberculosis Participate in Macrophage Invasion by Inducing Changes in the Organization of Plasma Membrane Lipids. *PLoS Pathog.* **2009**, *5*, e1000289, doi:10.1371/journal.ppat.1000289.

409. Murry, J.P.; Pandey, A.K.; Sassetti, C.M.; Rubin, E.J. Phthiocerol Dimycocerosate Transport Is Required for Resisting Interferon-γ–Independent Immunity. *J. Infect. Dis.* **2009**, *200*, 774–782, doi:10.1086/605128.

410. Arbués, A.; Malaga, W.; Constant, P.; Guilhot, C.; Prandi, J.; Astarie-Dequeker, C. Trisaccharides of Phenolic Glycolipids Confer Advantages to Pathogenic Mycobacteria through Manipulation of Host-Cell Pattern-Recognition Receptors. *ACS Chem. Biol.* **2016**, *11*, 2865–2875, doi:10.1021/acschembio.6b00568.

411. Elsaidi, H.R.H.; Lowary, T.L. Effect of phenolic glycolipids from Mycobacterium kansasii on proinflammatory cytokine release. A structure–activity relationship study. *Chem. Sci.* **2015**, *6*, 3161–3172, doi:10.1039/C4SC04004J.

412. Tran, V.; Ahn, S.K.; Ng, M.; Li, M.; Liu, J. Loss of Lipid Virulence Factors Reduces the Efficacy of the BCG Vaccine. *Sci. Rep.* **2016**, *6*, 1–12, doi:10.1038/srep29076.

413. Camacho, L.R.; Constant, P.; Raynaud, C.; Lanéelle, M.A.; Triccas, J.A.; Gicquel, B.; Daffé, M.; Guilhot, C. Analysis of the phthiocerol dimycocerosate locus of Mycobacterium tuberculosis. Evidence that this lipid is involved in the cell wall permeability barrier. *J. Biol. Chem.* **2001**, *276*, 19845–19854, doi:10.1074/jbc.M100662200.

414. Eckhardt, E.; Bastian, M. Animal models for human group 1 CD1 protein function. *Mol. Immunol.* **2021**, *130*, 159–163, doi:10.1016/j.molimm.2020.12.018.

415. Llorens-Fons, M.; Julián, E.; Luquin, M.; Pérez-Trujillo, M. Molecule confirmation and structure characterization of pentatriacontatrienyl mycolate in Mycobacterium smegmatis. *Chem. Phys. Lipids* **2018**, *212*, 138–143, doi:10.1016/J.CHEMPHYSLIP.2017.12.006.

8 - ANNEX I

Bacillus Calmette-Guérin (BCG) Therapy for Bladder Cancer: An Update

Sandra Guallar-Garrido, Esther Julián

9 - ANNEX II

Analysis of the Lipid Composition of Mycobacteria by Thin Layer Chromatography

Sandra Guallar-Garrido, Marina Luquin, Esther Julián

10 - ANNEX III

Each Mycobacterium Requires a Specific Culture Medium Composition for Triggering an Optimized Immunomodulatory and Antitumoral Effect

Sandra Guallar-Garrido, Víctor Campo-Pérez, Alejandro Sánchez-Chardi,

Marina Luquin and Esther Julián

11 - ANNEX IV

Mycobacterial surface lipidome remodeled by growth culture conditions drives/modulates the tumor immune microenvironment *in vivo* in intravesical bladder cancer treatment

Sandra Guallar-Garrido, Víctor Campo-Pérez, Míriam Pérez-Trujillo, Cecilia Cabrera, Jordi Senserrich, Alejandro Sánchez-Chardi, Rosa Maria Rabanal, Elisabet Gómez-Mora, Estela Noguera-Ortega, Marina Luquin and Esther Julián